

IntechOpen

# Ion Channels in Health and Sickness

*Edited by Kaneez Fatima Shad*





---

# **ION CHANNELS IN HEALTH AND SICKNESS**

---

Edited by **Kaneez Fatima Shad**

## **Ion Channels in Health and Sickness**

<http://dx.doi.org/10.5772/intechopen.72025>

Edited by Kaneez Fatima Shad

### **Contributors**

Zuzana Tomaskova, Katarina Mackova, Anton Misak, Viktoria Szuts, Jozsef Geza Kiss, Janos Andras Jarabin, Attila Nagy, Ferenc Otvos, Nikoletta Nagy, Roland Nagy, Katalin Halasy, Marta Szell, Laszlo Rovo, Tianbo Li, Wei Cheng, Tianhua Feng, Subha Kalyanamoorthy, Khaled Hasaan Barakat, Tian Li, Celio Castro Junior, Luana Ferreira, Marina Delgado, Juliana Silva, Duana Santos, Jun Chen, Fatima Shad Kaneez

### **© The Editor(s) and the Author(s) 2018**

The rights of the editor(s) and the author(s) have been asserted in accordance with the Copyright, Designs and Patents Act 1988. All rights to the book as a whole are reserved by INTECHOPEN LIMITED. The book as a whole (compilation) cannot be reproduced, distributed or used for commercial or non-commercial purposes without INTECHOPEN LIMITED's written permission. Enquiries concerning the use of the book should be directed to INTECHOPEN LIMITED rights and permissions department ([permissions@intechopen.com](mailto:permissions@intechopen.com)). Violations are liable to prosecution under the governing Copyright Law.



Individual chapters of this publication are distributed under the terms of the Creative Commons Attribution 3.0 Unported License which permits commercial use, distribution and reproduction of the individual chapters, provided the original author(s) and source publication are appropriately acknowledged. If so indicated, certain images may not be included under the Creative Commons license. In such cases users will need to obtain permission from the license holder to reproduce the material. More details and guidelines concerning content reuse and adaptation can be found at <http://www.intechopen.com/copyright-policy.html>.

### **Notice**

Statements and opinions expressed in the chapters are those of the individual contributors and not necessarily those of the editors or publisher. No responsibility is accepted for the accuracy of information contained in the published chapters. The publisher assumes no responsibility for any damage or injury to persons or property arising out of the use of any materials, instructions, methods or ideas contained in the book.

First published in London, United Kingdom, 2018 by IntechOpen

eBook (PDF) Published by IntechOpen, 2019

IntechOpen is the global imprint of INTECHOPEN LIMITED, registered in England and Wales, registration number:

11086078, The Shard, 25th floor, 32 London Bridge Street

London, SE19SG – United Kingdom

Printed in Croatia

British Library Cataloguing-in-Publication Data

A catalogue record for this book is available from the British Library

Additional hard and PDF copies can be obtained from [orders@intechopen.com](mailto:orders@intechopen.com)

Ion Channels in Health and Sickness

Edited by Kaneez Fatima Shad

p. cm.

Print ISBN 978-1-78984-227-2

Online ISBN 978-1-78984-228-9

eBook (PDF) ISBN 978-1-83881-642-1

# We are IntechOpen, the world's leading publisher of Open Access books Built by scientists, for scientists

**3,800+**

Open access books available

**116,000+**

International authors and editors

**120M+**

Downloads

**151**

Countries delivered to

Our authors are among the  
**Top 1%**

most cited scientists

**12.2%**

Contributors from top 500 universities



**WEB OF SCIENCE™**

Selection of our books indexed in the Book Citation Index  
in Web of Science™ Core Collection (BKCI)

Interested in publishing with us?  
Contact [book.department@intechopen.com](mailto:book.department@intechopen.com)

Numbers displayed above are based on latest data collected.  
For more information visit [www.intechopen.com](http://www.intechopen.com)





# Meet the editor



Professor Kaneez Fatima Shad completed her PhD in 1994 from the School of Physiology and Pharmacology Faculty of Medicine, University of New South Wales, Sydney, Australia. She is an Australian Neuroscientist with more than thirty-five years of experience in teaching neurosciences, neurophysiology and other medical and biological sciences to medical, dental, allied health and science students at postgraduate, graduate and undergraduate levels in various universities in Australia, USA, UAE, Bahrain, Pakistan and Brunei. She is currently back in Australia as a visiting Professor at the University of Technology Sydney where she is teaching undergraduates and supervising postgraduates. She is also teaching at the Australian Catholic University. She has fifty-five peer-reviewed publications, has edited four books, and written five book chapters.





---

# Contents

---

## **Preface XI**

### **Section 1 Introduction 1**

- Chapter 1 **Introductory Chapter: Ion Channels 3**  
Kaneez Fatima Shad, Saad Salman, Saifullah Afridi, Muniba Tariq  
and Sajid Asghar

### **Section 2 Monovalent Cations 11**

- Chapter 2 **Voltage-Gated Sodium Channels in Drug Discovery 13**  
Tianbo Li and Jun Chen
- Chapter 3 **Voltage-Gated Sodium Channel Drug Discovery Technologies  
and Challenges 45**  
Tianbo Li and Jun Chen
- Chapter 4 **Genetic Defects of Voltage-Gated Sodium Channel  $\alpha$  Subunit  
1 in Dravet Syndrome and the Patients' Response to  
Antiepileptic Drugs 57**  
Tian Li
- Chapter 5 **Altered Potassium Ion Homeostasis in Hearing Loss 79**  
Viktoria Szuts, Janos Andras Jarabin, Nikoletta Nagy, Ferenc Otvos,  
Roland Nagy, Attila Nagy, Katalin Halasy, Laszlo Rovo, Marta Szell  
and Jozsef Geza Kiss

### **Section 3 Divalent Cations 105**

- Chapter 6 **Role of Calcium Permeable Channels in Pain Processing 107**  
Célio Castro-Junior, Luana Ferreira, Marina Delgado, Juliana Silva  
and Duana Santos

Chapter 7 **L-Type Calcium Channels: Structure and Functions** 127  
Tianhua Feng, Subha Kalyanamoorthy and Khaled Barakat

**Section 4 Transient Receptor Potential (TRP)** 149

Chapter 8 **TRP Ion Channels: From Distribution to Assembly** 151  
Wei Cheng

**Section 5 Anions** 173

Chapter 9 **Lifting the Fog over Mitochondrial Chloride Channels** 175  
Katarina Mackova, Anton Misak and Zuzana Tomaskova

---

## Preface

---

In this book, we focus on the cationic, anionic and transient receptor potential channels. Cationic channels that are present in the plasma membrane allow positively charged ions (cations) such as sodium, potassium and calcium to pass through them to generate an action potential. Whereas, anionic channels present on the membranes of both plasma and intracellular organelles let negatively charged ions such as chlorides move through them. Anionic channels are very important in the regulation of the cell volume, trans-epithelial transport and electrical excitability. Similarly, transient receptor potential (TRP) channels are non-selective channels for cations such as sodium, potassium and magnesium and are involved in the regulation of sensory reception such as pain, temperature, pressure and light.

After the introductory chapter, this book is divided into four sections. Two sections focus on the cationic channels for monovalent ( $\text{Na}^+$ ,  $\text{K}^+$ ) and divalent ( $\text{Ca}^{2+}$ ) ions. The third segment is allocated to the transient receptor potential channels, which are non-selectively permeable to cations. The fourth section is for anionic ( $\text{Cl}^-$ ) channels.

In the monovalent cation section, there are three very interesting chapters on voltage gated sodium channels, discussing their role in health and sickness and the challenges and limitations during the development of drugs targeting these voltage gated sodium channels. A fascinating chapter on the role of potassium channels in hearing loss is also included in this section. The divalent cation section focuses on the structure function of calcium channels and their contribution in the painful states. The transient receptor potential section is based on a fascinating chapter discussing the distribution and assembly of TRP ion channels. The anionic section is created for an intriguing chapter on the role of chloride channels in the mitochondria.

This book is meant to be accessible for a broad range of readers from undergraduates, graduates, researchers and teachers in all biological disciplines and others who are interested in ion channels.

Production of this book would not have been possible without the contribution of the experts in their field and the continuous hard work of the author service manager from Intech Publication.

**Professor Kaneez Fatima Shad**  
School of Life Sciences  
Faculty of Science  
Centre for Health Technologies  
University of Technology Sydney, Australia



---

# Introduction

---



---

## Introductory Chapter: Ion Channels

---

Kaneez Fatima Shad, Saad Salman, Saifullah Afridi,  
Muniba Tariq and Sajid Asghar

Additional information is available at the end of the chapter

<http://dx.doi.org/10.5772/intechopen.80597>

---

### 1. Introduction

Ion channels are remarkable proteins, present in the lipid bilayer membrane of both animal and plant cells and their organelles, such as nucleus, endoplasmic reticulum, Golgi apparatus, mitochondria, chloroplasts, and lysosomes.

When we google the word “ion channel,” about 80,000,000 results pop up within 0.45 s. Scientists have been working on these amazing transmembrane proteins since the beginning of the last century, which has resulted in three sets of Nobel prizes in 1963, 1991, and 2003.

Sir John Carew Eccles, Alan Lloyd Hodgkin, and Andrew Fielding Huxley in 1963 received Nobel Prize for Physiology and Medicine for their discoveries concerning the ionic mechanisms involved in excitation and inhibition in the peripheral and central portions of the nerve cell membrane [1, 2]. Similarly, Erwin Neher and Bert Sakmann in 1991 proved that cell membranes have individual ion channels through which tiny currents can pass, which are big enough to generate communications between pre- and postsynaptic neurons by converting chemical or mechanical events into electrical signals [3, 4]. The Nobel Prize in Chemistry for 2003 was shared between two scientists Agre [5] and Roderick MacKinnon [6] who have made fundamental discoveries concerning how water and ions move through cell membranes.

In this book, we have **nine** very diverse and informative chapters including this introductory chapter on the importance of both cations and anions passing through these ion channels.

**First chapter** is the introductory chapter which briefly overview the other eight chapters included in this book, as well as discusses the diversity and classification of ion channels, nature and number of gating for these ion channels along with shedding some light on Channelopathies. **Second chapter** deals with the voltage-gated sodium channels in drug discovery. Sodium channels are the very first one to be discovered when Hodgkin and Katz were

performing their experiments on squid axons showing that there would be no action potential if sodium ions are not present in the extracellular fluid. In this chapter, genetic evolution and subtype distribution of this super family of voltage-gated sodium (Nav) channels are introduced, and there is a discussion about how the changes in the structure alter their functions. **Third chapter** argues the modulation of Nav by small and large molecules, along with the discussion on the major challenges for the Nav-targeted drug discoveries. **Fourth chapter** is taking us to a striking journey about how the genetic mutations bring change in their product proteins and resultant disorders such as Dravet syndrome. SCN1A gene is responsible for this condition and there is a word of caution for the medical practitioners to not prescribe sodium channel blockers for the epileptic patients with this mutation, as the medicine will aggravate their condition. **Fifth chapter** is about potassium channels: there are many different types of the potassium channels (many more than sodium ion channels). In this chapter, authors have discussed the role of two gap junction proteins—connexins and pannexins—in maintaining the homeostasis of potassium ions, taking cochlea as an example. Mutation in gap junction gene results in 50% of prelingual, recessive deafness. Authors developed a novel method for the early detection of the genetic mutations for the inner ear impairment. **Sixth chapter** is dealing with the structure and function of L-type calcium channels and how voltage-gated calcium channels (VGCCs) manage the electrical signaling of cells by allowing the selective-diffusion of calcium ions in response to the changes in the cellular membrane potential. Among the different VGCCs, the long-lasting or the L-type calcium channels (LTCCs) are prevalently expressed in a variety of cells, such as skeletal muscles, ventricular myocytes, smooth muscles, and dendritic cells and form the largest family of the VGCCs. Their wide expression pattern and significant role in diverse cellular events have made these channels the major targets for drug development. **Seventh chapter** is about the regulation of pain through calcium channels. In this chapter, authors present a large body of clinical, biochemical, biophysical, pharmacological, and genetic evidences pointing toward calcium-permeable channels as the key players in pain conditions. The primary goal of this chapter is to present an overview of the different classes of calcium-permeable channels and how they change to modulate the sensation of pain in acute and chronic states. **Eighth chapter** deals with the transient receptor potential (TRP) ion channels, from their distribution to their assembly. TRP ion channel superfamily is widely distributed from neuronal to nonneuronal tissues by serving as cellular sensors. TRP subunits can form both homomeric and heteromeric channels which are present either in the same subfamily or in the different subfamilies and diversify TRP channel functions. **Ninth chapter** discusses about the types of anionic and chloride channels present in the mitochondria. There are many types of chloride channels present in mitochondria, but two types are of major interest, i.e., one which is present in the inner mitochondrial membrane, responsible for the oscillations of membrane potential and the chloride intracellular ion channel (CLIC) localized in the cardiac mitochondrial membranes. These anion channels are very important both in health and diseased conditions. These channels are important for the regulation of PH and ROS along with the synchronization of the mitochondrial membrane potential.

In the following pages of Chapter 1, we will be looking at the role of gating in ion channels for the maintenance of normal physiology and how any of these alterations in the gating result in the channelopathies.



Before going any further, we would like to acknowledge the sculpture called the birth of an idea. It is a 1.5-m tall figurine of KcsA potassium channel, made up of wires and blown glass, representing the channel's lumen [7, 8]. This statue was commissioned to Julian Voss-Andreae by Nobel Prize winner Roderick Mackinnon.

There are three main types of ion channels, i.e., voltage-gated, extracellular ligand-gated, and intracellular ligand-gated along with two groups of miscellaneous ion channels. These ion channels are responsible for the transmission of signals between nerve and other types of electrically active cells [9, 10] through synapses and gap junctions [11, 12]. Alterations in the electrical potential of presynaptic neurons initiate the release of neurotransmitters from the vesicles in the synaptic cleft [13]. These chemicals move toward the postsynaptic cells through the diffusion and occupy their specific receptor sites on membranes and generate the electrical potential by opening ion channels [14]. Removal of neurotransmitters from the synaptic cleft is essential to avoid any effect on the nearby cells [14–16]. Cell signaling by neurotransmitters is far more adaptable and versatile as compared to the gap junctions [17].

## 2. Distinctive features of ion channels and ion transporter proteins

More than 10<sup>6</sup> ions are transported in a second through the ion channels without the help of metabolic energy like ATP, cotransport, or the active transport mechanism [18]. There are two types ion channels, nonselective or large pore and selective (archetypal) or small pores [19, 20]. Ions typically pass through the channel pores in the form of a single file almost as fast as they move through a free solution. In most of the ion channels, the passage across the pores is governed by a “gate.” The gate may be opened or closed in response to different factors such as: electrical signals, chemical signals, temperature, and the mechanical force [14, 15, 18]. In summary, ion channels are the integral membrane proteins which are usually present as assemblies of many subunit proteins [16, 19]. In most voltage-gated ion channels,  $\alpha$  subunit is the pore-forming subunit, while  $\beta$  and  $\gamma$  are the auxiliary subunits [21].

### 2.1. Diversity and classification of ion channels

There are many different types of ion channels distributed in each cell of our body; for example, in the cells of inner ear alone, there are about 300 ion channels [22]. Ion channels are mainly classified [23, 24] on the basis of the following:

1. The nature of gating;
2. The types of ions passing through the said gates;
3. The number of the gates.

#### 2.1.1. Classification by gating

Ion channels could be classified on the basis of gating, i.e., type of stimuli responsible for their opening and closing. Electrical gradient across the plasma membrane are responsible for the

opening and closing of voltage-gated ion channels [25, 26]; however, binding of the ligands to the channels is responsible for the activation and deactivation of ligand-gated ion channels [29].

#### 2.1.1.1. *Voltage-gated*

The opening and closing of the voltage-gated ion channels are dependent on the membrane potential, which can be divided into the following subtypes [25–28].

#### 2.1.1.2. *Ligand-gated*

These channels are also known as the ionotropic receptors and get opened in response to specific ligand molecules binding to the extracellular domain of the receptor proteins [28–30]. Binding of the ligand causes a conformational change in the channel protein that ultimately leads to the opening of the channel gate and subsequent ion flux across the plasma membrane occurs [31, 32]. Cation-permeable “nicotinic” acetylcholine receptors, ionotropic glutamate-gated receptors, acid-sensing ion channels (ASICs), ATP-gated P2X receptors, and the anion-permeable  $\gamma$ -aminobutyric acid-gated GABA receptors are a few examples of ligand-gated channels [29, 31, 33].

#### 2.1.1.3. *Other gating*

Activation and inactivation of ion channels by second messengers are included under this heading. Some examples are:

**Photon-mediated light-gated channels** are activated and deactivated in response to light and are synthesized in the laboratory. Some light-sensitive channels are present in nature such as channelrhodopsin. Photoreceptor proteins are also sensitive to light and are G protein gated too.

**Cyclic nucleotide-gated channels** are activated by hyperpolarization and are permeable to monovalent and divalent cations such as  $K^+$ ,  $Na^+$ , and  $Ca^{2+}$ .

**Temperature-gated channels** are the members of the transient receptor potential ion channel superfamily and are opened by hot or cold temperatures.

### 3. Channelopathies

Genetic and autoimmune disorders of the ion channels cause channelopathies. If a mutant gene encodes an ion channel protein that is present on the cell membrane of heart, muscles, or brain, it results in the development of diseases in these organs [34, 35]. For example, if a gene encoding  $Na^+$  channel is mutated, then the protein for that channel will be defected and will be incapable to function properly; for example, in myotonia, there is delayed muscle relaxation after voluntary contraction. The abnormal  $Na^+$  channels are not able to deactivate, thus initiating repeated membrane depolarizations and resultant muscle contractions. Similarly, abnormality of the  $K^+$  and  $Ca^{2+}$  channels in the brain can cause epilepsy. The repeated nerve firings result in convulsions and fits, known as epileptic seizures [36]. Generally, the cell repolarization is effected due to a defect in the voltage-gated ion channels such as  $K^+$ ,  $Ca^{2+}$ ,  $Cl^-$ , and  $Na^+$ . Similarly, any impediment in the Nav can lead to hyperkalemic periodic

paralysis [36, 37]. Stress, alarm, or strenuous activity can stimulate paramyotonia congenital (PC), potassium-aggravated myotonia (PAM), generalized epilepsy with febrile seizures plus (GEFS+), and episodic ataxia (EA), marked by acute bouts of extreme discoordination with or without myokymia [36, 37]. Similarly, familial hemiplegic migraine (FHM) and spinocerebellar ataxia are due to mutation in one or more of the 10 different genes encoding the potassium channels, which also causes a ventricular arrhythmia syndrome called the Long QT syndrome. This mutation ultimately affects the cardiac repolarization [38]. Another type of ventricular arrhythmia is caused by the mutations in genes coding for the voltage-gated sodium channels, and is known as the Brugada syndrome. Likewise, a mutation in the CFTR gene, which encodes for the chloride channel, causes cystic fibrosis [39].

Defect in the transient receptor potential cation channel, mucolipin subfamily (TRPML1) channel, due to a mutation in any of its genes results in mucopolipidosis type IV [34, 40, 41]. Some very vital events occur in the cancer cells due to the mutations and overexpression of genes encoding the ion channels; for example, glioblastoma multiform is marked by an increase in the number of receptors for glioma big potassium (gBK) channels and the CIC-3 chloride channels enabling the glioblastoma cells to move within the brain causing the diffuse growth patterns of these tumors.

## Author details

Kaneez Fatima Shad<sup>1\*</sup>, Saad Salman<sup>2,3</sup>, Saifullah Afridi<sup>3,4</sup>, Muniba Tariq<sup>3</sup> and Sajid Asghar<sup>2</sup>

\*Address all correspondence to: [ftmshad@gmail.com](mailto:ftmshad@gmail.com)

1 University of Technology Sydney, Sydney, Australia

2 Government College University, Faisalabad, Pakistan

3 The University of Lahore, Islamabad, Pakistan

4 Centre for Advanced Drug Research (CADR), COMSATS Institute of Information Technology (CIIT), Abbottabad, Pakistan

## References

- [1] Hodgkin AL, Huxley AF. Action potentials recorded from inside a nerve fibre. *Nature*. 1939;**144**:710
- [2] Hodgkin AL, Huxley AF. A quantitative description of membrane current and its application to conduction and excitation in nerve. *The Journal of Physiology*. 1952;**117**:500-544
- [3] Neher E, Sakmann B. Single-channel currents recorded from membrane of denervated frog muscle fibres. *Nature*. 1976;**260**:799
- [4] Neher E, Sakmann B, Steinbach JH. The extracellular patch clamp: A method for resolving currents through individual open channels in biological membranes. *Pflügers Archiv*. 1978;**375**:219-228

- [5] Agre P, King LS, Yasui M, Guggino WB, Ottersen OP, Fujiyoshi Y, et al. Aquaporin water channels—from atomic structure to clinical medicine. *The Journal of Physiology*. 2002;**542**:3-16
- [6] Mackinnon R. Determination of the subunit stoichiometry of a voltage-activated potassium channel. *Nature*. 1991;**350**:232
- [7] Voss-Andreae J. Protein sculptures: Life's building blocks inspire art. *Leonardo*. 2005;**38**:41-45
- [8] Voss-Andreae J. Quantum sculpture: Art inspired by the deeper nature of reality. In: *Aesthetics of Interdisciplinarity: Art and Mathematics*. Basel, Switzerland: Springer; 2017
- [9] Nusser Z. Creating diverse synapses from the same molecules. *Current Opinion in Neurobiology*. 2018;**51**:8-15
- [10] Stewart MG, Popov VI, Kraev IV, Medvedev N, Davies HA. Structure and Complexity of the Synapse and Dendritic Spine. *The Synapse*. Cambridge, Massachusetts, United States: Elsevier; 2014
- [11] Ashery U, Bielopolski N, Lavi A, Barak B, Michaeli L, Ben-Simon Y, et al. The Molecular Mechanisms Underlying Synaptic Transmission: A View of the Presynaptic Terminal. *The Synapse*. Cambridge, Massachusetts, United States: Elsevier; 2014
- [12] Raghavachari S, Lisman J. *Synaptic Transmission: Models*; 2009
- [13] Whalley K. Synaptic building blocks. *Nature Reviews Neuroscience*. 2018;**1**:388-389
- [14] Burch A, Tao-Cheng JH, Dosemeci A. A novel synaptic junction preparation for the identification and characterization of cleft proteins. *PLoS One*. 2017;**12**:e0174895
- [15] Lewis S. Synaptic transmission: A hare as well as a tortoise. *Nature Reviews Neuroscience*. 2018;**19**:183
- [16] Ohtaka-Maruyama C, Okamoto M, Endo K, Oshima M, Kaneko N, Yura K, et al. Synaptic transmission from subplate neurons controls radial migration of neocortical neurons. *Science*. 2018;**360**:313-317
- [17] Cervera J, Pietak A, Levin M, Mafe S. Bioelectrical coupling in multicellular domains regulated by gap junctions: A conceptual approach. *Bioelectrochemistry*. 2018;**123**:45-61
- [18] Li Y, Wang S, He G, Wu H, Pan F, Jiang Z. Facilitated transport of small molecules and ions for energy-efficient membranes. *Chemical Society Reviews*. 2015;**44**:103-118
- [19] Mandala V, Gelenter MD, Hong M. Transport-relevant protein conformational dynamics and water dynamics on multiple timescales in an archetypal proton channel—insights from solid-state NMR. *Journal of the American Chemical Society*. 2018;**140**:1514-1524
- [20] Tu YH, Cooper AJ, Teng B, Chang RB, Artiga DJ, Turner HN, et al. An evolutionarily conserved gene family encodes proton-selective ion channels. *Science*. 2018;**359**:1047-1050

- [21] Oyrer J, Maljevic S, Scheffer IE, Berkovic SF, Petrou S, Reid CA. Ion channels in genetic epilepsy: From genes and mechanisms to disease-targeted therapies. *Pharmacological Reviews*. 2018;**70**:142-173
- [22] Gabashvili IS, Sokolowski BH, Morton CC, Giersch AB. Ion channel gene expression in the inner ear. *Journal of the Association for Research in Otolaryngology*. 2007;**8**:305-328
- [23] Zdebik AA, Wangemann P, Jentsch TJ. Potassium ion movement in the inner ear: Insights from genetic disease and mouse models. *Physiology*. 2009;**24**:307-316
- [24] Zhang AH, Sharma G, Undheim EA, Jia X, Mobli M. A complicated complex: Ion channels, voltage sensing, cell membranes and peptide inhibitors. *Neuroscience Letters*. 2018;**679**:35-47
- [25] Brenowitz S, Duguid I, Kammermeier PJ. *Ion Channels: History, Diversity, and Impact*. Cold Spring Harbor Protocols; New York, United States. 2017. pdb. top092288
- [26] Dreyer I, Müller-Röber B, Köhler B. Voltage-gated ion channels. *Annual Plant Reviews*. 2004;**15**:169-215
- [27] Tikhonov DB, Zhorov BS. *3D Structures and Molecular Evolution of Ion Channels. Evolutionary Physiology and Biochemistry-Advances and Perspectives*. London, United Kingdom: InTech; 2018
- [28] Collingridge GL, Olsen RW, Peters J, Spedding MA. Nomenclature for ligand-gated ion channels. *Neuropharmacology*. 2009;**56**:2-5
- [29] Maathuis F. Ligand-gated ion channels. *Annual Plant Reviews*. 2018;**15**:216-246
- [30] Lev B, Murail S, Poitevin F, Cromer BA, Baaden M, Delarue M, Allen TW. String method solution of the gating pathways for a pentameric ligand-gated ion channel. In: *Proceedings of the National Academy of Sciences*. 2017b;**114**:E4158-E4167
- [31] Lev B, Murail S, Poitevin F, Cromer BA, Baaden M, Delarue M, Allen TW. Gating pathways for a pentameric ligand-gated ion channel solved by atomistic string method simulations. *Biophysical Journal*. 2017a;**112**:475a
- [32] Hu H, Nemečz À, Renterghem CV, Fourati Z, Sauguet L, Corringer PJ, Delarue M. Crystal structures of a pentameric ion channel gated by alkaline pH show a widely open pore and identify a cavity for modulation. In: *Proceedings of the National Academy of Sciences*. 2018;**115**:E3959-E3968
- [33] Sauguet L, Shahsavari A, Poitevin F, Huon C, Menny A, Nemečz À, Changeux JP, Corringer PJ, Delarue M. Crystal structures of a pentameric ligand-gated ion channel provide a mechanism for activation. In: *Proceedings of the National Academy of Sciences*. 2014;**111**:966-971
- [34] Caterina MJ. *An Introduction to Transient Receptor Potential Ion Channels and Their Roles in Disease. TRP Channels As Therapeutic Targets*. New York, United States: Elsevier; 2015

- [35] Zorina-Lichtenwalter K, Parisien M, Diatchenko L. Genetic studies of human neuropathic pain conditions: A review. *Pain*. 2018;**159**:583
- [36] Millichap JJ, Cooper EC. KCNQ2 potassium channel epileptic encephalopathy syndrome: Divorce of an electro-mechanical couple? *Epilepsy Currents*. 2012;**12**:150-152
- [37] Horvath GA, Demos M, Shyr C, Matthews A, Zhang L, Race S, et al. Secondary neurotransmitter deficiencies in epilepsy caused by voltage-gated sodium channelopathies: A potential treatment target? *Molecular Genetics and Metabolism*. 2016;**117**:42-48
- [38] Lolicato M, Arrigoni C, Mori T, Sekioka Y, Bryant C, Clark KA, et al. K2P2. 1 (TREK-1)-activator complexes reveal a cryptic selectivity filter binding site. *Biophysical Journal*. 2018;**114**:303a-304a
- [39] Themistocleous AC, Ramirez JD, Serra J, Bennett DL. The clinical approach to small fibre neuropathy and painful channelopathy. *Practical Neurology*. 2014;**14**:368-379
- [40] Sexton JE, Cox JJ, Zhao J, Wood JN. The genetics of pain: Implications for therapeutics. *Annual Review of Pharmacology and Toxicology*. 2018;**58**:123-142
- [41] Spillane J, Kullmann D, Hanna M. Genetic neurological channelopathies: Molecular genetics and clinical phenotypes. *The Journal of Neurology, Neurosurgery, and Psychiatry*. 2016;**87**:37-48

---

## Monovalent Cations

---





---

# Voltage-Gated Sodium Channels in Drug Discovery

---

Tianbo Li and Jun Chen

Additional information is available at the end of the chapter

<http://dx.doi.org/10.5772/intechopen.78256>

---

## Abstract

Voltage-gated sodium channels (Nav) control the initiation and propagation of action potential, and thus mediate a broad spectrum of physiological processes, including central and peripheral nervous systems' function, skeletal muscle contraction, and heart rhythm. Recent advances in elucidating the molecular basis of channelopathies implicating Nav channels are the most appealing druggable targets for pain and many other pathology conditions. This chapter overviews Nav super family from genetic evolution, distribution, human diseases/pathology association, highlighting the most recent structure function breakthrough. The second section will discuss current small and large Nav modulators, including traditional nonselective pore blockers, intracellular modulators, and extracellular modulators.

**Keywords:** voltage-gated sodium channel, Nav1.7, drug discovery

---

## 1. Introduction

Voltage-gated sodium channels (Nav) are large transmembrane proteins that conduct the flow of sodium ions down the electrochemical gradient through cell membranes. In excitable and nonexcitable cells, these channels control action potential initiation/propagation, cell motility, and proliferation. Na<sup>+</sup> currents were firstly discovered in 1949 by Hodgkin and Huxley in their study of action potentials in squid giant axon [1, 2]. This early work demonstrated that the resting membrane potential mostly depends on potassium permeability, whereas action potential is directly shaped by sodium permeability, which allows transient influx of Na<sup>+</sup> to raise membrane potentials and is followed by rapid inactivation within milliseconds. From 1950s to 1970s, studies from many laboratories established conceptual models and equations conceptualizing sodium channel function [3].

---

### 1.1. Membrane potential, Nernst and Goldman equations

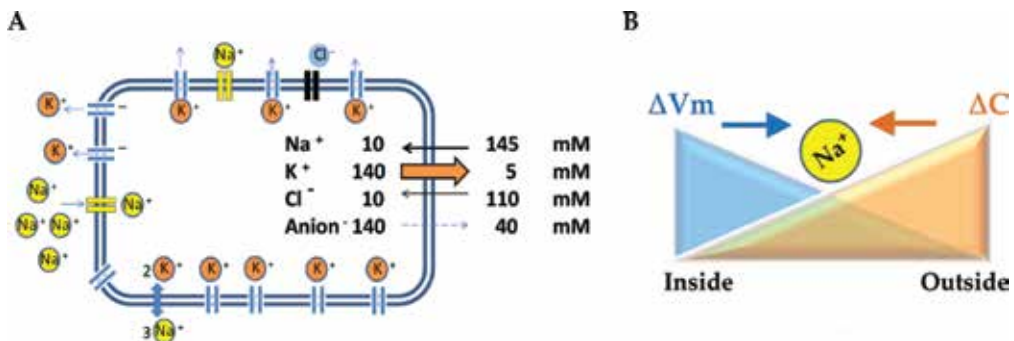
In a typical cell, sodium, potassium, chloride, and other membrane permeable ions are in unequal distribution across plasma membrane, **Figure 1A**. This unequal distribution and its resultant electrical gradient can be explained by Donnan equilibrium. For a specific ion, the electrical potential difference that exactly counterbalances diffusion due to the concentration difference is called the equilibrium potential for that specific ion. To use  $\text{Na}^+$  as an example, at equilibrium, the chemical force moving  $\text{Na}^+$  into the cell is balanced by the electrical force moving  $\text{Na}^+$  out of the cell (**Figure 1B**).

For each ion, the equilibrium (or reversal) potential,  $E_{ion}$ , can be calculated by the Nernst equation (Eq. (1)), where  $R$  = gas constant,  $8.135 \text{ J K}^{-1} \text{ mol}^{-1}$ ;  $T$  = temperature in K ( $273 + \text{temp}$  in  $^{\circ}\text{C}$ );  $z$  = valency of ion ( $\text{Na}^+ = 1$ ,  $\text{Ca}^{2+} = 2$ , and  $\text{Cl}^- = -1$ );  $F$  = Faraday's constant,  $9.684 \times 10^4 \text{ C mol}^{-1}$ . In a typical mammalian neuron with  $[\text{Na}^+]$ ,  $[\text{K}^+]$ , and  $[\text{Cl}^-]$  described in **Figure 1A**, based on Nernst equation, we can calculate  $E_{\text{Na}} = 67 \text{ mV}$ ,  $E_{\text{K}} = -83 \text{ mV}$ , and  $E_{\text{Cl}} = -61 \text{ mV}$ . In cell resting state, the experimental measured membrane potential  $E_m = -65 \text{ mV}$ . As indicated in **Figure 2**,  $\text{Na}^+$  has a tendency to flow into the cell due to  $E_m < E_{\text{Na}}$ , while  $\text{K}^+$  flow out of the cell ( $E_m > E_{\text{K}}$ ), and  $\text{Cl}^-$  near equilibrium ( $E_m \approx E_{\text{Cl}}$ ). These concentration and electrical gradients are maintained by the dynamic equilibrium of ion channels and active ion transporters, most importantly by sodium pump (Na/K-ATPase).

$$E_{ion} = \frac{RT}{zF} \ln \frac{[Ion]_{out}}{[Ion]_{in}} \quad (1)$$

$$= 58.2 \text{Log}_{10} \frac{[Ion]_{out}}{[Ion]_{in}} \quad (\text{when at } 20^{\circ}\text{C})$$

The whole cell membrane potential  $E_m$  can be calculated by all permeable ions' equilibrium potentials  $E_{ion}$  and their relative permeability  $P$ , which is described by Goldman-Hodgkin-Katz equation (GHK equation) (Eq. (2)). This equation explained the experimental finding that resting membrane potential is more depending on  $P_{\text{K}}$ , which is about 25-folds to  $P_{\text{Na}}$ .



**Figure 1.** (A) Unequal distribution of ions in a typical mammalian neuron and (B) Donnan equilibrium scheme shows that the balance of concentration gradient and electrical gradient drives  $\text{Na}^+$  movement toward inside or outside of the cell.

$$E_m = \frac{RT}{F} \ln \left( \frac{P_K[K^+]_{out} + P_{Na}[Na^+]_{out} + P_{Cl}[Cl^-]_{in}}{P_K[K^+]_{in} + P_{Na}[Na^+]_{in} + P_{Cl}[Cl^-]_{out}} \right) \quad (2)$$

$$= 58.2 \text{Log}_{10} \left( \frac{P_K[K^+]_{out} + P_{Na}[Na^+]_{out} + P_{Cl}[Cl^-]_{in}}{P_K[K^+]_{in} + P_{Na}[Na^+]_{in} + P_{Cl}[Cl^-]_{out}} \right) \quad (\text{when at } 20^\circ \text{C})$$

## 1.2. Hodgkin-Huxley model

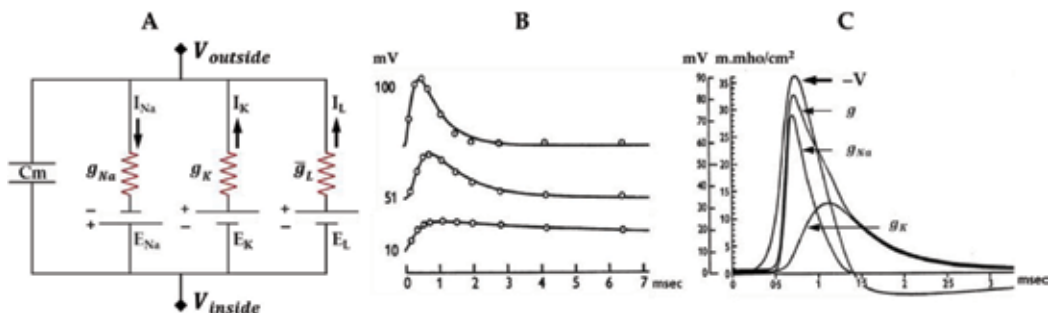
The Hodgkin-Huxley model describes how action potentials in neurons are initiated and propagated [4]. Originally developed to fit action potential dynamics of squid giant axon, this model has been successfully applied to a wide range of neurons. It describes the electrical properties of excitable membranes as typical electrical circuit components. For instance, the cell membrane is modeled as a capacitor with capacitance ( $C_m$ ) and ion channels are resistors with conductance of Na channel ( $g_{Na}$ ), K channel ( $g_K$ ), and leak channel ( $\bar{g}_L$ ).

From Hodgkin-Huxley model, the total cell membrane current,  $I$ , can be calculated by Eq. (4), where membrane potential  $V_m$ , ion conductances  $g_{Na}$  and  $g_K$ , sodium activation variable  $m$ , sodium inactivation variable  $h$ , potassium activation variable  $n$  are variable functions of time, whereas  $E_{Na}$ ,  $E_K$ ,  $E_L$ ,  $C_m$ , and  $\bar{g}_L$  are constants.

$$g_{Na} = \bar{g}_{Na} m^3 h_0 \left[ 1 - \exp \left( -\frac{t}{\tau_m} \right) \right]^3 \exp \left( -\frac{t}{\tau_h} \right) \quad (3)$$

$$I = C_m \frac{dV_m}{dt} + g_{Na} m^3 h (V_m - V_{Na}) + g_K n^4 (V_m - V_K) + g_L (V_m - V_L) \quad (4)$$

Hodgkin-Huxley model provides a relatively simple and experimentally testable equation to deduce  $Na^+$  conductance change with time and voltages (**Figure 2B**), and nerve action potential (**Figure 2C**). It also embodies the three key features of Nav channels: voltage-dependent activation (submillisecond scale), rapid inactivation (millisecond scale), and selective  $Na^+$  conductance.

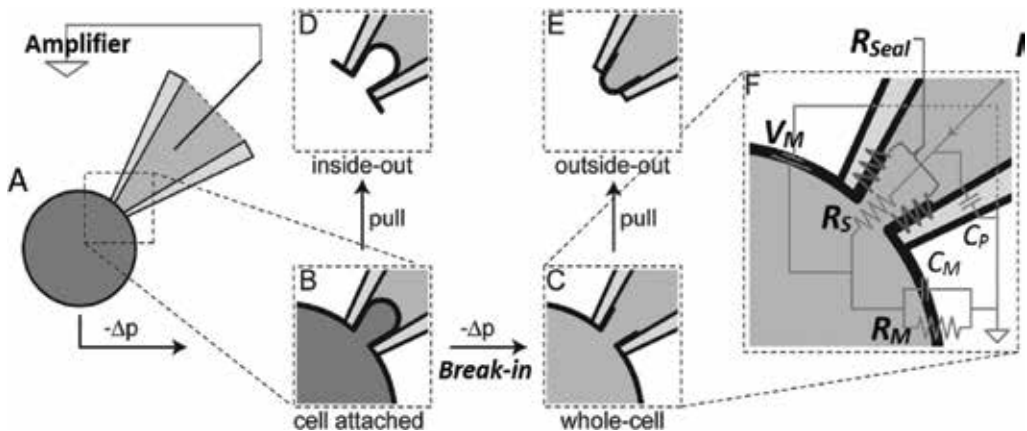


**Figure 2.** (A) Hodgkin-Huxley model, modified from Wikipedia. (B) Changes of sodium conductance associated with different depolarization voltages at 10, 51, and 100 mV. The circles are experimental sodium conductance, and the smooth curves are theoretical curves. (C) Calculated  $g_{Na}$ ,  $g_K$  components of total membrane conductance ( $g$ ) during propagated action potential ( $-V$ ). Modified from [4].

### 1.3. History and basic concepts of electrophysiology

Electrophysiology was originated by Luigi Galvani in studying “animal electricity” in 1780s. In 1903, an extracellular recording technique, electrocardiography, was invented by Willem Einthoven (1924 Nobel Laureate); in 1952, intracellular recording technique was developed by Alan Hodgkin and Andrew Huxley (1963 Nobel Laureates); and in 1976, Erwin Neher and Bert Sackmann (1991 Noble Laureates) succeeded in measuring the ionic current of single channels in the cell membrane by developing patch clamp technique. These works were fundamental in revealing the physiological function of ion channels. Since then, the field of electrophysiology had undergone rapid evolution, especially after the introduction of automated patch clamp in the early 2000s.

Manual patch clamp technique employs glass microelectrode(s) with desired filling solution and tip diameter to perform either voltage or current clamp. For larger cells, such as *Xenopus* oocytes, two-electrode voltage clamp (TEVC) is performed using two electrodes: one to measure membrane potential and the other to apply the current, with each tip diameter  $<1\ \mu\text{m}$  resulting in 10–100 M $\Omega$  resistances. For most other circumstances, a single electrode with an open tip diameter 1–3  $\mu\text{m}$  (1–3 M $\Omega$  resistances) is used for whole cells or small patches of cell membrane recording. A typical patch-clamp recording starts with cell attaching procedures including: placing glass tip next to a cell, using gentle suction, drawing a piece of the cell membrane to the microelectrode tip, and then letting glass tip to form a high-resistance seal with the cell membrane (ideally  $>1\text{G}\Omega$ , so-called “gigaseal”). By applying different following-up manipulations, the patch-clamp can be achieved in four configurations: cell-attached patch, whole-cell patch, inside-out patch, and outside-out patch, as shown in **Figure 3**.



**Figure 3.** Manual patch clamp configurations and procedures. After a cell is approached by a pipette (A), a high-resistance seal is achieved through application of negative pressure, resulting in the cell-attached configuration (B). Further application of negative pressure ruptures the membrane, resulting in the whole-cell configuration, i.e., electrical contact with the inside of the cell (C). Inside-out and outside-out configurations are achieved by pulling the pipette away from the cell (D and E). (F) An equivalent electrical circuit of a cell in whole-cell configuration during acquisition of data.  $V_M$  = membrane potential,  $I$  = whole current,  $R_{Seal}$  = seal resistance,  $R_S$  = series resistance,  $R_M$  = membrane resistance,  $C_P$  = pipette capacitance,  $C_M$  = membrane capacitance. Modified from [5].

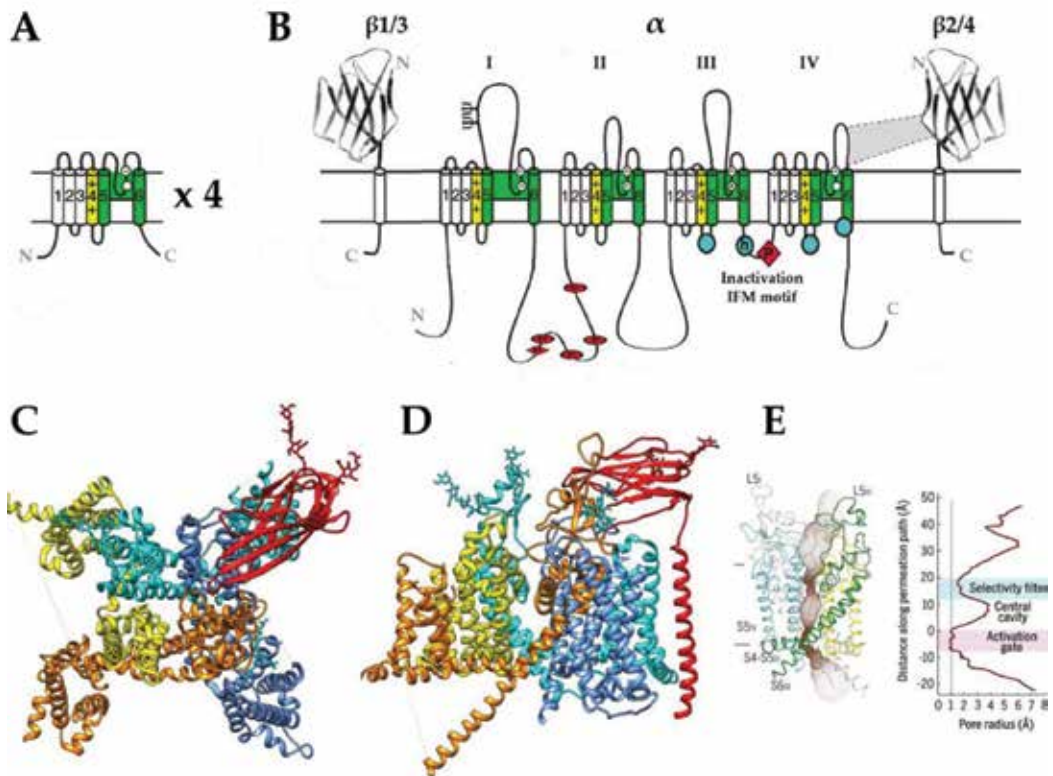
Many other electrophysiological techniques have been developed for various applications, including extracellular recordings such as electroencephalography (EEG), electrocardiography (ECG or EKG), and electromyography (EMG) for clinical diagnosis; artificial lipid bilayer recording for studying activities of reconstituted ion channel proteins; automated patch clamp recording to enable high-throughput recordings; and optogenetics to employ light to switch on and off ion channel activities. The technology evolution has brought the ion channel research and drug discovery to a new era, which will be discussed in later part of this chapter.

## 2. Nav channel general physiology

Nav channels were the first ion channel family discovered back in 1952 [1, 4] and cloned in 1984 [6]. Its pedigree spans across prokaryotic and eukaryotic kingdoms [7]. To date, ~500 Nav channels from bacteria (BacNavs) [8–10], and even more Nav channels from other species including fly [11], jellyfish [8], electric eel [12], cockroach [13], teleost fishes [8], and mammals have been cloned [14]. The BacNavs regulate the survival response to extreme pH, electrophiles, and hypoosmotic shock. Despite their markedly difference in physiology function, voltage dependence and kinetics, BacNavs share common features of mammalian Nav channels, thus serving as surrogates in the study of molecular evolution and channel architecture. Eukaryotic Navs display ultrafast kinetics, with milliseconds activation to inactivation, and high sodium ion selectivity,  $\text{Na}^+$  (1):  $\text{K}^+$  (0.14):  $\text{Rb}^+$  (0.02):  $\text{Cs}^+$  (0.005), which together enable them being responsible to initiate and transduce fast action potential firing in the vast electrical signaling pathways throughout the cardiovascular and nervous systems.

Nav family belongs to the voltage-gated ion channel (VGIC) superfamily, with less intrafamily variation comparing to the other two VGIC families, voltage-gated potassium channels (Kvs) and voltage-gated calcium channels (Cavs). The core functional unit of Nav channel is a tetrameric complex composed of four homologous domains (DI/II/III/IV), with each domain containing six transmembrane segments (S1–S6), an intracellular N-terminus and C-terminus. The first four transmembrane segments form a voltage-sensing domain (VSD) and the last two form the pore domain (PD). The central PD is responsible for ion-transduction through the structural top funnel, selectivity filter and gate, and all other domains are served as regulatory modlues for activation, fast and slow inactivation, albeit with different natures and structures.

Each eukaryotic Nav channel is composed of a single macromolecular  $\alpha$  subunit (~2000 amino acid residues, ~260 kDa), forming a pseudoheterotetrameric core functional unit, in association with one or more auxiliary  $\beta$  subunits ( $\beta 1$ ,  $\beta 2$ ,  $\beta 3$ , and/or  $\beta 4$ , ~35 kDa) [15] (**Figure 4**). While the prokaryotic Navs are formed by four separate  $\alpha$  subunit, similar to Kv channels, representing a simpler construction than eukaryotic Navs. A typical Nav channel has at least three distinct states, resting (closed), activated (open), inactivated (closed), which itself includes fast-inactivated (within milliseconds) and slow-inactivated (seconds), and recovering from inactivation (repriming), which is a period in which the channel is not available to open in response to a depolarization. Each Nav channel can be characterized by these different



**Figure 4.** Structures of voltage-gated sodium channels. Modified from [12, 15]. (A) Schematic representation of BacNav. (B) Schematic representation of eukaryotic Navs. (C and D) The top and side views of the cryo-EM structure of EeNav1.4- $\beta 1$  complex (PDB 5XSY). The  $\alpha$ -subunit domains DI-IV are colored orange, yellow, cyan, and blue, respectively, and the  $\beta 1$  subunit is colored red. (E) The pore domain sodium permeation path including selectivity filter, central cavity, and intracellular activation gate are colored in brown and annotated with pore radius.

voltage-dependent biophysiological properties, and pharmacological properties according to its expression pattern and modulation.

In human, there are 9 Nav channels (Nav1.1-1.9), which are encoded by the genes SCN1A, SCN2A, SCN3A, SCN4A, SCN5A, SCN8A, SCN9A, SCN10A, and SCN11A, respectively. A tenth isoform, Navx, is considered as atypical, as it contains key difference in DI/III/IV S4 VSDs and DIII-IV inactivation linker, also it is activated by augmentation of extracellular sodium (over 150 mM) instead of voltage. Thus, Navx was classified as a different Nav subfamily (type 2) [16, 17]. Based on the timeline of gene cloning, each  $\alpha$  subunit gene was assigned as SCN1A to SCN11A, and likewise, auxiliary  $\beta$  subunit genes were assigned as SCN1B to SCN4B, respectively (Table 1).

Due to their fundamental role in regulating central and peripheral nervous systems function, skeletal muscle contraction and heart rhythm, much of the early works on Navs involved characterizing their expression patterns, biophysiological properties, structure-function, and molecular pharmacology.

hNav isoform	Gene	Variant(s)	Human chromosome locus	UniProt	Homology*	TTX IC <sub>50</sub> (nM)	Primary tissue location	Therapeutic relevance
<b>Nine voltage-gated <math>\alpha</math> subunits</b>								
Nav1.1	SCN1A	3	2q24	P35498	90.0%	6	CNS, PNS	Epilepsy
Nav1.2	SCN2A	2	2q23–24	Q99250	90.8%	12	CNS, glia	Epilepsy, autism
Nav1.3	SCN3A	4	2q24	Q9NY46	90.0%	4	CNS, glia	Epilepsy
Nav1.4	SCN4A	1	17q23–25	P35499	76.8%	5	Skeletal muscle	Myotonia
Nav1.5	SCN5A	6	3p21	Q14524	79.4%	2000	Cardiac muscle	Cardiac rhythm disorders
Nav1.6	SCN8A	5	12q13	Q9UQD0	85.9%	1	CNS, PNS, glia	Ataxia, motor neuron disease
Nav1.7	SCN9A	4	2q24	Q15858	100%	4	Sensory neurons	Pain
Nav1.8	SCN10A	1	3p21–24	Q9Y5Y9	77.0%	60,000	Sensory neurons	Pain
Nav1.9	SCN11A	3	3p21–24	Q9UI33	70.4%	40,000	Sensory neurons	Pain
<b>One nonvoltage-gated <math>\alpha</math> subunits</b>								
Navx	SCN7A**	1	2p21-23	Q01118	71.2%		PNS, DRG, epithelia	
<b>Four <math>\beta</math> subunits</b>								
Nav $\beta$ 1	SCN1B	2	19q13	Q07699	100%		CNS, PNS, muscle	Epilepsy
Nav $\beta$ 2	SCN2B	1	11q23	O60939	53.1%		CNS	
Nav $\beta$ 3	SCN3B	1	11q23	Q9NY72	72.0%		CNS	
Nav $\beta$ 4	SCN4B	3	11q23	Q8IWT1	57.9%		CNS, thyroid	

Data from Universal Protein Resource (UniProt, <http://www.uniprot.org>).

\* $\alpha$ -subunit homology is calculated as the similarity between the most abundant isoform variant to Nav1.7 variant 3, which is the canonical sequence and position reference.

\*\*SCN6A and SCN7A are orthologs of a single atypical Nav gene (SCN7A in mouse, the same gene was denoted as SCN6A in human).

**Table 1.** Human Nav channel subunits' gene information.

## 2.1. Genetic evolution and expression

Compared to Cav and Kv channel family, the rise of Nav family is relatively recent [18]. The study of intron/exon organization suggested that Navs were evolved from the similarly structured Cav channels. This is supported by the finding that the four domains of Navs have higher similarity to their corresponding domains in the Cav channels than to each other. The ancestral Navs and Cavs genes might have evolved by two rounds of gene duplication, i.e., from an ancestral, single-domain Kv-like gene to a two-domain protein, then from a two-domain protein to a four-domain protein. This hypothesis is also in line with the observation that among the four domains of Navs, DI shares higher similarity with DIII, and DII shares higher similarity to DIV [19].

In choanoflagellate (the sister group of animals), the rapid long-distance communication among excitable cells is achieved at the emergence of Metazoa (represented by bilaterian animals and cnidarians) through the use of Nav channel [20, 21]. The gene organization, biophysical, and pharmacological properties of invertebrate sodium channels are largely similar to their mammalian counterparts, suggesting that the primordial Nav channels were established before the evolutionary separation of the invertebrates from the vertebrates, and evolution of Navs played a critical role in the emergence of nervous systems in animals [19, 22]. Of note, sodium selectivity might be acquired independently in BacNav and mammalian Nav channels as indicated by phylogenetic analysis [23]. Therefore, BacNav channels can serve as models for studying Navs structure function, but evolutionary variation should be taken into consideration.

Historically, the tissue distribution of mammalian Nav isoforms was obtained by methods such as quantitative PCR, expressed sequence tag (EST) profiling, and pharmacology study using isoform selective toxins. The more precise expression data were recently obtained by microarray [24, 25] and mRNA sequencing from Genotype-Tissue Expression (GTEx) project [26] (**Figure 5**). Now, we know that Nav1.1, Nav1.2, and Nav1.3 are predominantly expressed in central nervous system (CNS). Nav1.1 is the predominant channel in the caudal regions and the spinal cord, though relatively low-level expression of Nav1.1 has been shown in the peripheral nervous system (PNS). Nav1.2 is the highest expression isoform in the rostral regions. Nav1.3 peaks at birth but remains detectable at a lower level in adulthood. Interestingly, all of these CNS-enriched isoforms are sensitive to tetrodotoxin (TTX) at nanomolar concentrations, and their genes are clustered on chromosome 2 in both mice and humans.

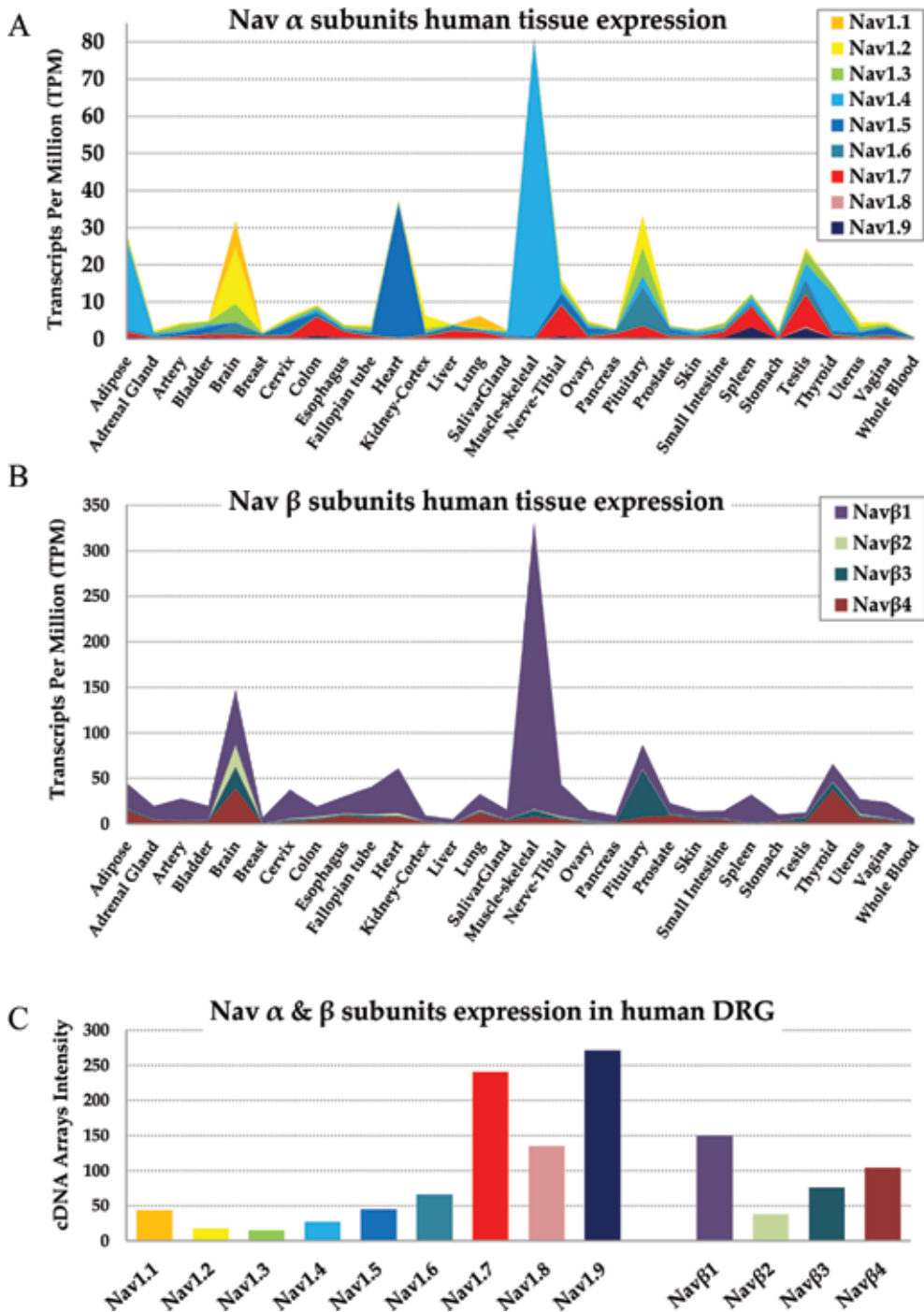
Nav1.4 and Nav1.5 exhibit strikingly high-level expression in muscle and heart, respectively. More sensitive approaches have detected Nav1.5 in the piriform cortex and limbic regions of the brain but at relatively low level [27]. These two Nav isoforms can be distinguished from each other and from the CNS isoforms on the basis of toxin sensitivity. Adult skeletal muscle-enriched Nav1.4 is sensitive to TTX and  $\mu$  conotoxin GIIIA at nanomolar concentrations, while the CNS-enriched channels are only sensitive to TTX, and heart-specific Nav1.5 is resistant to TTX. In addition, Nav1.4 is inhibited by nanomolar concentrations of  $\mu$  conotoxin PIIIA, whereas Nav1.2 is approximately 15-fold less sensitive, and Nav1.7 is resistant [28–30].

Nav1.6 appears to be abundantly expressed in both PNS and CNS tissues. Nav1.7, Nav1.8, and Nav1.9 are primarily expressed in PNS, including nociceptive neurons, A $\beta$ -fibers, C-fibers, and both large and small diameter dorsal root ganglion (DRG) [31]. This PNS-specific localization of Nav1.7, Nav1.8, and Nav1.9 make them attractive targets for developing isoform selective modulators to treat many PNS-related diseases and pathologic conditions.

## 2.2. Nav channel structure-function

The core functional unit of Nav channels is  $\alpha$  subunit. Each  $\alpha$  subtype is composed of a single polypeptide chain with  $\sim$ 2000 amino acid residues forming four pseudoheteromeric domains designated as DI to DIV. Nine  $\alpha$  subunits' protein sequence homology is greater than 70% (**Table 1**). The structure complexity and high-sequence homology make it difficult to design





**Figure 5.** Sodium channel body atlas in human. (A and B) Human Nav  $\alpha$  and  $\beta$  subunits tissue expression level from GTEx RNA-seq database (<https://www.gtexportal.org>). Gene expression level is presented as averaged tissue transcripts per million (TPM) value from 570 donors' 8555 samples. (C) Nav  $\alpha$  and  $\beta$  subunits' expression level in human DRG. Gene expression level is presented as averaged cDNA microarray intensity number from 214 human DRG samples [56].

subtype-selective drugs. In 2011, the first X-ray crystal structure of bacterial *Arcobacter butzleri* Nav channels (NavAb) was determined [32]. Subsequently, structures for several BacNavs and a BacNav-human Nav chimeric channel have been resolved, representing closed [33, 34], open [34, 35], and potentially inactive states of the channels [36, 37]. In 2017, the first two eukaryotic Nav structures for American cockroach and electric eel (Ee) Nav1.4- $\beta$ 1 complex were determined by using cryogenic electron microscopy (CryoEM) [12]. Findings from crystal and cryo-EM structures are mostly consistent, and collectively provided important insights into Nav channel structure-function and structure-based drug design.

**Voltage-sensing domains (VSDs).** The S1 to S4 segments form voltage-sensing domain. There are four VSDs in a sodium channel. Each VSD is featured by repetitively occurring positively charged Lys or Arg residues at every third position in S4. These charge clusters move toward the extracellular surface upon membrane depolarization and return to their resting positions upon membrane repolarization. Each VSD is connected to an intracellular S4-S5 linker, which transfers the movement of S4 segment to the central pore domain formed by S5-S6. Thus, the outward and inward movements of S4 result in channel opening and closing, respectively. Unlike homotetrameric Kvs and BacNavs, mammalian Nav channel's four VSDs possess distinctive sequence signature, conformation, and role in channel gating [12, 13]. For examples, the four VSDs have nonconserved intra- and extracellular loops, and the different charge clusters in S4, i.e., RRRR in DI, RRRRK in DII, KRRRR in DIII, and RRRRR in DIV. Also, the S2 in each VSD also makes asymmetric functional contributions to Nav channel activation and inactivation [38].

**Pore domain (PD):** the S5 to S6 segments from the four domains of the  $\alpha$  subunits enclose the central pore of the channel. The extracellular linker connecting S5-S6 is defined as pore-loop (P-loop), which can be separated into two  $\alpha$  helices named P1 and P2. The functional entities along the ion permeation pathway in PD include the selectivity filter (SF), the central cavity, and the intracellular activation gate, as shown in **Figure 4E**.

The outer vestibule and selectivity filter are formed in P-loop reentering membrane segments, designated as P1-SF-P2 funnel. Early study by comparing Navs with Cavs found that one residue, Asp/Glu/Lys/Ala (DEKA), at the corresponding locus in the middle of P1-P2 determines  $\text{Na}^+$  selectivity [39]. Structure studies confirmed that the asymmetric selectivity filter vestibule is constituted by the side chains of the signature DEKA residues and the carbonyl oxygens atoms of the two preceding residues in each domain, Thr/Gln (DI), Cys/Gly (DII), Thr/Phe (DIII), and The/Ser (DIV). Mutational study identified an additional outer ring above the selectivity filter, Glu/Glu/Met/Asp (EEMD), which significantly interfered the tetrodotoxin (TTX) binding [40, 41]. The outer vestibule and SF structures were further discerned by using bacteria KcsA channel X-ray structure as template and guanidinium toxins (TTX and saxitoxin, STX), which successfully defined the first pharmacological relevant site on Nav channels, site 1 [42]. After that, local anesthetic binding site was determined within the four fenestrations in PD, each with distinct shape and size [13, 43]. From studying a group of activators, including batrachotoxin (BTX), veratridine (VTD), grayanotoxin (GTX), and aconitine (ACD), the neurotoxin site 2 was determined in the inner cavity of PD [44, 45].

**Activation gate:** the activation gate of Nav channels was originally predicted to be at the inner end of the pore based on the study of local anesthetics, which exhibit usage-dependent blockage [46, 47]. From thiol-modifying reagent accessibility study, a  $\sim 3.8$  Å diameter constriction formed by a ring of conserved hydrophobic residues at the end of S6 (represented as DI-V440, DII-L795, DIII-I1287, DIV-I1590 in Nav1.4 and DI-Y405, DII-F960, DIII-F1449, DIV-F1752 in Nav1.7) was found to occlude only the pore at closed state but not at open state [48]. Recent cryo-EM structures confirmed that this activation gate is located at the cytoplasmic boundary level of the membrane [12]. Channelopathy study found that Nav1.7 DII S6 L955 deletion cause F960 side change conformational change in the activation gate. This mutation produces radial shift of the channel open at 25 mV more hyperpolarizing voltage, which renders hyperexcitability of DRG neurons to cause inherited erythromelalgia (IEM) [48].

**Fast inactivation:** while the channel opening is controlled by VSD and activation gate, the fast inactivation is regulated by a highly conserved Ile/Phe/Met (IFM) motif, which is localized in an intracellular loop connecting the domain DIII and DIV [49]. The IFM motif was originally discovered as a particle segment attached to the inner end of the pore. Study showed that pronase and N-bromoacetamide removed inactivation only when applied from intracellular side [50], and acetyl-KIFMK-amide peptides restored fast inactivation [51]. In the eukaryotic EeNav1.4- $\beta 1$  structure at open and resting states, the LFM motif (equivalent to IFM) in DIII-IV linker is plugged into the corner enclosed by the outer S4-S5 and inner S6 segments in DIII and DIV. Once the channel opens, the LFM motif acts as a hinged lid and folds into the intracellular mouth of the open pore to produce fast inactivation.

**Slow inactivation:** in contrast to fast inactivation (milliseconds scale), slow inactivation occurs in seconds during prolonged depolarization or rapid repetitive stimulations. Slow inactivation determines channel availability for action potential generation; thus, it endows neuronal tissues with memory of previous excitation, prevents excitation of skeletal muscle by mild hyperkalemia, and affects the conduction velocity and excitability of cardiac tissue. For the cardiac Nav1.5 channel, two putative proton sensor residuals in P-loop, C373 and H880, were responsible of tissue-acidification-induced slow inactivation underlying cardiac arrhythmia [52]. Other mutations, including DII S4-S5 linker L689I in Nav1.4, DII S6 Del-L955 in Nav1.7, have also been identified to impair slow inactivation, causing hyperkalemic periodic paralysis and inherited erythromelalgia, respectively [53, 54]. Voltage-clamp fluorimetry (VCF) study of Nav1.4 channels showed that that immobilization of DI and DII VSDs is involved in the development of slow inactivation, while DIII VSD is involved in the recovery from slow inactivation [55]. However, the structural basis for slow inactivation remains undefined.

### 2.3. Nav $\beta$ subunits

In vertebrates, five Nav auxiliary  $\beta$  subunits,  $\beta 1$ ,  $\beta 1B$ ,  $\beta 2$ ,  $\beta 3$ , and  $\beta 4$ , have been identified (SCN1B to SCN4B), with molecular weight ranging from 30 to 40 kD (Table 1) [57–60]. In invertebrates, auxiliary subunits such as tipE and Vssc  $\beta$  in drosophila bear no homology to vertebrate  $\beta$  subunits, suggesting a separate evolutionary pathway [61–63]. All  $\beta$  subunits comprise an amino terminal immunoglobulin (Ig) domain, a single transmembrane (TM)

segment, and an intracellular carboxyl-terminal, except for  $\beta$  1B (previously named  $\beta$ 1A), which is a  $\beta$ 1 splice variant that lacks TM segment [64].  $\beta$ 1 and  $\beta$ 3 interact with  $\alpha$  subunit noncovalently, whereas  $\beta$ 2 and  $\beta$ 4 bind to the  $\alpha$  subunit via a disulfide bond. All  $\beta$  isoforms are expressed in CNS, PNS, and cardiovascular systems, including excitable and nonexcitable cells, where they are part of the V-set immunoglobulin superfamily of cell adhesion molecules facilitating cell adhesion and cell migration.  $\beta$ 1 is highly expressed in skeletal and cardiac muscles, and the expression patterns of all  $\beta$  isoforms vary during development [65].  $\beta$  subunits play broad role in modulating Nav function. They regulate expression and membrane trafficking of  $\alpha$  subunits, modulate channel activation and inactivation, and interfere with toxin binding [66–68].

In 2017, the cryo-EM structure for EeNav1.4 in complex with the  $\beta$ 1 subunit was determined [12]. This structure provided a first glimpse into the interaction between  $\alpha$  and  $\beta$  subunits. The  $\beta$ 1 subunit interacts with the  $\alpha$  subunits as an ax, wherein its TM interacts with VSDIII within the membrane as the handle, while its Ig domain as the head interacts with DI-L5 and DIV-L6 extracellular loops and the intervening segment between DIII S1 and S2 (**Figure 4C and D**). Mutations in  $\beta$  subunits have been linked to many human diseases, including epilepsy, and cardiac arrhythmia, and sudden death syndromes. Although  $\beta$  subunit-specific drugs have not yet been developed, the Nav  $\beta$  subunit family remains a potential therapeutic target [68].

### 3. Channelopathy and therapeutic relevance

Nav channels are fundamentally important in a broad spectrum of physiological processes. Not surprisingly, genetic mutations of Nav channels result in many debilitating to severe phenotypes in CNS, PNS, cardiac, and neuromuscular systems. To date, at least ~50 human diseases have been attributed to aberrant activities of Nav channels; and hundreds of diseased related mutations of  $\alpha$  and the  $\beta$  subunits have been identified. These mutations lead to channel dysfunctions called channelopathies (summarized in **Table 2**) and suggest the disease association of respective channels.

#### 3.1. Pain

Nav1.7, 1.8, and 1.9 are highly expressed in sensory neurons. They control the excitability of nociceptive neurons, and thus are considered as therapeutic targets for pain relief [31, 71–74]. Among them, Nav1.7 was the first gene linked to human pain. In 2004, two missense mutations, I848T and L858H in SCN9A (Nav1.7), were associated with edema, redness, warmth, and bilateral pain in human inherited erythromelalgia (IEM) patients [75]. In 2006, three nonsense mutations, S459X, I767X, and W897X, were identified in congenital insensitivity to pain (CIP) patients [76]. Since then, additional gain-of-function mutations are associated with IEM, paroxysmal extreme pain disorder (PEPD), small fiber neuropathy (SFN), and additional loss-of-function mutations that are associated with CIP (**Figure 6**). The mechanism underlying these conditions was unraveled by characterizing biophysical properties of disease mutations

<b>Isoform</b>	<b>Channelopathies</b>	<b>Discovered mutant number</b>	<b>Discovery publication number</b>	
SCN1A	GEFS+2	Generalized epilepsy with febrile seizures plus 2	37	30
	EIEE6	Epileptic encephalopathy, early infantile, 6	317	41
	ICEGTC	Intractable childhood epilepsy with generalized tonic-clonic seizures	23	5
	FHM3	Migraine, familial hemiplegic, 3	5	4
	FEB3A	Febrile seizures, familial, 3A	2	2
SCN2A	BFIS3	Seizures, benign familial infantile 3	18	13
	EIEE11	Epileptic encephalopathy, early infantile, 11	50	21
	ASD	Autism spectrum disorders	16	1
SCN3A	CPE	Cryptogenic partial epilepsy	4	1
	ID	Intellectual disability	1	1
	AUTISM	Autism	2	1
	ADNSHL	Autosomal dominant nonsyndromic hearing loss	14	1
SCN4A	PMC	Paramyotonia congenita of von Eulenburg	16	16
	HOKPP2	Periodic paralysis hypokalemic 2	10	12
	HYPP	Periodic paralysis hyperkalemic	13	4
	NKPP	Periodic paralysis normokalemic	3	3
	MYOSCN4A	Myotonia SCN4A-related CMS16	14	13
	CMS16	Myasthenic syndrome, congenital, 16	3	3
SCN5A	PAM	Potassium-aggravated myotonias	6	1
	PFHB1A	Progressive familial heart block 1A	4	6
	LQT3	Long QT syndrome 3	123	30
	BRGDA1	Brugada syndrome 1	197	33
	SSS1	Sick sinus syndrome 1 VF1	2	3
	VF1	Familial paroxysmal ventricular fibrillation 1	1	1
	SIDS	Sudden infant death syndrome	2	1
	ATRST1	Atrial standstill 1	1	2
	CMD1E	Cardiomyopathy, dilated 1E	1	2
	ATFB10	Atrial fibrillation, familial, 10	9	2
MEPPC	Multifocal ectopic Purkinje-related premature contractions	3	4	
SCN8A	EIEE13	Epileptic encephalopathy, early infantile, 13	44	15
	BFIS5	Seizures, benign familial infantile, 5	1	2
SCN9A	IEM	Inherited erythralgia (primary erythralgia) pain	23	11
	CIP	Congenital insensitivity to pain	13	1
	PEPD	Paroxysmal extreme pain disorder	9	3
	GEFS+7	Generalized epilepsy with febrile seizures plus 7	2	1

Isoform	Channelopathies	Discovered mutant number	Discovery publication number
	FEB3B Febrile seizures, familial, 3B	2	1
	SFN Small fiber neuropathy	7	1
	DS (SMEI) Dravet syndrome (severe myoclonic epilepsy of infancy)	13	1
SCN10A	FEPS2 Episodic pain syndrome, familial, 2	2	1
	SFN Small fiber neuropathy	4	3
SCN11A	HSAN7 Neuropathy, hereditary sensory, and autonomic, 7	2	2
	FEPS3 Episodic pain syndrome, familial, 3	7	4
	SFN Small fiber neuropathy	4	4
SCN1B	ATFB13 Atrial fibrillation, familial, 13	2	1
	BRGDA5 Brugada syndrome 5	1	1
	EIEE52 Epileptic encephalopathy, early infantile, 52	2	2
	GEFS+1 Generalized epilepsy with febrile seizures plus 1	2	3
SCN2B	ATFB14 Atrial fibrillation, familial, 14	2	1
	BRGDA Brugada syndrome	1	1
SCN3B	ATFB16 Atrial fibrillation, familial, 16	4	2
	BRGDA7 Brugada syndrome 7	1	1
SCN4B	ATFB17 Atrial fibrillation, familial, 17	2	1
	LQT10 Long QT syndrome 10	1	1

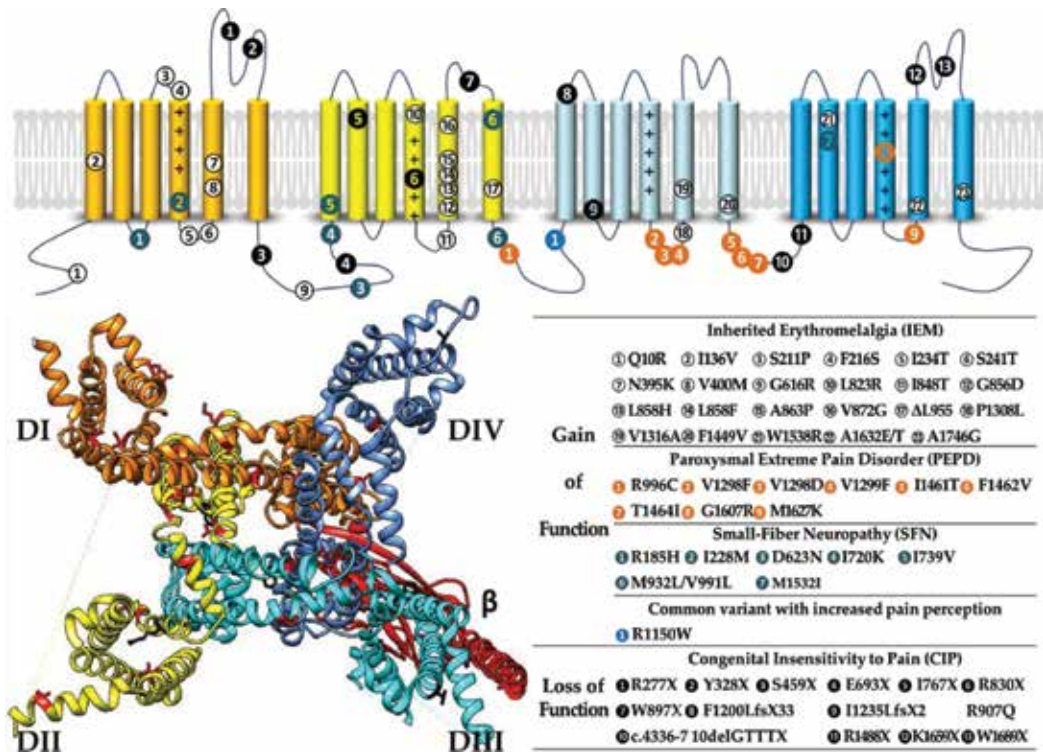
**Table 2.** Nav  $\alpha$  and  $\beta$  subunits' channelopathies data (updated in June, 2018 from database in <http://www.uniprot.org>).

[76] and nociceptor-specific Nav1.7 knockout [77]. Together, these studies have established that Nav1.7 is an essential and nonredundant requirement for nociception in humans.

While Nav1.7 is responsible for setting threshold for generation of action potentials, Nav1.8 and Nav1.9 contribute to the rising phase of action potentials in nociceptive neurons. Both channels are expressed in small-diameter DRG neurons, which include the C fibers that transmit nociceptive impulses [78]. Four gain-of-function Nav1.8 mutations (L554P, I1706V, A1304T, G1662S) have been identified, which lead to an increase in excitability in small-diameter neurons, underlying pain in small fiber neuropathy (SFN) [79–81]. In Nav1.9, gain-of-function mutations were recently reported to be associated with pain, albeit with opposing effects [82]. So far, naturally occurring loss-of-function mutations of Nav1.8 and Nav1.9 are yet to be described in humans; Nav1.8 and 1.9 are clearly important in the pain pathology and worth exploring as potential pain targets.

### 3.2. Epilepsy

Nav channel dysfunction is central to the pathophysiology of epileptic seizures, and many of the most widely used antiepileptic drugs, including phenytoin, carbamazepine, and lamotrigine,



**Figure 6.** Amino acid locations of Nav1.7 disease-related mutations on the Nav1.7 structure model. Modified from [12, 31, 69–71].

are Nav inhibitors. Many types of general epilepsy are resulted from mutations primarily in Nav1.1, and also in other Nav  $\alpha$  isoforms, including Nav1.2, Nav1.3, Nav1.6, Nav1.7, and Nav  $\beta$ 1. GEFS+ type 1 results from Nav  $\beta$ 1 mutation C387G, which destroys extracellular immunoglobulin domain and thus indirectly decreases rate of channel inactivation [83]. GEFS+ type 2 results from Nav1.1 mutations, such as T875 M (in DII-S4) and R1648H (in DIV-S4), which decrease Nav1.1 inactivation rate directly [84]. Worth noting, some epilepsy-associated Nav1.2 and Nav1.6 mutations cause a gain-of-function when characterized in transfected cells [85, 86]. Better understanding of clinical genetics and channel structure-function will facilitate the drug development for Nav-associated neurological diseases.

### 3.3. Cardiac arrhythmias

Mutations of Nav1.5 have been linked to long QT syndrome (LQTS). Recent study suggests that even modest depression of Nav1.5 expression may promote pathologic cardiac remodeling and progression of heart failure [87]. Since the first LQT-related Nav1.5 mutation being discovered in 1995 [88], more than a hundred Nav1.5 mutations that associate with distinct cardiac rhythm disorders, such as LQT syndrome subtype 3, Brugada syndrome, and cardiac conduction disease, have been identified [89]. These Nav1.5 mutations are spread out the whole protein. Most Nav1.5 mutations change biophysical property by increasing persistent

Na<sup>+</sup> current or gain-of-function, while in Brugada syndrome and cardiac conduction disease, most of the mutations are missense loss-of-function mutations. Because many mutations produce overlapping clinical phenotypes, it is crucial to understand genotype-phenotype correlations in Nav1.5 channelopathies for drug development.

### 3.4. Neuromuscular diseases

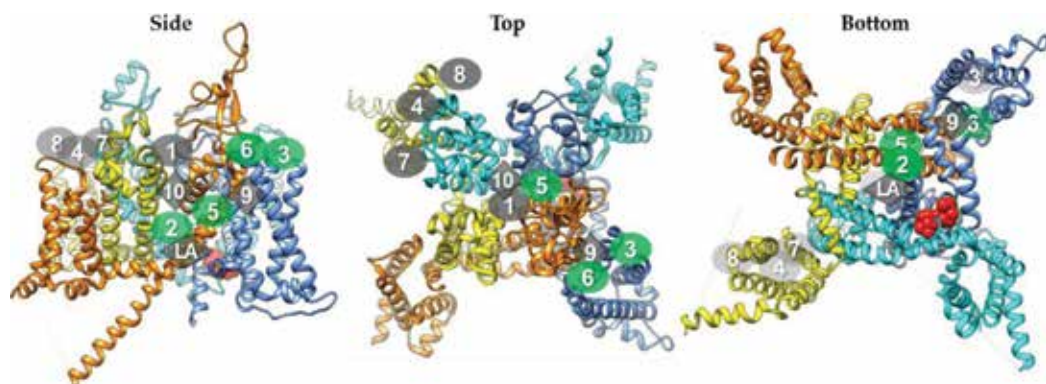
Mutations of Nav1.4 channel are associated with inherited neuromuscular diseases. For examples, the M1592V mutation causes hyperkalemic periodic paralysis (HYPP), in which increased levels of serum potassium lead to muscle hypoexcitability and paralysis; the R1448C mutation causes paramyotonia congenita (PMC), which is induced by cold and aggravated by increased muscle activity; and the G1306A mutation causes potassium-aggravated myotonias (PAM). These mutations affect either voltage-dependent activation or inactivation of Nav1.4, and are inherited in an autosomal dominant manner [90]. In contrast, most Nav1.6 mutations are recessive. An allelic mutation A107T in DIII S4-S5 caused ataxic phenotype by shifting Nav1.6 activation and inactivation to about 14 mV in the depolarizing direction, suggesting Nav1.6 is required for the complex spiking of cerebellar Purkinje cells and for persistent sodium current in several classes of neurons [91–93].

## 4. Nav modulation with small and large molecules

Nav channels have long been recognized as targets for treating pain, neurological disorders, and cardiac arrhythmias. In nature, Nav channels are the molecular targets of a broad range of neurotoxins including tetrodotoxin (TTX), saxitoxin (STX), veratridine (VTD), and batrachotoxin (BTX) from marine bacteria and plants, as well as peptide toxins such as ProToxin (ProTX), Huwentoxin (HwTX and  $\alpha$ -ScTXs) from the venoms of scorpions, spiders, sea anemones, and cone snails. Additionally, many Nav-targeting drugs have been developed, including local anesthesia (LA), antiarrhythmics (e.g., lidocaine, mexiletine), anticonvulsants (e.g., carbamazepine), and antidepressants (e.g., amitriptyline). In general, these drugs do not have subtype selectivity and have small therapeutic index. Recently, two series of highly isoform-selective compounds, aryl sulfonamides for Nav1.7 and phenyl imidazole for Nav1.8, have been reported [94, 95]. Besides small molecules, monoclonal antibody has also been proposed as an alternative strategy. Nonetheless, due to the high-sequence homology among all Nav isoforms, subtype selective targeting remains a challenge.

All nature or synthesized small and large modulators for Nav channels can be classified as pore blockers or gating modifiers. Pore blockers (e.g., TTX) physically occlude the pore, thereby inhibiting channel conductance. Often the blockade is tonic, or independent of states of the channels. Gating modifiers (aryl sulfonamides as example) preferentially modify activated or inactivated states, thus reducing currents progressively with increased stimulation duration and frequency.





**Figure 7.** Nav channel structural topology with drug binding sites. Domain DI/II/III/IV is colored orange, yellow, cyan, and blue, respectively. The IFM fast inactivation gate is shown in red sphere format. All currently identified eight Nav binding sites are labeled corresponding to its visibility. Binding sites leading to channel activation are in green, and binding sites leading to channel blockage are in gray. Seven natural toxin binding sites are labeled with oval, while local anesthetic, aryl sulfonamide, and phenyl imidazole binding sites are labeled with diamonds.

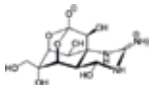
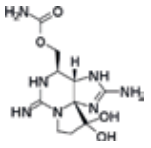
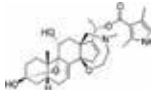
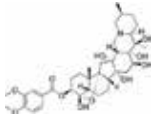
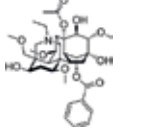
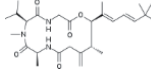
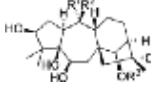
Based on their drug binding sites, Nav inhibitors can be classified into different groups (Figure 7 and Table 3).


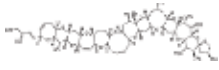
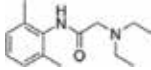
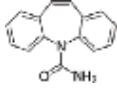
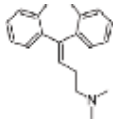
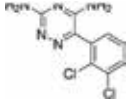
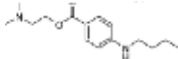
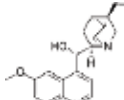
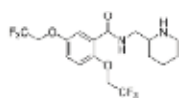
**Site 1: extracellular pore blocker.** This site is formed by the four P-loops and represents the binding site of two known groups of pore blockers, including small molecular guanidinium toxins from marine bacteria (TTX and STX), and 17–25 amino acids' peptide  $\mu$ -conotoxins from marine cone snail toxins [96–98]. These toxins physically plug the pore and thereby inhibit the sodium conductance.

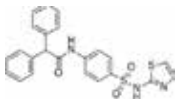
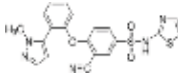
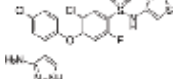
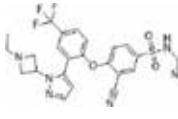
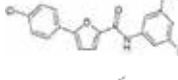
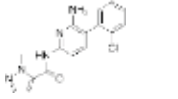
**Site 2: intracellular pore gating activator (state dependent).** The binding site is the fenestration site formed between DI-S6 and DIV-S6, which binds to many small lipid-soluble toxins including batrachotoxin (BTX) from frog, antillatoxin (ATX) from marine species, and veratridine (VTD), aconitine (ACT), and grayanotoxin (GTX) from plants. These modulators facilitate channel activation or prevent inactivation, thereby increasing channel conductance. They often have much higher affinity to the open and inactivated states of Nav channel as the binding fenestration exposed.

**Site 3: extracellular gating activator.** The binding site is localized in the DIV S3-S4 extracellular loop for two groups of peptide toxin activators: scorpion  $\alpha$ -toxins ( $\alpha$ -ScTxS) and sea. Upon binding, these modulators prevent the movement of DIV-S4, thus inhibiting transition to fast inactivation.

**Site 4: extracellular gating blocker.** The binding site is the DII S1-S2 and S3-S4 extracellular loop, which binds to four groups of peptide toxin blockers, including  $\beta$ -scorpion toxins ( $\beta$ -ScTxS),  $\beta$ -spider toxins,  $\mu$ O-conotoxins, and  $\iota$ -conotoxins. In general, these toxins block the DII-VSD conformational change and shift the voltage dependence of activation toward more hyperpolarized potentials, though the structural-based mechanism of action is not clear.

Binding site	Molecule group	Effect and application	Molecule examples	Structure or peptide PDB	Reference				
Site 1. DI-IV P-loop	Marine bacteria toxin	Block Na <sup>+</sup> conduction	Tetrodotoxin (TTX)		[96]				
			Saxitoxin (STX)		[97]				
	μ-Conotoxin			KIIIA	17 aa, 2LXG	[98]			
				PIIIA, PIIIB	22 aa, 1R9I	[98]			
				GIIIA, GIIB	23 aa, 1TCG	[98]			
				BuIIIB	25 aa, 2LOC	[98]			
SmIIIA	22 aa, 1Q2J	[98]							
Site 2. DI-DIV S6	Small lipid-soluble toxins	Prevent inactivation Nav agonist	Batrachotoxin (BTX)		[102]				
			Veratridine (VTD)		[103]				
			Aconitine (ACT)		[104]				
			Antillatoxin (ATX)		[105]				
			Grayanotoxin (GTX)		[106]				
			Site 3. DIV-S3-S4	α-Scorpion toxins	Prevent inactivation Nav agonist	Aah 2	64 aa, 1SEG	[107]	
LqhaIT	65 aa, 1LQH	[107]							
LqhIT2	62 aa, 2I6I	[107]							
Sea anemone toxins				BMK MI	64 aa, 1SN1	[107]			
				Type I: ATXI, etc.	46 aa, 1ATX	[108]			
				Type II: Rp2, etc.	48 aa	[108]			
				Type III: ATX3, etc.	27 aa, 1ANS	[108]			
				Site 4. DII S3-S4	β-Scorpion toxins (β-ScTxS)	Prevent activation	Cn2	67 aa, 1CN2	[109]

Binding site	Molecule group	Effect and application	Molecule examples	Structure or peptide PDB	Reference
			Ts1 (=Ts7, TsVII, Ts $\gamma$ )	61 aa, 1B7D	[109]
			Bj-xtrIT	77 aa, 1BCG	[109]
			LqhIT2	62 aa, 2I61	[109]
	$\beta$ -Spider toxins		ProTXI	35 aa, 2M9L	[110]
			ProTX II	30 aa, 2N9T	[110]
			HwTX-IV	35 aa, 1MB6	[111]
			Magi 5	29 aa, 2GX1	[112]
	$\mu$ O-conotoxins		$\mu$ O-MrVIB	31 aa, 1RMK	[113]
	$\iota$ -conotoxins		$\iota$ -RxIA	38 aa, 2JTU	[113]
Site 5. DI S6	Cyclic polyethers (dinoflagellate toxin)	Prevent inactivation, Nav agonist	Brevetoxins (PbTx)		[114]
			Ciguatoxins (CTX1)		[101]
Site 6. DIV S4	Cysteine knot 3 disulfide bridges	Conotoxins Nav agonist	$\delta$ -TxVIA	27 aa, 1FU3	[115]
			$\delta$ -EVIA	33 aa, 1G1P	[113]
Site 7. (LA) DIV S6	Local anesthetics	Local anesthetics Class Ib antiarrhythmic Neoropathic pain	Lidocaine		[116]
	State-dependent nonselective Na <sup>+</sup> conduction blockers	Antidepressant	Carbamazepine		[116]
		Antidepressant	Amitriptyline		[117]
		Anticonvulsant	Lamotrigine		[118]
		Local anesthetic	Tetracaine		[119]
		Class Ia antiarrhythmic	Quinidine		[120]
		Class Ic antiarrhythmic	Flecainide		[121]

Binding site	Molecule group	Effect and application	Molecule examples	Structure or peptide PDB	Reference
Site 8. DII S2	Cysteine knot	Conotoxins Nav antagonist	$\mu\text{O}\delta\text{-GVIII}$	35 aa, 2N8H	[100]
Site 9. DIV S4	Aryl sulfonamides	Nav1.7 selective blockers	ICA-121431 (Icagen)		[101]
			PF-04856264 (Pfizer)		[101]
			PF-05089771 (Pfizer)		[122]
			GX-936		[123]
Site 10	Phenyl imidazole	Nav1.8 selective blockers	A-803467		[124]
			PF-04531083 (Pfizer)		[95]

**Table 3.** Small molecules and toxin modulators for Nav channels.

**Site 5: intracellular pore gating activator (state dependent).** The fenestration site between DI-S6 and DIV-S5 binds two classes of cyclic polyether toxins from dinoflagellate: brevetoxins (PbTx) and ciguatoxins (CTX). These modulators have higher affinity to activated channel. Upon binding, they shift the activation and inactivation both to more hyperpolarizing voltage, thus keeping the channel hyperactive.

**Site 6: extracellular gating activator.** The DIV-S4 fenestration binds to  $\delta$ -conotoxins causing similar effects as site 3 toxins by slowing or inhibiting inactivation. Although sites 6 and 3 are structurally close to each other, however, the two categories activators do not compete with each other [99]. Site 6 activators trap DIV-S4 in outward conformation, thus leading to a persistent activation and prolongation of action potential.

**Site 7: local anesthetic (LA) binding site.** The inner cavity of channel pore, consisting of amino acid residues in S6 of DI, DIII, and DIV, forms the LA binding site. The LA binding site is highly conserved across Nav channels and accounts for the lack of subtype selectivity for most clinically used sodium channel blockers.

**Site 8: extracellular gating blocker.** The site was identified by studying a class of cone snail  $\mu\text{O}\text{S}$ -conotoxins blockers, such as  $\mu\text{O}\text{S}$ -GVIIJ. The putative binding site is close to a cysteine near DII P-loop (C910 in rNav1.2), which is responsible of the antagonist effect [100].

**Site 9: aryl sulfonamide site.** The unique Nav1.7 VSD4 binding site for the new series of aryl sulfonamide compounds, such as ICA-121431, PF-04856264 [101].

**Site 10: phenyl imidazole site.** The unique fenestration-selectivity filter site in Nav1.8 for the new series of phenyl imidazole compounds, such as A-803467, PF-04531083 [95].

## 5. Concluding remarks

Voltage-gated sodium channels play essential roles in physiological function, and historically, sodium channel blockers have been developed as local anesthetics and anticonvulsants. However, these early generation of sodium channel drugs were developed decades ago without the exact understanding of their molecular targets and mechanisms of action; their general lack of on-target potency and off-target selectivity renders narrow therapeutic windows. In recent years, several scientific frontiers have been rapidly evolving. First, the physiological functions of each sodium channel have been determined. Second, their associations to human diseases have been revealed in the form of “channelopathies.” Often both gain-of-function and loss-of-function mutations have been linked to human diseases, therefore pinpointing exactly the molecular targets. Third, the structural determination of sodium channels provides opportunities for structural-based drug design. Together, these progresses have ushered in a new, exciting era of sodium channel drug discovery.

## Acknowledgements

We gratefully acknowledge contributions from Genentech Inc. to support this publication.

## Conflict of interest

The authors are all employees of Genentech Inc. (a Roche Group Company) and declare no financial and conflict of interest in this chapter.

## Notes/thanks/other declarations

N/a.

## Author details

Tianbo Li\* and Jun Chen

\*Address all correspondence to: li.tianbo@gene.com

Department of Biochemical and Cellular Pharmacology, Genentech Inc., South San Francisco, California, USA

## References

- [1] Hodgkin AL, Huxley AF. Currents carried by sodium and potassium ions through the membrane of the giant axon of Loligo. *The Journal of Physiology*. 1952;**6**:449-472
- [2] Hodgkin AL, Katz B. The effect of sodium ions on the electrical activity of the giant axon of the squid. *The Journal of Physiology*. 1949;**8**:37-77
- [3] Armstrong CM. Sodium channels and gating currents. *Physiological Reviews*. 1981;**61**: 644-683. DOI: 10.1152/physrev.1981.61.3.644
- [4] Hodgkin AL, Huxley AF. A quantitative description of membrane current and its application to conduction and excitation in nerve. *The Journal of Physiology*. 1952;**117**:500-544
- [5] Pihl J, Sinclair J, Karlsson M, Orwar O. Microfluidics for cell-based assays. *Materials Today*. 2005;**8**:46-51. DOI: 10.1016/S1369-7021(05)71224-4
- [6] Noda M, Shimizu S, Tanabe T, Takai T, Kayano T, Ikeda T, Takahashi H, Nakayama H, Kanaoka Y, Minamino N, Kangawa K, Matsuo H, Raftery MA, Hirose T, Inayama S, Hayashida H, Miyata T, Numa S. Primary structure of *Electrophorus electricus* sodium channel deduced from cDNA sequence. *Nature*. 1984;**312**:121-127. DOI: 10.1038/312121a0
- [7] Hille B. *Ion Channels of Excitable Membranes*. 3rd ed. Sunderland, MA: Sinauer Associates Inc.; 2001
- [8] Spafford JD, Spencer AN, Gallin WJ. A putative voltage-gated sodium channel  $\alpha$  subunit (PpSCN1) from the hydrozoan jellyfish, *Polyorchis penicillatus*: Structural comparisons and evolutionary considerations. *Biochemical and Biophysical Research Communications*. 1998;**244**:772-780. DOI: 10.1006/bbrc.1998.8332
- [9] Ren D, Navarro B, Xu H, Yue L, Shi Q, Clapham DE. A prokaryotic voltage-gated sodium channel. *Science*. 2001;**294**:2372-2375. DOI: 10.1126/science.1065635
- [10] Payandeh J, Minor DL. Bacterial voltage-gated sodium channels (BacNaVs) from the soil, sea, and salt lakes enlighten molecular mechanisms of electrical signaling and pharmacology in the brain and heart. *Journal of Molecular Biology*. 2014;**427**:3-30. DOI: 10.1016/j.jmb.2014.08.010

- [11] Knipple DC, Doyle KE, Marsella-Herrick PA, Soderlund DM. Tight genetic linkage between the *kdr* insecticide resistance trait and a voltage-sensitive sodium channel gene in the house fly. *Proceedings of the National Academy of Sciences of the United States of America*. 1994;**91**:2483-2487
- [12] Yan Z, Zhou Q, Wang L, Wu J, Zhao Y, Huang G, Peng W, Shen H, Lei J, Yan N. Structure of the Nav1.4- $\beta$ 1 complex from electric eel. *Cell*. 2017;**170**:470-482.e11. DOI: 10.1016/j.cell.2017.06.039
- [13] Shen H, Zhou Q, Pan X, Li Z, Wu J, Yan N. Structure of a eukaryotic voltage-gated sodium channel at near-atomic resolution. *Science*. 2017;**355**:eaal4326. DOI: 10.1126/science.aal4326
- [14] Goldin AL. Resurgence of sodium channel research. *Annual Review of Physiology*. 2001; **63**:871-894. DOI: 10.1146/annurev.physiol.63.1.871
- [15] Yu FH, Catterall WA. Overview of the voltage-gated sodium channel family. *Genome Biology*. 2003;**4**:207
- [16] Noda M, Hiyama TY. The Nax Channel. What it is and what it does. *Neuroscience*. 2015; **21**:399-412. DOI: 10.1177/1073858414541009
- [17] George AL, Knittle TJ, Tamkun MM. Molecular cloning of an atypical voltage-gated sodium channel expressed in human heart and uterus: Evidence for a distinct gene family. *Proceedings of the National Academy of Sciences of the United States of America*. 1992; **89**:4893-4897
- [18] Strong M, Chandy KG, Gutman GA. Molecular evolution of voltage-sensitive ion channel genes: On the origins of electrical excitability. *Molecular Biology and Evolution*. 1993; **10**:221-242. DOI: 10.1093/oxfordjournals.molbev.a039986
- [19] Plummer NW, Meisler MH. Evolution and diversity of mammalian sodium channel genes. *Genomics*. 1999;**57**:323-331. DOI: 10.1006/GENO.1998.5735
- [20] Liebeskind BJ, Hillis DM, Zakon HH. Evolution of sodium channels predates the origin of nervous systems in animals. *Proceedings of the National Academy of Sciences of the United States of America*. 2011;**108**:9154-9159. DOI: 10.1073/pnas.1106363108
- [21] Moran Y, Barzilai MG, Liebeskind BJ, Zakon HH. Evolution of voltage-gated ion channels at the emergence of Metazoa. *The Journal of Experimental Biology*. 2015;**218**:515-525. DOI: 10.1242/jeb.110270
- [22] Lopreato GF, Lu Y, Southwell A, Atkinson NS, Hillis DM, Wilcox TP, Zakon HH. Evolution and divergence of sodium channel genes in vertebrates. *Proceedings of the National Academy of Sciences*. 2001;**98**:7588-7592. DOI: 10.1073/pnas.131171798
- [23] Liebeskind BJ, Hillis DM, Zakon HH. Independent acquisition of sodium selectivity in bacterial and animal sodium channels. *Current Biology*. 2013;**23**:R948-R949. DOI: 10.1016/J.CUB.2013.09.025

- [24] Raymond CK, Castle J, Garrett-Engle P, Armour CD, Kan Z, Tsinoremas N, Johnson JM. Expression of alternatively spliced sodium channel alpha-subunit genes. Unique splicing patterns are observed in dorsal root ganglia. *Journal of Biological Chemistry*. 2004;**279**: 46234-46241. DOI: 10.1074/jbc.M406387200
- [25] Parisien M, Khoury S, Chabot-Doré A-J, Sotocinal SG, Slade GD, Smith SB, Fillingim RB, Ohrbach R, Greenspan JD, Maixner W, Mogil JS, Belfer I, Diatchenko L. Effect of human genetic variability on gene expression in dorsal root ganglia and association with pain phenotypes. *Cell Reports*. 2017;**19**:1940-1952. DOI: 10.1016/j.celrep.2017.05.018
- [26] Ardlie KG, Deluca DS, Segre AV, Sullivan TJ, Young TR, Gelfand ET, Trowbridge CA, Maller JB, Tukiainen T, Lek M, Ward LD, Kheradpour P, Iriarte B, Meng Y, Palmer CD, Esko T, Winckler W, Hirschhorn JN, Kellis M, MacArthur DG, Getz G, Shabalin AA, Li G, Zhou Y-H, Nobel AB, Rusyn I, Wright FA, Lappalainen T, Ferreira PG, Ongen H, Rivas MA, Battle A, Mostafavi S, Monlong J, Sammeth M, Mele M, Reverter F, Goldmann JM, Koller D, Guigo R, McCarthy MI, Dermitzakis ET, Gamazon ER, Im HK, Konkashbaev A, Nicolae DL, Cox NJ, Flutre T, Wen X, Stephens M, Pritchard JK, Tu Z, Zhang B, Huang T, Long Q, Lin L, Yang J, Zhu J, Liu J, Brown A, Mestichelli B, Tidwell D, Lo E, Salvatore M, Shad S, Thomas JA, Lonsdale JT, Moser MT, Gillard BM, Karasik E, Ramsey K, Choi C, Foster BA, Syron J, Fleming J, Magazine H, Hasz R, Walters GD, Bridge JP, Miklos M, Sullivan S, Barker LK, Traino HM, Mosavel M, Siminoff LA, Valley DR, Rohrer DC, Jewell SD, Branton PA, Sobin LH, Barcus M, Qi L, McLean J, Hariharan P, Um KS, Wu S, Tabor D, Shive C, Smith AM, Buia SA, Undale AH, Robinson KL, Roche N, Valentino KM, Britton A, Burges R, Bradbury D, Hambright KW, Seleski J, Korzeniewski GE, Erickson K, Marcus Y, Tejada J, Taherian M, Lu C, Basile M, Mash DC, Volpi S, Struewing JP, Temple GF, Boyer J, Colantuoni D, Little R, Koester S, Carithers LJ, Moore HM, Guan P, Compton C, Sawyer SJ, Demchok JP, Vaught JB, Rabiner CA, Lockhart NC, Ardlie KG, Getz G, Wright FA, Kellis M, Volpi S, Dermitzakis ET. The genotype-tissue expression (GTEx) pilot analysis: Multitissue gene regulation in humans. *Science* (80-). 2015;**348**: 648-660. DOI: 10.1126/science.1262110
- [27] Hartmann HA, Colom LV, Sutherland ML, Noebels JL. Selective localization of cardiac SCN5A sodium channels in limbic regions of rat brain. *Nature Neuroscience*. 1999;**2**:593-595. DOI: 10.1038/10147
- [28] Safo P, Rosenbaum T, Shcherbatko A, Choi DY, Han E, Toledo-Aral JJ, Olivera BM, Brehm P, Mandel G. Distinction among neuronal subtypes of voltage-activated sodium channels by mu-conotoxin PIIIA. *The Journal of Neuroscience*. 2000;**20**:76-80
- [29] Moczydlowski E, Olivera BM, Gray WR, Strichartz GR. Discrimination of muscle and neuronal Na-channel subtypes by binding competition between [<sup>3</sup>H]saxitoxin and mu-conotoxins. *Proceedings of the National Academy of Sciences of the United States of America*. 1986;**83**:5321-5325
- [30] Cruz LJ, Gray WR, Olivera BM, Zeikus RD, Kerr L, Yoshikami D, Moczydlowski E. Conus geographus toxins that discriminate between neuronal and muscle sodium channels. *The Journal of Biological Chemistry*. 1985;**260**:9280-9288



- [31] Dib-Hajj SD, Yang Y, Black JA, Waxman SG. The Na(V)1.7 sodium channel: from molecule to man. *Nature Reviews Neuroscience*. 2013;**14**:49-62. DOI: 10.1038/nrn3404
- [32] Payandeh J, Scheuer T, Zheng N, Catterall WA. The crystal structure of a voltage-gated sodium channel. *Nature*. 2011;**475**:353-358. DOI: 10.1038/nature10238
- [33] Overington JP, Al-Lazikani B, Hopkins AL. How many drug targets are there? *Nature Reviews. Drug Discovery*. 2006;**5**:993-996. DOI: 10.1038/nrd2199
- [34] McCusker EC, Bagn eris C, Naylor CE, Cole AR, D'Avanzo N, Nichols CG, Wallace BA. Structure of a bacterial voltage-gated sodium channel pore reveals mechanisms of opening and closing. *Nature Communications*. 2012;**3**:1102. DOI: 10.1038/ncomms2077
- [35] Sula A, Booker J, Ng LCT, Naylor CE, DeCaen PG, Wallace BA. The complete structure of an activated open sodium channel. *Nature Communications*. 2017;**8**:14205. DOI: 10.1038/ncomms14205
- [36] De Lera Ruiz M, Kraus RL. Voltage-gated sodium channels: Structure, function, pharmacology, and clinical indications. *Journal of Medicinal Chemistry*. 2015;**58**:7093-7118. DOI: 10.1021/jm501981g
- [37] Zhang X, Ren W, DeCaen P, Yan C, Tao X, Tang L, Wang J, Hasegawa K, Kumasaka T, He J, Wang J, Clapham DE, Yan N. Crystal structure of an orthologue of the NaChBac voltage-gated sodium channel. *Nature*. 2012;**486**:130-134. DOI: 10.1038/nature11054
- [38] Pless SA, Elstone FD, Niciforovic AP, Galpin JD, Yang R, Kurata HT, Ahern CA. Asymmetric functional contributions of acidic and aromatic side chains in sodium channel voltage-sensor domains. *The Journal of General Physiology*. 2014;**143**:645-656. DOI: 10.1085/jgp.201311036
- [39] Heinemann SH, Terlau H, St uhmer W, Imoto K, Numa S. Calcium channel characteristics conferred on the sodium channel by single mutations. *Nature*. 1992;**356**:441-443. DOI: 10.1038/356441a0
- [40] Agnew WS, Moore AC, Levinson SR, Raftery MA. Identification of a large molecular weight peptide associated with a tetrodotoxin binding protein from the electroplax of *Electrophorus electricus*. *Biochemical and Biophysical Research Communications*. 1980;**92**:860-866. DOI: 10.1016/0006-291X(80)90782-2
- [41] Miller JA, Agnew WS, Levinson SR. Principal glycopeptide of the tetrodotoxin/saxitoxin binding protein from *Electrophorus electricus*: Isolation and partial chemical and physical characterization. *Biochemistry*. 1983;**22**:462-470
- [42] Fozzard HA, Lipkind GM. The tetrodotoxin binding site is within the outer vestibule of the sodium channel. *Marine Drugs*. 2010;**8**:219-234. DOI: 10.3390/md8020219
- [43] Ahern CA, Eastwood AL, Dougherty DA, Horn R. Electrostatic contributions of aromatic residues in the local anesthetic receptor of voltage-gated sodium channels. *Circulation Research*. 2008;**102**:86-94. DOI: 10.1161/CIRCRESAHA.107.160663

- [44] Wang S-Y, Tikhonov DB, Mitchell J, Zhorov BS, Wang GK. Irreversible block of cardiac mutant Na<sup>+</sup> channels by batrachotoxin. *Channels (Austin)*. n.d.;**1**:179-188
- [45] Du Y, Garden DP, Wang L, Zhorov BS, Dong K. Identification of new batrachotoxin-sensing residues in segment IIIIS6 of the sodium channel. *The Journal of Biological Chemistry*. 2011;**286**:13151-13160. DOI: 10.1074/jbc.M110.208496
- [46] Strichartz GR. The inhibition of sodium currents in myelinated nerve by quaternary derivatives of lidocaine. *The Journal of General Physiology*. 1973;**62**:37-57
- [47] Armstrong CM, Bezanilla F. Charge movement associated with the opening and closing of the activation gates of the Na channels. *The Journal of General Physiology*. 1974;**63**:533-552
- [48] Oelstrom K, Goldschen-Ohm MP, Holmgren M, Chanda B. Evolutionarily conserved intracellular gate of voltage-dependent sodium channels. *Nature Communications*. 2014;**5**:3420. DOI: 10.1038/ncomms4420
- [49] West JW, Patton DE, Scheuer T, Wang Y, Goldin AL, Catterall WA. A cluster of hydrophobic amino acid residues required for fast Na(+)-channel inactivation. *Proceedings of the National Academy of Sciences of the United States of America*. 1992;**89**:10910-10914
- [50] Oxford GS, Wu CH, Narahashi T. Removal of sodium channel inactivation in squid giant axons by n-bromoacetamide. *The Journal of General Physiology*. 1978;**71**:227-247
- [51] Eaholtz G, Scheuer T, Catterall WA. Restoration of inactivation and block of open sodium channels by an inactivation gate peptide. *Neuron*. 1994;**12**:1041-1048
- [52] Jones DK, Peters CH, Allard CR, Claydon TW, Ruben PC. Proton sensors in the pore domain of the cardiac voltage-gated sodium channel. *The Journal of Biological Chemistry*. 2013;**288**:4782-4791. DOI: 10.1074/jbc.M112.434266
- [53] Cheng X, Dib-Hajj SD, Tyrrell L, te Morsche RH, Drenth JPH, Waxman SG. Deletion mutation of sodium channel NaV1.7 in inherited erythromelalgia: enhanced slow inactivation modulates dorsal root ganglion neuron hyperexcitability. *Brain*. 2011;**134**:1972-1986. DOI: 10.1093/brain/awr143
- [54] Bendahhou S, Cummins TR, Kula RW, Fu Y-H, Ptáček LJ. Impairment of slow inactivation as a common mechanism for periodic paralysis in DIIS4-S5. *Neurology*. 2002;**58**:1266-1272
- [55] Silva JR, Goldstein SAN. Voltage-sensor movements describe slow inactivation of voltage-gated sodium channels I: Wild-type skeletal muscle Na(V)1.4. *Journal of General Physiology*. 2013;**141**:309-321. DOI: 10.1085/jgp.201210909
- [56] Goldin AL, Barchi RL, Caldwell JH, Hofmann F, Howe JR, Hunter JC, Kallen RG, Mandel G, Meisler MH, Netter YB, Noda M, Tamkun MM, Waxman SG, Wood JN, Catterall WA. Nomenclature of voltage-gated sodium channels. *Neuron*. 2000;**28**:365-368. DOI: 10.1016/S0896-6273(00)00116-1

- [57] Isom LL, Ragsdale DS, De Jongh KS, Westenbroek RE, Reber BF, Scheuer T, Catterall WA. Structure and function of the beta 2 subunit of brain sodium channels, a transmembrane glycoprotein with a CAM motif. *Cell*. 1995;**83**:433-442
- [58] Yu FH, Westenbroek RE, Silos-Santiago I, McCormick KA, Lawson D, Ge P, Ferreira H, Lilly J, DiStefano PS, Catterall WA, Scheuer T, Curtis R. Sodium channel beta4, a new disulfide-linked auxiliary subunit with similarity to beta2. *The Journal of Neuroscience*. 2003;**23**:7577-7585
- [59] Morgan K, Stevens EB, Shah B, Cox PJ, Dixon AK, Lee K, Pinnock RD, Hughes J, Richardson PJ, Mizuguchi K, Jackson AP. Beta 3: An additional auxiliary subunit of the voltage-sensitive sodium channel that modulates channel gating with distinct kinetics. *Proceedings of the National Academy of Sciences of the United States of America*. 2000;**97**(5):2308-2313. DOI: 10.1073/pnas.030362197
- [60] Isom LL, De Jongh KS, Patton DE, Reber BF, Offord J, Charbonneau H, Walsh K, Goldin AL, Catterall WA. Primary structure and functional expression of the beta 1 subunit of the rat brain sodium channel. *Science*. 1992;**256**:839-842
- [61] Feng G, Deák P, Chopra M, Hall LM. Cloning and functional analysis of TipE, a novel membrane protein that enhances *Drosophila* para sodium channel function. *Cell*. 1995;**82**:1001-1011
- [62] Lee SH, Smith TJ, Ingles PJ, Soderlund DM. Cloning and functional characterization of a putative sodium channel auxiliary subunit gene from the house fly (*Musca domestica*). *Insect Biochemistry and Molecular Biology*. 2000;**30**:479-487
- [63] Molinarolo S, Lee S, Leisle L, Lueck JD, Granata D, Carnevale V, Ahern CA. Cross-Kingdom auxiliary subunit modulation of a voltage-gated Sodium channel. *The Journal of biological chemistry*. 2018;**293**(14):4981-4992. DOI: 10.1074/JBC.RA117.000852
- [64] Kazen-Gillespie KA, Ragsdale DS, D'Andrea MR, Mattei LN, Rogers KE, Isom LL. Cloning, localization, and functional expression of sodium channel beta1A subunits. *The Journal of Biological Chemistry*. 2000;**275**:1079-1088. DOI: 10.1074/JBC.275.2.1079
- [65] Hull JM, Isom LL. Voltage-gated sodium channel  $\beta$  subunits: The power outside the pore in brain development and disease. *Neuropharmacology*. 2018;**132**:43-57. DOI: 10.1016/j.neuropharm.2017.09.018
- [66] Brackenbury WJ, Isom LL. Na<sup>+</sup> channel  $\beta$  subunits: Overachievers of the ion channel family. *Frontiers in Pharmacology*. 2011;**2**:53. DOI: 10.3389/fphar.2011.00053
- [67] Baroni D, Moran O. On the multiple roles of the voltage gated sodium channel  $\beta$ 1 subunit in genetic diseases. *Frontiers in Pharmacology*. 2015;**6**:108. DOI: 10.3389/fphar.2015.00108
- [68] O'Malley HA, Isom LL. Sodium channel  $\beta$  subunits: Emerging targets in channelopathies. *Annual Review of Physiology*. 2015;**77**:481-504. DOI: 10.1146/annurev-physiol-021014-071846

- [69] Drenth JPH, Waxman SG. Mutations in sodium-channel gene SCN9A cause a spectrum of human genetic pain disorders. *The Journal of Clinical Investigation*. 2007;**117**:3603-3610. DOI: 10.1172/JCI33297.type
- [70] Dib-Hajj SD, Binshtok AM, Cummins TR, Jarvis MF, Samad T, Zimmermann K. Voltage-gated sodium channels in pain states: Role in pathophysiology and targets for treatment. *Brain Research Reviews*. 2009;**60**:65-83. DOI: 10.1016/j.brainresrev.2008.12.005
- [71] Huang W, Liu M, Yan SF, Yan N. Structure-based assessment of disease-related mutations in human voltage-gated sodium channels. *Protein & Cell*. 2017;**8**:401-438. DOI: 10.1007/s13238-017-0372-z
- [72] Emery EC, Luiz AP, Wood JN. Nav1.7 and other voltage-gated sodium channels as drug targets for pain relief. *Expert Opinion on Therapeutic Targets*. 2016;**20**:975-983. DOI: 10.1517/14728222.2016.1162295
- [73] Fritz J, Wang KC, Carrino JA. Magnetic resonance neurography-guided nerve blocks for the diagnosis and treatment of chronic pelvic pain syndrome. *Neuroimaging Clinics of North America*. 2014;**24**:211-234. DOI: 10.1016/J.NIC.2013.03.028
- [74] Zorina-Lichtenwalter K, Parisien M, Diatchenko L. Genetic studies of human neuropathic pain conditions: A review. *Pain*. 2018;**159**:583-594. DOI: 10.1097/j.pain.0000000000001099
- [75] Yang Y, Wang Y, Li S, Xu Z, Li H, Ma L, Fan J, Bu D, Liu B, Fan Z, Wu G, Jin J, Ding B, Zhu X, Shen Y. Mutations in SCN9A, encoding a sodium channel alpha subunit, in patients with primary erythralgia. *Journal of Medical Genetics*. 2004;**41**:171-174
- [76] Cox JJ, Reimann F, Nicholas AK, Thornton G, Roberts E, Springell K, Karbani G, Jafri H, Mannan J, Raashid Y, Al-Gazali L, Hamamy H, Valente EM, Gorman S, Williams R, McHale DP, Wood JN, Gribble FM, Woods CG. An SCN9A channelopathy causes congenital inability to experience pain. *Nature*. 2006;**444**:894-898. DOI: 10.1038/nature05413
- [77] Nassar MA, Stirling LC, Forlani G, Baker MD, Matthews EA, Dickenson AH, Wood JN. Nociceptor-specific gene deletion reveals a major role for Nav1.7 (PN1) in acute and inflammatory pain. *Proceedings of the National Academy of Sciences*. 2004;**101**:12706-12711. DOI:10.1073/pnas.0404915101
- [78] Dib-Hajj SD, Tyrrell L, Cummins TR, Black JA, Wood PM, Waxman SG. Two tetrodotoxin-resistant sodium channels in human dorsal root ganglion neurons. *FEBS Letters*. 1999;**462**:117-120
- [79] Faber CG, Lauria G, Merkies ISJ, Cheng X, Han C, Ahn H-S, Persson A-K, Hoeijmakers JGJ, Gerrits MM, Pierro T, Lombardi R, Kapetis D, Dib-Hajj SD, Waxman SG. Gain-of-function Nav1.8 mutations in painful neuropathy. *Proceedings of the National Academy of Sciences of the United States of America*. 2012;**109**:19444-19449. DOI: 10.1073/pnas.1216080109
- [80] Huang J, Yang Y, Zhao P, Gerrits MM, Hoeijmakers JGJ, Bekelaar K, Merkies ISJ, Faber CG, Dib-Hajj SD, Waxman SG. Small-fiber neuropathy Nav1.8 mutation shifts activation

- to hyperpolarized potentials and increases excitability of dorsal root ganglion neurons. *Journal of Neuroscience*. 2013;**33**:14087-14097. DOI: 10.1523/JNEUROSCI.2710-13.2013
- [81] Han C, Vasylyev D, Macala LJ, Gerrits MM, Hoeijmakers JGJ, Bekelaar KJ, Dib-Hajj SD, Faber CG, Merkies ISJ, Waxman SG. The G1662S NaV1.8 mutation in small fibre neuropathy: impaired inactivation underlying DRG neuron hyperexcitability. *Journal of Neurology, Neurosurgery, and Psychiatry*. 2014;**85**:499-505. DOI: 10.1136/jnnp-2013-306095
- [82] Dib-Hajj SD, Black JA, Waxman SG. NaV1.9: A sodium channel linked to human pain. *Nature Reviews Neuroscience*. 2015;**16**:511-519. DOI: 10.1038/nrn3977
- [83] Wallace RH, Wang DW, Singh R, Scheffer IE, George AL, Phillips HA, Saar K, Reis A, Johnson EW, Sutherland GR, Berkovic SF, Mulley JC. Febrile seizures and generalized epilepsy associated with a mutation in the Na<sup>+</sup>-channel  $\beta$ 1 subunit gene SCN1B. *Nature Genetics*. 1998;**19**:366-370. DOI: 10.1038/1252
- [84] Escayg A, MacDonald BT, Meisler MH, Baulac S, Huberfeld G, An-Gourfinkel I, Brice A, LeGuern E, Moulard B, Chaigne D, Buresi C, Malafosse A. Mutations of SCN1A, encoding a neuronal sodium channel, in two families with GEFS+2. *Nature Genetics*. 2000;**24**:343-345. DOI: 10.1038/74159
- [85] Estacion M, O'Brien JE, Conravey A, Hammer MF, Waxman SG, Dib-Hajj SD, Meisler MH. A novel de novo mutation of SCN8A (Nav1.6) with enhanced channel activation in a child with epileptic encephalopathy. *Neurobiology of Diseases*. 2014;**69**:117-123. DOI: 10.1016/j.nbd.2014.05.017
- [86] Mantegazza M, Curia G, Biagini G, Ragsdale DS, Avoli M. Voltage-gated sodium channels as therapeutic targets in epilepsy and other neurological disorders. *Lancet Neurology*. 2010;**9**:413-424. DOI: 10.1016/S1474-4422(10)70059-4
- [87] Park DS, Fishman GI. SCN5A: The greatest HITS collection. *The Journal of Clinical Investigation*. 2018;**128**:913-915. DOI: 10.1172/JCI99927
- [88] Wang Q, Shen J, Splawski I, Atkinson D, Li Z, Robinson JL, Moss AJ, Towbin JA, Keating MT. SCN5A mutations associated with an inherited cardiac arrhythmia, long QT syndrome. *Cell*. 1995;**80**:805-811
- [89] Zimmer T, Surber R. SCN5A channelopathies—An update on mutations and mechanisms. *Progress in Biophysics and Molecular Biology*. 2008;**98**:120-136. DOI: 10.1016/j.pbiomolbio.2008.10.005
- [90] Cannon SC. From mutation to myotonia in sodium channel disorders. *Neuromuscular Disorders*. 1997;**7**:241-249
- [91] Meisler MH, Sprunger LK, Plummer NW, Escayg A, Jones JM. Ion channel mutations in mouse models of inherited neurological disease. *Annals of Medicine*. 1997;**29**:569-574
- [92] Kohrman DC, Smith MR, Goldin AL, Harris J, Meisler MH. A missense mutation in the sodium channel Scn8a is responsible for cerebellar ataxia in the mouse mutant jolting. *The Journal of Neuroscience*. 1996;**16**:5993-5999

- [93] Meisler MH, Plummer NW, Burgess DL, Buchner DA, Sprunger LK. Allelic mutations of the sodium channel SCN8A reveal multiple cellular and physiological functions. *Genetica*. 2004;**122**:37-45
- [94] Focken T, Liu S, Chahal N, Dauphinais M, Grimwood ME, Chowdhury S, Hemeon I, Bichler P, Bogucki D, Waldbrook M, Bankar G, Sojo LE, Young C, Lin S, Shuart N, Kwan R, Pang J, Chang JH, Safina BS, Sutherlin DP, Johnson JP, Dehnhardt CM, Mansour TS, Oballa RM, Cohen CJ, Robinette CL. Discovery of aryl sulfonamides as isoform-selective inhibitors of Nav1.7 with efficacy in rodent pain models. *ACS Medicinal Chemistry Letters*. 2016;**7**:277-282. DOI: 10.1021/acsmedchemlett.5b00447
- [95] Bagal SK, Kemp MI, Bungay PJ, Hay TL, Murata Y, Payne CE, Stevens EB, Brown A, Blakemore DC, Corbett MS, Miller DC, Omoto K, Warmus JS. Discovery and optimization of potent and highly subtype selective Nav1.8 inhibitors with reduced cardiovascular liabilities. *Medchemcomm*. 2016;**7**:1925-1931. DOI: 10.1039/C6MD00281A
- [96] Narahashi T. Tetrodotoxin: A brief history. *Proceedings of the Japan Academy. Series B, Physical and Biological Sciences*. 2008;**84**:147-154
- [97] French RJ, Worley JF, Krueger BK. Voltage-dependent block by saxitoxin of sodium channels incorporated into planar lipid bilayers. *Biophysical Journal*. 1984;**45**:301-310. DOI: 10.1016/S0006-3495(84)84156-9
- [98] Wilson MJ, Yoshikami D, Azam L, Gajewiak J, Olivera BM, Bulaj G, Zhang M-M.  $\mu$ -Conotoxins that differentially block sodium channels Nav1.1 through 1.8 identify those responsible for action potentials in sciatic nerve. *Proceedings of the National Academy of Sciences of the United States of America*. 2011;**108**:10302-10307. DOI: 10.1073/pnas.1107027108
- [99] Leipold E, Hansel A, Olivera BM, Terlau H, Heinemann SH. Molecular interaction of delta-conotoxins with voltage-gated sodium channels. *FEBS Letters*. 2005;**579**:3881-3884. DOI: 10.1016/j.febslet.2005.05.077
- [100] Gajewiak J, Azam L, Imperial J, Walewska A, Green BR, Bandyopadhyay PK, Raghuraman S, Ueberheide B, Bern M, Zhou HM, Minassian NA, Hagan RH, Flinspach M, Liu Y, Bulaj G, Wickenden AD, Olivera BM, Yoshikami D, Zhang M-M. A disulfide tether stabilizes the block of sodium channels by the conotoxin  $\mu$ Os-GVIIJ. *Proceedings of the National Academy of Sciences of the United States of America*. 2014;**111**:2758-2763. DOI: 10.1073/pnas.1324189111
- [101] Strachan LC, Lewis RJ, Nicholson GM. Differential actions of pacific ciguatoxin-1 on sodium channel subtypes in mammalian sensory neurons. *The Journal of Pharmacology and Experimental Therapeutics*. 1999;**288**:379-388
- [102] Wang S-Y, Mitchell J, Tikhonov DB, Zhorov BS, Wang GK. How batrachotoxin modifies the sodium channel permeation pathway: Computer modeling and site-directed mutagenesis. *Molecular Pharmacology*. 2005;**69**:788-795. DOI: 10.1124/mol.105.018200

- [103] Wang GK, Wang S-Y. Veratridine block of rat skeletal muscle Nav1.4 sodium channels in the inner vestibule. *Journal of Physiology*. 2003;**548**:667-675. DOI: 10.1113/jphysiol.2002.035469
- [104] Ghiasuddin SM, Soderlund DM. Mouse brain synaptosomal sodium channels: Activation by aconitine, batrachotoxin, and veratridine, and inhibition by tetrodotoxin. *Comparative Biochemistry and Physiology. C*. 1984;**77**:267-271
- [105] Cao Z, Gerwick WH, Murray TF. Antillatoxin is a sodium channel activator that displays unique efficacy in heterologously expressed rNav1.2, rNav1.4 and rNav1.5 alpha subunits. *BMC Neuroscience*. 2010;**11**:154. DOI: 10.1186/1471-2202-11-154
- [106] Jansen SA, Kleerekooper I, Hofman ZLM, Kappen IFPM, Stary-Weinzinger A, van der Heyden MAG. Grayanotoxin poisoning: 'Mad Honey Disease' and beyond. *Cardiovascular Toxicology*. 2012;**12**:208-215. DOI: 10.1007/s12012-012-9162-2
- [107] Bosmans F, Tytgat J. Voltage-gated sodium channel modulation by scorpion alpha-toxins. *Toxicon*. 2007;**49**:142-158. DOI: 10.1016/j.toxicon.2006.09.023
- [108] Moran Y, Gordon D, Gurevitz M. Sea anemone toxins affecting voltage-gated sodium channels—Molecular and evolutionary features. *Toxicon*. 2009;**54**:1089-1101. DOI: 10.1016/j.toxicon.2009.02.028
- [109] Pedraza Escalona M, Possani LD. Scorpion beta-toxins and voltage-gated sodium channels: interactions and effects. *Frontiers in Bioscience (Landmark Ed.)*. 2013;**18**:572-587
- [110] Middleton RE, Warren VA, Kraus RL, Hwang JC, Liu CJ, Dai G, Brochu RM, Kohler MG, Gao Y-D, Garsky VM, Bogusky MJ, Mehl JT, Cohen CJ, Smith MM. Two tarantula peptides inhibit activation of multiple sodium channels. *Biochemistry*. 2002;**41**:14734-14747
- [111] Xiao Y, Luo X, Kuang F, Deng M, Wang M, Zeng X, Liang S. Synthesis and characterization of huwentoxin-IV, a neurotoxin inhibiting central neuronal sodium channels. *Toxicon*. 2008;**51**:230-239. DOI: 10.1016/j.toxicon.2007.09.008
- [112] Bosmans F, Swartz KJ. Targeting voltage sensors in sodium channels with spider toxins. *Trends in Pharmacological Sciences*. 2010;**31**:175-182. DOI: 10.1016/j.tips.2009.12.007
- [113] Green BR, Olivera BM. Venom Peptides From Cone Snails. *Current Topics in Membrane*. 2016;**78**:65-86. DOI: 10.1016/bs.ctm.2016.07.001
- [114] Dechraoui MY, Naar J, Pauillac S, Legrand AM. Ciguatoxins and brevetoxins, neurotoxic polyether compounds active on sodium channels. *Toxicon*. 1999;**37**:125-143
- [115] Hasson A, Fainzilber M, Gordon D, Zlotkin E, Spira ME. Alteration of sodium currents by new peptide toxins from the venom of a molluscivorous *Conus* snail. *The European Journal of Neuroscience*. 1993;**5**:56-64
- [116] Tanelian DL, Brose WG. Neuropathic pain can be relieved by drugs that are use-dependent sodium channel blockers: Lidocaine, carbamazepine, and mexiletine. *Anesthesiology*. 1991;**74**:949-951

- [117] Song JH, Ham SS, Shin YK, Lee CS. Amitriptyline modulation of Na(+) channels in rat dorsal root ganglion neurons. *European Journal of Pharmacology*. 2000;**401**:297-305
- [118] Yasam VR, Jakki SL, Senthil V, Eswaramoorthy M, Shanmuganathan S, Arjunan K, Nanjan M. A pharmacological overview of lamotrigine for the treatment of epilepsy. *Expert Review of Clinical Pharmacology*. 2016;**9**:1533-1546. DOI: 10.1080/17512433.2016.1254041
- [119] Ragsdale DS, McPhee JC, Scheuer T, Catterall WA. Molecular determinants of state-dependent block of Na<sup>+</sup> channels by local anesthetics. *Science*. 1994;**265**:1724-1728
- [120] Grace AA, Camm AJ. Quinidine. *The New England Journal of Medicine*. 1998;**338**:35-45. DOI: 10.1056/NEJM199801013380107
- [121] Watanabe H, Chopra N, Laver D, Hwang HS, Davies SS, Roach DE, Duff HJ, Roden DM, Wilde AAM, Knollmann BC. Flecainide prevents catecholaminergic polymorphic ventricular tachycardia in mice and humans. *Nature Medicine*. 2009;**15**:380-383. DOI: 10.1038/nm.1942
- [122] Pfizer. Efficacy of PF-05089771 in treating postoperative dental pain. *ClinicalTrials.Gov*. 2012. <https://clinicaltrials.gov/ct2/show/NCT01529346> [Accessed: March 18, 2018]
- [123] Ahuja S, Mukund S, Deng L, Khakh K, Chang E, Ho H, Shriver S, Young C, Lin S, Johnson JP Jr, Wu P, Li J, Coons M, Tam C, Brillantes B, Sampang H, Mortara K, Bowman KK, Clark KR, Estevez A, Xie Z, Verschoof H, Grimwood M, Dehnhardt C, Andrez JC, Focken T, Sutherlin DP, Safina BS, Starovasnik MA, Ortwine DF, Franke Y, Cohen CJ, Hackos DH, Koth CM, Payandeh J. Structural basis of Nav1.7 inhibition by an isoform-selective small-molecule antagonist. *Science (80-)*. 2015;**350**:aac5464. DOI: 10.1126/science.aac5464
- [124] Jarvis MF, Honore P, Shieh CC, Chapman M, Joshi S, Zhang XF, Kort M, Carroll W, Marron B, Atkinson R, Thomas J, Liu D, Krambis M, Liu Y, McGaraughty S, Chu K, Roeloffs R, Zhong C, Mikusa JP, Hernandez G, Gauvin D, Wade C, Zhu C, Pai M, Scanio M, Shi L, Drizin I, Gregg R, Matulenko M, Hakeem A, Gross M, Johnson M, Marsh K, Wagoner PK, Sullivan JP, Faltynek CR, Krafft DS. A-803467, a potent and selective Nav1.8 sodium channel blocker, attenuates neuropathic and inflammatory pain in the rat. *Proceedings of the National Academy of Sciences of the United States of America*. 2007;**104**:8520-8525. DOI: 10.1073/pnas.0611364104



---

# Voltage-Gated Sodium Channel Drug Discovery Technologies and Challenges

---

Tianbo Li and Jun Chen

Additional information is available at the end of the chapter

<http://dx.doi.org/10.5772/intechopen.80370>

---

## Abstract

Voltage-gated sodium (Nav) channels represent an important class of drug target for pain and many other pathology conditions. Despite the recent advances in channelopathies and structure-function studies, the discovery of Nav channel therapeutics is still facing a major challenge from the limitation of assay technologies. This chapter will focus on advancement and challenge of Nav drug discovery technologies including nonelectrophysiological assays, extracellular electrophysiological assays, and the newly evolved high-throughput automated patch clamp (APC) technologies.

**Keywords:** voltage-gated sodium channel, drug discovery, uHTS, APC

---

## 1. Introduction

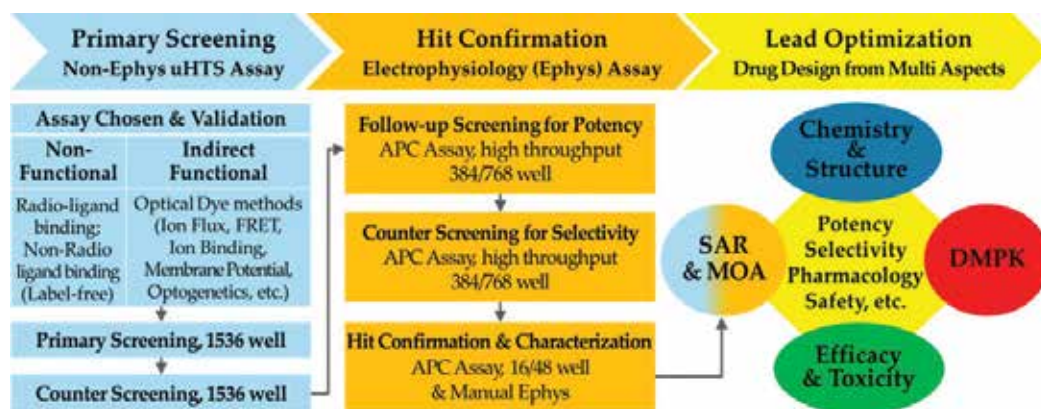
Nav channels are among the most well-characterized drug targets for pain, epilepsy, cardiac arrhythmias, and neuromuscular diseases. Current Nav drugs were developed empirically, in most cases without knowing their precise molecular targets. Even though new clinical indications have been found for these early-generation Nav modulators, their lack of sufficient isoform selectivity significantly limits the therapeutic outcomes. For example, when lidocaine is used to treat neuropathic pain, it causes cardiac toxicity due to inhibition of Nav1.5 and causes sedation, convulsion, and cardiac arrhythmias due to inhibition of CNS Nav channels.

Subtype-selective modulation of Nav channels is essential for target drug development but extremely difficult to achieve due to high sequence homology in the Nav family. The problem is further confounded by the current screening assays. Several assay platforms, such as radioligand binding, ion flux, and fluorescence membrane potential assays, have existed

---

for several decades. They are cost-effective and amenable to high-throughput screening. However these assays have significant limitations. For instance, the ligand binding assays could not provide functional effects (e.g., agonism vs. antagonism). Ion flux and membrane potential assays only measure channel function indirectly and are prone to artifacts such as autofluorescence, ionophore, and cellular toxicity. Electrophysiology is considered as the gold standard. However, traditional electrophysiology is significantly limited by its low throughput and labor intense. In the past decade, the emergence of automated electrophysiology has significantly increased the throughput, making it feasible to screen compounds using electrophysiology.

Same as any other drug targets, ion channel drug discovery refers to the process by which new candidate medications are discovered. This is a drug early development process lying between target validation biology research and drug clinic development. The process of ion channel drug discovery can be arbitrarily divided to three stages: primary screening, hit confirmation, and lead optimization (**Figure 1**). At the stage of primary screening, a large number (up to millions) of compounds are screened using various non- or indirect functional high-throughput assay, such as radioligand binding, ion flux, or membrane potential assays. Often, a small set of tool compounds are used to validate the assay. After obtaining correlation to electrophysiology, the assay is chosen for ultra high-throughput screening (uHTS) development and used for primary screening. Companion assays are also developed for counter screening to reduce assay artifacts or assess selectivity against other irrelevant targets. The uHTS assay performance is evaluated by assay stability, assay window, and hit rate, which is usually around 0.1% resulting in tens of thousands of potential hits. At the hit confirmation stage, often automated patch clamp (APC) platforms are used to test HTS hits. Hits are conformed, and their selectivity is confirmed by counter screening against other relevant isoforms. At the lead optimization stage, compounds are optimized on multiple fronts, including potency, selectivity, DMPK properties, efficacy, and toxicity.



**Figure 1.** Ion channel drug discovery strategy. Strategies for the implementation of multiple assay platforms in Nav channel drug discovery in the three stages of drug early development: SAR, structure-action relation; MOA, mechanism of action; DMPK, drug metabolism and pharmacokinetics.

## 2. Nonelectrophysiological technologies

Nonelectrophysiological assays include nonfunctional assays and indirect functional assays. Under nonfunctional assay category, there are radioligand binding, fluorescence polarization (FP), fluorescence resonance energy transfer (FRET), and a series of fragment-based lead discovery assays. These assays can detect high-affinity binding, which makes them useful for kinetic studies and lead optimization. However, their major limitation is that the ligand binding sometimes does not translate into functional effects.

Indirect functional assays include ion flux assay and fluorescence membrane potential assays. These assays do not have precise voltage control and do not directly measure channel conductance. Hence, these assays are prone to false positives from autofluorescence, ionophore, off-target effect, and cellular toxicity and in many cases cannot detect state-dependent modulators, thus needing to be redesigned [1] and validated using tool compounds in early assay development stage. Overall, these indirect functional assays have been commonly used for Nav channel drug discovery primary screening, due to their functional correlation and uHTS amenable assay properties.

### 2.1. Radioligand binding assays

Radioligand binding assays have been extensively employed for various targets. These assays are cost-efficient, amenable for automation, and relatively easy to perform. Due to the lack of functional information, this assay format is usually not used for primary screening, but often employed during lead optimization stage to determine binding affinity, kinetics, and mechanism of action.

Ligand binding assays address the affinity between a ligand and its target:  $K = 1/K_d$ , which can be measured from kinetic experiments. In association experiments, multiple  $K_{obs}$  are measured at different ligand concentrations [C]. And  $K_{off}$  is measured in dissociation experiment at equilibrium condition. Then the association  $K_{on}$  and dissociation  $K_{off}$  rate constants can be calculated from Eq. 1, and  $K_d$  can be calculated from Eq. 2:

$$K_{ob} = K_{off} + K_{on} \times [C] \quad (1)$$

$$K_d = K_{off}/K_{on} \quad (2)$$

Binding experiments are relatively easy to perform and achieve high throughput. The assay development needs to avoid multiple issues, such as non-equilibrium dissociation and ligand depletions, which can be exacerbated by undetected impurities in the ligands studied.

Based on the nature of binding assays, the major limitation of this assay is that the studying subject compound needs to bind to the same or allosterically linked site of the ligand. This is particularly the case for Nav channels' target, due to Nav channels' high complexity and the high homology between intra- $\alpha$  subunit four domains and nine inter-Nav subtypes.

## 2.2. Nonradioligand binding assays

Traditional nonradioligand binding assays use fluorescence labeling to detect binding, including fluorescence polarization (FP) to measure the change in the rotational speed of a fluorescent-labeled ligand once it is bound; total internal reflection fluorescence (TIRF) labels target instead of ligand to measure fluorescence rotational change upon ligand binding; fluorescence resonance energy transfer (FRET) labels both ligand and target with a pair of donor and acceptor fluorescent molecules to measure fluorescent energy transfer. All these methods require that fluorescence labeling should not interfere with target-ligand interaction.

Another category of nonradioligand drug binding assays is fragment-based lead discovery (FBLD) technologies. Among them, nuclear magnetic resonance (NMR) spectroscopy is considered as the gold standard, as it measures chemical shift between free and bound targets in  $^{15}\text{N}/^1\text{H}$ ,  $^{13}\text{C}/^1\text{H}$ , and/or other labeled atom's two-dimensional correlation spectra to provide molecular interaction information [2]. In the past decade, many label-free technologies emerged to provide new options (Table 1). Isothermal titration calorimetry (ITC) and microscale thermophoresis (MST) technologies measure thermodynamic change associated with ligand binding in solution. A quartz crystal microbalance (QCM) measures a mass variation per unit area via the change in frequency of a quartz crystal resonator. Surface plasmon resonance (SPR), second harmonic generation (SHG), and biolayer interferometry (BLI) measure optical change through a sensor, which usually requires immobilizing one binding reaction component on the sensor surface. Typical applications of these FBLD technologies include fragment-based screening, binding studies for target engagement,  $K_d$  measurements, and protein conformational changes. Many of these methods, such as surface plasmon resonance (SPR), can provide insights to enzymatic reactions by directly monitoring and quantifying the binding and depletion of the reaction components in real time. The advancement of increased sensitivity and implementation of automated systems have broadened the use of FBLD technologies in drug discovery, especially in lead optimization drug discovery stage mechanism-of-action studies.

## 2.3. Membrane potential assays

Membrane potential assays have been widely used in Nav channel drug discovery. Two types of membrane potential assays have been developed [3, 4]. One uses membrane potential dye and fluorescence imaging plate reader (FLIPR) (Molecular Devices, Sunnyvale, CA). Another measures fluorescence resonance energy transfer (FRET) between a voltage-sensing oxonol acceptor and a fluorescent membrane-bound coumarin dye. Both methods have been used to identify modulators for Nav1.6, Nav1.7, and Nav1.8.

The major drawback for these assays is their reliance on using nonphysiological relevant toxin openers (e.g., veratridine, deltamethrin, or batrachotoxin) to elicit channel response. These toxins remove inactivation and causes persistent channel opening through its binding to the intracellular pore domain (Site 2). The assay can successfully detect inhibition by TTX and tetracaine, but it fails to detect Nav1.7-selective aryl sulfonamides, such as PF-05089771 and GX-936. A new strategy of eliminating key LA binding site mutation N1742 K in Nav1.7,

	Nuclear magnetic resonance (NMR)	Isothermal titration calorimetry (ITC)	Microscale thermophoresis (MST)	Quartz crystal microbalance (QCM)	Surface plasmon resonance (SPR)	Second harmonic generation (SHG)	Biolayer interferometry (BLI)
Kinetics	No	No	Yes	Yes	Yes	Yes	Yes
Immobilization-free	Yes	Yes	Yes	No	No	No	No
Label-free	Optional	Yes	Optional	Yes	Yes	No	Yes
Throughput	Medium	Low	Medium	High	Medium	High	Yes
Sensitivity	High	Medium	Medium	High	High	High	Low
Mass dependent	No	Yes	Yes	Yes	Yes	No	Yes
Sample amount	High	High	Low	Low	Low	<1 ug	Low
Costs	High	Low	Medium	Medium	High	High	Medium
Vendor	Multi	NanoTemper, etc.		Q-Sense, etc.	Multi	Biodesy	FortéBio

**Table 1.** Fragment-based lead discovery (FBLD) technologies in drug discovery.

combined with using a new activator 1K $\alpha$ PMTX, was recently reported [1]. This new assay was able to detect aryl sulfonamides, with significantly reduced sensitivity to LAs, hence shifting the assay toward non-pore-binding mechanism. Such a mechanism-specific assay design can be applied to other ion channels to facilitate discovering subtype-selective drug.

## 2.4. Ion flux assays

Early ion flux assays were primarily developed on radionuclide ions such as  $^{45}\text{Ca}^{2+}$  and  $^{22}\text{Na}^+$ . However, in the 1980s the development of ion-selective fluorescent dye-based indicators revolutionized the measurement of ion flux assay. This method provides an indirect functional detection for ion channel activity, especially for calcium and potassium channels due to the robust signals of calcium dye and thallium dye. Unfortunately, fluorescent  $\text{Na}^+$  dyes have relatively weak signals and are not amenable to reporting  $\text{Na}^+$  concentration. However,  $\text{Na}^+$  concentration can be quantitated by using atomic absorption spectroscopy (AAS). Additionally, radioisotopic  $^{22}\text{Na}^+$  still can be used as a tracer for Nav flux assay [5].

## 3. Extracellular electrophysiological technologies

Extracellular electrophysiological recording technologies employ direct or indirect electrical stimuli to a population of cell, in most cases a whole well confluent cell, and record target ion channel activity either from direct electrical signal or indirect fluorescent dye methods. These methods provide electrophysiological-involved functional assays at extracellular level, which usually represent a more physiological relevant environment, thus different from non-electrophysiological assays and typical single-cell and subcell-level electrophysiological patch clamp assays.

### 3.1. Optogenetics assay

The integration of optogenetics tools with membrane potential assays provides a powerful approach for Nav channel research and drug discovery [6]. Instead of using nonphysiological stimuli, optogenetics controls membrane potential by using light-activated channelrhodopsins (ChR2, ChR1, VChR1, and SFOs); therefore, channels can be populated to specific state, and state-dependent modulators can be identified. After optimizing the performance of channelrhodopsins and voltage reporters, this technique may contribute to Nav channel drug discovery. One potential drawback could be the introduction of false positives derived from interferences with channelrhodopsins and membrane potential dyes.

### 3.2. Electric field stimulation (EFS) assay

Recently, electric field stimulation (EFS) assay has been reported in studying Nav1.7 function in cultured rat sensory neurons. This method utilizes electrical field stimulation to evoke action potential and record action potential-driven calcium transients in the neurons through live cell imaging. This method provides a novel functional phenotypic assay platform to study voltage-gated ion channels in the network of excitable primary cell and induced pluripotent stem cell [7].

### 3.3. Multielectrode arrays (MEA)

Multielectrode arrays (MEAs) are a useful tool for monitoring the functional activity of several individual, electrically excitable cells within a larger population. MEA platforms enable noninvasive, longitudinal monitoring of cellular networks over weeks and months, so activity patterns during development and functional effects of acute and chronic treatment paradigms could be determined [8–10]. Recently, the availability of multiwell MEA plates has allowed for increased throughput, offering the ability to perform complete concentration-effect curves on cell populations.

## 4. Classical electrophysiological technologies

Single-cell-based electrophysiology remains the gold standard assay for Nav channel research, since it controls membrane voltage and measures ionic current directly, therefore assessing channel activities at distinct states. Despite the high information content, the utility of manual patch clamp electrophysiology is significantly limited by high demand for labor and skills. Therefore, automated patch clamp (APC) platforms have emerged to meet this challenge.

### 4.1. APC development and advancement

Many automated patch clamp (APC) technology platforms have been developed in the past decade [11, 12]. These include lipid bilayer recording (e.g., Orbit, from Nanion Technologies), *Xenopus* oocytes' two-electrode recording (e.g., OpusXpress, from Molecular Devices), glass pipette electrode recording (e.g., FlyScreen 8500, from Flyion), continuous microfluidic-based recording (e.g., IonFlux, Mercury, from Fluxion), and most notably chip- or plate-based planar recording technologies (Table 2, IonWorks HT, Quattro, PatchXpress 7000A, IonWorks Quattro, and Barracuda from Molecular Devices; QPatch16, QPatch HT, Qube from Sophion; Port-a-Patch, Patchliner SyncroPatch 96, 384PE, 768PE from Nanion). Among the planar platforms, the third-generation IonWorks Barracuda, Qube, and SyncroPatch 384PE/768PE have gained the most attention due to their high throughput, i.e., recording 384 or more cells in parallel.

IonWorks Barracuda was launched in 2010 and was applied for compound screening on hERG, CaV2.2, and Nav channels [13–15]. Barracuda uses perforated-patch configuration; the seal resistance was ~120 M $\Omega$  for single-hole mode and ~35 M $\Omega$  for population patch mode (64 holes). In 2014, Qube (Biolin Scientific, Sweden) and SyncroPatch (Nanion Technologies, German) were introduced with promised giga-seal data quality. Both platforms use 384 channel digital amplifier and 384 pipetting robot, borosilicate glass-based single- or multi-hole chips, and programmable negative pressure to achieve whole-cell configuration. However, they also differ in many regards. For example, Qube adopts an in-chip microfluid design to enable solution exchange, while SyncroPatch uses a liquid handler (e.g., BiomeK) so the system can be integrated for automation. SyncroPatch also can integrate two 384 modules into one robot platform, so 768 well parallel recording is feasible.

Feature	Manual	Dynaflow	Port-a-Patch	IonFlux/Mercury HT	IonWorks Barracuda	QPatch HT/HTX	Patchliner	Qube	SyncoPatch 768PE
Company		Celtec tricon	Nantion	Fluxion Bioscience	MDC/MDS	Sophion	Nantion	Sophion	Nantion
Throughput/run	1	1	1	32	384	48	16	384	768
Substrate material	Glass	Silicone rubber	Glass	Silicone rubber	Polyimide	Silicon oxide	Glass	Glass	Glass
Seal resistance, GΩ	>1	>1	>1	-0.1	-0.2	>1	>1	>1	>1
Access resistance, MΩ	<10	<10	<10	>10	15	<10	<10	<10	<10
Parallel recordings	1	96	1	64	384	48	16	384	384*2
Unique recording	1	16	1	32	384	48	8	384	768
Amplifier channels	1	96	1	32	384	48	8	384	384/768
Number of pipettes	1 or 2	1	N/A	N/A	384	8	8	384	384
Solution switch time (100%)	<10 ms	30 ms (100%)	100 ms	50 ms (100%)	50 ms	80 ms	≤20 ms	50 ms	50 ms
Compound washout	Yes	Yes	Yes	Yes	No	Yes	Yes	Yes	Yes
Compound additions	Yes	Yes	Yes	Yes	No	No	Yes	Yes	Yes
Unlimited compound additions	Yes	Yes	Yes	Yes	No	No	Yes	Yes	Yes
Internal perfusion	Yes	No	Yes	No	No	No	Yes	Yes	Yes
Rs Cslow compensation	Yes	Yes	Yes	No	No	Yes	Yes	Yes	Yes
In/out-side out configuration	Yes	No	No	No	No	No	No	No	No
Single-cell recordings	Yes	Yes	Yes	Yes	Yes	Yes	Yes	Yes	Yes
Population recordings	No	No	No	Yes 20/well	Yes 64/well	Yes 10/well	No	Yes 10/well	Yes 8/4/well
Implement date	1976		2004	2009		2009			2014

Table 2. Automated patch system comparison.



## 4.2. APC assay challenges

Even though the APC platform is superior to other nonfunctional or indirect functional assay methods by offering precise control of voltage-gated ion channels' physiological condition and direct measurement of channel activity, this technology faces many challenges including throughput, success rate, stability, integrating high-throughput data analysis, and lowering the equipment and consumable costs. The recently launched third-generation APC systems are intended to meet these challenges as a "primary screener" to perform both robust high-throughput screening and high-quality recording to support drug discovery and ion channel research. In order to bring out the best APC performance for each ion channel assay, there are many parameters that can be considered for optimization which will be discussed in the following section.

### 4.2.1. Cell line development and cell preparation

Since APC patches cell randomly from the cell suspension solution added into the system, the cell quality is critical for every APC assay. If it's possible, researcher should always pursue the best cell membrane electrophysiological property which includes homogeneous and high-target ion channel expression for good recording signal, high cell capacitance for easier cell catching, and good membrane property to facilitate achieving whole-cell configuration and stable recording. There are many methods that can be used to improve target expression such as choosing high expression host cell and expression system and test different medium and culture conditions. It is reported that using a gentle cell dissociation method followed by a thorough cell debris-removing protocol and adjusting cell solution density will improve APC success rate [16]. Also keeping the cell in serum-free medium and at lower temperature may improve current [17]. In cell line development and preparation optimization, it is vital to validate the target channel response by characterizing its electrophysiological and pharmacological properties by using reference compounds.

### 4.2.2. APC cell catching and forming whole-cell protocol

Two important parameters have to be optimized for APC recording, which are cell catching and breaking in pressure protocols and intracellular and extracellular solution compositions. Many APC systems allow programming advanced pressure protocol including holding, ramping, and rupturing steps to achieve best whole-cell configuration success rate. And some target and cell may be more sensitive to intracellular cesium and extracellular calcium ion concentrations, which usually help to achieve giga-seal. Since each target and cell line is different, one optimized pressure and solution protocol may not work well for other targets and cells.

### 4.2.3. Drug applications

Different APC systems utilize either vial (in lower-throughput platform) or plate (in higher-throughput platform) format source to deliver compound mostly by using automated liquid handler. Compound application usually is executed after recording signal reaching stable. Based on the APC system compound adding and washing capability and recording stability,

researchers chose to apply multiple concentrations of a compound to one recording, which usually decrease recording success rate but increase throughput comparing to single-dose application per recording. Also in order to avoid compound sticking to its container or pipette, the siliconizing reagent for glass and other surfaces can be included in the compound buffer after being validated using reference compounds.

#### *4.2.4. Recording stability*

In order to validate the pharmaceutical effect from adding compound, it's important to include positive and negative controls to monitor recording stability. In the ideal condition, the negative control recording should remain stable throughout the whole experiment, which requires cell membrane seal resistance, cell capacitance, and series resistance to remain stable. To achieve this, each APC assay usually needs to be optimized with various conditions, including intracellular and extracellular solution compositions, voltage protocol, pressure protocol, and experimental procedure design. Many times, the current decrease independent of any compound application can be observed, which is called "rundown." For Nav channel, rundown is usually caused by the holding membrane voltage ( $V_m$ ), in which the closer  $V_m$  to half inactivation, the stronger slow inactivation-inducing effect will occur. So in order to examine inactive state-dependent modulator, the Nav assay voltage protocol has to be well designed and validated.

#### *4.2.5. High-throughput data analysis*

High-throughput data analysis is another major challenge in developing APC assay, especially in performing high-throughput screening. It is essential to build a robust high-throughput data analysis method in the assay development stage. To achieve this, two issues need to be overcome. One is data reduction strategy, which means extracting key parameters from each current sweep, such as peak current amplitude for signal change analysis, and three recording quality control (QC) parameters including seal resistance, cell capacitance, and series resistance. Another issue is to develop a robust and reliable data QC strategy to exclude poor-quality recordings, which can be achieved by using self-developed script program or commercial available software by setting proper QC criteria for the three QC parameters' value and stabilities at the desired time points of the experiment.

## **5. Concluding remarks**

The advancement of technologies has made significant impact on Nav channel research and drug discovery in the past decade. As true for all drug screenings, no universal screening strategy can fit for all needs. Currently, primary uHTS is usually performed by using a validated non-electrophysiological functional assay and followed up by APC assay for potential hits' confirmation and characterization. Overall, the advancement of high-throughput APC coupled with rational assay designs has offered unprecedented capacity for Nav channel drug discovery.

## Acknowledgements

We gratefully acknowledge contributions from Genentech Inc. to support this publication.

## Conflict of interest

The authors are all employees of Genentech Inc. (a Roche Group Company) and declare no financial and conflict of interest in this article.

## Author details

Tianbo Li\* and Jun Chen

\*Address all correspondence to: [li.tianbo@gene.com](mailto:li.tianbo@gene.com)

Department of Biochemical and Cellular Pharmacology, Genentech (Roche Group),  
South San Francisco, California, USA

## References

- [1] Chernov-Rogan T, Li T, Lu G, Verschoof H, Khakh K, et al. Mechanism-specific assay design facilitates the discovery of Nav1.7-selective inhibitors. *Proceedings of the National Academy of Sciences of the United States of America*. 2018;**115**:E792-E801. DOI: 10.1073/pnas.1713701115
- [2] Pellicchia M, Bertini I, Cowburn D, Dalvit C, Giralt E, et al. Perspectives on NMR in drug discovery: A technique comes of age. *Nature Reviews Drug Discovery*. 2008;**7**:738-745. DOI: 10.1038/nrd2606
- [3] Finley M, Cassaday J, Kreamer T, Li X, Solly K, et al. Kinetic analysis of membrane potential dye response to Nav1.7 channel activation identifies antagonists with pharmacological selectivity against Nav1.5. *Journal of Biomolecular Screening*. 2016;**21**:480-489. DOI: 10.1177/1087057116629669
- [4] Liu CJ, Priest BT, Bugianesi RM, Dulski PM, Felix JP, et al. A high-capacity membrane potential FRET-based assay for Nav1.8 channels. *Assay and Drug Development Technologies*. 2006;**4**:37-48. DOI: 10.1089/adt.2006.4.37
- [5] Fitch RW, Daly JW. Phosphorimaging detection and quantitation for isotopic ion flux assays. *Analytical Biochemistry*. 2005;**342**:260-270. DOI: 10.1016/j.ab.2005.04.041

- [6] Zhang H, Cohen AE. Optogenetic approaches to drug discovery in neuroscience and beyond. *Trends in Biotechnology*. 2017;**35**:625-639. DOI: 10.1016/j.tibtech.2017.04.002
- [7] Yuste R, MacLean J, Vogelstein J, Paninski L. Imaging action potentials with calcium indicators. *Cold Spring Harbor Protocols*. 2011;**2011**:985-989. DOI: 10.1101/pdb.prot5650
- [8] McConnell ER, McClain MA, Ross J, LeFew WR, Shafer TJ. Evaluation of multi-well microelectrode arrays for neurotoxicity screening using a chemical training set. *Neurotoxicology*. 2012;**33**:1048-1057. DOI: 10.1016/j.neuro.2012.05.001
- [9] Newberry K, Wang S, Hoque N, Kiss L, Ahlijanian MK, Herrington J, Graef JD. Development of a spontaneously active dorsal root ganglia assay using multiwell multielectrode arrays. *Journal of Neurophysiology*. 2016;**115**:3217-3228. DOI: 10.1152/jn.01122.2015
- [10] Massobrio P, Tessadori J, Chiappalone M, Ghirardi M. *In Vitro* studies of neuronal networks and synaptic plasticity in invertebrates and in mammals using multielectrode arrays. *Neural Plasticity*. 2015;**2015**:1-18. DOI: 10.1155/2015/196195
- [11] Picones A, Loza-Huerta A, Segura-Chama P, Lara-Figueroa CO. Contribution of Automated Technologies to Ion Channel Drug Discovery. *Advances in Protein Chemistry and Structural Biology*. 2016;**104**:357-378. DOI: 10.1016/bs.apcsb.2016.01.002. Epub 2016 Mar 3
- [12] Comley J. Automated patch clamping finally achieves high throughput! *Drug Discovery World*. 2014;**4**:45-56
- [13] Mannikko R, Bridgland-Taylor MH, Pye H, Swallow S, Abi-Gerges N, et al. Pharmacological and electrophysiological characterization of AZSMO-23, an activator of the hERG K(+) channel. *British Journal of Pharmacology*. 2015. DOI: 10.1111/bph.13115
- [14] Cerne R, Wakulchik M, Li B, Burris KD, Priest BT. Optimization of a high-throughput assay for calcium channel modulators on IonWorks Barracuda. *Assay and Drug Development Technologies*. 2016;**14**:75-83. DOI: 10.1089/adt.2015.678
- [15] Cerne R, Wakulchik M, Krambis MJ, Burris KD, Priest BT. IonWorks Barracuda assay for assessment of state-dependent sodium channel modulators. *Assay and Drug Development Technologies*. 2016;**14**:84-92. DOI: 10.1089/adt.2015.677
- [16] Li T, Lu G, Chiang EY, Chernov-Rogan T, Grogan JL, Chen J. High-throughput electrophysiological assays for voltage gated ion channels using SyncroPatch 768PE. *PLoS One*. 2017;**12**:e0180154. DOI: 10.1371/journal.pone.0180154
- [17] Danker T, Möller C. Early identification of hERG liability in drug discovery programs by automated patch clamp. *Frontiers in Pharmacology*. 2014;**5**:203. DOI: 10.3389/fphar.2014.00203

---

# Genetic Defects of Voltage-Gated Sodium Channel $\alpha$ Subunit 1 in Dravet Syndrome and the Patients' Response to Antiepileptic Drugs

---

Tian Li

Additional information is available at the end of the chapter

<http://dx.doi.org/10.5772/intechopen.76390>

---

## Abstract

In the past decade, hundreds of mutations have been found in the *SCN1A* (sodium voltage-gated channel  $\alpha$  subunit 1) gene in the epileptic patients. The functioning of the *SCN1A* gene products is intensively studied in the neuroscience field. The loss-of-function mutations of the *SCN1A* gene are the causative factor of Dravet syndrome, an intractable epilepsy syndrome. With the loss-of-function  $\text{Na}_v1.1$  (the protein encoded by *SCN1A* gene), the selective dysfunction of the inhibitory parvalbumin (PV) interneurons impairs the balance of excitatory and inhibitory synaptic inputs to the downstream neurons, and causes the hyperexcitability of the neuronal network. The underlying mechanism is that the axon initial segments (AISs) of inhibitory parvalbumin interneurons predominantly express  $\text{Na}_v1.1$ , particularly in the proximal end of the AISs. The deficiency of  $\text{Na}_v1.1$  weakens the excitability of the inhibitory parvalbumin neurons and leads to the hyperexcitability of the neuronal network. The sodium channel blockers, one category of the antiepileptic drugs (AEDs) that specifically block the activity of VGSCs, may potentially worsen the defect of  $\text{Na}_v1.1$  of the PV interneurons in the patients with the *SCN1A* gene loss-of-function mutations, aggravate the clinical manifestation, and increase the seizure frequency of those patients.

**Keywords:** epilepsy, Dravet syndrome, voltage-gated sodium channel, axon initial segment, interneuron

---

## 1. Introduction

Voltage-gated sodium channels (VGSCs) play an essential role in the generation of the action potentials, which are the primary way for the communication between the excitable cells,

---

particularly the neurons. The action potential is the fast method to collect the afferent sensory information and to relay the efferent motor commands in the nervous system. The pathways to transfer the action potentials rely on the organized expression and the proper functioning of VGSCs [1]. The genetic mutations that cause the defected expression of VGSCs or the malfunction of the altered VGSC gene products impair the physiological function of conduction pathway [2], nerve nuclei [3], and cortical neurons [4]. Epilepsy is a common multifactorial neurological disease that is caused by both environmental and genetic factors [5]. Several ion-channel genes are evidently associated with epilepsy, such as *SCN1A* [6], *SCN2A* (sodium voltage-gated channel  $\alpha$  subunit 2) [7], *SCN8A* (sodium voltage-gated channel  $\alpha$  subunit 8) [8], *GABRA1* (gamma-aminobutyric acid type A receptor  $\alpha$  1 subunit), *GABRG2* (gamma-aminobutyric acid type A receptor  $\gamma$ 2 subunit) [9], and *KCNA2* (potassium voltage-gated channel subfamily A member 2) [10]. Those genes predominantly control at least one critical event in a specific neuron type or/and a particular subcellular region during the physiological functioning of the neurons. The irreversible dysfunction of those gene products leads to the permanent pathological alteration of the targeted neurons and increases the susceptibility to seizures.

## 2. VGSC $\alpha$ subunit 1 and Dravet syndrome

$\text{Na}_v1.1$  existing in the majority in the brain and was labeled at the soma and dendrites of the neurons in the early studies, referred as  $\text{Na}^+$  channel subtype RI, or Type I  $\text{Na}^+$  channel alpha-subunit [11, 12]. Nowadays, more than 1000 mutations [13] have been found in the *SCN1A* genes. They have been believed as the causative factors of generalized epilepsy with febrile seizure plus (GEFS+) [14], Dravet syndrome (severe myoclonic epilepsy of infancy—SMEI) [15], and migraine [16]. The *SCN1A* gene could be called as “an epilepsy gene” because of its close relationship with febrile seizures and the epilepsies with antecedent febrile seizures [13]. Dravet syndrome has been intensively studied within *SCN1A* gene mutations, the related functional analysis [6, 17], and the high phenotype-genotype correlations to *SCN1A* gene [18]. It is a rare disease of 1-to-40,000 incidence in the USA at estimate and 1-per-15,700 incidence in northern California with evidence [19]. The debilitating clinical progress goes from the “febrile stage” in the first year of life, the “worsening stage” until the age of 6 years, to the “stabilization stage” in the rest of life [20]. The clinical case may have the family history of epilepsy or febrile seizures, no previous medical history (an apparently normal baby), and the generalized or unilateral febrile seizures beginning in the first year followed by myoclonic jerks, partial seizures, atypical absence, and status epilepticus. The patients progressively lose the neurological functioning, such as retarded psychomotor development, ataxia, pyramidal signs, interictal myoclonus, intellectual deficiency or cognitive impairment, and personality disorders [21]. A French pediatrician, Dr. Charlotte Dravet, first described the rare disease in 1978 [22], and in 2001, Lieve Claes team in Belgium found seven *SCN1A* gene mutations in SMEI patients, including four frame-shift and truncation mutations (c.657-658delAG, c.3299-3300insAA, c.5010-5013delGTTT, and c.5536-5539delAAAC), one nonsense mutation (c.664C>T), one splice donor mutation

(IVS22+1G>A), and one missense mutation (c.2956C>T) [15]. The subsequent genotyping studies indicated that the *SCN1A* gene truncation mutations appeared with the higher frequency in Dravet syndrome than in the milder phenotype of febrile seizure-related epilepsy, and furthermore, the cognitive function impairment of the *SCN1A*-positive epilepsy patients also associated with the truncation variants, regardless of age at seizure onset [23]. Those truncation mutations severely alter the molecular structure of sodium channel, reduce the expression amount of the *SCN1A* gene products, and hence severely impact the  $\text{Na}_v1.1$ -VGSC functioning in the neurons. The underlying pathogenic mechanism of one-allele truncation could be due to the haploinsufficiency (the loss of the half amount of  $\text{Na}_v1.1$ ) [24] or a dominant-negative effect that represents the mutated proteins (truncated  $\text{Na}_v1.1$ ) negatively affect wild-type products (normal allele-expressed  $\text{Na}_v1.1$ ) [25]. However, the truncated  $\text{Na}_v1.1$  protein in the human brain sample of a patient with Dravet syndrome was not detected, while the mRNA of both the wild-type and the truncation mutations was equally expressed. It was explained as the endoplasmic reticulum-associated degradation of the misfolded or misassembled protein caused the absence of the truncated  $\text{Na}_v1.1$  protein [26]. Therefore, the lower expression of the  $\text{Na}_v1.1$  protein, the haploinsufficiency of *SCN1A* gene, should be the main pathogenesis of *SCN1A* truncation mutations. The remaining mutations of *SCN1A* gene causing Dravet syndrome are the missense and splice-site mutations that mistakenly code the amino acids building the pore-forming region of VGSC [27] and cause the severe impairment of the function and electrophysiological properties of the  $\text{Na}_v1.1$  protein (VGSC  $\alpha$  subunit 1) [28–30].

Both the haploinsufficiency and the pore-forming mutations of *SCN1A* gene impact the VGSC function severely because structurally the  $\text{Na}_v1.1$  protein constructs the main part of VGSC complex. This type of sodium channel is made up of a large pore-forming glycosylated  $\alpha$  subunit and one or two small  $\beta$  subunits non-covalently ( $\beta1$  or  $\beta3$ ) or covalently ( $\beta2$  or  $\beta4$ ) associated with the large  $\alpha$  subunit. The  $\alpha$  subunit is coded by *SCN1A-SCN11A* gene ( $\text{Na}_v1.1$ - $\text{Na}_v1.9$  protein) and responsible for the generation of transmembrane sodium current. The  $\beta$  subunits regulate the electrophysiological properties of sodium current (the gating and kinetics of  $\alpha$  subunits) and the subcellular location or expression of  $\alpha$  subunit [31]. Those mutations disable the main part of VGSC,  $\alpha$  subunit, by either the insufficient amount of subunit for the complex resembling or the structurally altered subunit to make the malfunctioning complex. The primary structure of the VGSC  $\alpha$  subunit contains four internally repeated transmembrane domains (I–IV). Each domain includes six  $\alpha$ -helical transmembrane segments (S1–S6). The S1–S4 segments are the voltage-sensing module, and the S5–S6 segments are the pore-forming module (D400, E755, K1237, and A1529 in each of four homologous domains, forming part of the selectivity filter [32]). Nine members of VGSC  $\alpha$  subunits ( $\text{Na}_v1.1$ – $\text{Na}_v1.9$ ) have been identified with similar complex structure and functional properties [33].  $\text{Na}_v1.1$  is tetrodotoxin (TTX)-sensitive and could be blocked by nanomolar concentrations of TTX [34].  $\text{Na}_v1.1$ ,  $\text{Na}_v1.2$  (*SCN2A*),  $\text{Na}_v1.3$  (*SCN3A*), and  $\text{Na}_v1.6$  (*SCN8A*) primarily locate in central nervous system and are the primary subtypes of VGSCs in the neurons of brain and spinal cord [35]. Four subtypes of VGSC  $\alpha$  subunits in the central nervous system express in the specific neuron types and the specific subcellular location [36, 37].

### 3. Animal models and pathogenic mechanism of Dravet syndrome

Based on the genotyping results that the *SCN1A*-gene truncation mutations are found in the large percentage of patients with Dravet syndrome [18], the scientists produce the genetic models to disrupt the *SCN1A* gene by truncation mutations. They successfully duplicate the clinical features in mouse models of Dravet syndrome, such as spontaneous and frequent seizures, impaired neurological function, and premature death [4, 38, 39]. Yu et al. at the University of Washington, USA, first replaced the last exon (Exon 26) of *SCN1A* gene of 129/SvJ and C57BL/6 mice with neomycin-resistance gene cassette to make the truncation at the domain IV, S3 segment of Na<sub>v</sub>1.1 protein. By measuring whole-cell sodium currents of the dissociated neurons, the authors found a substantial decrease in the sodium current amplitude and other significant alteration of electrophysiological features, which indicated the reduced amount of the functional VGSCs in *Scn1a*<sup>-/-</sup> and *Scn1a*<sup>+/-</sup> interneurons. They also confirmed that in those GABAergic inhibitory interneurons the VGSC subtype Na<sub>v</sub>1.3 was upregulated to compensate the reduced functional Na<sub>v</sub>1.1 protein, without the apparent increase of Na<sub>v</sub>1.2 and Na<sub>v</sub>1.6 [4]. The group of Mistry at the Vanderbilt University, USA, generated another *SCN1A* gene truncation mice in 2014 by disrupting Exon 1 of the *SCN1A* gene. They measured the electrophysiological features of acutely dissociated hippocampal neurons and found that the sodium channel density was lower in GABAergic interneurons of the *Scn1a*<sup>+/-</sup> mice. Furthermore, the sodium channel density in excitatory pyramidal neurons of *Scn1a*<sup>+/-</sup> mice was also elevated, which potentially correlated with age-dependent lethality. Although the phenotype severity was variable due to the factors of strain and age of mice with Dravet syndrome, the findings first emphasized the contribution of pyramidal neuron hyperexcitability during the pathological process in the study of animal model [38]. Both of the studies point out that the imbalance of electrophysiological activities of the excitatory (pyramidal neurons) and the inhibitory neurons (GABAergic interneurons) is the fundamental pathogenesis to cause the intractable seizures in mice with Dravet syndrome that had the *SCN1A* gene truncation mutations.

Furthermore, the Ogiwara group in Japan provided the results from an *SCN1A* truncation knock-in mouse model, which displayed the specific subcellular region of Na<sub>v</sub>1.1 deficiency in those dysfunctional inhibitory neurons. By inserting the nonsense mutation R1407X into mouse *SCN1A* gene, the authors found that the truncated Na<sub>v</sub>1.1 protein was not detectable in either *Scn1a*<sup>RX/RX</sup> or *Scn1a*<sup>+RX</sup> knock-in mice. In the neocortex of those developing mouse brain, only a subpopulation of the neocortical neurons, the parvalbumin-positive interneurons (PV neurons), had the Na<sub>v</sub>1.1 immunostaining signals, predominantly at the axon initial segments (AISs). Consequently, the *Scn1a*<sup>+RX</sup> neocortical PV interneuron (GAD67+), fast-spiking interneurons, displayed the spike amplitude decrement during prolonged spike trains [6, 39]. That important study proved the specific functional defect of the PV neurons and the critical pathophysiological role of the PV neurons in Dravet syndrome. Moreover, in an in-vivo animal study, using the advanced techniques, such as optogenetics, local field potential, and multiunit activity signals recording, the authors surprisingly found that the spontaneous cortical activity of *Scn1a*<sup>+/-</sup> mice did not alter in vivo. Although after sacrificing those mice, they could recognize the seizure-related pathological changes in the brain slices, such as the hypoexcitability of the parvalbumin and somatostatin interneurons, the rapid propagation of epileptiform activity, and the pathogenic synaptic adaptations [40]. Therefore, we could reason



that the interneuron hypoexcitability should exist much earlier than the electroencephalography (EEG)-positive findings in the patients with Dravet syndrome.

The other type of *SCN1A* gene mutations causing Dravet syndrome is the missense mutation in the pore-forming region of VGSC. Another group in Japan, using gene-driven ENU mutagenesis technique, generated *Scn1a*-targeted rats carrying a missense mutation N1417H miscoding the amino acid in the third pore region of VGSC [29]. The clinical feature of the N1417H rat was milder than that of truncation *Scn1a* mouse models. The rat had neither spontaneous seizures nor apparent pathological abnormality in the brain in the earlier life, but at postnatal week 5, after a hot water bath about 3.5 min, the rats exhibited clonic seizures. The susceptibility to hyperthermia-induced seizures increased with age. The hippocampal GABAergic interneurons of the N1417H rats were hypoexcitable with the reduced action potential amplitude. The authors believed that the clinical phenotype of the N1417H rat was close to that of generalized epilepsy with febrile seizure plus (GEFS+) [41]. However, the common pathogenic mechanism of the truncation mutations and the pore-forming region mutations of  $\text{Na}_v1.1$  is the selective interneuron dysfunction and hypoexcitability due to the  $\text{Na}_v1.1$  deficiency or malfunction. The results from the study of the N1417H rat enhance the hypothesis that the selective impairment of the PV interneurons is the primary pathogenesis of febrile seizure-related epilepsy syndrome, the clinical spectrum from GEFS+ to Dravet syndrome [18].

#### 4. Inhibitory interneurons and the features for their specialties

During the processing of the neuronal activities in the central nervous system, the simultaneous excitation and inhibition assure the proper excitability of the neuronal network and the precise control of the neuronal functions. Inhibition in the cortex is generated by the GABAergic neurons, which make up about 20% of the cortical neuronal population. Compared with the pyramidal cells (excitatory neurons), they have the smaller size and much shorter-range projects of the axon to form the local circuit with the nearby neurons and layers [42]. The interneurons could generate the long-lasting currents, the faster reaction to stimuli, and the higher-frequency signal transmission. The inhibition in a neuronal microcircuit could apply at the right millisecond (timing) and with the precise amount (dosing) exactly matching the inhibitory demand [42, 43]. The defects of GABAergic neuronal function have been identified as the contributive factors to the neuronal diseases, such as epilepsy, schizophrenia, and autism spectrum disorders [44, 45]. The cell therapy strategy of the GABAergic neurons for epilepsy was applied in several significant studies of epileptic model and stem cells [44, 46]. In the studies of animal models of Dravet syndrome, the constitutive  $\text{Na}_v1.1$  knockout selectively impacted the functioning of the inhibitory parvalbumin interneurons, spared the detectable dysfunction of the excitatory neurons, and caused by the imbalance of excitation and inhibition, which led to the spontaneous and intractable seizures [4, 38, 39]. On the background of the  $\text{Na}_v1.1$  knockout specifically in the PV neurons, the addition of  $\text{Na}_v1.1$  knockout specifically in the excitatory neurons could alleviate the clinical manifestation of Dravet syndrome [6] and potentially re-balance the excitatory and inhibitory neuronal activity. Based on those results, we can understand that the balancing status of inhibitory neurons and excitatory neurons functioning is the determinant of the clinical phenotypes of Drave syndrome.

The several types of inhibitory interneurons are called as “basket” cells, “chandelier” cells, and “Martinotti” cells due to their morphological features. Because of their morphological advantages, they connect and inhibit the particular compartment of principal neurons [42]. The “basket” cells have the highly branched axons that innervate the target somas and the proximal dendrites of pyramidal neurons, as the axonal branches appear like baskets surrounding the pyramidal neurons. In hippocampus CA1, the parvalbumin-expressing basket cells (PVBCs, 26% of CA1 interneurons) are more than the cholecystokinin-expressing basket cells (CCKBCs, 12% of CA1 interneurons) [47]. The PVBCs place 99% output to connect the pyramidal cells and the rest 1% output to form the gap junctions and reciprocal synaptic connections onto themselves or other interneurons generating gamma oscillation [48, 49]. The “chandelier” cells that are also parvalbumin positive have the “cartridges” shape of the axonal arbors that selectively inhibit the AISs of pyramidal cells, and hence they are also called the axon-axonic cells providing precise control of the action potential generation of pyramidal cells [48, 50, 51]. The axon-axonic cells represent about 15% of all PV hippocampal interneurons [47]. The “Martinotti” cells target the apical dendritic tuft and express the somatostatin and calbindin but not parvalbumin or vasoactive intestinal peptide (VIP) [52]. In the hippocampus, the rest of PV cells is “Bistratified” cells, which represent about 25% of PV hippocampal interneurons with the PV-immunosignal on the somatodendritic compartments. In the PVBCs, the Na<sup>+</sup> channels are sparse in the dendrites where K<sup>+</sup> channels predominate. The Na<sup>+</sup> channels cluster at the AIS of PVBCs. In fact, 99% of PVBC Na<sup>+</sup> channels are located in the axonal compartment [53]. The unique feature of the high-density distribution of Na<sup>+</sup> channels at the PVBC AISs determines the fast-spiking pattern of the PVBCs, which typically generate uniform, non-changing, and high-frequency discharge [54].

## 5. AIS and VGSC

Axon initial segment (AIS) contains the high density of sodium and potassium channels; the scaffolding protein ankyrin G (AnkG),  $\beta$ IV spectrin, and extracellular matrix-binding protein neurofascin; and the ion channel-associated protein FGF14 (fibroblast growth factor 14). Those are necessary to help the sodium channels locate and cluster at the AIS [55]. The AIS has the lowest threshold for action potential initiation because of the highest density of sodium channels when compared with somatodendritic compartment [53]. The proper functioning of AIS is essential for action potential initiation and adaptive cell excitability of both pyramidal cells (excitatory neurons) and GABAergic interneurons (inhibitory neurons). Many factors regulate the function of the sodium channels at the AIS [55, 56]. First, the distinctive VGSC  $\alpha$  subunit types express in specific neuronal types and the particular regions of AIS. In the human brain tissue, the fluorescence signals of Na<sub>v</sub>1.1 have been found at the thinly AnkG-labeled AIS, which putatively belongs to the interneurons, while Na<sub>v</sub>1.2 and Na<sub>v</sub>1.6 are located at the AISs of human cortical pyramidal cells [51]. Na<sub>v</sub>1.6, the low-threshold sodium channel subtype, accumulates at the distal end of AIS of cortical pyramidal cells, which is responsible for generating the action potentials. The high-threshold Na<sub>v</sub>1.2 locates at the proximal end of AIS of cortical pyramidal cells, which regulates the action potential backpropagation [57]. The

$\text{Na}_v1.1$  has been found at the proximal end of AIS of cortical and cerebellar interneurons and the axons of main olfactory bulb neurons. The  $\text{Na}_v1.1$  immunosignals predominantly outline the axons of the parvalbumin-positive neurons [58]. The action potential threshold of  $\text{Na}_v1.6$  is more hyperpolarized (15–25 mV lower) than that of both  $\text{Na}_v1.2$  and  $\text{Na}_v1.1$ . Unlike  $\text{Na}_v1.6$  more likely producing a persistent current,  $\text{Na}_v1.1$  and  $\text{Na}_v1.2$  show the apparent use-dependent inactivation (higher than 20 Hz) [59, 60]. Therefore, the accumulated  $\text{Na}_v1.6$  at the distal end of the AIS facilitates the action potential initiation, while  $\text{Na}_v1.2$  and  $\text{Na}_v1.1$  subunits gathering at the proximal end of AIS prevent the high-frequency firing of nerve cells backward.

Second, the molecule complex at AIS, composed of the ion channels (Kv1, T-type  $\text{Ca}^{2+}$  channel) and ligands (FGF14, VGSC  $\beta$  subunit 1, and  $\beta\text{IV}$  spectrin), directly or indirectly cooperates with  $\text{Na}^+$  channel and regulates the neuronal excitability. FGF14 could directly interact with the C-terminal of VGSC  $\alpha$  subunit ( $\text{Na}_v1.1$ ,  $\text{Na}_v1.2$ ,  $\text{Na}_v1.6$ ) in the transfected HEK293 cells [61]. The *fgf14*<sup>-/-</sup> mice showed the significantly reduced number of the PV interneurons, but the pyramidal neuron number was unchanged in the CA1 hippocampus region. This change cooperated with the reduced GAD67 immunosignals in PV cell soma, the reduced gamma oscillations in CA1 stratum radiatum layer, and the deficits in spatial working memory, which was displayed by the eight-arm maze test [62]. Because the FGF14 is a complementary protein of  $\text{Na}_v1.1$ ,  $\text{Na}_v1.2$ , and  $\text{Na}_v1.6$  at the AIS [61, 63, 64], the pyramidal cells of the *fgf14*<sup>-/-</sup> mice should have been affected as well due to the loss of FGF14: $\text{Na}_v1.6$  and FGF14: $\text{Na}_v1.2$  complex. Why are the PV cells the first or most to be affected by FGF14 protein defect or the FGF14: $\text{Na}_v1.1$  complex deficiency? What makes the FGF14: $\text{Na}_v1.1$  critical for the excitability of the PV cells and finally impact on the number of the live PV cells? Similarly, the  $\text{Na}_v1.1$ -predominant proximal end of the AIS only occupies a small part of the AIS of the PV cells, and why the  $\text{Na}_v1.1$  deficiency impairs the PV cell functions dramatically and causes the Dravet syndrome? We expect the promising studies and explanation in future. Other molecules in the AIS complex, such as VGSC  $\beta$  subunit and AnkG, have been recognized as the ligand or the anchoring protein to stabilize the VGSC  $\alpha$  subunit and regulate their functions at the AIS [65, 66].

Third, the location and the size of the AIS can be adapted for the neuronal activity and the long-term plasticity. The longer AIS, the higher excitability of the neuron. The more proximal location of the AIS, the higher excitability of the neuron. The chronic depolarization of the dissociated neurons moved the AIS distally and then decreased the neuronal excitability. The dynamic regulation of the AIS location through activity-dependent structural reorganization relied on the activation of T-type voltage-gated calcium channels and the elevation of intracellular  $[\text{Ca}^{2+}]$  [67]. On the other hand, the experiments to eliminate the sensory stimuli made the AIS longer with little change in  $\text{Na}^+$  channel density and ion channel composition at the AIS, which increased the whole cell  $\text{Na}^+$  current, and the neuronal excitability. However, those adaptive responses also depend on the neuronal types due to the distinctions of the AIS location of different neurons under the standard conditions [67]. In the PV interneurons, the action potentials are generated at 20  $\mu\text{m}$  away from the soma at the AIS [53], which means the proximal part of the AIS of the PV neurons locates even closer than 20  $\mu\text{m}$  since the action potential generates at the beginning of the distal part of the AIS. The AIS of the PV neurons locates more proximal than the AIS of pyramidal cells that has been observed at 20–60  $\mu\text{m}$  from the soma by ankyrin G staining [68]. Using specific neuronal marker labeling,

Höfflin et al. saw the AISs of the pyramidal neurons were significantly longer than that of the interneurons [69]. Based on those findings of the PV interneurons and their AISs, neuroscientists may have many interests in the regulatory mechanisms of  $\text{Na}_v1.1$  cooperative functioning and adaptive response to the neuronal activity, coupling with the dynamic plasticity of the PV interneuron AIS.

With the specialized output structures of PV interneurons (“basket” or “chandelier cartridge”), the interactions of the PV interneurons (PVBCs or chandelier cells) and the pyramidal cells, inhibitory synapses, are accordingly subject to the dynamic regulation of adaptive neuronal functioning and the AIS plasticity. The chandelier cell axon terminals only contact the AISs of pyramidal cells and have three to five boutons per cartridge. The innervation patterns are similar at different postnatal age. Multiple chandelier cells (four at estimate) connect one pyramidal cell, while one chandelier cell contacts 35–50% of pyramidal cells in the traversed area by its axonal arbor [70]. The inhibitory synapses exist in the innervation of a chandelier cell to the pyramidal cell by nature. The innervation could be visible by labeling the chandelier cells (pre-synaptic component) with the marker of GABA membrane transporter 1 (GAT1) or parvalbumin (PV) and labeling the post-synaptic pyramidal cell AIS with GABA<sub>A</sub> receptor  $\alpha_2$  subunit. The structures and functioning status of those synapses keep updated to meet the dynamic developmental demands [71, 72] and are impacted in the specific areas by pathological conditions, such as epilepsy and schizophrenia [73, 74].

## 6. Treatment to Dravet syndrome and therapeutic response

Dravet syndrome is an intractable epileptic encephalopathy with the unfavorable outcome. The most commonly used AEDs for patients with Dravet syndrome include valproate, topiramate, benzodiazepines, stiripentol, and potassium bromide [22]. Because the high percentage of patients with Dravet syndrome have the *SCN1A* gene mutations [18], some AEDs should be avoided, such as the sodium channel blockers (lamotrigine [75] and carbamazepine [76]), to prevent the inhibition of the rest  $\text{Na}_v1.1$  functioning in PV interneurons. Guerrini et al. retrospectively reviewed 21 Dravet syndrome cases and found that 80% (17) patients with lamotrigine treatment showed >50% increase in seizure frequency for 2 months and then ceased the lamotrigine treatment [75]. In a large-sized (276 patients) study, Shi et al. showed the evidence that the treatment of carbamazepine to Dravet syndrome was either not effective (<50% seizure reduction) or worsening the clinical condition (>25% increase in seizure frequency) [76]. Considering the high percentage of *SCN1A* gene mutations in Dravet syndrome and the potential risk of worsening seizures by AEDs, the clinicians recommend a screening test to detect the *SCN1A* gene mutations for the suspected patients with Dravet syndrome (the initially normal infants suffering from prolonged, recurrent, febrile, and hemiclonic seizures induced by bathing). The purpose of the screening test is to optimize AEDs and rehabilitation therapy [77, 78] at the earlier stage of the disease. The test can be done with the direct sequencing of the coding exons of *SCN1A* gene or multiplex ligation-dependent probe amplification [79]. There are an increasing number of the adult patients with the intractable seizures, who finally are diagnosed with Dravet syndrome. They may retain the partial seizures,

secondary generalized clonic-tonic seizures [80], and intellectual disability, which are all not the characteristic symptoms for the diagnosis of Dravet syndrome. It is not occasional that those underdiagnosed patients with Dravet syndrome have been treated with sodium channel blockers, such as carbamazepine and oxcarbazepine, for years. However, the attempt to withdraw the treatment of carbamazepine or oxcarbazepine from those adult patients is still risky for seizure frequency rebound, withdrawal-related seizure, and sudden death [81].

Valproate is the most frequently used AED to treat Dravet syndrome. Shi et al. found that 87% of *SCN1A* mutation patients and 78% of *SCN1A* negative patients were using valproate. About 52% of *SCN1A* mutation patients and 41% *SCN1A* negative patients responded to the valproate treatment (>50% reduction in seizure frequency). Bromide (potassium bromide and sodium bromide) was the most effective AED. About 41% *SCN1A* mutation patients and 21% *SCN1A* negative patients used bromide with 71% and 94% responder rate, respectively. The *SCN1A* negative patients had the significantly higher responder rate to bromide, when compared with *SCN1A* mutation patients [76]. Bromide therapy was usually used in combination with valproate (100%), topiramate (91%), clobazam (75%), levetiracetam (66%), and so on. After 3 months of treatment, 81% of patients (26/32) had >50% reduction in seizure frequency, and after 12 months of treatment, 47% of patients (15/32) still maintained >50% seizure reduction [82]. Verapamil add-on treatment was reported in two pediatric patients with Dravet syndrome. They gained the long-period (13 months and 20 months) seizure free with the verapamil dosage of 1.5 mg/kg/day. As a result of a long period of seizure free, the patient's neurological and cognitive function improved significantly [83]. Levetiracetam add-on treatment was proved as an effective therapy to Dravet syndrome by an open-label clinical trial. The dose was titrated up to 50–60 mg/kg/day within 5- to 6-week up-titration phase and maintained in a 12-week evaluation phase. The responder rate ranged from 44.4 to 64.2% varied by the distinctive seizure types [84]. Stiripentol is one of the commonly used medications for Dravet syndrome. Because of its fair tolerability profile, stiripentol is frequently added within valproate and clobazam and maintained in the triple long-term therapy remedy (96% patients). However, the effectiveness of stiripentol is not ideal for seizure control. De Liso et al. evaluated 54 patients with Dravet syndrome after stiripentol maintenance at the dose of 35–50 mg/kg/day. They found that 96% of patients continued to have clonic or tonic-clonic seizures (38% of patients had the seizure frequency more than three times per month, 40% of patients remained seizure frequency once to three times per month, and the rest of patients remained yearly seizures) [85]. Balestrini and Sisodiya observed stiripentol add-on treatment in 13 patients with Dravet syndrome. Only 23% of patients (3/13) gained >50% reduction in seizure frequency, 23% of patients (3/13) showed seizure worsening, 23% of patients (3/13) showed no change, and 15% of patients (2/13) showed <50% reduction in seizure frequency [86]. Obviously, the responder rate or effectiveness of the pharmacological treatment of Dravet syndrome is not ideal. The clinicians also assessed the vagus nerve stimulation for Dravet syndrome treatment. Fulton et al. placed the vagus nerve stimulation for 12 patients with Dravet syndrome and assessed the seizure control after 6 months. Nine of them showed >50% reduction in generalized tonic-clonic seizures, and four of them showed the cognitive function improvement [87]. Neuroscientist screened the potential therapeutic agents and tested their effectiveness in vivo in the experimental setting. *Scn1Lab* zebrafish model was

used for the fast drug screening for *SCN1A*-mutated Dravet syndrome. Baraban et al. applied the molecules in the swimming bath of the mutant or control zebrafish, tracked the swimming velocity and behaviors of the zebrafish, and identified clemizole that could inhibit seizure behavior and electrographic seizures of the mutant zebrafish [88]. Ohmori et al. found that the intraperitoneal methylphenidate could improve the behavior (hyperactivity, anxiety-like behavior, and spatial learning impairments) of N1417H-*Scn1a* mice and significantly suppress the hot bath-induced seizures [89]. Similar to the results from human case studies, the N1417H-*Scn1a* mice showed the good therapeutic response to potassium bromide (reduced seizure duration) without significant impairment in motor coordination [90].

## 7. Discussion

Epilepsy is a chronic neurological disease worldwide, which jeopardizes the patients' lives, burdens the patients' family and caregivers, and requires to be concerned with the increasing attention to the affordable therapies, the effectiveness of current treatment strategies, and the social support to the patients and the caregivers. The pharmaceutical therapy (the application of AEDs) is the most commonly used strategy to fight against epilepsy. However, 30% of epilepsy patients are resistant to the optimized AED treatment without obvious precipitating factors [95]. Dravet syndrome might be an intractable and adverse form of extremity, which requires the multiple AED remedy (**Table 1**) and resistant to many AEDs over time [22]. The two major mechanisms are responsible for the resistance to AEDs in chronic epilepsy. One is the desensitization or modification of the molecular targets of AEDs during the chronic pathological process (frequent and recurring seizures), and the other is the overexpression of multidrug transporters, such as P-glycoprotein [96]. The sodium channel blocker is one of the main classes of AEDs. The genetic polymorphisms of the molecular targets, VGSC  $\alpha$  subunits, are significantly associated with AED resistance. The genetic variant of *SCN2A* IVS7-32A>G (rs2304016) did not alter the *SCN2A* mRNA expression quantity or the exon splicing but had statistically significant association with AED resistance [97]. The calcium channel is also the therapeutic target of some AEDs, such as retigabine and ethosuximide (ETS). The genetic association study of drug-resistant epilepsy in the Chinese Han population displayed that the specific haplotype of the gene-coding calcium voltage-gated channel subunit alpha1 A (*CACNA1A*) was the risk factor for AED resistance [98]. How do those polymorphisms facilitate the desensitization of the AED target? We still need the extended functional studies to reveal the underlying mechanism. For instance, a significant cell functional study of the human brain samples collected from the surgery of hippocampal sclerosis resection provided the evidence of one mechanism of AED resistance (the modification of the cellular target of AEDs). Some categories of AEDs (benzodiazepines and barbiturates) stimulate the gamma-aminobutyric acid ( $\text{GABA}_A$ ) receptor and increase the intracellular concentration of chloride and synaptic inhibition. However, the expected  $\text{GABA}_A$ ergic response of the treated pyramid cells relies on the proper functioning and the normal expression profile of chloride transporters (Na-K-2Cl cotransporter NKCC1 and K-Cl cotransporter KCC2). Otherwise, the  $\text{GABA}_A$  receptor activation depolarize the postsynaptic compartments, which contributes to the epileptiform activity in the stimulated pyramidal cells. In fact, in the temporal lobe epilepsy biopsy tissue, a small group of pyramidal cells downregulated the expression of KCC2 and

Agent or medication	Main action for treatment	Dosage in the treatment	Responder rate (>50% reduction)	Retain period (year)	Retain combination remedy	Aggravation rate (>25% increase)	Cause of death (SE or SUDEP)
Valproate (VPA)	Na <sup>+</sup> Ca <sup>2+</sup> channel ↓ GABA ↑ GLUT ↑ [91]	30–50 mg/kg/d [92]	52 and 41% [76]		VPA + Br VPA + CZP + Br		SUDEP [92]
Topiramate (TPM)	Na <sup>+</sup> Ca <sup>2+</sup> channel ↓ GABA ↑ GLUT ↑ [91]	7.5–15 mg/kg/d [92]	57 and 33% [76]		VPA + CLB + Br [81]	17% [82]	
Clobazam (CLB)	GABA ↑ [91]	0.2–1 mg/kg/d [92]	44 and 48% [76]		VPA + Br VPA + CLB + Br [81]		SUDEP [92]
Clonazepam (CZP)	GABA ↑ [91]	0.03–0.1 mg/kg/d [92]	44 and 38% [76]		VPA + Br VPA + CZP + Br [81]		
Zonisamide (ZNS)	Na <sup>+</sup> Ca <sup>2+</sup> channel ↓ [91]		36 and 38% [76]			44% [82]	
Phenobarbital (PHB)	GABA ↑ [91]		29 and 35% [76]				
Phenytoin (PHT)	Sodium channel blocker [91]		10 and 29% [76]			50% [82]	
Stiripentol (STP)	GABAergic enhancer [93]	35–50 mg/kg/d [85]	23% [86]	5 [86]	VPA + CLB CLB + TPM VPA + TPM [86]	23% [86] 6% [82]	
Bromide (Br)	Stabilize the excitable membrane through hyperpolarization [94]	30–70 mg/kg/d [76] 30–106 mg/kg/d [82]	71 and 94% [76] 81% [82]	2.5 [76] 2 [82]	VPA + Br VPA + CZP + Br VPA + CLB + Br [76] VPA + TPM + CLB [82]		
Levetiracetam (LEV)	Act as a neuromodulator	50–60 mg/kg/d [84]	44–64% [84]		VPA + TPM + LEV [84] VPA + CLB + LEV [84]	5% [82]	
Lamotrigine (LTG)	Sodium channel blocker [91]	2.5–12.5 mg/kg/d [75]	5% (1/21) [75]	14 m <sup>f</sup> [75]	VPA + CZP + CLB [75]	57% [82] 80% [75]	SUDEP [92]

Agent or medication	Main action for treatment	Dosage in the treatment	Responder rate (>50% reduction)	Retain period (year)	Retain combination remedy	Aggravation rate (>25% increase)	Cause of death (SE or SUDEP)
Carbamazepine (CBZ)	Sodium channel blocker [91]	200–900 mg/day [81]	9% [76]	0.9–>20 [81]	VPA CLB STP ZNS LEV CLN TPM PHT [81]	33% [81] 71% [82] 21% [76]	SUDEP, SE [81]
Oxcarbazepine (OXC)	Sodium channel blocker [91]	600–1200 mg/day [81]	Withdrawal + complete stop	0.1–>20 [81]	VPA CBZ ZNS LEV CLN PHB [81]	72% [82]	SUDEP [81]
Verapamil	Voltage-gated calcium channel blocker [83]	1.5 mg/kg/d [83]	2/2 [83]	13–>20 m <sup>a</sup>	VPA TPM PHT ETS <sup>+</sup> [83]		
Clemizole	H1 antagonist [88]	100 µM swim bath (zebrafish)	Significant reduce seizure behavior	Single dose	Monotherapy [88]		
Methyphenidate	Increase dopamine release (rat) [89]	0.5–2.0 mg/kg i.p. [89]	Significant improvement	Single dose	Monotherapy [89]		

<sup>a</sup>SUDEP, sudden unexpected death in epilepsy; SE, status epilepticus.

<sup>m</sup>m: month.

<sup>+</sup>ETS, ethosuximide.

**Table 1.** The commonly used AEDs and the experimental therapies that have been applied in the treatment of Dravet syndrome.



led to depolarizing the postsynaptic neurons [99]. Because Dravet syndrome would be treated intensively with multiple AEDs for a long time, the multifaceted mechanisms might involve the AED resistance during the disease development. They could be the pathological alteration of the target cells at cellular/molecular level (downregulation of KCC2 in the pyramidal cells) or the overexpression of multidrug transporter genes that code ATP-binding cassette transporters 1–4 (*ABCB1-4*) in the epileptogenic zone (hippocampal sclerosis) [100]. The research interests might arise from those points in the future neuroscience and epileptology fields.

## 8. Conclusions

Dravet syndrome, an intractable epilepsy syndrome, affects the initially normal infants with febrile or non-febrile seizures, myoclonic seizures, hemiclonic seizures, and developmental delay. The *SCN1A* gene mutations are frequently found in patients with Dravet syndrome with “severe” genotypes, such as truncation or pore-region missense mutations. The *SCN1A* haplo-deficiency mice display spontaneous seizures, cognitive impairment, and premature death, similar to human clinical phenotype of Dravet syndrome. The electrophysiological findings indicate that the parvalbumin-expressing interneurons in those mice are dysfunctional and hypoexcitable. The selective dysfunction of PV interneurons causes the imbalance of excitatory and inhibitory control to the principal neurons and neuronal network. The immunostaining has confirmed that  $\text{Na}_v1.1$  highly expresses at the axon initial segment of PV interneurons. Due to the complex and dynamic plasticity of AIS and the adaptation response of ion channels to neuronal activity, the  $\text{Na}_v1.1$  functioning within the AIS plasticity of PV interneurons and mutant pathogenesis remains unknown and would bring out the intensive studies in future. Patients with Dravet syndrome are always treated with multiple AEDs with disappointing outcome (**Table 1**). The most commonly used and retained AED in the treatment is valproate. The most evidently effective medication is bromide. With the aim to optimize the pharmacological treatment and encourage the earlier intervention to neurological development, the early genetic screening test of *SCN1A* gene is recommended to the possible patients with Dravet syndrome. Patients with Dravet syndrome should avoid the sodium channel blockers to prevent greater extent inhibition of  $\text{Na}_v1.1$  function that potentially worsens the seizures. We expect that the more promising results would be generated in the experimental therapy studies of Dravet syndrome and provide the valuable resources to help the patients with Dravet syndrome and overcome the devastating disease.

## Acknowledgements

The author greatly appreciates the financial support from Postdoctoral Startup Research Foundation of Guangzhou Human Resource Department (310109-011).

## Conflict of interest

The author declares that there is no conflict of interest.

## Author details

Tian Li

Address all correspondence to: [vivienne\\_tian@hotmail.com](mailto:vivienne_tian@hotmail.com)

Guangzhou Medical University, Guangzhou, China

## References

- [1] Kruger LC, Isom LL. Voltage-gated Na<sup>+</sup> channels: Not just for conduction. *Cold Spring Harbor Perspectives in Biology*. 2016;**8**(6). pii: a029264. DOI: 10.1101/cshperspect.a029264
- [2] Hoeijmakers JG, Faber CG, Lauria G, Merckies IS, Waxman SG. Small-fibre neuropathies—Advances in diagnosis, pathophysiology and management. *Nature Reviews. Neurology*. 2012;**8**(7):369-379. DOI: 10.1038/nrneuro.2012.97
- [3] Chen K, Godfrey DA, Ilyas O, Xu J, Preston TW. Cerebellum-related characteristics of Scn8a-mutant mice. *Cerebellum*. 2009;**8**(3):192-201. DOI: 10.1007/s12311-009-0110-z. Epub 2009 May 8
- [4] Yu FH, Mantegazza M, Westenbroek RE, Robbins CA, Kalume F, Burton KA, et al. Reduced sodium current in GABAergic interneurons in a mouse model of severe myoclonic epilepsy in infancy. *Nature Neuroscience*. 2006;**9**(9):1142-1149. Epub 2006 Aug 20
- [5] Ferraro TN, Dlugos DJ, Buono RJ. Role of genetics in the diagnosis and treatment of epilepsy. *Expert Review of Neurotherapeutics*. 2006;**6**(12):1789-1800
- [6] Ogiwara I, Iwasato T, Miyamoto H, Iwata R, Yamagata T, Mazaki E, et al. Na<sub>v</sub>1.1 haploinsufficiency in excitatory neurons ameliorates seizure-associated sudden death in a mouse model of Dravet syndrome. *Human Molecular Genetics*. 2013;**22**(23):4784-4804. DOI: 10.1093/hmg/ddt331. Epub 2013 Aug 6
- [7] Shi X, Yasumoto S, Kurahashi H, Nakagawa E, Fukasawa T, Uchiya S, Hirose S. Clinical spectrum of SCN2A mutations. *Brain & Development*. 2012 Aug;**34**(7):541-545. DOI: 10.1016/j.braindev.2011.09.016. Epub 2011 Oct 24
- [8] Wagnon JL, Meisler MH. Recurrent and non-recurrent mutations of SCN8A in epileptic encephalopathy. *Frontiers in Neurology*. 2015 May;**6**:104. DOI: 10.3389/fneur.2015.00104. eCollection 2015
- [9] Hirose S. Mutant GABA(A) receptor subunits in genetic (idiopathic) epilepsy. *Progress in Brain Research*. 2014;**213**:55-85. DOI: 10.1016/B978-0-444-63326-2.00003-X
- [10] Syrbe S, Hedrich UBS, Riesch E, Djémié T, Müller S, Möller RS, et al. De novo loss- or gain-of-function mutations in KCNA2 cause epileptic encephalopathy. *Nature Genetics*. 2015 Apr;**47**(4):393-399. DOI: 10.1038/ng.3239. Epub 2015 Mar 9

- [11] Westenbroek RE, Merrick DK, Catterall WA. Differential subcellular localization of the RI and RII Na<sup>+</sup> channel subtypes in central neurons. *Neuron*. 1989 Dec;**3**(6):695-704
- [12] Gong B, Rhodes KJ, Bekele-Arcuri Z, Trimmer JS. Type I and type II Na<sup>+</sup> channel alpha-subunit polypeptides exhibit distinct spatial and temporal patterning, and association with auxiliary subunits in rat brain. *The Journal of Comparative Neurology*. 1999 Sep;**412**(2):342-352
- [13] Meng H, Xu HQ, Yu L, Lin GW, He N, Su T, et al. The SCN1A mutation database: Updating information and analysis of the relationships among genotype, functional alteration, and phenotype. *Human Mutation*. 2015 Jun;**36**(6):573-580. DOI: 10.1002/humu.22782. Epub 2015 Apr 13
- [14] Escayg A, MacDonald BT, Meisler MH, Baulac S, Huberfeld G, An-Gourfinkel I, Malafosse A. Mutations of SCN1A, encoding a neuronal sodium channel, in two families with GEFS+2. *Nature Genetics*. 2000;**24**:343-345
- [15] Claes L, Del-Favero J, Ceulemans B, Lagae L, Van Broeckhoven C, De Jonghe P. De novo mutations in the sodium-channel gene SCN1A cause severe myoclonic epilepsy of infancy. *American Journal of Human Genetics*. 2001 Jun;**68**(6):1327-1332. Epub 2001 May 15
- [16] Weller CM, Pelzer N, de Vries B, López MA, De Fàbregues O, Pascual J, et al. Two novel SCN1A mutations identified in families with familial hemiplegic migraine. *Cephalalgia*. 2014 Nov;**34**(13):1062-1069. DOI: 10.1177/0333102414529195
- [17] Cheah CS, Yu FH, Westenbroek RE, Kalume FK, Oakley JC, Potter GB, et al. Specific deletion of Na<sub>v</sub>1.1 sodium channels in inhibitory interneurons causes seizures and premature death in a mouse model of Dravet syndrome. *Proceedings of the National Academy of Sciences of the United States of America*. 2012 Sep;**109**(36):14646-14651. DOI: 10.1073/pnas.1211591109. Epub 2012 Aug 20
- [18] Miller IO, Sotero de Menezes MA. SCN1A-related seizure disorders. In: Adam MP, Ardinger HH, Pagon RA, Wallace SE, Bean LJH, Stephens K, Amemiya A, Editors. *GeneReviews*® [Internet]. Seattle (WA): University of Washington, Seattle; 1993-2018. 2007 Nov 29 [Updated 2014 May 15]
- [19] Wu YW, Sullivan J, McDaniel SS, Meisler MH, Walsh EM, Li SX, Kuzniewicz MW. Incidence of Dravet Syndrome in a US Population. *Pediatrics*. 2015 Nov;**136**(5):e1310-e1315. DOI: 10.1542/peds.2015-1807. Epub 2015 Oct 5
- [20] Gataullina S, Dulac O. From genotype to phenotype in Dravet disease. *Seizure*. 2017 Jan;**44**:58-64. DOI: 10.1016/j.seizure.2016.10.014. Epub 2016 Oct 21. Review
- [21] Dravet C. Dravet syndrome history. *Developmental Medicine and Child Neurology*. 2011 Apr;**53**(Suppl 2):1-6. DOI: 10.1111/j.1469-8749.2011.03964.x
- [22] Dravet C, Oguni H. Dravet syndrome (severe myoclonic epilepsy in infancy). *Handbook of Clinical Neurology*. 2013;**111**:627-633. DOI: 10.1016/B978-0-444-52891-9.00065-8

- [23] Ishii A, Watkins JC, Chen D, Hirose S, Hammer MF. Clinical implications of SCN1A missense and truncation variants in a large Japanese cohort with Dravet syndrome. *Epilepsia*. 2017 Feb;**58**(2):282-290. DOI: 10.1111/epi.13639. Epub 2016 Dec 24
- [24] Bechi G, Scalmani P, Schiavon E, Rusconi R, Franceschetti S, Mantegazza M. Pure haploinsufficiency for Dravet syndrome Na(V)1.1 (SCN1A) sodium channel truncating mutations. *Epilepsia*. 2012 Jan;**53**(1):87-100. DOI: 10.1111/j.1528-1167.2011.03346.x. Epub 2011 Dec 9
- [25] Kamiya K, Kaneda M, Sugawara T, Mazaki E, Okamura N, Montal M, et al. A nonsense mutation of the sodium channel gene SCN2A in a patient with intractable epilepsy and mental decline. *The Journal of Neuroscience*. 2004;**24**:2690-2698
- [26] McArdle EJ, Kunic JD, George AL Jr. Novel SCN1A frameshift mutation with absence of truncated Na<sub>v</sub>1.1 protein in severe myoclonic epilepsy of infancy. *American Journal of Medical Genetics. Part A*. 2008 Sep;**146A**(18):2421-2423. DOI: 10.1002/ajmg.a.32448
- [27] Marini C, Scheffer IE, Nabbout R, Suls A, De Jonghe P, Zara F, Guerrini R. The genetics of Dravet syndrome. *Epilepsia*. 2011 Apr;**52**(Suppl 2):24-29. DOI: 10.1111/j.1528-1167.2011.02997.x
- [28] Hilber K, Sandtner W, Kudlacek O, Glaaser IW, Weisz E, Kyle JW, et al. The selectivity filter of the voltage-gated sodium channel is involved in channel activation. *The Journal of Biological Chemistry*. 2001 Jul;**276**(30):27831-27839. Epub 2001 May 29
- [29] Ohno Y, Ishihara S, Mashimo T, Sofue N, Shimizu S, Imaoku T, et al. Scn1a missense mutation causes limbic hyperexcitability and vulnerability to experimental febrile seizures. *Neurobiology of Disease*. 2011 Feb;**41**(2):261-269. DOI: 10.1016/j.nbd.2010.09.013. Epub 2010 Sep 25
- [30] Mashimo T, Ohmori I, Ouchida M, Ohno Y, Tsurumi T, Miki T, et al. A missense mutation of the gene encoding voltage-dependent sodium channel (Na<sub>v</sub>1.1) confers susceptibility to febrile seizures in rats. *The Journal of Neuroscience*. 2010 Apr;**30**(16):5744-5753. DOI: 10.1523/JNEUROSCI.3360-09.2010
- [31] Meadows L, Malhotra JD, Stetzer A, Isom LL, Ragsdale DS. The intracellular segment of the sodium channel beta 1 subunit is required for its efficient association with the channel alpha subunit. *Journal of Neurochemistry*. 2001;**76**(6):1871-1878
- [32] Yamagishi T, Li RA, Hsu K, Marbán E, Tomaselli GF. Molecular architecture of the voltage-dependent Na channel: Functional evidence for alpha helices in the pore. *The Journal of General Physiology*. 2001 Aug;**118**(2):171-182
- [33] Mantegazza M, Catterall WA. Voltage-gated Na<sup>+</sup> channels: Structure, function, and pathophysiology. In: Noebels JL, Avoli M, Rogawski MA, Olsen RW, Delgado-Escueta AV, Editors. *Jasper's Basic Mechanisms of the Epilepsies* [Internet]. 4th ed. Bethesda (MD): National Center for Biotechnology Information (US); 2012
- [34] Tsukamoto T, Chiba Y, Wakamori M, Yamada T, Tsunogae S, Cho Y, et al. Differential binding of tetrodotoxin and its derivatives to voltage-sensitive sodium channel subtypes

( $\text{Na}_v$  1.1 to  $\text{Na}_v$  1.7). *British Journal of Pharmacology*. 2017;**174**(21):3881-3892. DOI: 10.1111/bph.13985. Epub 2017 Sep 20

- [35] Onwuli DO, Beltran-Alvarez P. An update on transcriptional and post-translational regulation of brain voltage-gated sodium channels. *Amino Acids*. 2016 Mar;**48**(3):641-651. DOI: 10.1007/s00726-015-2122-y. Epub 2015 Oct 27
- [36] Patel RR, Barbosa C, Xiao Y, Cummins TR. Human  $\text{Na}_v$ 1.6 channels generate larger resurgent currents than human  $\text{Na}_v$ 1.1 channels, but the  $\text{Na}_v$ beta4 peptide does not protect either isoform from use-dependent reduction. *PLoS One*. 2015 Jul;**10**(7):e0133485. DOI: 10.1371/journal.pone.0133485. eCollection 2015
- [37] Kaneko Y, Watanabe S. Expression of  $\text{Na}_v$ 1.1 in rat retinal AII amacrine cells. *Neuroscience Letters*. 2007 Sep;**424**(2):83-88. Epub 2007 Aug 1
- [38] Mistry AM, Thompson CH, Miller AR, Vanoye CG, George AL Jr, Kearney JA. Strain- and age-dependent hippocampal neuron sodium currents correlate with epilepsy severity in Dravet syndrome mice. *Neurobiology of Disease*. 2014 May;**65**:1-11. DOI: 10.1016/j.nbd.2014.01.006. Epub 2014 Jan 14
- [39] Ogiwara I, Miyamoto H, Morita N, Atapour N, Mazaki E, Inoue I, et al.  $\text{Na}_v$ 1.1 localizes to axons of parvalbumin-positive inhibitory interneurons: A circuit basis for epileptic seizures in mice carrying an *Scn1a* gene mutation. *The Journal of Neuroscience*. 2007 May;**27**(22):5903-5914
- [40] De Stasi AM, Farisello P, Marcon I, Cavallari S, Forli A, Vecchia D, et al. Unaltered network activity and Interneuronal firing during spontaneous cortical dynamics in vivo in a mouse model of severe myoclonic epilepsy of infancy. *Cerebral Cortex*. 2016 Apr;**26**(4):1778-1794. DOI: 10.1093/cercor/bhw002. Epub 2016 Jan 26
- [41] Tang B, Dutt K, Papale L, Rusconi R, Shankar A, Hunter J, et al. A BAC transgenic mouse model reveals neuron subtype-specific effects of a generalized epilepsy with febrile seizures plus (GEFS+) mutation. *Neurobiology of Disease*. 2009 Jul;**35**(1):91-102. DOI: 10.1016/j.nbd.2009.04.007. Epub 2009 May 3
- [42] Isaacson JS, Scanziani M. How inhibition shapes cortical activity. *Neuron*. 2011 Oct;**72**(2):231-243. DOI: 10.1016/j.neuron.2011.09.027
- [43] Markram H, Toledo-Rodriguez M, Wang Y, Gupta A, Silberberg G, Wu C. Interneurons of the neocortical inhibitory system. *Nature Reviews. Neuroscience*. 2004 Oct;**5**(10):793-807
- [44] Hunt RF, Baraban SC. Interneuron transplantation as a treatment for epilepsy. *Cold Spring Harbor Perspectives in Medicine*. 2015 Dec;**5**(12):pii: a022376
- [45] Shetty AK, Upadhyaya D. GABA-ergic cell therapy for epilepsy: Advances, limitations and challenges. *Neuroscience and Biobehavioral Reviews*. 2016 Mar;**62**:35-47. DOI: 10.1016/j.neubiorev.2015.12.014
- [46] DeRosa BA, Belle KC, Thomas BJ, Cukier HN, Pericak-Vance MA, Vance JM, Dykxhoorn DM. hVGAT-mCherry:A novel molecular tool for analysis of GABAergic neurons

- derived from human pluripotent stem cells. *Molecular and Cellular Neurosciences*. 2015 Sep;**68**:244-257. DOI: 10.1016/j.mcn.2015.08.007
- [47] Bezaire MJ, Soltesz I. Quantitative assessment of CA1 local circuits: Knowledge base for interneuron-pyramidal cell connectivity. *Hippocampus*. 2013 Sep;**23**(9):751-785. DOI: 10.1002/hipo.22141. Epub 2013 Jul 10
- [48] Baude A, Bleasdale C, Dalezios Y, Somogyi P, Klausberger T. Immunoreactivity for the GABAA receptor alpha1 subunit, somatostatin and Connexin 36 distinguishes axoaxonic, basket, and bistratified interneurons of the rat hippocampus. *Cerebral Cortex*. 2007 Sep;**17**(9):2094-2107. Epub 2006 Nov 22
- [49] Pawelzik H, Hughes DI, Thomson AM. Modulation of inhibitory autapses and synapses on rat CA1 interneurons by GABA(A) receptor ligands. *The Journal of Physiology*. 2003 Feb;**546**(Pt 3):701-716
- [50] Somogyi P, Nunzi MG, Gorio A, Smith AD. A new type of specific interneuron in the monkey hippocampus forming synapses exclusively with the axon initial segments of pyramidal cells. *Brain Research*. 1983 Jan;**259**(1):137-142
- [51] Tian C, Wang K, Ke W, Guo H, Shu Y. Molecular identity of axonal sodium channels in human cortical pyramidal cells. *Frontiers in Cellular Neuroscience*. 2014 Sep;**8**:297. DOI: 10.3389/fncel.2014.00297. eCollection 2014
- [52] Sugino K, Hempel CM, Miller MN, Hattox AM, Shapiro P, Wu C, et al. Molecular taxonomy of major neuronal classes in the adult mouse forebrain. *Nature Neuroscience*. 2006 Jan;**9**(1):99-107. Epub 2005 Dec 20
- [53] Hu H, Jonas P. A supercritical density of Na(+) channels ensures fast signaling in GABAergic interneuron axons. *Nature Neuroscience*. 2014 May;**17**(5):686-693. DOI: 10.1038/nn.3678. Epub 2014 Mar 23
- [54] Li T, Tian C, Scalmani P, Frassoni C, Mantegazza M, Wang Y, et al. Action potential initiation in neocortical inhibitory interneurons. *PLoS Biology*. 2014;**12**(9):e1001944. DOI: 10.1371/journal.pbio.1001944. eCollection 2014 Sep
- [55] Grubb MS, Burrone J. Activity-dependent relocation of the axon initial segment fine-tunes neuronal excitability. *Nature*. 2010 Jun;**465**(7301):1070-1074. DOI: 10.1038/nature09160. Epub 2010 Jun 13
- [56] Grubb MS, Shu Y, Kuba H, Rasband MN, Wimmer VC, Bender KJ. Short- and long-term plasticity at the axon initial segment. *The Journal of Neuroscience*. 2011 Nov;**31**(45):16049-16055. DOI: 10.1523/JNEUROSCI.4064-11.2011
- [57] Hu W, Tian C, Li T, Yang M, Hou H, Shu Y. Distinct contributions of Na(v)1.6 and Na(v)1.2 in action potential initiation and backpropagation. *Nature Neuroscience*. 2009 Aug;**12**(8):996-1002. DOI: 10.1038/nn.2359. Epub 2009 Jul 26
- [58] Lorincz A, Nusser Z. Cell-type-dependent molecular composition of the axon initial segment. *The Journal of Neuroscience*. 2008 Dec;**28**(53):14329-14340. DOI: 10.1523/JNEUROSCI.4833-08.2008

- [59] Rush AM, Dib-Hajj SD, Waxman SG. Electrophysiological properties of two axonal sodium channels,  $\text{Na}_v1.2$  and  $\text{Na}_v1.6$ , expressed in mouse spinal sensory neurones. *The Journal of Physiology*. 2005 May; **564**(Pt 3):803-815. Epub 2005 Mar 10
- [60] Spampinato J, Escayg A, Meisler MH, Goldin AL. Functional effects of two voltage-gated sodium channel mutations that cause generalized epilepsy with febrile seizures plus type 2. *The Journal of Neuroscience*. 2001 Oct; **21**(19):7481-7490
- [61] Laezza F, Lampert A, Kozel MA, Gerber BR, Rush AM, Nerbonne JM, et al. FGF14 N-terminal splice variants differentially modulate  $\text{Na}_v1.2$  and  $\text{Na}_v1.6$ -encoded sodium-channels. *Molecular and Cellular Neurosciences*. 2009 Oct; **42**(2):90-101. DOI: 10.1016/j.mcn.2009.05.007. Epub 2009 May 22
- [62] Alshammari TK, Alshammari MA, Nenov MN, Hoxha E, Cambiaghi M, Marcinno A, et al. Genetic deletion of fibroblast growth factor 14 recapitulates phenotypic alterations underlying cognitive impairment associated with schizophrenia. *Translational Psychiatry*. 2016 May; **6**:e806. doi: 10.1038/tp.2016.66
- [63] Goetz R, Dover K, Laezza F, Shtraizent N, Huang X, Tchetchik D, et al. Crystal structure of a fibroblast growth factor homologous factor (FHF) defines a conserved surface on FHF s for binding and modulation of voltage-gated sodium channels. *The Journal of Biological Chemistry*. 2009; **284**(26):17883-17896. DOI: 10.1074/jbc.M109.001842. Epub 2009 Apr 30
- [64] Shavkunov AI, Panova N, Prasai A, Veselenak R, Bourne N, Stoilova-McPhie S, Laezza F. Bioluminescence methodology for the detection of protein-protein interactions within the voltage-gated sodium channel macromolecular complex. *ASSAY and Drug Development Technologies*. 2012 Apr; **10**(2):148-60. doi: 10.1089/adt.2011.413. Epub 2012 Feb 24
- [65] Jones SL, Svitkina TM. Axon initial segment cytoskeleton: Architecture, development, and role in neuron polarity. *Neural Plasticity*. 2016; **2016**:6808293. DOI: 10.1155/2016/6808293. Epub 2016 Jul 17
- [66] Brackenbury WJ, Calhoun JD, Chen C, Miyazaki H, Nukina N, Oyama F, et al. Functional reciprocity between  $\text{Na}^+$  channel  $\text{Na}_v1.6$  and beta1 subunits in the coordinated regulation of excitability and neurite outgrowth. *Proceedings of the National Academy of Sciences of the United States of America*. 2010 Feb; **107**(5):2283-2288. DOI: 10.1073/pnas.0909434107. Epub 2010 Jan 19
- [67] Kuba H, Oichi Y, Ohmori H. Presynaptic activity regulates  $\text{Na}^+$  channel distribution at the axon initial segment. *Nature*. 2010 Jun; **465**(7301):1075-1078. DOI: 10.1038/nature09087. Epub 2010 Jun 13
- [68] Wefelmeyer W, Cattaert D, Burrone J. Activity-dependent mismatch between axo-axonic synapses and the axon initial segment controls neuronal output. *Proceedings of the National Academy of Sciences of the United States of America*. 2015 Aug; **112**(31):9757-9762. DOI: 10.1073/pnas.1502902112. Epub 2015 Jul 20

- [69] Höfflin F, Jack A, Riedel C, Mack-Bucher J, Roos J, Corcelli C, et al. Heterogeneity of the axon initial segment in interneurons and pyramidal cells of rodent visual cortex. *Frontiers in Cellular Neuroscience*. 2017 Nov;**11**:332. DOI: 10.3389/fncel.2017.00332. eCollection 2017
- [70] Inan M, Blázquez-Llorca L, Merchán-Pérez A, Anderson SA, DeFelipe J, Yuste R. Dense and overlapping innervation of pyramidal neurons by chandelier cells. *The Journal of Neuroscience*. 2013 Jan;**33**(5):1907-1914. DOI: 10.1523/JNEUROSCI.4049-12.2013
- [71] Cruz DA, Eggan SM, Lewis DA. Postnatal development of pre- and postsynaptic GABA markers at chandelier cell connections with pyramidal neurons in monkey prefrontal cortex. *The Journal of Comparative Neurology*. 2003 Oct;**465**(3):385-400
- [72] Hardwick C, French SJ, Southam E, Totterdell S. A comparison of possible markers for chandelier cartridges in rat medial prefrontal cortex and hippocampus. *Brain Research*. 2005 Jan;**1031**(2):238-244
- [73] Bloomfield C, French SJ, Jones DN, Reavill C, Southam E, Cilia J, Totterdell S. Chandelier cartridges in the prefrontal cortex are reduced in isolation reared rats. *Synapse*. 2008 Aug;**62**(8):628-631. DOI: 10.1002/syn.20521
- [74] Pierri JN, Chaudry AS, Woo TU, Lewis DA. Alterations in chandelier neuron axon terminals in the prefrontal cortex of schizophrenic subjects. *The American Journal of Psychiatry*. 1999 Nov;**156**(11):1709-1719
- [75] Guerrini R, Dravet C, Genton P, Belmonte A, Kaminska A, Dulac O. Lamotrigine and seizure aggravation in severe myoclonic epilepsy. *Epilepsia*. 1998 May;**39**(5):508-512
- [76] Shi XY, Tomonoh Y, Wang WZ, Ishii A, Higurashi N, Kurahashi H, et al. Efficacy of anti-epileptic drugs for the treatment of Dravet syndrome with different genotypes. *Brain & Development*. 2016 Jan;**38**(1):40-46. DOI: 10.1016/j.braindev.2015.06.008. Epub 2015 Jul 13
- [77] Hirose S, Scheffer IE, Marini C, De Jonghe P, Andermann E, Goldman AM, et al. SCN1A testing for epilepsy: Application in clinical practice. *Epilepsia*. 2013 May;**54**(5):946-952. DOI: 10.1111/epi.12168. Epub 2013 Apr 15
- [78] Hattori J, Ouchida M, Ono J, Miyake S, Maniwa S, Mimaki N, et al. A screening test for the prediction of Dravet syndrome before one year of age. *Epilepsia*. 2008 Apr;**49**(4):626-633. Epub 2007 Dec 11
- [79] Stenhouse SA, Ellis R, Zuberi S. SCN1A genetic test for Dravet Syndrome (severe myoclonic epilepsy of infancy and its clinical subtypes) for use in the diagnosis, prognosis, treatment and management of Dravet syndrome. *PLOS Currents*. 2013;**5**. pii: ecurrents.eogt.c553b83d745dd79bfb61eaf35e522b0b. DOI: 10.1371/currents.eogt.c553b83d745dd79bfb61eaf35e522b0b
- [80] Connolly MB. Dravet syndrome: Diagnosis and long-term course. *The Canadian Journal of Neurological Sciences*. 2016 Jun;**43**(Suppl 3):S3-S8. DOI: 10.1017/cjn.2016.243
- [81] Snoeijen-Schouwenaars FM, Veendrick MJ, an Mierlo P, van Erp G, de Louw AJ, Kleine BU, et al. Carbamazepine and oxcarbazepine in adult patients with Dravet syndrome:



- Friend or foe? *Seizure* 2015 Jul;**29**:114-118. DOI: 10.1016/j.seizure.2015.03.010. Epub 2015 Apr 13
- [82] Lotte J, Haberlandt E, Neubauer B, Staudt M, Kluger GJ. Bromide in patients with SCN1A-mutations manifesting as Dravet syndrome. *Neuropediatrics*. 2012 Feb;**43**(1):17-21. DOI: 10.1055/s-0032-1307454. Epub 2012 Mar 19
- [83] Iannetti P, Parisi P, Spalice A, Ruggieri M, Zara F. Addition of verapamil in the treatment of severe myoclonic epilepsy in infancy. *Epilepsy Research*. 2009 Jul;**85**(1):89-95. DOI: 10.1016/j.eplepsyres.2009.02.014. Epub 2009 Mar 20
- [84] Striano P, Coppola A, Pezzella M, Ciampa C, Specchio N, Ragona F, et al. An open-label trial of levetiracetam in severe myoclonic epilepsy of infancy. *Neurology* 2007 Jul;**69**(3):250-254
- [85] De Liso P, Chemaly N, Laschet J, Barnerias C, Hully M, Leunen D, et al. Patients with Dravet syndrome in the era of stiripentol: A French cohort cross-sectional study. *Epilepsy Research* 2016 Sep;**125**:42-46. doi: 10.1016/j.eplepsyres.2016.05.012. Epub 2016 May 28
- [86] Balestrini S, Sisodiya SM. Audit of use of stiripentol in adults with Dravet syndrome. *Acta Neurologica Scandinavica*. 2017 Jan;**135**(1):73-79. DOI: 10.1111/ane.12611. Epub 2016 May 27
- [87] Fulton SP, Van Poppel K, McGregor AL, Mudigoudar B, Wheless JW. Vagus nerve stimulation in intractable epilepsy associated with SCN1A gene abnormalities. *Journal of Child Neurology*. 2017 Apr;**32**(5):494-498. DOI: 10.1177/0883073816687221. Epub 2017 Jan 12
- [88] Baraban SC, Dinday MT, Hortopan GA. Drug screening in *Scn1a* zebrafish mutant identifies clemizole as a potential Dravet syndrome treatment. *Nature Communications*. 2013;**4**:2410. DOI: 10.1038/ncomms3410
- [89] Ohmori I, Kawakami N, Liu S, Wang H, Miyazaki I, Asanuma M, et al. Methylphenidate improves learning impairments and hyperthermia-induced seizures caused by an *Scn1a* mutation. *Epilepsia*. 2014 Oct;**55**(10):1558-1567. DOI: 10.1111/epi.12750
- [90] Hayashi K, Ueshima S, Ouchida M, Mashimo T, Nishiki T, Sendo T, et al. Therapy for hyperthermia-induced seizures in *Scn1a* mutant rats. *Epilepsia*. 2011 May;**52**(5):1010-1017. DOI: 10.1111/j.1528-1167.2011.03046.x
- [91] Kwan P, Sills GJ, Brodie MJ. The mechanisms of action of commonly used antiepileptic drugs. *Pharmacology & Therapeutics*. 2001 Apr;**90**(1):21-34
- [92] Ceulemans B, Boel M, Claes L, Dom L, Willekens H, Thiry P, Lagae L. Severe myoclonic epilepsy in infancy: Toward an optimal treatment. *Journal of Child Neurology*. 2004 Jul;**19**(7):516-521
- [93] Trojnar MK, Wojtal K, Trojnar MP, Czuczwar SJ. Stiripentol. A novel antiepileptic drug. *Pharmacological Reports*. 2005 Mar-Apr;**57**(2):154-160
- [94] Ryan M, Baumann RJ. Use and monitoring of bromides in epilepsy treatment. *Pediatric Neurology*. 1999 Aug;**21**(2):523-528

- [95] Kwan P, Brodie MJ. Early identification of refractory epilepsy. *The New England Journal of Medicine*. 2000 Feb;**342**(5):314-319
- [96] Wang GX, Wang DW, Liu Y, Ma YH. Intractable epilepsy and the P-glycoprotein hypothesis. *The International Journal of Neuroscience*. 2016;**126**(5):385-392. DOI: 10.3109/00207454.2015.1038710. Epub 2015 Jul 2
- [97] Kwan P, Poon WS, Ng HK, Kang DE, Wong V, Ng PW, Lui CH, Sin NC, Wong KS, Baum L. Multidrug resistance in epilepsy and polymorphisms in the voltage-gated sodium channel genes SCN1A, SCN2A, and SCN3A: Correlation among phenotype, genotype, and mRNA expression. *Pharmacogenetics and Genomics*. 2008 Nov;**18**(11):989-998. DOI: 10.1097/FPC.0b013e3283117d67
- [98] Lv N, Qu J, Long H, Zhou L, Cao Y, Long L, Liu Z, Xiao B. Association study between polymorphisms in the CACNA1A, CACNA1C, and CACNA1H genes and drug-resistant epilepsy in the Chinese Han population. *Seizure*. 2015 Aug;**30**:64-69. DOI: 10.1016/j.seizure.2015.05.013. Epub 2015 May 28
- [99] Huberfeld G, Wittner L, Clemenceau S, Baulac M, Kaila K, Miles R, Rivera C. Perturbed chloride homeostasis and GABAergic signaling in human temporal lobe epilepsy. *The Journal of Neuroscience*. 2007 Sep;**27**(37):9866-9873
- [100] Lachos J, Zatzoni M, Wieser HG, Fritschy JM, Langmann T, Schmitz G, et al. Characterization of the gene expression profile of human hippocampus in mesial temporal lobe epilepsy with hippocampal sclerosis. *Epilepsy Research and Treatment*. 2011;**2011**:758407. DOI: 10.1155/2011/758407. Epub 2011 Mar 6

---

# **Altered Potassium Ion Homeostasis in Hearing Loss**

## *Altered Expression of Connexins and Kir2.1 Potassium Ion Channels in Hearing Loss Patients*

---

Viktoria Szuts, Janos Andras Jarabin, Nikoletta Nagy,  
Ferenc Otvos, Roland Nagy, Attila Nagy,  
Katalin Halasy, Laszlo Rovo, Marta Szell and  
Jozsef Geza Kiss

Additional information is available at the end of the chapter

<http://dx.doi.org/10.5772/intechopen.77732>

---

### **Abstract**

Connexins, Kv-type ion channels, and pannexins have a dominant role in maintaining the potassium ion homeostasis in the cochlea. The cellular background currents are sustained by Kir2.1 ion channels; however, their involvement in the hearing system is less clear. In this study, the mutations of gap junction proteins beta 2 (GJB2), beta 3 (GJB3) and beta 6 (GJB6) were screened in the white Caucasian population in Hungary using gene mapping and immunofluorescence methods from translated proteins of these genes—connexins on blood cells. Expression of connexins and Kir2.1 ion channels was investigated in the blood cells of deaf patients prior to cochlear implantation, and the results show significantly decreased amounts of connexin26 and connexin43. In addition, the coexpression of Kir2.1 ion channels with synapse-associated 97 proteins was partially impaired. Our investigation revealed a reduced level of Kir2.1 channels in deaf patients indicating a crucial role for the functional Shaker superfamily of K<sup>+</sup> channels in the non-diseased hearing system.

**Keywords:** hearing loss, cochlea, GJB gene mutation, connexin26, connexin43, Kir2.1 ion channels, lymphocytes

---

## **1. Introduction**

Mutations in connexin26 (Cx26) and connexin30 (Cx30) have frequently been associated with hearing loss and deafness, and some Cx26 mutations have also been found to contribute to

---

over 50% of hearing loss or nonsyndromic deafness cases in different human populations investigated in the last decades [1–6].

Recently, a fast and new non-invasive method has been developed in our laboratory to identify mutated genes for GJB2 leading to hearing loss or deafness [7]. This method has allowed us to collect and store the dried blood spots (DBS) in Guthrie cards for mutation analysis or expressed proteins of genes. The early detection of genetic mutations for inner ear impairment is crucial to provide hearing rehabilitation with an outstanding functional outcome, i.e. to maintain the development of the peripheral and central auditory pathway for unhindered future benefits. There are a number of modern technologies in the field of cochlear implantation and to fulfill this aim it is crucial to address the audiological and logopedical progress in a timely manner.

Cx26 and connexin43 (Cx43) have a major role in cell-to-cell interactions and in the permeability of the channels for diverse ions and small molecules, which maintain the physiological condition of the cochlea [1, 8]. Connexins form hemichannels in the cochlea where the Cx26 channels are the most abundant and are involved in the potassium-recycling pathway of the cochlea. Translated proteins from GJ genes make up channels by head-to-head docking of two connexin hexamers referred to as hemichannels (HCs) or connexons; one from each neighboring cell [9, 10]. Cx26 proteins were localized in the outer membrane of the cochlea.

The position of mutations in the GJB2 gene (Cx26 protein) is different across certain populations. The known mutation in the populations of northern European descent is a base pair deletion at position 35 in the GJB2 gene (known as 35delG; Cx26 protein) while the 235delC mutation, which occurs more frequently in Asian populations, misses a base pair at position 235 (Cx26 protein) [11–13]. Furthermore, patients with a single base pair deletion at position 167 (167delT) (Cx26 protein) are commonly found in communities of eastern European (Ashkenazi) Jewish ancestry [14, 15].

Different connexins may be important factors in the flawless cell-to-cell interactions that maintain the fast electrogenic mechanisms between the cochlea and neuronal system [16]. Other ion currents are also involved in this process. The voltage-dependent inward rectifier potassium current ( $I_{K1}$ ) has a role in maintaining the resting membrane potential, contributing to the beginning and the final repolarization in all cells. The  $I_{K1}$  current in different tissues is sustained mostly by Kir2.x (Kir2.1, Kir2.2, and Kir2.3) ion channels [17–23]. Auxiliary subunits and the synapse-associated protein 97 (SAP97) modulate the function of these channels [24, 25].  $I_{K1}$  currents have a fundamental role in muscle cells, but their molecular background in the hearing system is still uncertain. We have limited information on the impact of the altered gap-junctions [26] and Kir2.1 in the inner membrane of the cochlea [20, 21, 27], the neural connection and the expressed potassium ion channels on blood cells. The exploration of the type and mechanism of these channels is one of the aims of the present work.

Hereditary hearing diseases are known to be associated with mutations, such as the autosomal recessive non-syndromic hearing loss (ARNSHL), seizures, sensorineural deafness [5, 28–30], Pendred syndrome (PDS) [5, 29–31], deafness [7, 27–35], and rarely the hearing loss overlaps with Andersen-Tawil syndrome [2, 36, 37]. The Andersen-Tawil syndrome is characterized by mutated KCNJ2 genes expressing malfunctioned Kir2.1 proteins, which leads to functional abnormalities and causing deafness with cardiomyopathy [36–38].

The  $I_{K1}$  current is sustained by ion channels that consist of heteromeric assemblies of Kir2.1, Kir2.2, and Kir2.3  $\alpha$ -subunits [22, 39]. This current significantly contributes to the maintenance and regulation of the resting membrane potential [17, 40] and strongly affects the final repolarization of the action potential (AP) [8, 9, 17, 18, 41]. The Kir2.x channels are under the control of the intracellular scaffolding, trafficking and regulatory proteins, which strongly adjust their physiological functions. Kir2.x isoforms colocalize with membrane associated guanylate kinase (MAGUK) proteins [24, 42]. One of these is the SAP97 anchoring protein, which has an important interaction with Kir2.x channel complexes in neuronal cells and myocytes [25, 42, 43]. Various Kir2.x isoforms may cooperate differently with the MAGUK proteins in the complexes that traffic Kir2.x ion channels to the plasma membrane (PM), and anchor and stabilize these channels into the sarcolemma of cardiac muscle [22, 25, 43]. The Kir2.1 channels may be exported from the Golgi in a signal-dependent manner and this process may be disrupted by certain diseases [44]. The age-dependent SAP97 expression in the human heart was evaluated for the first time in our laboratory [45], and it seems that the regulation and modulation of these ion channel complexes have a strong effect in the development of different tissue types in diverse hereditary diseases associated with cardiomyopathy and deafness too [36–39, 46]. These genes have demonstrated a gender differences and have been remodeled in cardiomyopathy [40, 41].  $I_{K1}$  currents are active during the time course of AP [20, 21, 47, 48], but their molecular background basis is poorly characterized on blood cells.

Our hypothesis states that connexins and Kir2.x ion channels, which are impaired at the transcription and translated protein level in deafness, have an essential function in the hearing system. The aim of this study was to monitor the mutations of expressed GJs and KCNJ2 genes in the Hungarian population and to screen the expression of hearing-related genes and proteins involved in the maintenance of the ionic homeostasis in the cochlea. An additional goal was to find an opportunity to obtain cells from the body that present the disrupted ionic status control characteristic of the pathophysiological condition of deafness. For this purpose, we used non-invasive methods to find the representative and irrevocable changes in peripheral blood cells of patients. Our group has previously demonstrated that connexin ion channels, especially the Cx26 mutations, are characteristic indicators in patients with hearing loss [7, 48]. In this study we investigated ion channels related to connexins in patients with altered hearing and detected the expression level of Cx26, Cx43 and Kir2.1 channels in the blood cells. Patients have hearing defects and these results highlight to the role of gap junctions and hemichannels in  $K^+$  removal and recycling in the inner ear, as well as possible roles for nutrient passage in the cochlea [9, 26, 48].

## 2. Material and methods

### 2.1. Human patients

Eighty consecutive, non-randomized profoundly hearing-impaired cochlear implant candidates were recruited in this study cohort; 45 females and 35 males aged between 0.5 and 72 years (average:  $25.8 \pm 24.4$  years). The control group was made up of 13 subjects with objectively measured binaural normal hearing sensitivity; 7 females and 6 males aged between 3

and 59 years (average:  $27.4 \pm 17.2$  years) (**Tables 1** and **2**). Details of patient demographics, clinical diagnoses, and genetic investigations are presented in **Table 1**. All patients in the diseased group had nonsyndromic sensorineural hearing loss, without any organic abnormalities (neither anatomical nor developmental alterations) including overlapping diseases. Prior to cochlear implantation, patients did not receive medication. The investigations conformed to the Declaration of Helsinki. Experimental protocols were authorized by the University of Szeged and National Scientific Research Ethical Review Boards (No. 38/2014). The blood cells were taken and kept in cold ( $4\text{--}6^\circ\text{C}$ ) for 2–4 h prior to investigations.

## 2.2. Objective tests used for the evaluation of hearing sensitivity

### 2.2.1. Impedance audiometry

#### 2.2.1.1. Tympanometry

A measurement of compliance change in the middle ear apparatus to transmit sounds to the inner ear as air pressure is varied in the external auditory canal [49, 50]. Equipment used: r36m Clinical Middle Ear Analyzer (Resonance, Gazzaniga, Italy).

#### 2.2.1.2. Acoustic reflex test

Following high intensity acoustic stimulation, a sudden decrease in compliance occurs with an approximate 10 ms delay as a consequence of the contraction of the stapedius muscle. Equipment used: r36m Clinical Middle Ear Analyzer (Resonance, Gazzaniga, Italy).

Patients	Sex	Age	Diagnosis	Mutation
1	F	5.0	ND	NO
2	M	39.0	ND	NO
3	F	59.0	ND	NO
4	F	16.7	ND	NO
5	F	57.9	ND	NO
6	M	22.0	ND	NO
7	M	23.9	ND	NO
8	M	22.1	ND	NO
9	F	24.0	ND	NO
10	M	17.9	ND	NO
11	F	17.9	ND	NO
12	F	17.7	ND	NO
13	M	3.0	ND	NO

ND: Non-Diseased; F: female; M: male.

**Table 1.** Data of non-diseased patients without mutations in GJB2 (Cx26) genes in Hungarian population: non-diseased patients.

<b>Patients</b>	<b>Sex</b>	<b>Age</b>	<b>Diagnosis</b>	<b>Mutation</b>
1	M	1.7	Hearing loss	
2	M	46.3	Hearing loss	
3	M	2.5	Hearing loss	GJB2 (heterozygote c.35delG)
4	F	4.4	Hearing loss	
5	F	1.1	Hearing loss	
6	M	2.8	Hearing loss	
7	M	16.1	Hearing loss	
8	M	23.5	Hearing loss	
9	M	1.4	Hearing loss	GJB2 (homozygote c.35delG)
10	F	14.5	Hearing loss	
11	F	26.9	Hearing loss	
12	F	27.6	Hearing loss	GJB2 (homozygote c.35delG)
13	M	14.5	Hearing loss	
14	F	1.8	Hearing loss	
15	F	65.7	Hearing loss	
16	F	64.6	Hearing loss	GJB2 (homozygote c.35delG)
17	M	2.1	Hearing loss	GJB2 (heterozygote c.35delG)
18	M	70.4	Hearing loss	
19	F	70.0	Hearing loss	
20	F	41.9	Hearing loss	
21	F	1.8	Hearing loss	
22	F	71.0	Hearing loss	
23	F	2.2	Hearing loss	GJB2 (heterozygote missense c.101 T/C p.Met34Thr (rs35887622, CM077555, CM970679))
24	F	9.9	Hearing loss	GJB2 (homozygote c.35delG)
25	M	6.9	Hearing loss	GJB2 (heterozygote c.35delG)
26	F	1.9	Hearing loss	GJB2 (homozygote c.35delG)
27	M	2.7	Hearing loss	GJB2 (homozygote c.35delG)
28	M	1.3	Hearing loss	
29	F	2.9	Hearing loss	GJB2 (homozygote c.35delG)
30	M	5.4	Hearing loss	GJB2 (heterozygote c.35delG)
31	M	69.6	Hearing loss	
32	F	11.3	Hearing loss	
33	F	54.0	Hearing loss	
34	F	69.5	Hearing loss	

<b>Patients</b>	<b>Sex</b>	<b>Age</b>	<b>Diagnosis</b>	<b>Mutation</b>
35	F	23.7	Hearing loss	
36	M	3.1	Hearing loss	
37	M	61.6	Hearing loss	
38	F	15.4	Hearing loss	
39	F	27.7	Hearing loss	
40	F	76.9	Hearing loss	
41	F	41.7	Hearing loss	
42	M	2.0	Hearing loss	
43	M	1.2	Hearing loss	
44	M	2.6	Hearing loss	GJB2 (heterozygote missense c.119c/a p.Ala40Glu (rs111033296, CM051511))
45	F	48.0	Hearing loss	
46	F	59.1	Hearing loss	GJB2: c.101 T/C p.Met34Thr rs35887622 homozygote, GJB2: c.139G/T p.Glu47Ter rs104894398 homozygote
47	M	52.7	Hearing loss	GJB2: c.35delG homozygote
48	M	19.7	Hearing loss	
49	M	2.6	Hearing loss	GJB2 (homozygote c.35delG)
50	M	6.6	Hearing loss	
51	M	58.5	Hearing loss	
52	M	13.2	Hearing loss	
53	F	27.3	Hearing loss	
54	F	34.9	Hearing loss	
55	F	58.9	Hearing loss	
56	F	29.8	Hearing loss	
57	F	49.2	Hearing loss	
58	F	77.3	Hearing loss	
59	M	51.2	Hearing loss	
60	M	3.1	Hearing loss	GJB2 (homozygote c.35delG)
61	M	52.6	Hearing loss	
62	F	40.9	Hearing loss	GJB2 (heterozygote c.35delG)
63	F	5.7	Hearing loss	
64	M	1.5	Hearing loss	GJB2 (homozygote c.35delG)
65	F	2.5	Hearing loss	
66	F	2.0	Hearing loss	



Patients	Sex	Age	Diagnosis	Mutation
67	F	64.6	Hearing loss	GJB3 (c.316C/T p.Arg106Cys (rs147106166) heterozygote)
68	F	2.8	Hearing loss	
69	F	7.1	Hearing loss	
70	M	23.7	Hearing loss	
71	F	66.5	Hearing loss	
72	M	68.7	Hearing loss	
73	F	5.9	Hearing loss	GJB2 (heterozygote c.35delG)
74	M	6.2	Hearing loss	
75	F	20.9	Hearing loss	
76	M	9.4	Hearing loss	GJB2 (heterozygote c.35delG)
77	F	45.2	Hearing loss	
78	M	1.4	Hearing loss	
79	F	3.4	Hearing loss	
80	F	55.8	Hearing loss	

F: female; M: male. Mutation of GJB3 gene.

**Table 2.** Data of hearing loss patients carrying mutations in GJB2 (Cx26) genes in Hungarian population: patients with hearing loss.

### 2.2.2. Otoacoustic emission (OAE)

Spontaneous and evoked sound waves that originate from the inner ear are transmitted through the ossicles and the eardrum into the external auditory meatus can be measured. Equipment used: Eclipse EP15 (Interacoustics A/S, Middelfart, Denmark [51].

### 2.2.3. Auditory brain stem responses (ABR)

Auditory brain stem responses are far-field potentials that measure all ranges of the early auditory evoked potentials (AEP) using signal averaging [52, 53]. It consists of a series of seven waves (I-VII.) occurring within about 10 ms from stimulus onset [54]. Applied stimuli: Click and CE-Chirp LS. Equipment used: Eclipse EP15 (Interacoustics A/S, Middelfart, Denmark). Click stimulus: used to test the critical high frequency region (approximately 2–4 kHz). Chirp stimulus: applied to activate the entire cochlea instantaneously.

### 2.2.4. Auditory steady state responses (ASSR)

Auditory steady state responses are AEPs that are used to objectively estimate the hearing sensitivity in individuals with normal hearing sensitivity and with various degrees and configurations of sensorineural hearing loss (SNHL) [55]. Equipment used: Eclipse EP15 (Interacoustics A/S, Middelfart, Denmark) [50, 55].

### 2.3. Genetic investigations

Peripheral blood samples were drawn from the affected patients ( $n = 80$ ). Genomic DNA was isolated following the instructions of QIAamp DNA Blood Mini Kit (Qiagen, USA). The coding regions and the flanking introns of the GJB2, GJB3 and GJB6 genes were amplified by polymerase chain reaction (PCR) using DreamTaq Green PCR Master Mix (Thermo Scientific, USA). Primer sequences used for the genetic analyses were designed with Primer 3 (<http://bioinfo.ut.ee/primer3/>) online software. The quality and quantity of PCR products were measured by electrophoresis on 2% agarose gel (SeaKem LE agarose, Lonza), which were used as templates for sequencing. Direct sequencing of PCR products was performed on a traditional capillary sequencer (ABI Prism 7000) and compared with the wild-type gene sequences using the Ensemble Genome Browser.

### 2.4. Immunofluorescence

Blood samples were collected in parallel for protein analyses in tubes containing EDTA as anti-coagulant. Blood cells of non-diseased and hearing loss patients were washed with phosphate buffer saline (PBS, pH 7.3) and centrifuged gently. Cells, mostly lymphocytes, were attached to slides, blocked with 2% bovine serum albumin and incubated overnight at 4°C with mouse anti-Cx26 (1:100 dilution, Millipore, USA), or rabbit anti-Cx43 (1:100 dilution, Cell Signaling Technology, USA), or rabbit anti-Kir2.1 antibodies (1:100 dilution, Alomone Ltd., Jerusalem) with mouse anti-SAP97 (1:300 dilution, LifeSpan, USA) [48]. After washing with PBS, the cells were incubated with Alexa 488-labeled anti-rabbit IgG (1:400 dilution; Molecular Probes, USA) plus Cy3-conjugated anti-mouse IgG (1:400 dilution; Jackson Immuno Research Laboratories, Inc., USA) secondary antibodies and counterstained with 2,4 diamino-2-phenylindol (DAPI) (Hoechst 33258) for 10 minutes. Detection was performed using an Olympus FV1000 confocal laser scanning microscope (Olympus Life Science Europa GmbH, Hamburg, Germany). The scale bar was labeled in every figure ( $n = 2-3$  specimens for each antibody staining) from 12 patients and the analysis was performed using Fluoview ver. 4.0 programme.

## 3. Results

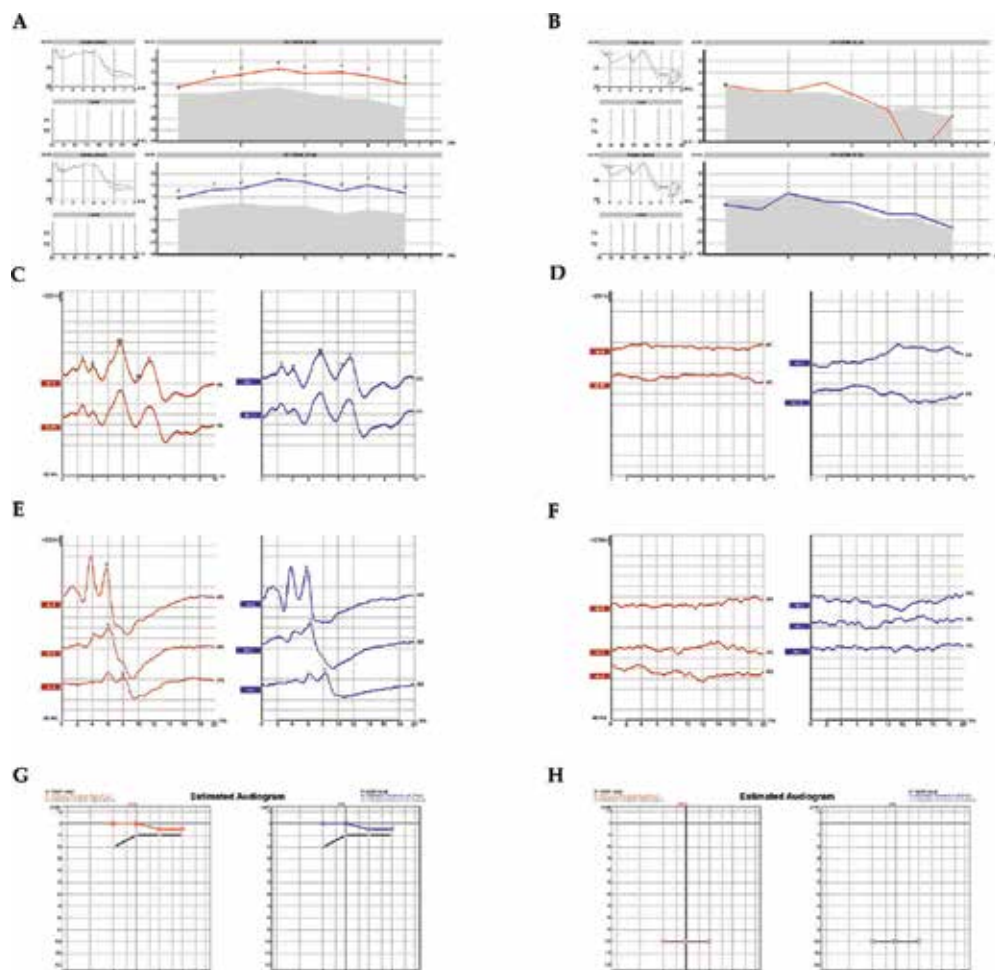
### 3.1. Examination of patients expecting cochlear implantation

The outer ear was inspected by physical examination and found to be anatomically and functionally intact in all subjects prior to any hearing assessment (**Figure 1A–H**). Hearing sensitivity was subsequently evaluated with objective procedures, applying the crosscheck principle to achieve reliable results, confirmed by multiple analyses [49]. The middle ear is essentially an impedance matching system. Impedance is simply a measure of acceptance or rejection of the energy per unit time. While transmitted through the tympanic membrane and other structures of the middle ear, acoustic signals can be modified, depending on the mass, the elasticity and the resistance of the system that would determine the amount of energy accepted or reflected. The overall configuration of tympanometry and acoustic reflex tests provide greater authority and assurance in the evaluation of middle ear pathologies and conductive hearing

loss. Middle ear analysis was performed prior to any other tests to unquestionably exclude any pathology that might alter subsequent results [49, 50]. Otoacoustic emissions (OAEs) indicate the functional integrity of the outer hair cells in the inner ear [49, 51]. The source that generates retrograde sound transmission is the frequency following cell-vibration of the outer hair cells, representing their active, non-linear characteristics. There is a distinction between spontaneous emissions (SOAE) and evoked emissions (EOAE). Several modes of stimulation and registration (i.e. post or pre-stimulatory) are known to provide information about outer hair cell function [49, 50]. Distortion product otoacoustic emission (DPOAE) [49, 51] is one of them. Representative results of a non-diseased subject (**Table 1**), (**Figure 1A, C, E, G**) and a hearing-impaired patient (**Table 2**), (**Figure 1B, D, F, H**) are presented. All curves are color-coded: red lines represent the right ear while blue lines represent the left ear. **Figure 1A** and **B** clearly shows that the active, non-linear vibrations of the outer hair cells to an external sound stimulus are sensitively recordable with DPOAE exhibiting the normal function of the endocochlear cellular amplification mechanisms (**Figure 1A**). In hearing-impaired patients, DPOAE can be registered up to a moderate degree of sensorineural hearing loss; however, the signal tapers off beyond a certain extent (**Figure 1B**). Neural responses during an auditory brainstem response test (ABR) are generated subcortically by the auditory nerve and subsequent brain stem fiber tracts and nuclei. Using either click or chirp stimuli is still the gold standard for electro-physiologically assessing the integrity of the auditory nerve and the brain stem pathways as they lead the electrical stimuli towards the cortex [52–55] (**Figure 1C** and **D**). Neuronal junction points in the brainstem as generator relay structures are identified in the form of waves on the electrophysiological recordings in normal subjects (**Figure 1C**); while these points are not registered in patients with a profound hearing loss (**Figure 1D**). Using CE Chirp-LS stimuli (**Figure 1E** and **F**) while registering ABRs, the synchronous activation is achieved in the cochlea, thus a more prominent wave IV-V is observed in a non-diseased patient (**Figure 1E**). In patients with profound hearing loss, ABRs are missing (**Figure 1F**). Auditory steady state responses on amplitude-modulated stimuli are highly relevant, since it takes many years to objectively estimate hearing sensitivity in individuals with normal hearing and with various degrees and configurations of SNHL. The objective estimation of hearing sensitivity is performed by auditory steady-state response (ASSR) tests (**Figure 1G** and **H**). In a non-diseased subject, normal thresholds were registered on all the measured frequencies (**Figure 1G**); while a profound hearing loss is demonstrated in a patient with hereditary sensorineural deafness (**Figure 1H**).

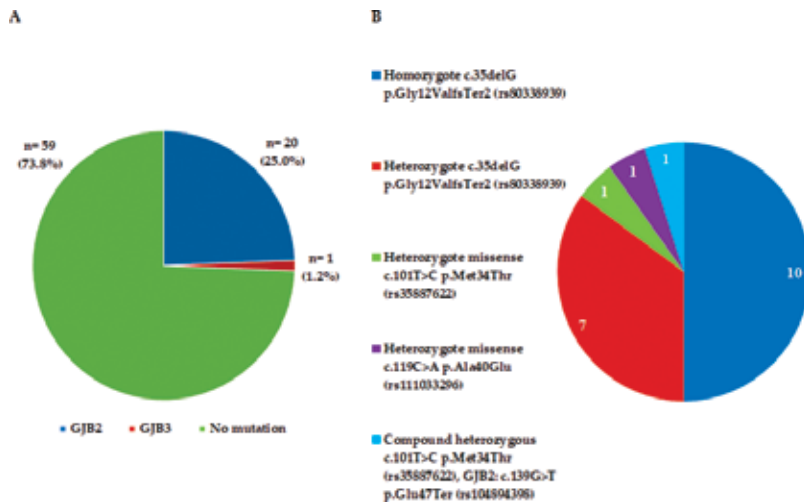
### 3.2. Mutation of connexin genes in blood cells in patients with hearing loss

In all patients the most frequently occurring GJ genes in the cochlea were tested for mutations of GJB genes from DNA of blood cells as described above. **Figure 2** shows the distribution in patients from Hungary involving 13 non-diseased patients and 80 patients selected for cochlear implantation. The results of the mutation analysis of GJB2, GJB3 and GJB6 genes are shown in **Figure 2A**. 25.0% of hearing loss patients carried a mutation in the GJB2 gene, and only 1 out of 80 patients (1.2%) had a mutation in the GJB3 gene (**Figure 2A**). Mutations in GJB6 genes were not detected in this study (**Table 1**). In the ancestors of the Hungarian Caucasian population, the 35delG mutation in the GJB2 gene appeared most frequently in homozygous state (50%) (**Figure 2B**) and c.35delG (p.Gly12ValfsTer2 (rs80338939)) in heterozygotes (50%). Among the



**Figure 1.** Objective clinical measures of the auditory function in patients with hearing loss. Representative results of a non-diseased patient (A, C, E, G) and a patient with impaired hearing (B, D, F, H) are presented. All curves are color-coded. Red represents the right ear, and blue represents the left ear. A-B: The active, non-linear vibrations of the outer hair cells to external sound stimuli are sensitively recordable with the distortion product otoacoustic emission test (DPOAE) exhibiting the normal function of the endocochlear cellular amplification mechanisms (A). In hearing impaired patients, DPOAE can be registered up to a moderate degree of sensorineural hearing loss. However, the signal tapers off beyond a certain extent (B). C-D: Auditory brainstem response tests (ABR) precisely reveals the functional integrity of the vestibulocochlear nerve leading the electrical stimuli towards the cortex. Neuronal junction points in the brainstem as generator relay structures are identified in the form of waves in the electrophysiological recordings in normal subjects (C); however, they are not present in patients with a profound hearing loss (D). E-F: The objective estimation of hearing sensitivity was performed by auditory steady-state response (ASSR) tests. In a non-diseased subject, normal thresholds were registered on all the measured frequencies (E), while a profound hearing loss is shown in a patient with hereditary sensorineural deafness (F). G-H: Used while registering ABRs, synchronous activation is achieved in the cochlea, thus a more prominent CE chirp-LS stimuli wave IV-V is observed in a non-diseased subject (G). In patients with profound hearing loss, ABRs are missing (H).

heterozygotes, the tests showed 35% mutations of heterozygote c.35delG p.Gly12ValfsTer2 (rs80338939), 5% heterozygote missense c.101T>C p.Met34Thr (rs35887622), 5% heterozygote missense c.119C>A p.Ala40Glu (rs111033296) and 5% of compound heterozygous c.101T>C



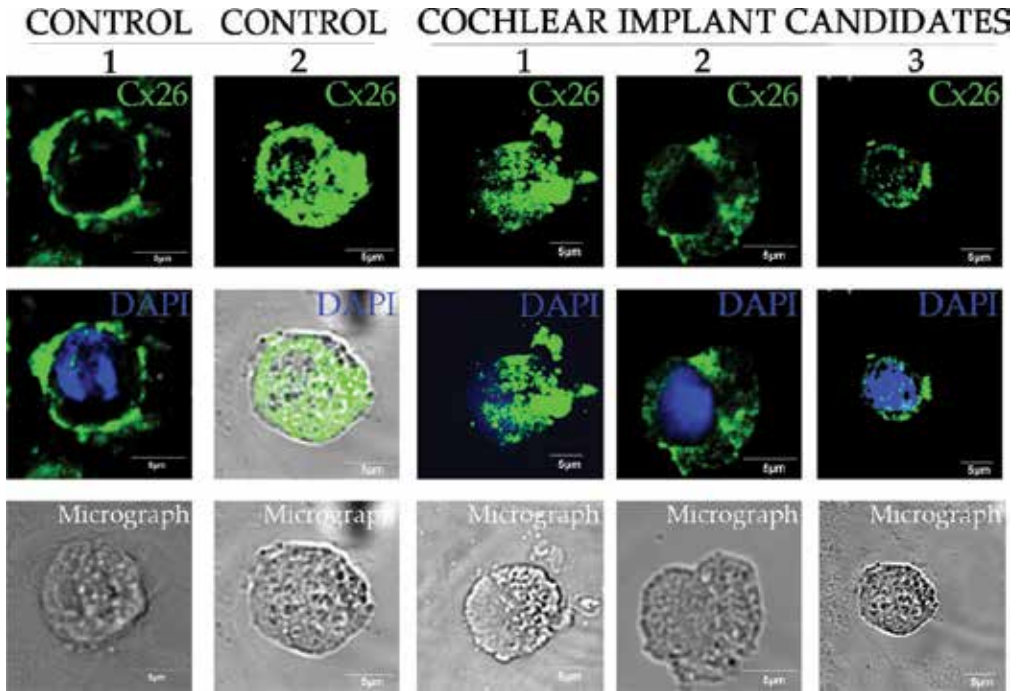
**Figure 2.** Genetic mutations for GJB genes were tested in hearing loss patients prior to implantation (n = 80). (A) Prevalence of GJB2 and GJB3 gene mutations in subjects with non-syndromic hearing impairment (n = 21/80). (B) Prevalence of different GJB2 mutations in subjects with non-syndromic hearing impairment (n = 20/80).

p.Met34Thr (rs35887622), GJB2: c.139G>T p.Glu47Ter (rs104894398). The distribution of these ratios for homozygotes and heterozygotes may change with time, but the rate of this change cannot be estimated at this moment.

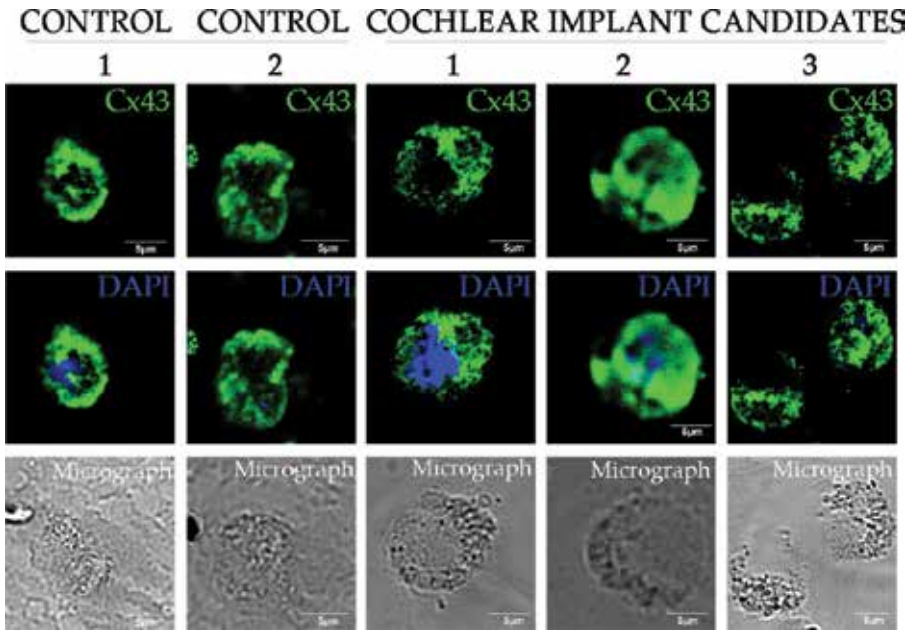
### 3.3. Distribution of connexins and Kir2.1 ion channels with modulators on blood cells

The expression of Cx26 and Cx43 channel proteins was abundant in non-diseased patients (control 1 and 2) but much poorer in blood cells of deaf patients as seen in **Figure 3** and variable in hearing loss patients (see 1–3 on **Figure 4**). In all cells, the nuclei were counterstained with DAPI (blue) and scale bars are shown on each image. Thirteen patients with hearing loss were tested for ion channels and compared to controls (with same age and sex) in each experiment. The protein pattern of both Cx26 and Cx43 changed on the surface of blood cells (**Figures 3** and **4**), appearing as large patches in the control cells and reorganized in smaller groups of connexins in diseased cells. Furthermore, the shape of the area around the nucleus was round in diseased cells and the cytosol was disintegrated. The protein level of Cx26 was variable on the surface of blood cells from patients with hearing loss. We could not identify the GJB2 gene mutation in Patient 1, but Patient 2 and 3 showed mutations with decreased protein level of Cx26. We suppose that Patient 1 has a mutation in another type of gene.

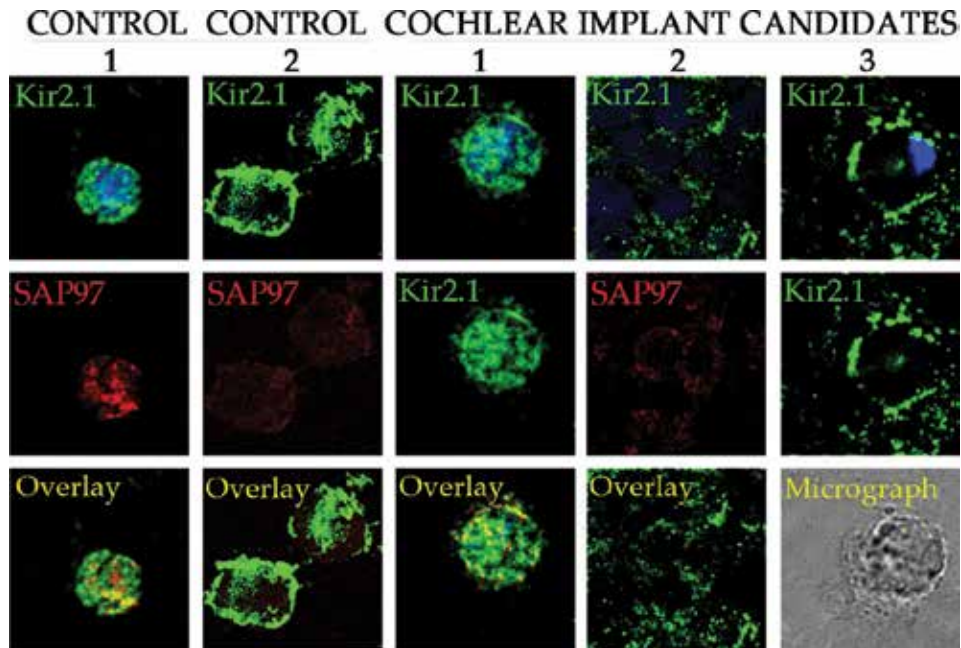
The Kir2.1 ion channels colocalized with SAP97 protein in non-diseased patients, but we determined only partial or no overlaid channel complexes (**Figure 5**) in cells from cochlear implant candidates. The protein pattern was altered and the levels were decreased in hearing loss patients compared to controls. The SAP97 anchoring protein is redistributed in the blood cells and do not colocalize often with Kir2.1 channels in diseased cells. The levels of Kir2.1



**Figure 3.** Pattern of connexin26 ion channels on blood cells of patients expecting cochlear implantation. Cx26: Connexin26, DAPI: 2,4-diamino-2-phenylindole.



**Figure 4.** Alteration of protein levels of connexin43 ion channels in blood cells in patients with deafness. Representative figures from non-diseased and hearing loss patients. Cx43: Connexin43; DAPI: 2,4-diamino-2-phenylindole.



**Figure 5.** The disrupted protein pattern and coexpression of Kir2.1 ion channel with declined SAP97 on blood cells of hearing loss patients. SAP97: Synapse-associated protein 97; DAPI: 2,4-diamino-2-phenylindole.

protein were varied in each cochlear implant candidates, just as in Patient 1 compared to Patient 2 or 3. The amount of SAP97 declined in the lymphocytes of Patient 2 and 3 with *GJB2* gene mutations. The Kir2.1 channels did not perfectly colocalize with SAP97 in the lymphocytes of Patients 1–3 with hearing loss (**Figure 5**).

#### 4. Discussion

The main purpose of this study was to detect the mutations of genes *GJB2*, *GJB3* and *GJB6* as well as the translated proteins Cx26, Cx43 and Kir2.1 ion channels from blood cells in cochlear implant candidates. The cochlear implantation was required in hearing impaired patients for based on indication criteria. Hearing sensitivity was evaluated with objective methodologies [56], applying the crosscheck principle. The outer and middle ear anatomy and function proved to be normal in all the recruited subjects of this cohort.

The study provided the following key results: (1) the different *GJB* mutations were detected in hearing loss in 50% homozygote and 50% heterozygote form for *GJB* genes in a Hungarian population. (2) Cx43 levels decreased moderately in blood cells. (3) Our investigation revealed a reduced level for Kir2.1 channels as well as for the SAP97 protein. (4) The extent of colocalization of Kir2.1 ion channels with SAP97 anchoring proteins was less marked or partially redistributed in blood cells from patients with hearing loss. (5) Cx26 mutation impacts hearing loss.

#### 4.1. Significance of connexins in hearing system and alteration in deafness

These data are consistent with earlier reports on the decrease of GJB2 gene expression in deafness [7, 57], and this study is the first to demonstrate the declined Cx26 protein level in patients carrying these mutations. Recently, more than 100 mutations have been reported, among which the GJB2 gene mutations are the most common cause of nonsyndromic deafness [1]. In this study we demonstrated a similar ratio of GJB2 gene mutations in a Hungarian population in accordance with the earlier findings of Nagy et al. [7]. Additionally, more heterozygote forms were identified in this investigation. The position of joint mutations differs across many populations. This very likely holds true for other genes as well, but GJB2 gene is probably the most examined gene among the genes involved in hearing-related problems. The allelic frequency of three GJB2 gene mutations have been shown to exhibit differences based on ethnicity, which in some cases also translated to geographic regions [11]. The 35delG mutation of the coding exon of GJB2 gene has a frequency of 2–4% in the Caucasian population [58]. Geographically this holds true for Europe, the Middle East and some populations in North America.

The GJB2 gene encodes the Cx26 protein, which assembles to form channels between the cells in the cochlea. These gap junction proteins allow the rapid removal of  $K^+$  from the base of hair cells, resulting in the recycling of this ion back to the endolymph to maintain the cochlear homeostasis in humans [59]. Kamiya et al. investigated the expression of Cx26 and Cx30 in the gap junction macromolecular complex [60], where Cx26 is the most abundant channel in the cochlea of mice. They concluded that the disruption of Cx26 was the earliest alteration of the Cx26-dependent gap junction plaque during the embryonic development of mice with connexin-associated deafness. The degradation of the gap junction macromolecular complex leads to loss of hearing function [60] caused by diets [61].

The abnormal or missing gap junctions likely alter the level of potassium ions, which may affect the function and survival of cells that are essential for hearing in the inner ear. The spatial and temporal heteromeric associations of Cx26 and Cx30 proteins in the inner ear have been confirmed earlier [26, 62]. This finding has not been reconfirmed until now. Forge's results had an essential role to understand the pathophysiologic processes of nonsyndromic deafness caused by mutations in GJB2 genes.

Previously, we have demonstrated that the Cx26 mutation frequently occurs in the Hungarian population [7]. In this study we demonstrated that the ratio of homozygotes and heterozygotes is 1.0:1.0 in the mutated GJB2 genes, which suggests that the frequency of heterozygotes is rather high in hearing impaired patients. Further investigations are required to identify additional mutated genes. The combination of heterozygote forms of additional channels may also be involved in the causes leading to deafness in the Caucasian population, because about 73.8% of hearing impaired subjects is not carriers for mutations of the GJB2 gene.

Connexins are 25% more abundant in the sensory epithelial cells of the inner ear than in mammalian supporting cell types and these cells infrequently contain more than 100,000 channels. Forge and co-workers have demonstrated [62] that four connexin isotypes, Cx26, Cx30, Cx31 and Cx43, can be found in different mammalian species, in the cochlea and three of them,



Cx26, Cx30 and Cx43, in the vestibular organs. The spatial distribution of connexins in the inner ear has been extensively investigated and it was suggested that these connexin channels are isolated both spatially and functionally. The Cx26 and Cx30 are found in supporting cells of the organ of Corti, in the basal cell region of the stria vascularis, and in type 1 fibrocytes of the spiral ligament, but no other connexin type was detected in this area. Cx31 localizes around the type 2 fibrocytes and below the spiral prominence. Cx30 was not expressed here and the amount of Cx26 expression was low in the above areas [62]. Cx43 was only detected in one region where “tension fibrocytes” line the inner aspect of the otic capsule. It is an important result that Cx26 colocalizes with Cx30 as detected by electron microscopic and immunoprecipitation methods for protein expression.

The majority of gap junction forming proteins in the inner ear potassium-recycling pathway includes Cx26, Cx30 and Cx43. The heteromeric association of Cx26 and Cx30 proteins indicates a fine regulation in the connexin composition of the gap junction channels in the inner membrane of the cochlea, and the altered potassium homeostasis might also be related to the redistributed ion channels on blood cells. The heteromeric coexpression of Cx40-Cx43-Cx45 was evaluated by Desplantez et al. [63, 64] in liver cells, and low levels of Cx40/Cx43 coexpression was detected in heart tissues demonstrating that the Cx40:Cx43 ratio regulates the composition and electrical properties of gap junctions [65–68], which may also be the case in the cochlea.

The age of the 35delG mutation was estimated by Van Lear and co-workers [12]. This mutation was tested in ancestors for about 500 generations, indicating an approximate age of 10,000 years in various populations. The mutations in the Hungarian Caucasian population demonstrate a European average.

We saw a high expression of Cx26 and Cx43 proteins in the blood cells of non-diseased patients where the high intensity staining on the surface of cells indicated a high abundance of Cx26. In the presence of the GJB2 gene mutation, the Cx26 protein level decreased and the pattern of the distribution was disrupted. These results suggest that the expression of GJB2 gene is regulated at the level of transcription and translation in non-diseased patients. Furthermore, it supported the results that the GJB2 gene deficiency is presumably associated with cochlear developmental disorders [66].

Our results indicate that the absence or a reduced presence of Cx26 channels contributes to the development of deafness in humans, which is in support of earlier results [1, 7, 57]. The widely distributed Cx26 and Cx30 and Cx43 proteins have an essential role in the regulation of early ear development [9, 26, 35] and also in the regulation of potassium pathways in the inner ear of adults [26, 62, 67].

#### **4.2. The possible role of Kir2.1 ion channels in the cochlea**

Kir2.x ion channels have an important physiological function in transporting potassium ions back into the cells, but the mutations of these ion channels are rarely detected. The role of Kir2.1 ion channels, well-known in Andersen-Tawil syndrome, has only recently been

confirmed for deafness [36, 37, 69], and this suggests the importance of in the auditory system. The spatial and temporal localization of Kir2.x channels has been mapped in the inner ear by Forge et al. [62], Jagger et al. [26] and its significance has been described by Meredith et al. [70]. Kir2.1 was characterized as a strong inwardly rectifying ion channel in the vestibular type II hair cells by Zampini et al. [18], Correia et al. [71] in avian and mammalian settings too [47, 69]. An inwardly rectifying potassium channel itself, Kir5.1 plays a vital role in regulating cochlear K<sup>+</sup> circulation which is necessary for normal hearing, and it has age-related reduction in expression [71] just like SAP97, but contrary to the Kir2.1 ion channels [45]. The developmental study by Ruan et al. [20, 21] carried out in mouse has shown the temporal pattern of Kir2.1 channels in different parts of the hearing system. Kir2.1 has a temporal expression in the hair cells of mouse cochleae that correlates with the functional maturation of the hair cells and the neurons. The stronger signals were generally detected in the apical parts of the cochlea and on row 3 outer hair cells after birth. However, the Kir2.1 ion channels in human adults have been detected mostly in the vestibular system. In all types of cells the mutations of these channels still indicated that the homomer and heteromer Kir2.x channel compositions are necessary in the mammalian inner ear. Lewin and Holt [47], and also Meredith and Rennie [70] identified the functional contribution of Kir2.1 in the I<sub>K1</sub> current in utricle hair cells. They demonstrated that Kir2.1 is required for I<sub>K1</sub> currents in type II utricle hair cells and that Kir2.1 contributes to the hyperpolarized resting potentials [46] and also to the fast, small amplitude receptor potentials.

The effective functioning of the Kir2.x protein tripartite complex, requires an association of proteins involving SAP97 and calcium calmodulin kinase II (CaMKII) with Kir2.1 ion channels, and Kir2.6 ion channel also has an essential role to deliver the matured Kir2.x protein to the membrane surface [42, 43]. In this study, we showed that the amount of Kir2.1 channel was close to the control in hearing loss patients where we could not detect GJB2 gene mutations. The low level of SAP97 anchoring protein decreased drastically in hearing loss patients. Our results confirmed the colocalization of Kir2.1 ion channel with SAP97 anchoring protein in non-diseased patients but only partial colocalization with disrupted clustering occurred on the surface of blood cells in patients with deafness. This redistribution of the Kir2.1 channel complex, and also the clearly visible reorganization of Cx26 and Cx43 channels, suggests the instability of Kir2.1 and connexin macromolecule complexes in blood cells. This redistribution of Kir2.1 ion channels and Cx26 on the surface of blood cells may lead to a weakened physiological function of Kir2.1 channels and gap junctions, which, in turn, may influence the potassium homeostasis in the sensorineural system [73, 74]. These direct or indirect interactions are essential for the normal physiological function of the Kir2.1 complex and inward rectifier currents contributing to normal potassium ion homeostasis [71, 72].

The development of new diagnostic techniques for molecular biology analysis together with deep insights into molecular physiology requires subcellular nanotechnology tools in biomedical research and clinical diagnostics. In this study, we report on hearing impaired patients with a series of hearing screenings using modern equipment, and we have developed a new molecular method to study the critical potassium ion channels contributing to normal cochlear function.

## 5. Conclusion

Altered expression of Cx26 with Kir2.1 ion channel complex in hearing loss patients profoundly determines the potassium-recycling pathway and the alteration of these channels in blood cells in deafness detectable using molecular tools.

The Kir2.x ion channels and connexin channels may have an essential role in the  $I_{K1}$  currents of the cochlea and vestibule during the development process and may serve as diagnostic markers in the early stage of the pathophysiology of hearing loss.

## Acknowledgements

This study was supported by grant EFOP-3.6.2-16-2017-00009, which supported MSz, NN, JGK, JAJ, and RN. VSz was supported through the NKFIH-112688 and OTKA K112688 grants. The authors thank Professor Dr. Gyozo Garab and his group for complementary protein studies, Dr. Ferhan Ayaydin, Zsuzsanna Koszo, Ildiko Kelemen Valkonyne, and Peter Deak for their assistance in confocal microscopy.

## Conflict of interest

The authors have nothing to disclose.

## Author contributions

MS was the mentor who guided the genetic research study; JAJ and LR tested patients and wrote the manuscript; NN designed and performed the genetic analyses; JGK, AN, RN KH, VSZ carried out protein experiments, analyzed data, and VSZ, FO, JAJ and KH wrote the first draft of the manuscript.

## Abbreviation

ABR	auditory brain stem responses
AEP	auditory evoked potentials
AP	action potential
ARNSHL	autosomal recessive non-syndromic hearing loss

ASSR	auditory steady-state responses
CaMKII	calcium calmodulin kinase II
Cx26	connexin26
Cx30	connexin30
Cx31	connexin31
Cx43	connexin43
Cx45	connexin45
DAPI	2,4-diamino-2-phenylindole
DBS	dried blood spots
DNA	deoxyribonucleic acid
DPOAE	distortion product otoacoustic emission
EDTA	ethylenediaminetetraacetic acid
EOAE	evoked otoacoustic emissions
GJB2	gap junction protein beta 2
GJB3	gap junction protein beta 3
GJB6	gap junction protein beta 6
HC	hemichannel
Kv-type	voltage-gated potassium channel
Kir2.x	potassium inward-rectifier ion channel 2.x
MAGUK	membrane associated guanylate kinase
OAE	otoacoustic emission
PCR	polymerase chain reaction
PDS	Pendred syndrome
PM	plasma membrane
SAP97	synapse-associated protein 97
SNHL	sensorineural hearing loss
SOAE	spontaneous otoacoustic emission

## Author details

Viktoria Szuts<sup>1,2\*</sup>, Janos Andras Jarabin<sup>3</sup>, Nikoletta Nagy<sup>4</sup>, Ferenc Otvos<sup>5</sup>, Roland Nagy<sup>3</sup>, Attila Nagy<sup>3,6</sup>, Katalin Halasy<sup>7</sup>, Laszlo Rovo<sup>3</sup>, Marta Szell<sup>4,8</sup> and Jozsef Geza Kiss<sup>3</sup>

\*Address all correspondence to: [szutsvik@hotmail.com](mailto:szutsvik@hotmail.com)

1 Institute of Plant Biology, Biological Research Centre, Hungarian Academy of Sciences, Szeged, Hungary

2 Department of Food Engineering, Faculty of Engineering, University of Szeged, Szeged, Hungary

3 Department of Oto-Rhino-Laryngology and Head-Neck, Faculty of Medicine, University of Szeged, Szeged, Hungary

4 Department of Medical Genetics, Faculty of Medicine, University of Szeged, Szeged, Hungary

5 Institute of Biochemistry, Biological Research Centre, Hungarian Academy of Sciences, Szeged, Hungary

6 Department of Medical Physics and Informatics, Faculty of Medicine and Faculty of Sciences and Informatics, University of Szeged, Szeged, Hungary

7 Department of Anatomy and Histology, University of Veterinary Medicine, Budapest, Hungary

8 MTA-SZTE Dermatological Research Group, University of Szeged, Szeged, Hungary

## References

- [1] Kemperman MH, Hoefsloot LH, Cremers CWRJ. Hearing loss and connexin 26. *Journal of the Royal Society of Medicine*. 2002;**95**(4):171-177. DOI: 10.1258/jrsm.95.4.171
- [2] Zelante L, Gasparini P, Estivill X, Melchionda S, D'Agruma L, Govea N, Milá M, Della Monica M, Lutfi J, Shohat M, Mansfield E, Delgrosso K, Rappaport E, Surrey S, Fortina P. Connexin26 mutations associated with the most common form of non-syndromic neurosensory autosomal recessive deafness (DFNB1) in Mediterraneans. *Human Molecular Genetics*. 1997;**6**(9):1605-1609. DOI: 10.1093/hmg/6.9.1605
- [3] Estivill X, Rabionet R. The Connexin-deafness homepage World Wide Web URL: [<http://www.iro.es/deafness>] [Accessed: November 2001]
- [4] Marlin S, Garabédian EN, Roger G, Moatti L, Matha N, Lewin P, Petit C, Denoyelle F. Connexin 26 gene mutations in congenitally deaf children: Pitfalls for genetic counseling. *Archives of Otolaryngology – Head & Neck Surgery*. 2001;**127**(8):927-933

- [5] Mueller RF, Nehammer A, Middleton A, Houseman M, Taylor GR, Bitner-Glindzciz M, Van Camp G, Parker M, Young ID, Davis A, Newton VE, Lench NJ. Congenital non-syndromal sensorineural hearing impairment due to connexin 26 gene mutations—Molecular and audiological findings. *International Journal of Pediatric Otorhinolaryngology*. 1999;**50**(1):3-13. DOI: 10.1016/S0165-5876(99)00242-6
- [6] Chan DK, Schrijver I, Chang KW. Connexin-26-associated deafness: Phenotypic variability and progression of hearing loss. *Genetics in Medicine*. 2010;**12**(3):174-181. DOI: 10.1097/GIM.0b013e3181d0d42b
- [7] Nagy AL, Csáki R, Klem J, Rovó L, Tóth F, Tálosi G, Jóri J, Kovács K, Kiss JG. Minimally invasive genetic screen for GJB2 related deafness using dried blood spots. *International Journal of Pediatric Otorhinolaryngology*. 2010;**74**(1):75-81. DOI: 10.1016/j.ijporl.2009.10.021
- [8] Pointis G, Gilleron J, Carette D, Segretain D. Physiological and physiopathological aspects of connexins and communicating gap junctions in spermatogenesis. *Philosophical Transactions of the Royal Society, B: Biological Sciences*. 2010;**365**(1546):1607-1620. DOI: 10.1098/rstb.2009.0114
- [9] Forge A, Jagger DJ, Kelly JJ, Taylor RR. Connexin30-mediated intercellular communication plays an essential role in epithelial repair in the cochlea. *Journal of Cell Science*. 2013;**126**(7):1703-1712. DOI: 10.1242/jcs.125476
- [10] Fiori MC, Reuss L, Cuello LG, Altenberg GA. Functional analysis and regulation of purified connexin hemichannels. *Frontiers in Physiology*. 2014:71. DOI: 10.3389/fphys.2014.00071
- [11] Shearer AE, Eppsteiner RW, Booth KT, Ephraim SS, Gurrola J, Simpson A, Black-Ziegelbein EA, Joshi S, Ravi H, Giuffre AC, Happe S, Hildebrand MS, Azaiez H, Bayazit YA, Emin Erdal M, Lopez-Escamez JA, Gazquez I, Tamayo ML, Gelvez NY, Leal GL, Jalas C, Ekstein J, Yang T, Usami S, Kahrizi K, Bazazzadegan N, Najmabadi H, Scheetz TE, Braun TA, Casavant TL, LeProust EM, Smith RJ. Utilizing ethnic-specific differences in minor allele frequency to recategorize reported pathogenic deafness variants. *American Journal of Human Genetics*. 2014;**95**(4):445-453. DOI: 10.1016/j.ajhg.2014.09.001
- [12] Van Laer L, Coucke P, Mueller RF, Caethoven G, Flothmann K, Prasad SD, Chamberlin GP, Houseman M, Taylor GR, Van de Heyning CM, Franssen E, Rowland J, Cucci RA, Smith RJH, Van Camp G, Van Camp G. A common founder for the 35delG GJB2 gene mutation in connexin 26 hearing impairment. *Journal of Medical Genetics*. 2001;**38**(8):515-518. DOI: 10.1136/jmg.38.8.515
- [13] Mahdiah N, Rabbani B. Statistical study of 35delG mutation of GJB2 gene: A meta-analysis of carrier frequency. *International Journal of Audiology*. 2009;**48**(6):363-370. DOI: 10.1080/14992020802607449
- [14] Morell RJ, Kim HJ, Hood LJ, Goforth L, Friderici K, Fisher R, Van Camp G, Berlin CI, Oddoux C, Ostrer H, Keats B, Friedman TB. Mutations in the connexin 26 gene (GJB2)

- among Ashkenazi Jews with nonsyndromic recessive deafness [see comments]. *The New England Journal of Medicine*. 1998;**339**:1500-1505. DOI: 10.1056/NEJM199811193392103
- [15] Lerer I, Sagi M, Malamud E, Levi H, Raas-Rothschild A, Abeliovich D. Contribution of connexin 26 mutations to nonsyndromic deafness in Ashkenazi patients and the variable phenotypic effect of the mutation 167delT. *American Journal of Medical Genetics*. 2000;**95**(1):53-56. DOI: 10.1002/1096-8628(20001106)95:1<53::AID-AJMG11>3.0.CO;2-2
- [16] Kelley PM, Cohn E, Kimberling WJ. Connexin 26: Required for normal auditory function. *Brain Research Reviews*. 2000;**32**:184-188. DOI: 10.1016/S0165-0173(99)00080-6
- [17] Hibino H, Inanobe A, Furutani K, Murakami S, Findlay I, Kurachi Y. Inwardly rectifying potassium channels: Their structure, function, and physiological roles. *Physiological Reviews*. 2010;**90**(1):291-366. DOI: 10.1152/physrev.00021.2009
- [18] Zampini V, Masetto S, Correia MJ. Elementary properties of Kir2.1, a strong inwardly rectifying K<sup>+</sup> channel expressed by pigeon vestibular type II hair cells. *Neuroscience*. 2008;**155**(4):1250-1261. DOI: 10.1016/j.neuroscience.2008.06.048
- [19] Hofherr A. Selective Golgi export of Kir2.1 controls the stoichiometry of functional Kir2.X channel heteromers. *Journal of Cell Science*. 2005;**118**(9):1935-1943. DOI: 10.1242/jcs.02322
- [20] Ruan Q, Chen D, Wang Z, Chi F, Yin S, Wang J. Topological and developmental expression gradients of Kir2.1, an inward rectifier K<sup>+</sup> channel, in spiral ganglion and cochlear hair cells of mouse inner ear. *Developmental Neuroscience*. 2008;**30**(6):374-388. DOI: 10.1159/000164687
- [21] Ruan Q, Chen D, Wang Z, Chi F, He J, Wang J, Yin S. Effects of Kir2.1 gene transfection in cochlear hair cells and application of neurotrophic factors on survival and neurite growth of co-cultured cochlear spiral ganglion neurons. *Molecular and Cellular Neurosciences*. 2010;**43**(3):326-339. DOI: 10.1016/j.mcn.2009.12.006
- [22] Rook MB. Physiologic function of I(K1) requires a combination of Kir2 isoforms. *Heart Rhythm*. 2007;**4**(4):497-498. DOI: 10.1016/j.hrthm.2006.12.041
- [23] Anumonwo JMB, Lopatin AN. Cardiac strong inward rectifier potassium channels. *Journal of Molecular and Cellular Cardiology*. 2010;**48**(1):45-54. DOI: 10.1016/j.yjmcc.2009.08.013
- [24] Leonoudakis D, Conti LR, Radeke CM, McGuire LMM, Vandenberg CA. A multi-protein trafficking complex composed of SAP97, CASK, Veli, and Mint1 is associated with inward rectifier Kir2 potassium channels. *The Journal of Biological Chemistry*. 2004;**279**(18):19051-19063. DOI: 10.1074/jbc.M400284200
- [25] Vaidyanathan R, Taffet SM, Vikstrom KL, Anumonwo JMB. Regulation of cardiac inward rectifier potassium current (IK1) by synapse-associated protein-97. *The Journal of Biological Chemistry*. 2010;**285**(36):28000-28009. DOI: 10.1074/jbc.M110.110858
- [26] Jagger DJ, Forge A. Connexins and gap junctions in the inner ear – It's not just about K<sup>+</sup> recycling. *Cell and Tissue Research*. 2015;**360**(3):633-644. DOI: 10.1007/s00441-014-2029-z

- [27] Isomoto S, Kondo C, Kurachi Y. Inwardly rectifying potassium channels: Their molecular heterogeneity and function. *The Japanese Journal of Physiology*. 1997;**47**(1):11-39. DOI: 10.2170/jjphysiol.47.11
- [28] Kelsell DP, Dunlop J, Stevens HP, Lench NJ, Liang JN, Parry G, Mueller RF, Leigh IM. Connexin 26 mutations in hereditary non-syndromic sensorineural deafness. *Nature*. 1997;**387**:80-83. DOI: 10.1038/387080a0
- [29] Abdelhadi O, Iancu D, Stanescu H, Kleta R, Bockenbauer D. EAST syndrome: Clinical, pathophysiological, and genetic aspects of mutations in KCNJ10. *Rare Diseases*. 2016;**4**(1):e1195043. DOI: 10.1080/21675511.2016.1195043
- [30] Csanády M, Faragó M, Forster T, Hógye M, Gy P. Study of the course of inheritance of dilated familial cardiomyopathy. *European Heart Journal*. 1991;**12**:191
- [31] Denoyelle F, Marlin S, Weil D, Moatti L, Chauvin P, Garabédian EN, Petit C. Clinical features of the prevalent form of childhood deafness, DFNB1, due to a connexin-26 gene defect: Implications for genetic counselling. *Lancet*. 1999;**353**:1298-1303. DOI: 10.1016/S0140-6736(98)11071-1
- [32] Abe S, Usami S, Shinkawa H, Kelley PM, Kimberling WJ. Prevalent connexin 26 gene (GJB2) mutations in Japanese. *Journal of Medical Genetics*. 2000;**37**:41-43
- [33] Marlin S, Garabedian EN, Roger G, Moatti L, Matha N, Lewin P, Petit C, Denoyelle F. Connexin 26 gene mutations in congenitally deaf children: Pitfalls for genetic counselling. *Archives of Otolaryngology – Head & Neck Surgery*. 2001;**127**:927-933
- [34] Martini A, Calzolari F, Sensi A. Genetic syndromes involving hearing. *International Journal of Pediatric Otorhinolaryngology*. 2009;**73**(Sp1):S2-S12. DOI: 10.1016/S0165-5876(09)70002-3
- [35] Nickel R. Forge a gap junctions and connexins in the inner ear: Their roles in homeostasis and deafness. *Current Opinion in Otolaryngology & Head and Neck Surgery*. 2008 Oct;**16**(5):452-457. DOI: 10.1523/JNEUROSCI.1932-14.2014
- [36] Plaster NM, Tawil R, Tristani-Firouzi M, Canún S, Bendahhou S, Tsunoda A, Donaldson MR, Iannaccone ST, Brunt E, Barohn R, Clark J, Deymeer F, George AL, Fish FA, Hahn A, Nitu A, Ozdemir C, Serdaroglu P, Subramony SH, Wolfe G, Fu YH, Ptáček LJ. Mutations in Kir2.1 cause the developmental and episodic electrical phenotypes of Andersen's syndrome. *Cell*. 2001;**105**(4):511-519. DOI: 10.1016/S0092-8674(01)00342-7
- [37] Tristani-Firouzi M, Etheridge SP. Kir 2.1 channelopathies: The Andersen-Tawil syndrome. *Pflügers Archiv / European Journal of Physiology*. 2010;**460**(2):289-294. DOI: 10.1007/s00424-010-0820-6
- [38] Jun AI, McGuirt WT, Hinojosa R, Green GE, Fischel-Ghodsian N, Smith RJ. Temporal bone histopathology in connexin 26-related hearing loss. *Laryngoscope*. 2000;**110**:269-275. DOI: 10.1097/00005537-200002010-00016



- [39] Zobel C, Cho HC, Nguyen TT, Pekhletski R, Diaz RJ, Wilson GJ, Backx PH. Molecular dissection of the inward rectifier potassium current ( $I_{K1}$ ) in rabbit cardiomyocytes: Evidence for heteromeric co-assembly of  $K_{ir2.1}$  and  $K_{ir2.2}$ . *The Journal of Physiology*. 2003;**550**(Pt 2): 365-372. DOI: 10.1113/jphysiol.2002.036400
- [40] Gaborit N, Varro A, Le Bouter S, Szuts V, Escande D, Nattel S, Demolombe S. Gender-related differences in ion-channel and transporter subunit expression in non-diseased human hearts. *Journal of Molecular and Cellular Cardiology*. 2010;**49**:639-646. DOI: 10.1016/j.yjmcc.2010.06.005
- [41] Yanni J, Tellez TO, Mackewski JO, Mackiewicz U, Beresewich A, Beresewicz A, Billeter R, Dobrzynski H, Boyett M. Changes of ion channels gene expression underlying heart failure induced sinoatrial node dysfunction. *Circular Heart Failure*. 2011;**4**:496-508. DOI: 10.1161/CIRCHEARTFAILURE.110.957647
- [42] Muströph J, Maier SL, Wagner S. CaMKII regulation of cardiac K channels. *Frontiers in Pharmacology*. 2014;**5**:1-12. DOI: 10.1016/j.pharmthera.2016.10.006
- [43] Dassau L, Conti RL, Radekr MC, Ptacek JL, Vandenberg AC. Kir2.6 regulates the surface expression of Kir2.X inward rectifier potassium channels. *The Journal of Biological Chemistry*. 2011;**286**:9526-9541. DOI: 10.1074/jbc.M110.170597
- [44] Ma D, Taneja TK, Hagen BM, Kim B-Y, Ortega B, Lederer WJ, Welling PA. Golgi export of the Kir2.1 channel is driven by a trafficking signal located within its tertiary structure. *Cell*. 2011;**145**:1102-1115. DOI: 10.1016/j.cell.2011.06.007
- [45] Szuts V, Menesi D, Varga-Orvos Z, Zvara A, Houshmand N, Bitay M, Bogats G, Virag L, Baczko I, Szalontai B, Geramipour A, Cotella D, Wettwer E, Ravens U, Deak F, Puskas LG, Papp JG, Kiss I, Varro A, Jost N. Altered expression of genes for Kir ion channels in dilated cardiomyopathy. *Canadian Journal of Physiology and Pharmacology*. 2013;**91**(8):648-656. DOI: 10.1139/cjpp-2012-0413
- [46] Horwitz GC, Risner-Janiczek JR, Jones SM, Holt JR. HCN channels expressed in the inner ear are necessary for normal balance function. *The Journal of Neuroscience*. 2011;**31**:16814-16825
- [47] Levin ME, Holt JR. The function and molecular identity of inward rectifier channels in vestibular hair cells of the mouse inner ear. *Journal of Neurophysiology*. 2012;**108**(1):175-186. DOI: 10.1152/jn.00098.2012
- [48] Szuts V, Fazekas P, Kovacs A, Nagy A, Deak P, Jarabin JA, Otvos F, Cs V, Szecsi M, Halasy K, Rovo L, Kiss JG. Connexins and Kir2.1 ion channels modulated in hearing loss patients before cochlear implantation. International congress of cochlear implantation & OMAI congress, Szeged, Hungary, 2016 June. *Otorhinolaryngologica Hungarica*. 2016;**62**(Suppl.A):A38
- [49] Hoth S, Baljić I. Current audiological diagnostics. *GMSCurrent Topic Otorhinolaryngology Head & Neck Surgery*. 2017 Dec;**16**:Doc09. DOI: 10.3205/cto000148

- [50] François M, Dehan E, Carlevan M, Dumont H. Use of auditory steady-state responses in children and comparison with other electrophysiological and behavioral tests. *European Annals of Otorhinolaryngology, Head and Neck Diseases*. 2016;**133**(5):331-335. DOI: 10.1016/j.anorl.2016.07.008
- [51] Janssen T, Gehr DD, Klein A, Muller J. Distortion product otoacoustic emissions for hearing threshold estimation and differentiation between middle-ear and cochlear disorders in neonates. *The Journal of the Acoustical Society of America*. 2005;**117**(5):2969-2979. DOI: 10.1121/1.1853101
- [52] McCreery RW, Kaminski J, Beauchaine K, Lenzen N, Simms K, Gorga MP. The impact of degree of hearing loss on auditory brainstem response predictions of behavioral thresholds. *Ear and Hearing*. 2015;**36**(3):309-319. DOI: 10.1097/AUD.0000000000000120
- [53] Rodrigues GRI, Ramos N, Lewis DR. Comparing auditory brainstem responses (ABRs) to toneburst and narrow band CE-chirp in young infants. *International Journal of Pediatric Otorhinolaryngology*. 2013;**77**(9):1555-1560. DOI: 10.1016/j.ijporl.2013.07.003
- [54] Curthoys IS. The new vestibular stimuli: Sound and vibration—Anatomical, physiological and clinical evidence. *Experimental Brain Research*. 2017;**235**(4):957-972. DOI: 10.1007/s00221-017-4874-y
- [55] Kristensen SGB, Elberling C. Auditory brainstem responses to level-specific chirps in normal-hearing adults. *Journal of the American Academy of Audiology*. 2012;**23**(9):712-721. DOI: 10.3766/jaaa.23.9.5
- [56] Korczak P, Smart J, Delgado RM, Strobel T, Bradford C. Auditory steady-state responses. *Journal of the American Academy of Audiology*. 2012;**23**(3):146-170. DOI: 10.3766/jaaa.23.3.3
- [57] Cremers, Frans PM. Genetic causes of hearing loss. *Current Opinion in Neurology*. February 1998;**11**(1):11-16
- [58] Qu Y, Tang W, Zhou B, Ahmad S, Chang Q, Li X, Lin X. Early developmental expression of connexin26 in the cochlea contributes to its dominate functional role in the cochlear gap junctions. *Biochemical and Biophysical Research Communications*. 2012;**417**(1):245-250. DOI: 10.1016/j.bbrc.2011.11.093
- [59] Kikuchi T, Kimura RS, Paul DL, Takasaka T, Adams JC. Gap junction systems in the mammalian cochlea. *Brain Research Reviews*. 2000;**32**:163-166
- [60] Kamiya K, Yum SW, Kurebayashi N, Muraki M, Ogawa K, Karasawa K, Miwa A, Guo X, Gotoh S, Sugitani Y, Yamanaka H, Ito-Kawashima S, Iizuka T, Sakurai T, Noda T, Minowa O, Ikeda K. Assembly of the cochlear gap junction macromolecular complex requires connexin 26. *The Journal of Clinical Investigation*. 2014 Apr;**124**(4):1598-1607. DOI: 10.1172/JCI67621
- [61] Wu X, Wang Y, Sun Y, Chen S, Zhang S, Shen L, Huang X, Lin X, Kong W. Reduced expression of Connexin26 and its DNA promoter hypermethylation in the inner ear of mimetic aging rats induced by D-galactose. *Biochemical and Biophysical Research Communications*. 2014;**452**(3):340-346. DOI: 10.1016/j.bbrc.2014.08.063

- [62] Forge A, Becker D, Casalotti S, Edwards J, Marziano N, Nevill G. Gap junctions in the inner ear: Comparison of distribution patterns in different vertebrates and assessment of Connexin composition in mammals. *The Journal of Comparative Neurology*. 2003;**467**(2):207-231. DOI: 10.1002/cne.10916
- [63] Desplantez T, Grikscheit K, Thomas NM, Peters NS, Severs NJ, Dupont E. Relating specific connexin co-expression ratio to connexon composition and gap junction function. *Journal of Molecular and Cellular Cardiology*. 2015 Dec;**89**(Pt B):195-202. DOI: 10.1016/j.yjmcc.2015.11
- [64] Desplantez T. Cardiac Cx43, Cx40 and Cx45 co-assembling: Involvement of connexins epitopes in formation of hemichannels and Gap junction channels. *BMC Cell Biology*. 2017 Jan 17;**18**(Suppl 1):3. DOI: 10.1186/s12860-016-0118-4
- [65] Chaigne S, Dupuis S, Constantin MDT. Co-expressed cardiac connexins: Dependence on the Cx43:Cx40 ratio in regulating the gap junction channel make-up and electrical properties. *Cardiovascular Research Supplements*. 2014;**103**(Supplement 1):S20. DOI: 10.1093/cvr/cvu082.58
- [66] Dupuis S, Chaigne S, Constantin M, Desplantez T. Dependence of the cardiac connexins Cx43:Cx45 ratio on the formation of gap junction channels and their electrical properties. *Cardiovascular Research Supplements*. 2014;**103**(Suppl. 1):S116-S117. DOI: 10.1093/cvr/cvu098.68
- [67] Chan DK, Chang KW. GJB2-associated hearing loss: Systematic review of worldwide prevalence, genotype, and auditory phenotype. *The Laryngoscope*. 2014 Feb;**124**(2):E34-E53. DOI: 10.1371/journal.pone.0167850
- [68] Liu W, Li H, Edin F, Brännström J, Glueckert R, Schrott-Fischer A, Molnar M, Pacholsky D, Pfaller K, Rask-Andersen H. Molecular composition and distribution of gap junctions in the sensory epithelium of the human cochlea—a super-resolution structured illumination microscopy (SR-SIM) study. *Upsala Journal of Medical Sciences*. 2017 Aug;**122**(3):160-170. DOI: 10.1080/03009734.2017.1322645
- [69] Lu CW, Lin JH, Rajawat YS, Jerng H, Rami TG, Sanchez X, DeFreitas G, Carabello B, DeMayo F, Kearney DL, Miller G, Li H, Pfaffinger PJ, Bowles NE, Khoury DS, Towbin JA. Functional and clinical characterization of a mutation in KCNJ2 associated with Andersen-Tawil syndrome. *Journal of Medical Genetics*. 2006;**43**(8):653-659
- [70] Meredith FL, Rennie KJ. Channeling your inner ear potassium: K<sup>+</sup> channels in vestibular hair cells. *Hearing Research*. 2016;**338**:40e51. DOI: 10.1016/j.heares.2016.01.015
- [71] Correia MJ, Wood TG, Prusak D, Weng T, Rennie KJ, Wang HQ. Molecular characterization of an inward rectifier channel (IKir) found in avian vestibular hair cells: cloning and expression of pKir2.1. *Physiol Genomics*. 2004;**19**(2):155-169. PMID: 15316115
- [72] Pan C, Chu H, Lai Y, Sun Y, Du Z, Liu CJ, Tong T, Chen QL, Bing D, Tao Y. Downregulation of inwardly rectifying potassium channel 5.1 expression in C57BL/6J cochlear lateral wall. *Journal of Huazhong University Science of Technology [Medical Science]*. 2016;**36**(3):406-409

- [73] Collado MS, Holt JR. Can neurosphere production help restore inner ear transduction? *Proceedings of the National Academy of Sciences of the United States of America*. 2009 Jan 6;**106**(1):8-9. DOI: 10.1073/pnas.0811804106
- [74] Forge A, Taylor RR, Dawson SJ, Lovett M, Jagger DJ. Disruption of SorCS2 reveals differences in the regulation of stereociliary bundle formation between hair cell types in the inner ear. *PLoS Genetics*. 2017 Mar 27;**13**(3):e1006692. DOI: 10.1371/journal.pgen.1006692

---

## Divalent Cations

---



---

# Role of Calcium Permeable Channels in Pain Processing

---

Célio Castro-Junior, Luana Ferreira, Marina Delgado,  
Juliana Silva and Duana Santos

Additional information is available at the end of the chapter

<http://dx.doi.org/10.5772/intechopen.77996>

---

## Abstract

Calcium-permeable channels control intracellular calcium dynamics in both neuronal and nonneuronal cells to orchestrate sensory functions including pain. Calcium entering the cell throughout these channels is associated with transduction, transmission, processing, and modulation of pain signals. Clinic, genetic, biochemical, biophysical and pharmacological evidence points toward calcium-permeable channels as the key players in acute and persistent pain conditions. Ligand-gated calcium channels such as TRP channels or some subtypes of voltage-gated calcium channels shows abnormal functioning in persistent pain states. Also, NMDA receptors can be unlocked from their physiological  $Mg^{2+}$  blockade under persistent pain states to culminate with central sensitization. The primary goal of this chapter is to present an overview of the functioning of different classes of calcium-permeable channels and how they become altered to modulate the sensation of pain in acute and chronic states. The most important evidence from classical and recent studies will be discussed trying to depict ways of modulating those channels as a strategy for better pain control.

**Keywords:** pain, sensitization, calcium channels, NMDA receptors, VGCC's, TRP channels

---

## 1. Introduction

### 1.1. Overall pain neurobiology

For a better understanding of how calcium channels regulation is involved in pain states, it is relevant define pain and discusses overall aspects of the transmission and modulation of pain signals throughout the nervous system. Pain is defined as “an unpleasant sensory and emotional experience associated with actual or potential tissue damage, or described in terms of

---

such damage". This definition was proposed by Harold Merskey in 1964 and was adopted by the International Association of the Study of Pain (IASP) and since 1979 is the most accepted definition for pain worldwide. That definition clearly mention the sensory aspect of pain. As an organic sensorial modality, pain processing relies on electrical signal transmission throughout the nervous system. Despite the fact that emotional features of an individual directly interferes with final pain interpretation, this chapter is focused on the sensory aspects (also called nociception) of pain and how calcium-permeable channels are involved in pain processing.

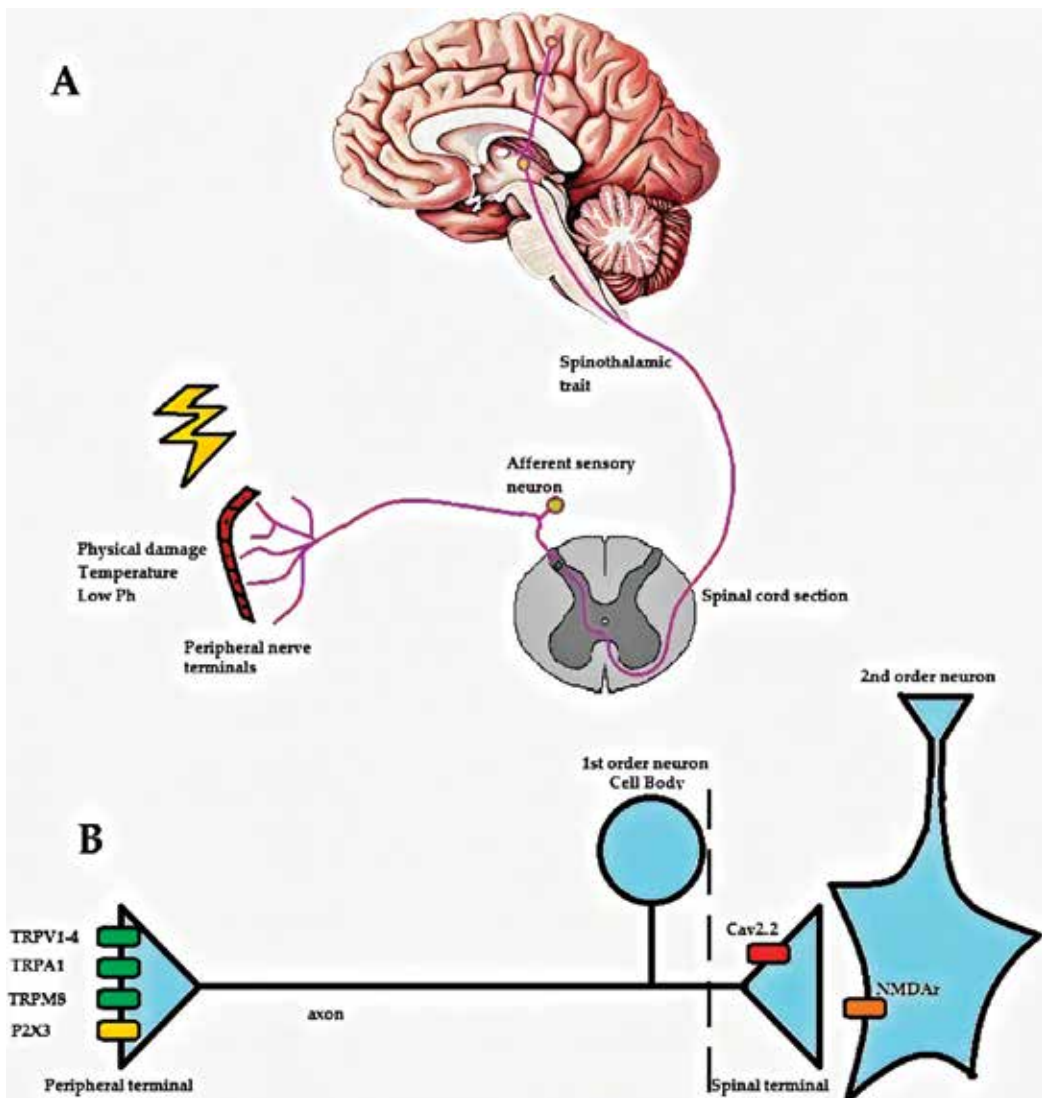
The macroscopic pathway of pain signals comprises a well-accepted route throughout the peripheral and central nervous system (**Figure 1A**). Detection of noxious stimuli may occur in skin, muscle, joints, and internal organs. Generated signals travel from periphery to the spinal cord through axons of sensory afferent fibers. Once those fibers enter the spinal cord through the dorsal horn, they made synapses with second order neurons that convey synaptic release of neurotransmitter into new action potentials. That action potential travels up along the spinal cord mainly through spinothalamic tract until the thalamus where a new synapse occurs and pain can be initially perceived by its intensity. From the thalamus, signals diverge to different brain areas mainly the somatosensory cortex and limbic systems allowing a more broad interpretation and association of pain with emotional experiences (**Figure 1**). This ascending path is counterbalanced by a descending circuitry that connects with the ascending fibers to facilitate or reduce the traffic of electrical pain signals to the brain.

## 1.2. Calcium channels in the pain pathway

Importantly, the ion channels present at the membrane of neurons of the above pathway functionally orchestrate the generation and processing of pain signals (**Figure 1B**). Although calcium channels are the focus of this chapter, sodium and potassium channels also holds prominent contribution of signal transmission mainly on the conduction of the bioelectrical pain signals. Noxious stimuli are initially transduced into electrical signals by the peripheral end of sensory neurons. Those terminals convey diverse sensory modalities such as pain, itch, discriminative touch into action potentials. Some terminals belong to a subset of fibers that are specialized on the detection of noxious stimuli (delta and C fibers). Some of the markers associated with specific nociceptive fibers include calcium-permeable channels such as the cold/menthol receptor TRPM8, the heat vanilloid receptor TRPV1, the mustard oil receptor TRPA1 and the purinergic receptor P2X3.

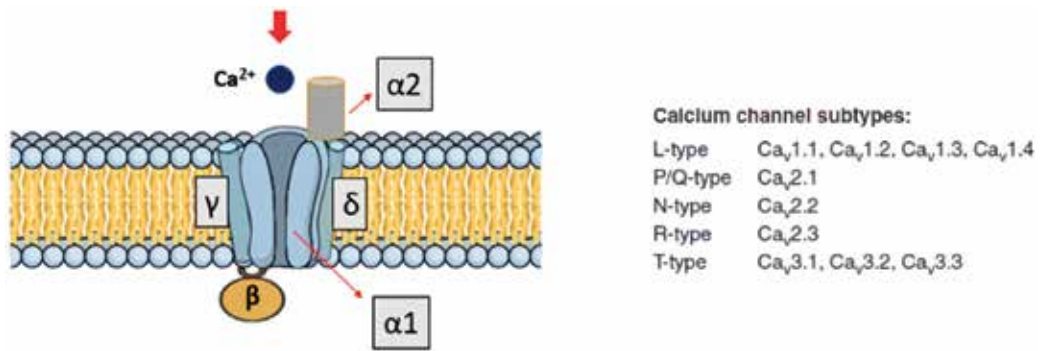
Those markers consist of cation-permeable channels that activate in response to noxious stimuli (e.g. TRPA1 respond to noxious cold and TRPV1 to heat) to allow mainly sodium and calcium influx into the nerve terminal contributing for action potential generation. At the central terminal of sensorial afferent neurons, the action potential triggers the opening of voltage-gated calcium channels and the consecutive influx of calcium ions cause exocytosis of excitatory neurotransmitter (glutamate) which further depolarize a second order neuron in the spinal cord. The expression pattern of N-type voltage gated calcium channels at the dorsal horn of spinal cord is consistent with the role of VGCC's in afferent/spinal synapses. Furthermore, null mice for the N-type channels show higher threshold for thermal and mechanical





**Figure 1.** Afferent processing of nociceptive signals: (A) peripheral nerve terminals trigger action potential in response to harmful stimuli. Electrical potentials reach the spinal cord throughout axons from sensory afferent fibers. At the dorsal horn of spinal cord those afferent fibers make synapse with 2nd order neurons that project to thalamus and then to other brain areas to allow central processing of pain; (B) differential cellular distribution of distinct calcium permeable channels in the ascending pain pathway.

sensitivity. Nevertheless, other subtypes of VGCC's also contribute to this process but N-type channels are the most relevant and studied in this process. The propagation of action potential through thalamus depends on the summation of synaptic potentials received by the 2nd order neuron. Glutamate released on those synapses activate NMDA and AMPA receptors to allow calcium and sodium entry providing a rapid onset depolarization process, thus 3rd and consecutive neurons can be activated (Figure 2).



**Figure 2.** Overall molecular assembly and classification of a voltage gated calcium channels.

Normal pain has an evolutionary purpose of protecting us from harmful environments. Thus, the neurochemical cascade of normal pain relies on the proper function of calcium and other ion channels to allow a physiologic functioning of our sensorial system. However, when pain goes untreated, or when some pathological process goes embedded, maladaptive changes can occur. Ion channels may become differentially expressed, badly recycled, differentially phosphorylated or even unblocked by endogenous ions, therefore, activation thresholds are altered, or ion conductance is increased for a given input, so bioelectrical facilitation occurs with pain signals culminating in a state known as sensitization. The sensitization is present in several chronic pain conditions transforming pain in a worldwide public health problem whose treatment is largely inefficient and challenging. The precise role of calcium channels in the pain process is a very pursued scientific theme. The currently available tools for genetic and molecular studies are unraveling new putative targets that could be controlled in order to promote new options for better pain management.

This chapter presents an overview of current state of art of the knowledge on calcium-permeable channels associated to pain processing. Their divisions, classifications, and way of control are discussed in the view of signaling transmission in pain. Finally, we present how the current understanding of this theme may turn into therapeutic opportunities to treat pain.

## 2. The role of voltage-gated calcium channels (VGCC) in pain

As the name says, these channels are able to respond to variations in the electric field that trigger changes in its conformation, which allows these channels to transit between open or closed states [1]. Therefore, calcium can flow into the intracellular space at depolarized voltages within the peak of action potentials. In this topic, we will give an overview of the updated data involving VGCC's and how they contribute to the pain pathway. Specific details of molecular composition and classification are given in previews chapters of this book.

In resume, VGCC can be classified as L, N, P/Q, R and T and are distinguished by their different sensitivity for some pharmacological agents and their channel conductance kinetics based on their voltage activation properties. The VGCC classes can be further divided into two groups by

their voltage activation properties: the high-voltage activated type (L, N, P/Q and R-type) and the low voltage activated the T-type channel [2, 3]. Besides their biophysical and pharmacological features, different calcium channel isoforms show distinct cellular and subcellular distributions to fulfill specific functional roles. These diverse functional roles ultimately pose a challenge when drawing new calcium channel modulators with low risk of adverse effects.

Several evidences suggest that some subtypes of VGCC have greater involvement in pain pathways than others. The action potentials of neurons are able to reach the central terminals of a sensory neuron, activating voltage-gated calcium channels and allowing calcium influx in the cell, which triggers synaptic vesicle exocytosis containing the neurotransmitters. In sensory neurons of the pain pathway, neurotransmitters such as glutamate, substance P, and CGRP are released after activation of  $\text{Ca}^{2+}$  channels, mainly the L, N and P/Q type [4]. Due to their prominent role in pain processing signals, Calcium channels are considered important targets for the treatment the treatment of pain [5].

### 2.1. N-type ( $\text{Ca}_{v2.2}$ )

This channel is a hetero-oligomeric complex consisting of  $\alpha_{1B}$ ,  $\beta$ , and  $\alpha_2\delta$  subunits (**Figure 2**). N-type channels are present in synaptic terminals of the dorsal horn of spinal cord and in DRG neurons [5]. These channels are not restricted to pain pathways; they are in fact widely distributed in the central nervous system. Some studies show that these channels are proportionally more expressed in small than in large sensory neurons. One of the important functions of N-type is the control of neurotransmitter release. A region in the linker between domains II and III of N-type channel forms a binding site for the proteins coupled to the membrane, allowing the release of neurotransmitters [6, 7].

In animal models of neuropathic pain, N-type channel has been shown to underlie significant changes in their levels and composition. N-type channels are considered the main targets for the development of new analgesics. Studies have shown that knockout mice for N-type channels display higher thresholds for pain perception when compared to their wild-type [8]. The calcium channel blocker known as ziconotide shows proven clinical efficacy against pain when administered intrathecally [9].

### 2.2. L-type ( $\text{Ca}_{v1.1}$ $\text{Ca}_{v1.2}$ $\text{Ca}_{v1.3}$ $\text{Ca}_{v1.4}$ )

L-type  $\text{Ca}_{v1.2}$  and  $\text{Ca}_{v1.3}$  have been reported to be up or down regulated in DRG of neuropathic pain [10]. Studies on the antinociceptive effect of L-type calcium channel blockers combined to opioids have reported significantly higher antinociceptive effect [11]. In sensory neurons, L-type  $\text{Ca}^{2+}$  channels appear to be involved in nociception since nifedipine, a L-type blocker, inhibits the release of substance P induced by inflammation [12].

### 2.3. P/Q-type ( $\text{Ca}_{v2.1}$ )

The  $\text{Ca}_{v2.1}$  subunit drives both P-type and Q-type currents. This channel is expressed in Purkinje and Granular cells but is not restricted to neurons only. In glutamatergic and GABAergic synapses the P/Q currents are essential for the release of neurotransmitters [13].

P/Q-type have an important role in the regulation of neurotransmitter release at central neurons. Although the role of P/Q-type calcium channels in migraine is well established, the participation of these calcium currents in pain signaling is much less understood. The Nagoya mutant mouse carries a loss of function mutation in P/Q channels and shows reduced inflammatory pain phenotype. Although complete deletion of P/Q channels leads to hyposensitivity to neuropathic pain, they paradoxically show increased thermal acute nociception. Indeed, mice that completely lack P/Q presents motor deficit that compromises normal life span. Therefore, although P/Q may contribute to pain signaling, they have a much more limited role than N-type and T-type channels.

#### 2.4. T-type ( $\text{Ca}_{V3.1}$ , $\text{Ca}_{V3.2}$ , $\text{Ca}_{V3.3}$ ) low voltage

T-type calcium channels evoke secretion from the neuroendocrine cells and are capable of associating with the synaptic vesicle release machinery. These channels are activated by membrane potentials close to the resting potential, with low threshold; its inactivation is rapid and reactivation requires a strong hyperpolarization. Due to their hyperpolarized activation range T-type is notoriously associated with the regulation of neuronal excitability. Their main role is probably in the rhythmic action potentials of muscle cells and neurons [14]. T-type channel can be found at dorsal horn of spinal cord, in various subpopulations of primary afferent neurons suggesting, thus, a role of these channels in pain signaling. The activity of T-type is increased in the afferent fibers in chronic pain conditions, such as traumatic nerve injury, metabolic nerve diabetic neuropathy or toxic neuropathies induced by chemotherapy [15]. Conversely, Ethosuximide, a T-type channel blocker, produce analgesia in pain models in rodents.

#### 2.5. R-type ( $\text{Ca}_{V2.3}$ )

R-type channels contribute to neurotransmitter release at certain synapses and are strongly involved in memory and neuronal learning [16] but are also linked to the regulation of neuronal excitability in a number of neuronal subtypes including DRG neurons.  $\text{Ca}_{V2.3}$  channels contribute to pain signaling mechanisms; however, the exact roles of these channels remain to be clarified. These channels are present in the somatosensory neurons of the peripheral ganglia, implying them as components of the pain pathways. Genetic research approaches confirmed this, with R-type knockout mice exhibiting reduced pain perception [8]. Like N-type channels, R-type are upregulated in neuropathic pain associated with nerve damage. SNX-482 is a synthetic peptide derived from the venom of the tarantula *Hysteroocrates gigas* that specifically blocks R-type channels. Intrathecal administration of SNX-482 causes analgesia in models of neuropathic pain [17].

### 3. TRP family and pain

TRP channels represent an extended protein family consisting of more than 30 distinct subtypes of channels. TRP channels were firstly characterized on the *Drosophila melanogaster* eye, in which they act depolarizing the photoreceptor cells in response to light. These channels have characteristics of

polymodal activation since temperature changes, pH alterations and chemicals (ex. Capsaicin) can activate those channels. Once activated, calcium and sodium flow from the extracellular space through these channels to convert the stimuli into locally spreading membrane depolarizations, propagating action potentials to the spinal cord and higher brain centers.

Since the cloning of the first vanilloid receptor (TRPV1), six subfamilies have been described: vanilloid (TRPV), canonical (TRPC), melastatin (TRPM), ankyrin (TRPA), polycystin (TRPP), and mucolipin (TRPML) [18]. The members of the above superfamily participate in the molecular mechanisms of pain signaling by acting as transducers of harmful thermal, mechanical and chemical stimuli, for review see [19]. TRP channels are found not only in neurons but also in a wide variety of cell types, including smooth muscle, epithelial, and immune cells. Since this book chapter is focused on calcium channels and pain, special attention will be given for the role of TRP channels mainly those expressed in sensorial neurons. Therefore, we will discuss the role of TRPV1, TRPA1, TRPV4, and TRPM8 in more details since they are the most well characterized so far regarding their role in the pain pathway. For a more broad view of all TRP members and their respective functions see [20].

Although TRP channels share little similarity between subfamilies, they exhibit a similar membrane topology. Four subunits are required to form a TRP functional channel. Each subunit contains six membrane-spanning helices (termed S1–S6) as well as a pore-forming loop between S5 and S6 that enables the distinct cation selectivity and permeability among TRP channels. Details of the structural and biochemical characterization of TRP channels are presented in previews chapters from this book.

In addition to their pivotal role in the transduction of harmful stimuli into membrane depolarization, a growing number of evidence have been shown that these channels are regulated by pro-inflammatory mediators, such as, serotonin, bradykinin, prostaglandins, proteases, chemokines, and growth factors, confirming how essential these channels are for the sensitization of the afferent pain pathway [21]. Given that these channels are of tremendous importance in somatosensory perception, their dysregulation, as well as the increased expression and sensitivity, is often associated with inflammatory and neuropathic pain [22].

### 3.1. TRPV1 channel

The first characterized nociceptive TRP channel was the transient receptor potential vanilloid type 1 (TRPV1) that was cloned in 1997 using an expression-cloning screening strategy [138]. TRPV1 is a cation permeable channel that is expressed in nociceptive fibers and is responsible for the detection of noxious stimuli from the periphery such as low pH, temperature rises ( $>42^{\circ}\text{C}$ ), osmolality changes, arachidonic acid metabolites, second inflammatory messenger and capsaicin (irritant compound of the chili). TRPV1 channel expression has been reported in small to medium neurons, widely expressed in the central and peripheral nervous system, gastrointestinal tract, bladder epithelium and skin [23]. Because of locating pattern as well as activating properties, the TRPV1 receptors have a key role in the pain transmission.

Topically applied capsaicin and related vanilloid compounds produce burning pain by depolarizing specific subsets of C and A $\delta$  nociceptors due to TRPV1 expression on those fibers.

Type II A $\delta$  nociceptors have a much lower heat threshold, but a very high mechanical threshold. The activity of this afferent almost certainly mediates the “first” acute pain response to noxious heat. The unmyelinated C fibers are also heterogeneous. Like the myelinated afferents, most C fibers are polymodal, that is, they include a population which is sensitive to both heat and mechanical stimuli [24]. Those of greater interest are the heat-responsive, but mechanically insensitive, unmyelinated afferents (so-called silent nociceptors) that develop mechanical sensitivity only in the setting of injury [25].

Studies have shown that other inflammatory mediators such as prostaglandin E<sub>2</sub> (PGE<sub>2</sub>) trigger sensitization of TRPV1 channels via phosphorylation, leading to development of thermal hyperalgesia [26]. Conversely, the lack of such sensitization in TRPV1-knockout mice provides genetic evidence for the idea that TRPV1 is a key component of the mechanism through which inflammation produces thermal hyperalgesia [27]. The interaction result in a deep decrease in the channel’s thermal activation threshold, as well as an increase in the magnitude of responses at suprathreshold temperatures—the biophysical equivalents of allodynia and hyperalgesia, respectively.

TRP channels are activated or positively modulated by phospholipase C-mediated cleavage of plasma membrane phosphatidylinositol 4,5 bisphosphate (PIP<sub>2</sub>). Of course, those are many downstream consequences of this action, including a decrease in membrane PIP<sub>2</sub>, increased levels of diacylglycerol and its metabolites, and increased cytoplasmic calcium, as well as consequent activation of protein kinases. In the case of TRPV1, the most, if not all, of these pathways have been implicated in the sensitization process.

Nevertheless, TRPV1 modulation is one of most relevant to tissue injury-evoked pain hypersensitivity, particularly in the development of inflammation. This would include conditions such as sunburn, infections, rheumatoid or osteoarthritis, and inflammatory bowel disease. Another interesting example includes pain from bone cancer, where tumor growth and bone destruction are accompanied by tissue acidosis, as well as the production of cytokines, neurotrophins, and prostaglandins that can, altogether modulate TRPV1 to cause sensitization.

Several studies have proposed a fundamental role of TRPV1 in hypersensitivity states that result from tissue inflammation, including thermal and mechanical hyperalgesia [28]. Due to its high expression in nociceptors, TRPV1, therefore, blockers of TRPV1 have been shown to have analgesic properties. However, while capsaicin is able to produce central and peripheral sensitization associated with secondary hyperalgesia, prolonged or repetitive administration of capsaicin locally on the epidermis results in channel desensitization, a condition that can result in analgesia [29]. Surprisingly, attempts to develop TRPV1 antagonists have been less successful than the use of TRPV1 agonist such as capsaicin. Given the role of this channel in the regulation of body temperature [30], most of the antagonists tested in preclinical and human studies presented hyperthermic side effects [31].

### 3.2. TRPA1 channel

TRPA1 receptor was originally identified and cloned by Jaquemar et al. in 1999 [32]. In both humans and rodents, TRPA1 is expressed in a subpopulation of small-diameter peptidergic

nociceptors of the dorsal root, nodose, and trigeminal ganglia, along with TRPV1. TRPA1 channel is expressed in vagal and primary afferent fibers innervating the bladder, the pancreas, the heart, the respiratory tract, and the gastrointestinal tract [33].

This channel is activated by a variety of noxious stimuli, including cold temperatures, pungent natural compounds, and environmental irritants as menthol, mustard oil, wasabi and horseradish [34]. TRPA1 is a major effector of the known proinflammatory mediator bradykinin, which elicits sensory neuron excitation *ex vivo* and hyperalgesia *in vivo* [35]. TRPA1 is also modulated indirectly by proalgesic agents, such as bradykinin, which act by PLC-coupled receptors. Studies have evidenced that TRPA1-deficient mice show dramatically reduced cellular and behavioral responses to all of these agents, as well as a reduction in tissue injury-evoked thermal and mechanical hypersensitivity [36].

Genetic evidence in humans also point toward a role of TRPA1 in pain signaling. A recent study described a gain-of-function mutation in humans suffering from episodic pain syndromes. This autosomal dominant mutation occurs in the fourth transmembrane domain of TRPA1 and generates normal pharmacological profile of this receptor but increases inward current at resting potentials. Since cold temperature is a trigger of enhanced pain perception in that human cohort study, the authors confirm the role of the TRPA1 channel as a noxious cold sensor as well as an irritant sensor [37].

Pha1 $\beta$ , the peptide purified from the venom of the armed spider *Phoneutria nigriventer*, which previously has been shown to exhibit antinociceptive effects [38, 39], and its recombinant form (CTK 01512–2) have now been identified as selective and potent TRPA1 channel antagonist with antihyperalgesic effects in a relevant model of neuropathic pain [40]. These findings, in addition to the reinforcing the role of TRPA1 channels in pain transmission, suggest Pha1 $\beta$  and CTK 01512–2 as novel strategies for the treatment of painful conditions where TRPA1 channels might be involved.

### 3.3. TRPV4 channel

TRPV4 has been considered the main molecular candidate for sensing osmotic changes, pressure, and shear stress in neurons and muscle tissue thus contributing to pain transduction associated to these stimuli [41, 42]. TRPV4 regulates intracellular calcium signaling, temperature sensing, osmotic and mechanic transduction, as well as maintenance of cell volume and energy homeostasis [43]. It is present in various cell types, including endothelial and epithelial cells, chondrocytes, and adipocytes. For being expressed in DRG and trigeminal ganglia neurons, has suggested a role in pain responses to mechanical stimuli in somatic tissue and visceral organs [33]. Like TRPV1 and TRPA1, TRPV4 is also activated by polyunsaturated fatty acids. Metabolites of arachidonic acid activate TRPV4 by an indirect mechanism involving the cytochrome P-450, therefore, suggesting a role of TRPV4 in inflammatory associated sensitization process.

### 3.4. TRPM8 channel

TRPM8 channel is considered as the primary sensor of cold in mammalian. TRPM8 channels are present in 10% of small DRG and trigeminal ganglia neurons, is activated by temperature

of below 25°C and by agents as menthol and eucalyptol and that do not express the classical markers of nociceptors such as TRPV1 and CGRP, suggesting that TRPM8 is a cold thermosensor for non-noxious temperatures [44]. However, studies have reported that acute activation or inhibition of TRPM8 can have analgesic effects either on visceral or neuropathic pain [45, 46].

#### 4. Ionotropic glutamate receptors

Numerous ion channels of many types of receptors, including the ionotropic glutamate receptors, contribute to the detection and processing the pain signals. The function of these channels is detection the information from primary afferent neurons of mechanical and chemical insults, generation of action potentials, regulation of neuronal firing patterns, provide the initiation of neurotransmitter release at the dorsal horn synapses and the ensuring activation of spinal cord neurons that project to pain centers in the brain. The ionotropic glutamate receptors are involved in the mechanisms underlying peripheral and central sensitization and are important for pain sensation and pain perception. Changes in channel expression and function of NMDA receptors are thought to contribute to chronic pain states.

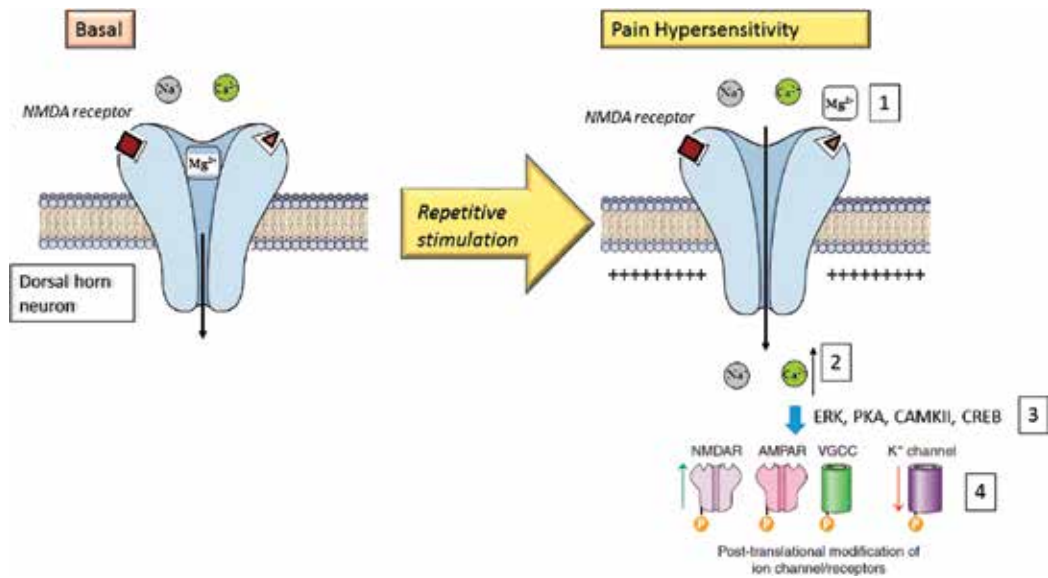
NMDA and AMPA receptors are expressed in secondary sensory neurons of the spinal cord, some interneurons and in neurons of supraspinal central nervous system. The ionotropic glutamate receptors include three pharmacologically and genetically distinct receptor types, named N-methyl-D-aspartate receptor (NMDA),  $\alpha$ -amino-3-hydroxy-5-methylisazole-4-propionic acid receptor (AMPA) and kainate receptors.

At the molecular level, seven homologous genes code for NMDA subunits and are categorized into three major classes: GluN1/NR1, (Grin 1), GluN2/NR2 (Grin 2A, Grin2B, Grin2C, Grin2D) and GluN3/NR3 (Grin 3A, Grin 3B). The GluN1 subtype is essential for NMDA function and is expressed in the majority of the central nervous system, while differential expression of Glu2 subtype variants accounts for differences in the functional properties of NMDA receptors. A typically functional NMDA receptor contains two GluN1 and two GluN2 genetically encoded subunits (for review see [28]).

Glutamate and aspartate are the principal excitatory neurotransmitters that act on postsynaptic ionotropic glutamate receptors in response to noxious stimulation [47]. As the most studied ionotropic glutamate receptor in pain is the NMDA receptor, it will be described in more details. NMDA receptors represent the most recognized postsynaptic source of calcium rise in the neurons, regulated by many kinases, phosphatases, and other enzymes. Moreover, NMDA activation is the major component of inflammatory and neuropathic pain. These receptors have independent mechanisms for facilitating excitatory and boosting synaptic transmission and, in this way, are important in the pain system [48].

The pore of NMDA receptor is permeable to monovalent cations such as sodium and potassium and divalent cations including calcium. Activation of NMDA receptors requires the binding of L-glutamate and glycine as an obligatory co-agonist. However, at physiological resting membrane potential, the pore is largely blocked by extracellular magnesium ions





**Figure 3.** NMDA receptor activation and dorsal horn neuronal windup. Left: under basal physiological conditions, NMDA receptor is in a non-potentiated, with reduced sodium and calcium inward currents due to the blockage of magnesium ions from the extracellular space. Right: repetitive stimulation from pre synaptic afferent inputs causes relief of  $Mg^{2+}$  blockage (1). Calcium elevation in cytosol (2) activates kinase cascades including ERK, PKA, CAMKII (3) that leads to an upregulation in the activity of excitatory ion channels through posttranslational modifications (4) culminating in persistent changes in dorsal horn excitability.

(**Figure 3**). The cumulative depolarization produced during central sensitization leads to a relief of NMDA receptors blockade by magnesium causing an increase in intracellular calcium, synaptic depolarization and transmission and neuronal excitability. The process known as windup is the initial activity-dependent event that increases the synaptic responses and triggers central sensitization. Wind up is a form of physiological pain characterized by a successive increase in the output of a dorsal horn neuron produced by repetitive noxious stimuli [28].

Windup and Cumulative depolarization activates convergent signaling cascades from NK1, G protein-coupled metabotropic receptors (mGluR) and tyrosine kinase receptors, all present in the superficial dorsal horn leading to suppression of magnesium blockade of NMDA channels and enhance NMDA channels gating and function [48]. In dorsal horn neurons, NMDA receptors are known to be regulated by AMPA channel and unregulated by tyrosine kinase family (Src). During central sensitization, the Src enhance the NMDA receptor function raising intracellular calcium and activating de calcium/calmodulin-dependent kinase II (CaMKII) and protein kinase C (PKC) [48].

Downstream to the  $Mg^{2+}$  unblock of NMDA receptors, the flow of sodium and calcium ions through NMDA receptors leads to depolarization of the synaptic membrane and facilitate the excitatory postsynaptic potentials (EPSPs) and cause an increase of intracellular calcium concentrations. The intracellular calcium causes activation of kinases, including protein kinase A (PKA), protein kinase C (PKC) and extracellular signal-regulated kinase (ERK). The

NMDA-dependent activation of these kinases can, in turn, increase the excitability of voltage-gated-calcium channels as well as inhibit the voltage-gated-potassium channels (for review, see [28]). Furthermore, calcium entry through AMPA receptors may also contribute to the downregulation of inhibitory glycinergic synaptic function in spinal cord neurons culminating with even more facilitation of the ascending of pain signals. **Figure 3** shows the activation of NMDA receptors.

Central sensitization is a result from activity-dependent changes in spinal neuronal function and involves both long-term potentiation of individual synapses as well as the increased excitability of neurons within the spine cord dorsal horn [48]. Most of the excitatory input to pain pathway neurons is subthreshold, and increased gain results in the recruitment of these inputs to the output of the neurons, causing them to fire to normally ineffective inputs. These changes constitute central sensitization and are responsible for pain produced by low threshold afferent inputs and the spread of hypersensitivity to regions beyond injured tissue [48]. As it has been stated, NMDA receptors are considered the most validated molecular player responsible for sensitization process at the spinal cord.

## 5. Therapeutical opportunities

The prominent role of calcium permeable channels in the pain pathway represents the opportunity of controlling those channels for improving pharmacotherapeutic pain management. To date, several analgesic agents exert their effects by functionally interacting with calcium channels. The most well-recognized strategies that are already in use comprehends pore inhibition of voltage-gated calcium channels—with focus on N-type channels; inhibition of VGCC's by binding on  $\alpha_2\delta$  auxiliary subunit; inhibition or desensitization of vanilloid receptors mainly TRPV1 and inhibition of NMDA receptors. Although there is an ever-growing number of substances discovered to act on the above targets, the number of those with use approved for humans is still small.

Ziconotide (Prialt™) was developed and approved as a first-in-class synthetic version of  $\omega$ -conotoxin MVIIA, a peptide blocker of  $Ca_{V2.2}$  channels. It was approved by US Food and Drug Administration and European Medicines Agency for the management of severe chronic pain associated with cancer, acquired immune deficiency syndrome (AIDS) and neuropathies—refractory to other current pain medications. Despite the clinical efficacy of ziconotide to treat severe pain, its impracticalities of intrathecal administration, low therapeutical index, and severe neurotoxic effects have restricted its use to rare circumstances. Ziconotide is the first and unique drug, so far, derived from an animal toxin to be approved for use in pain management, in humans [49].

The consecutive need for a more favorable ratio of anti-nociception to side effect has led to the discovery of new conotoxins that already translated from basic bench to bed side research (for review, see [50]). CVID is another  $\omega$ -conotoxin with remarkable analgesic actions. AM-336 (leconotide) is the synthetic version of CVID that has been tested as a therapeutic agent and has completed phase II clinical trial. Compared with ziconotide, CVID has improved specificity for

N-type VGCCs showing, thus, improved efficacy and fewer cardiovascular side effects. Similar to CVID, CVIE and CVIF are  $\omega$ -conotoxins capable of blocking N-type channels and completely and reversibly relieve mechanical allodynia in rodent models of neuropathic pain. Due to their inherently large size and hydrophilic nature, peptides, in general, are unable to cross the blood-brain barrier. Therefore, the methods for administering  $\omega$ -conopeptides are limited to intrathecal delivery. Therefore, alternative strategies are needed, for example, the use of nonpeptidic small molecules that has limited systemic degradation. Another strategy is the development of state-dependent channel blockers who preferentially inhibits the calcium channel when they are in activated state which appears in highly active pain fibers. A few numbers of state-dependent blockers is currently under development, for review see [51], but all of them are still in a pre-clinical phase of testing.

Several pharmaceutical companies have T-type voltage gated calcium channels on their list of targets to manage pain. It has been shown that T-type channels are expressed in a subset of primary afferent neurons and have been implicated in synaptic release in the spinal cord suggesting a role of these channels in pain processing. Consistent with this idea, systemic or intrathecal administration of ethosuximide or mibefradil (T-type calcium channel blockers) mediates analgesia in rodents [52]. Indeed, in the recent years, a new generation of both state-dependent and state-independent T-type blockers appeared (ex. TTA-P2, TTA-A2, and Z123212) and both mediate analgesia in rodent models of pain [14]. Near future will show if clinical drugs emerge.

The most frequently prescribed calcium channels modulation for neuropathic pain are the gabapentinoids. These drugs were initially designed to perform as analogues of GABA and originally indicated for the treatment of epilepsy. However, it becomes empirically evident that this class of drugs is very efficient in attenuating pain in postherpetic neuralgia, diabetic neuropathy, and fibromyalgia. Thus, initial off-label use of gabapentinoids turns into approved used for palliative care neuropathic pain states. The main clinically used gabapentinoids include gabapentin and the newer derivative pregabalin. Gabapentinoids were identified as ligands for the auxiliary voltage-gated calcium channel subunit  $\alpha_2\delta$  although they also bind to GABA receptors but with lower affinity. The interaction of gabapentinoids with the  $\alpha_2\delta$  subunit is required for the antinociceptive activity of gabapentinoids given the lack of correspondent efficacy in null mice [53]. By binding to  $\alpha_2\delta$  subunit, gabapentinoids acts as inhibitors of  $\alpha_2\delta$  subunit-containing VDCC's therefore inhibiting neurotransmitter release. At the cellular level, it is unclear how gabapentinoids inhibit neurotransmitter release. It is suggested they inhibit axonal trafficking of  $\alpha_2\delta$  subunit and thus the recycling of calcium channel complexes, which is elevated in injured primary afferents.

Blocking N-methyl D-aspartate (NMDA) receptors inhibits the wind-up phenomenon of spinal dorsal horn neurons. Given this phenomenon is a key event in the pain sensitization process, NMDA ionophore antagonists have been shown to have potent attenuating effects in pain states, though not approved, in humans. Numerous NMDA antagonists have been employed for preclinical work. These include channel blockers such as ketamine, and memantine [54]. NMDAR antagonists e.g. ketamine and dextromethorphan, are generally effective in patients with neuropathic pain such as complex regional pain syndrome and painful diabetic neuropathy [55]. Main observed side effects of these antagonists include neuronal toxicity and

profound psychotomimetic effects. Then, current usage of these class of drugs to treat pain is off-label usage.

TRP channels are also promising targets for drug discovery. The initial focus of research was on TRP channels that are expressed on nociceptive neurons. Indeed, a number of potent, small-molecule TRPV1, TRPV3, and TRPA1 antagonists have already entered clinical trials as novel analgesic agents but this is a rapidly expanding and changing field. Although there has been considerable excitement around the therapeutic potential of this channel family since the cloning and identification of TRPV1 channels as the capsaicin receptor more than 20 years ago, only modulators of a few channels have been tested clinically. TRPV1 channel antagonists have suffered from side effects related to the channel's role in temperature sensation. Paradoxically, high dose formulations of capsaicin have reached the market and shown therapeutic utility. A number of potent, small molecule antagonists of TRPA1 channels have recently advanced into clinical trials for the treatment of inflammatory and neuropathic pain, and TRPM8 antagonists are following closely behind for cold allodynia. Other TRP channels such as TRPV3, V4, and TRPM2 have also attracted significant attention [56].

## 6. Conclusions

The calcium flow throughout ion channels in the membrane of sensory neurons convey information about how pain signals are transduced, transported and interpreted by the nervous system. Regarding the gating control of calcium channels, the voltage-gated (mainly N-type) and the ligand-gated (mainly vanilloid receptors and NMDAR) are the most well characterized to show a close association with pain processing. The normal function of these channels helps to control pain in their primitive purpose that is the protection from harmful environment. However, maladaptive changes of these channels (eg. altered expression levels or modulation by intracellular phosphorylative cascades) may end up with chronification or even exacerbation of pain signals transforming it into a public health problem. Although the majority of clinical trials are disappointing so far, a progressive approach to clinical trials designs with calcium channels modulators will be key to the success of future therapeutic approaches. Alternative approaches include the rational search for drug combination regimens applying calcium channels modulators associated with other drugs. Concurrently, basic research may also help to identify novel targets, for example, splice variants of calcium channels that have a more specific role in pain processing. Therefore, new target-specific drugs could also improve the efficacy and toxicity profiles for pain management.

## Acknowledgements

We thank Dr. Marcus Vinícius Gomez for critical review and constructive commentaries. Also to Dr. Caio Aoki and to Sabrina Queiroz for their valuable assistance. Also, thank for CAPES and FAPEMIG (CBB-APQ-03767-16) for supporting the scholarship of LF and DCS.

## Conflict of interest

All the authors declare they have no conflicts of interest.

## Appendices and nomenclature

TRP	Transient receptor potential
VGCC	Voltage gated calcium channels
NMDAR	N-methyl D-aspartate receptor
GABA	Gamma aminobutyric acid
DRG	Dorsal root ganglion
ERK	Extracellular signal regulated kinase
PKA	Protein kinase A
CAMK	Calcium calmodulin kinase
EPSP	Excitatory postsynaptic potentials
PLC	Phospho lipase C
CAPES	Coordenação de Aperfeiçoamento de Pessoal de Nível Superior
FAPEMIG	Fundação de Amparo a Pesquisa de Minas Gerais

## Author details

Célio Castro-Junior\*, Luana Ferreira, Marina Delgado, Juliana Silva and Duana Santos

\*Address all correspondence to: [celiojunior@santacasabh.org.br](mailto:celiojunior@santacasabh.org.br)

Neuropharmacology Laboratory, Institute for Education and Research, Hospital Santa Casa, Belo Horizonte, MG, Brazil

## References

- [1] Gribkoff VK. The role of voltage-gated calcium channels in pain and nociception. *Seminars in Cell & Developmental Biology*. 2006;**17**(5):555-564
- [2] Catterall WA, Perez-Reyes E, Snutch TP, Striessnig J. International Union of Pharmacology. XLVIII. Nomenclature and structure-function relationships of voltage-gated calcium channels. *Pharmacological Reviews*. 2005;**57**(4):411-425

- [3] Ertel EA, Campbell KP, Harpold MM, Hofmann F, Mori Y, Perez-Reyes E, et al. Nomenclature of voltage-gated calcium channels. *Neuron*. 2000;**25**(3):533-535
- [4] Evans AR, Nicol GD, Vasko MR. Differential regulation of evoked peptide release by voltage-sensitive calcium channels in rat sensory neurons. *Brain Research*. 1996;**712**(2):265-273
- [5] Park J, Luo ZD. Calcium channel functions in pain processing. *Channels*. 2010;**4**(6):510-517
- [6] Mochida S, Yokoyama CT, Kim DK, Itoh K, Catterall WA. Evidence for a voltage-dependent enhancement of neurotransmitter release mediated via the synaptic protein interaction site of N-type  $\text{Ca}^{2+}$  channels. *Proceedings of the National Academy of Sciences of the United States of America*. 1998;**95**(24):14523-14528
- [7] Yokoyama CT, Sheng ZH, Catterall WA. Phosphorylation of the synaptic protein interaction site on N-type calcium channels inhibits interactions with SNARE proteins. *The Journal of Neuroscience: The Official Journal of the Society for Neuroscience*. 1997;**17**(18):6929-6938
- [8] Saegusa H, Kurihara T, Zong S, Minowa O, Kazuno A, Han W, et al. Altered pain responses in mice lacking alpha 1E subunit of the voltage-dependent  $\text{Ca}^{2+}$  channel. *Proceedings of the National Academy of Sciences of the United States of America*. 2000;**97**(11):6132-6137
- [9] Staats PS, Hekmat H, Staats AW. The psychological behaviorism theory of pain and the placebo: Its principles and results of research application. *Advances in Psychosomatic Medicine*. 2004;**25**:28-40
- [10] Radwani H, Lopez-Gonzalez MJ, Cattaert D, Roca-Lapirot O, Dobremez E, Bouali-Benazzouz R, et al. Cav1.2 and Cav1.3 L-type calcium channels independently control short- and long-term sensitization to pain. *The Journal of Physiology*. 2016;**594**(22):6607-6626
- [11] Gullapalli S, Ramarao P. L-type  $\text{Ca}^{2+}$  channel modulation by dihydropyridines potentiates kappa-opioid receptor agonist induced acute analgesia and inhibits development of tolerance in rats. *Neuropharmacology*. 2002;**42**(4):467-475
- [12] Vedder H, Otten U. Biosynthesis and release of tachykinins from rat sensory neurons in culture. *Journal of Neuroscience Research*. 1991;**30**(2):288-299
- [13] Turner TJ, Adams ME, Dunlap K. Calcium channels coupled to glutamate release identified by omega-Aga-IVA. *Science*. 1992;**258**(5080):310-313
- [14] Bourinet E, Francois A, Laffray S. T-type calcium channels in neuropathic pain. *Pain*. 2016;**157**(Suppl 1):S15-S22
- [15] Kawabata A. Targeting  $\text{Ca}(v)3.2$  T-type calcium channels as a therapeutic strategy for chemotherapy-induced neuropathic pain. *Nihon Yakurigaku Zasshi*. 2013;**141**(2):81-84
- [16] Fang Z, Park CK, Li HY, Kim HY, Park SH, Jung SJ, et al. Molecular basis of  $\text{Ca}(v)2.3$  calcium channels in rat nociceptive neurons. *The Journal of Biological Chemistry*. 2007;**282**(7):4757-4764

- [17] Matthews EA, Bee LA, Stephens GJ, Dickenson AH. The Cav2.3 calcium channel antagonist SNX-482 reduces dorsal horn neuronal responses in a rat model of chronic neuropathic pain. *The European Journal of Neuroscience*. 2007;**25**(12):3561-3569
- [18] Nilius B, Owsianik G, Voets T, Peters JA. Transient receptor potential cation channels in disease. *Physiological Reviews*. 2007;**87**(1):165-217
- [19] O'Neill J, Brock C, Olesen AE, Andresen T, Nilsson M, Dickenson AH. Unravelling the mystery of capsaicin: A tool to understand and treat pain. *Pharmacological Reviews*. 2012;**64**(4):939-971
- [20] Ramsey IS, Delling M, Clapham DE. An introduction to TRP channels. *Annual Review of Physiology*. 2006;**68**:619-647
- [21] Vay L, Gu C, McNaughton PA. The thermo-TRP ion channel family: Properties and therapeutic implications. *British Journal of Pharmacology*. 2012;**165**(4):787-801
- [22] Salat K, Moniczewski A, Librowski T. Transient receptor potential channels—Emerging novel drug targets for the treatment of pain. *Current Medicinal Chemistry*. 2013;**20**(11):1409-1436
- [23] Myers BR, Julius D. TRP channel structural biology: New roles for an old fold. *Neuron*. 2007;**54**(6):847-850
- [24] Perl ER. Ideas about pain, a historical view. *Nature Reviews Neuroscience*. 2007;**8**(1):71-80
- [25] Schmidt R, Schmelz M, Forster C, Ringkamp M, Torebjork E, Handwerker H. Novel classes of responsive and unresponsive C nociceptors in human skin. *The Journal of Neuroscience: The Official Journal of the Society for Neuroscience*. 1995;**15**(1 Pt 1):333-341
- [26] Hu HJ, Bhawe G, RWt G. Prostaglandin and protein kinase A-dependent modulation of vanilloid receptor function by metabotropic glutamate receptor 5: Potential mechanism for thermal hyperalgesia. *The Journal of Neuroscience: The Official Journal of the Society for Neuroscience*. 2002;**22**(17):7444-7452
- [27] Caterina MJ, Leffler A, Malmberg AB, Martin WJ, Trafton J, Petersen-Zeitze KR, et al. Impaired nociception and pain sensation in mice lacking the capsaicin receptor. *Science*. 2000;**288**(5464):306-313
- [28] Bourinet E, Altier C, Hildebrand ME, Trang T, Salter MW, Zamponi GW. Calcium-permeable ion channels in pain signaling. *Physiological Reviews*. 2014;**94**(1):81-140
- [29] Jancso G, Kiraly E, Jancso-Gabor A. Pharmacologically induced selective degeneration of chemosensitive primary sensory neurones. *Nature*. 1977;**270**(5639):741-743
- [30] Garami A, Pakai E, Oliveira DL, Steiner AA, Wanner SP, Almeida MC, et al. Thermoregulatory phenotype of the Trpv1 knockout mouse: Thermo-effector dysbalance with hyperkinesis. *The Journal of Neuroscience: The Official Journal of the Society for Neuroscience*. 2011;**31**(5):1721-1733

- [31] Moran MM, McAlexander MA, Biro T, Szallasi A. Transient receptor potential channels as therapeutic targets. *Nature Reviews Drug Discovery*. 2011;**10**(8):601-620
- [32] Jaquemar D, Schenker T, Trueb B. An ankyrin-like protein with transmembrane domains is specifically lost after oncogenic transformation of human fibroblasts. *The Journal of Biological Chemistry*. 1999;**274**(11):7325-7333
- [33] Nilius B, Appendino G, Owsianik G. The transient receptor potential channel TRPA1: From gene to pathophysiology. *Pflugers Archiv: European Journal of Physiology*. 2012; **464**(5):425-458
- [34] Macpherson LJ, Dubin AE, Evans MJ, Marr F, Schultz PG, Cravatt BF, et al. Noxious compounds activate TRPA1 ion channels through covalent modification of cysteines. *Nature*. 2007;**445**(7127):541-545
- [35] Bandell M, Story GM, Hwang SW, Viswanath V, Eid SR, Petrus MJ, et al. Noxious cold ion channel TRPA1 is activated by pungent compounds and bradykinin. *Neuron*. 2004;**41**(6): 849-857
- [36] Kwan KY, Allchorne AJ, Vollrath MA, Christensen AP, Zhang DS, Woolf CJ, et al. TRPA1 contributes to cold, mechanical, and chemical nociception but is not essential for hair-cell transduction. *Neuron*. 2006;**50**(2):277-289
- [37] Kremeyer B, Lopera F, Cox JJ, Momin A, Rugiero F, Marsh S, et al. A gain-of-function mutation in TRPA1 causes familial episodic pain syndrome. *Neuron*. 2010;**66**(5):671-680
- [38] Rigo FK, Trevisan G, Rosa F, Dalmolin GD, Otuki MF, Cueto AP, et al. Spider peptide Phalpha1beta induces analgesic effect in a model of cancer pain. *Cancer Science*. 2013; **104**(9):1226-1230
- [39] Souza AH, Ferreira J, Cordeiro Mdo N, Vieira LB, De Castro CJ, Trevisan G, et al. Analgesic effect in rodents of native and recombinant Ph alpha 1beta toxin, a high-voltage-activated calcium channel blocker isolated from armed spider venom. *Pain*. 2008;**140**(1): 115-126
- [40] Tonello R, Fusi C, Materazzi S, Marone IM, De Logu F, Benemei S, et al. The peptide Phalpha1beta, from spider venom, acts as a TRPA1 channel antagonist with antinociceptive effects in mice. *British Journal of Pharmacology*. 2017;**174**(1):57-69
- [41] Nilius B, Voets T. The puzzle of TRPV4 channelopathies. *EMBO Reports*. 2013;**14**(2):152-163
- [42] Ho TC, Horn NA, Huynh T, Kelava L, Lansman JB. Evidence TRPV4 contributes to mechanosensitive ion channels in mouse skeletal muscle fibers. *Channels*. 2012;**6**(4):246-254
- [43] Ye L, Kleiner S, Wu J, Sah R, Gupta RK, Banks AS, et al. TRPV4 is a regulator of adipose oxidative metabolism, inflammation, and energy homeostasis. *Cell*. 2012;**151**(1):96-110
- [44] McKemy DD, Neuhausser WM, Julius D. Identification of a cold receptor reveals a general role for TRP channels in thermosensation. *Nature*. 2002;**416**(6876):52-58



- [45] Harrington AM, Hughes PA, Martin CM, Yang J, Castro J, Isaacs NJ, et al. A novel role for TRPM8 in visceral afferent function. *Pain*. 2011;**152**(7):1459-1468
- [46] Proudfoot CJ, Garry EM, Cottrell DF, Rosie R, Anderson H, Robertson DC, et al. Analgesia mediated by the TRPM8 cold receptor in chronic neuropathic pain. *Current Biology: CB*. 2006;**16**(16):1591-1605
- [47] Voscopoulos C, Lema M. When does acute pain become chronic? *British Journal of Anaesthesia*. 2010;**105**(Suppl 1):i69-i85
- [48] Woolf CJ, Salter MW. Neuronal plasticity: Increasing the gain in pain. *Science*. 2000;**288**(5472):1765-1769
- [49] Sanford M. Intrathecal ziconotide: A review of its use in patients with chronic pain refractory to other systemic or intrathecal analgesics. *CNS Drugs*. 2013;**27**(11):989-1002
- [50] Adams DJ, Callaghan B, Berecki G. Analgesic conotoxins: Block and G protein-coupled receptor modulation of N-type (Ca(V) 2.2) calcium channels. *British Journal of Pharmacology*. 2012;**166**(2):486-500
- [51] Patel R, Montagut-Bordas C, Dickenson AH. Calcium channel modulation as a target in chronic pain control. *British Journal of Pharmacology*. 2017. [Epub ahead of print]
- [52] Dogrul A, Gardell LR, Ossipov MH, Tulunay FC, Lai J, Porreca F. Reversal of experimental neuropathic pain by T-type calcium channel blockers. *Pain*. 2003;**105**(1-2):159-168
- [53] Field MJ, Cox PJ, Stott E, Melrose H, Offord J, Su TZ, et al. Identification of the alpha2-delta-1 subunit of voltage-dependent calcium channels as a molecular target for pain mediating the analgesic actions of pregabalin. *Proceedings of the National Academy of Sciences of the United States of America*. 2006;**103**(46):17537-17542
- [54]Coderre TJ, Van Empel I. The utility of excitatory amino acid (EAA) antagonists as analgesic agents. II. Assessment of the antinociceptive activity of combinations of competitive and non-competitive NMDA antagonists with agents acting at allosteric-glycine and polyamine receptor sites. *Pain*. 1994;**59**(3):353-359
- [55] Zhou HY, Chen SR, Pan HL. Targeting N-methyl-D-aspartate receptors for treatment of neuropathic pain. *Expert Review of Clinical Pharmacology*. 2011;**4**(3):379-388
- [56] Moran MM, Szallasi A. Targeting nociceptive transient receptor potential channels to treat chronic pain: Current state of the field. *British Journal of Pharmacology*. 2017. [Epub ahead of print]



---

# L-Type Calcium Channels: Structure and Functions

---

Tianhua Feng, Subha Kalyaanamoorthy and  
Khaled Barakat

Additional information is available at the end of the chapter

<http://dx.doi.org/10.5772/intechopen.77305>

---

## Abstract

Voltage-gated calcium channels (VGCCs) manage the electrical signaling of cells by allowing the selective-diffusion of calcium ions in response to the changes in the cellular membrane potential. Among the different VGCCs, the long-lasting or the L-type calcium channels (LTCCs) are prevalently expressed in a variety of cells, such as skeletal muscle, ventricular myocytes, smooth muscles and dendritic cells and forms the largest family of the VGCCs. Their wide expression pattern and significant role in diverse cellular events, including neurotransmission, cell cycle, muscular contraction, cardiac action potential and gene expression, has made these channels the major targets for drug development. In this book chapter, we aim to provide a comprehensive overview of the different VGCCs and focus on the sequence-structure-function properties of the LTCCs. Our chapter will summarize and review the various experimental and computational analyses performed on the structures of the LTCCs and their implications in drug discovery applications.

**Keywords:** CaV1.2, L-type calcium channel, ion channel blocker, high-voltage activation, low-voltage activation

---

## 1. Introduction

### 1.1. L-type calcium channel introduction

The voltage-gated calcium channels (VGCCs/CaVs), are transmembrane ion channel proteins that selectively conduct calcium ions through the cell membrane in response to the membrane potential during depolarization. In 1953, Paul Fatt and Bernard Katz discovered the existence of calcium-conducting ion channels in the crustacean muscle [1]. Following the initial discovery of the presence of calcium conducting ion channels in the crustacean muscle cells, several

reports confirmed the presence of these channels in various mammalian cell types including, skeletal, cardiac muscles and all excitable cells. These calcium channels were firstly classified into two types based on their activation voltage and conductance, the high-voltage-activated (HVA) and the low-voltage-activated (LVA) calcium channels [2]. The HVA and LVA channels were reported to have distinct gating properties and pharmacological profiles [2, 3]. Hess et al. [4] found that the HVA channels are sensitive to 1,4-dihydropyridine (DHPs) antagonists and DHPs agonists help in stabilizing the HVA channels in the open-conducting state for a prolonged time. Interestingly, some of the identified HVA calcium channels exhibited preferences to different tissues and different sensitivity to DHP and other toxin antagonists, which led to the identification and classification of diverse HVA channels.

DHP-sensitive channels were found to be present in various cells and exhibited a long-lasting activation length and hence are called the DHP channel or the L-type calcium channel (LTCC) [5, 6].  $\omega$ -CTX-sensitive calcium channels were pronounced for their roles in the nervous system and are thus classified as N-type (non-L or neuronal) channels.  $\omega$ -AGA-sensitive channels were initially found in the Purkinje cells of the cerebellum and are, therefore, named as P-type channels. Another close homolog of the P-type channel produced by alternative splicing of the CACNA1A gene was found and is referred to as the Q-type calcium channel. In addition to these three types of HVA, some calcium-conducting channels were found to be insensitive to any of these antagonists and have been classified as R-type (resistant) channels (Table 1).

Only one type of calcium channel has been reported among the LVA channels, namely, the transient-opening calcium channel (also called T-type channel). The T-type channels are similar to L-type channels in their diverse expression and antagonist resistant properties. However, small single-channel conductance and ability to be activated at lower membrane potentials make them distinct from the L-type channels.

The prevalence of N-, P/Q-, and R-channels in neurons, and L- and T-channels in broad cellular types, shows the distinctive functional roles of the calcium channels. Besides their role in the characterization of the homologous channels, the calcium channel antagonists remain promising for their ability to specifically-modulate the different types of channels [10]. The varied sensitivities of the HVA and LVA channels to different antagonists show the potential for engineering these antagonists to selectively-alter the calcium conduction in different cells for various functions.

Type	Antagonists sensitivity					Ref
	1,4-DHP	Phenylalkylamine	Benzothiazepine	$\omega$ -CTX	$\omega$ -AGA	
CaV1 L-type	Blocks	Blocks	Blocks	Resistant	Resistant	[7]
CaV2.1P/Q-type	Resistant	Resistant	Resistant	Resistant	Blocks	[8]
CaV2.2 N-type	Resistant	Resistant	Resistant	Blocks	Resistant	[9]
CaV2.3 R-type	Resistant	Resistant	Resistant	Resistant	Resistant	[9]

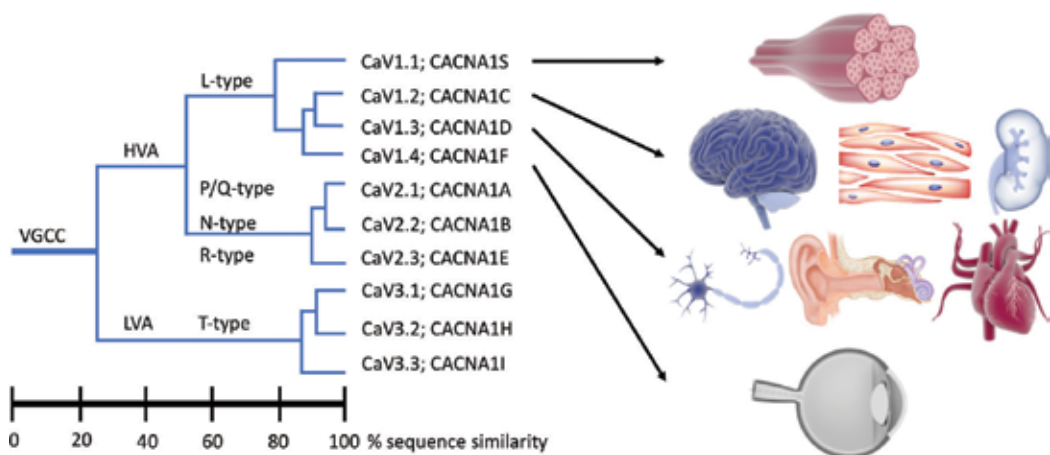
**Table 1.** Blocker sensitivities of different HVA channels.

Ten mammalian VGCCs have been identified, of which the L-type calcium channel includes four members, CaV1.1-CaV1.4, the P-/Q-type includes CaV2.1, the N-type includes CaV2.2, the R-type includes CaV2.3, and the T-type includes three members, CaV3.1–3.3. Their sequence similarity and evolutionary relationship are shown in **Figure 1**. The following sections of the chapter will focus on comprehending the structure, and function of the LTCCs and their implications in drug discovery applications.

## 1.2. Distribution of LTCCs

The distribution of LTCCs varies widely across its' members as their functions vary in different excitable cells [9]. Transcripts for all L-type channel isoforms have been detected in lymphocytes for endocrine functions [11]. Among the four LTCCs types, CaV1.1 is mainly distributed in skeletal muscle and plays a role in muscle contraction. It is co-expressed with ryanodine receptors (RYRs) in GABAergic neurons, which produces gamma-aminobutyric acid (GABA) [12]. CaV1.2 and CaV1.3 show a highly overlapping expression pattern in many tissues and are mostly present in same cell types, such as in adrenal chromaffin cells, cardiac and neuronal cells [13]. CaV1.2 and CaV1.3 are predominantly located post-synaptically on the cell soma and in the spine and shaft of dendrites in the neurons [14]. CaV1.2 and CaV1.3 are also expressed in the sinoatrial node (SAN) and atrial cardiomyocytes and play a role in cardiac pacemaker activity [15]. In cardiomyocytes, CaV1.2 is mainly involved in the excitation-contraction coupling. CaV1.3 are found in the pancreas and kidney, where it correlates with endocrine secretion, and in the cochlea to regulate the auditory transduction (**Figure 1**). CaV1.4 is primarily expressed in the retinal cells and helps in normal visual functions [16].

When the LTCCs detect the electrical signal on the cell membrane, they transform these signals into other physiological activities, such as contraction of the muscle, secretion of hormones, and regulation of genes [18, 19]. These processes can generally be summarized as excitation-contraction [18], excitation-secretion [19], and excitation-transcription coupling [12], respectively.



**Figure 1.** Phylogenetic tree showing the evolutionary relationship among the members of the VGCCs [2, 17]. And, the major distribution of the four LTCC isoforms in human tissues [12, 13, 18]. The tree was constructed using the Clustal omega. The scale in the figure shows the percentage of sequence identity in the CaV $\alpha_1$  subunit of different channels.

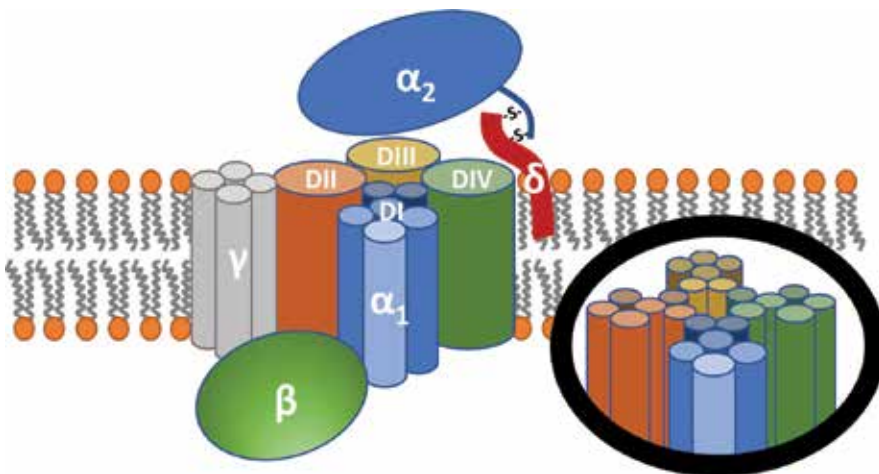
## 2. Sequence-structure organization of L-type calcium channels

### 2.1. LTCC: domain organization

The purified LTCCs contains five subunits, the principal or pore-forming subunit,  $\alpha_1$  (170 kDa) and different auxiliary subunits,  $\alpha_2$  (150 kDa),  $\beta$  (50–78 kDa),  $\delta$  (17–25 kDa), and  $\gamma$  (32 kDa). The auxiliary subunits are non-covalently linked to the  $\alpha_1$  subunit for modulating the biophysical properties and trafficking of the  $\alpha_1$  subunit onto the membrane [20]. The  $\alpha_1$  subunit corresponds to the pore-forming segment of LTCC to allow the passage of  $\text{Ca}^{2+}$  ions and is composed of approximately 2000 amino acids (AAs). The other components serve as auxiliary subunits and modify the function of the channel. For example, the  $\beta$  subunit and  $\alpha_2\delta$ -subunit accelerate the activation and deactivation kinetics of the channel and significantly increases the maximal-conductance of ionic current [21]. The  $\beta$  subunit, which lacks the membrane-spanning region, is localized on the intracellular region of the channel. The  $\alpha_2$  and  $\delta$  subunit, although expressed by a single gene, are cleaved into two separate proteins during post-translational modification resulting in a glycosylated extracellular  $\alpha_2$  and a smaller membrane-spanning  $\delta$  subunit that are held together ( $\alpha_2\delta$ -subunit) by a disulfide bond. The transmembrane  $\gamma$ -subunit, another component of LTCCs has not been found in CaV1.2 and CaV1.3 of the cardiac cells [13]. The  $\gamma$ -subunit has not been extensively studied because of their relatively limited distribution and trivial functional roles. **Figure 2** shows the arrangement of CaV subunits.

### 2.2. LTCC: sequence and splice variants

The pore-forming  $\alpha_1$ -subunits are expressed by 10 genes, the CACNA1S (CaV1.1 $\alpha_1$ ), CACNA1C (CaV1.2 $\alpha_1$ ), the CACNA1D (CaV1.3 $\alpha_1$ ), the CACNA1F (CaV1.4 $\alpha_1$ ), the CACNA1A (CaV2.1 $\alpha_1$ ), the



**Figure 2.** The LTCC complex. The pore-forming transmembrane  $\alpha_1$ -subunit, the intracellular  $\beta$ -subunit, the extracellular  $\alpha_2$ -subunit co-linked with the transmembrane  $\delta$ -subunit, and the transmembrane  $\gamma$ -subunit are shown [3, 13].

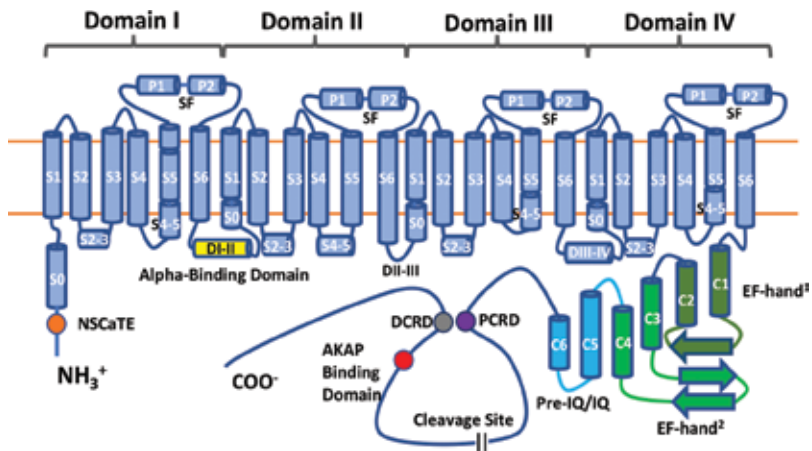
CACNA1B (CaV2.2 $\alpha_1$ ), the CACNA1E (CaV2.3 $\alpha_1$ ), the CACNA1G (CaV3.1 $\alpha_1$ ), the CACNA1H (CaV3.2 $\alpha_1$ ), and the CACNA1I (CaV3.3 $\alpha_1$ ). The members of the three families (CaV1, CaV2, and CaV3) share high sequence similarity (above 80%). In particular, the CaV1 and CaV2 families have relatively high sequence similarity, when compared with that of the LVA CaV3 family. All these channels have large numbers of potential splice variants expressed in different tissues [12]. The splicing sites are mainly distributed in the structurally flexible regions, such as N-terminal, C-terminal, and linkers between the transmembrane domains. They contribute to regulation of genes, gaining diversity in proteins, and in fine-tuning the physiological functions of the channel.

### 2.3. Domain organization

The LTCC polypeptide forms a heterotetramer and includes the pore-forming transmembrane  $\alpha_1$ -subunit, the intracellular  $\beta$  subunit, and an extracellular  $\alpha_2\delta$  subunit. Most of the pharmacological and gating properties of LTCCs are accomplished by their  $\alpha_1$ -subunits. The structural topology of the  $\alpha_1$ -subunits is highly conserved among the members of the LTCCs and is made up of the cytoplasmic N- and C-terminal domains and four intervening transmembrane domains (DI-DIV). Each transmembrane domain is composed of six transmembrane  $\alpha$ -helices (S1–S6), where S1–S4 helices are known as the voltage sensing domain (VSD), and S5–S6 forms the pore domain [22]. VSD detects the changes in the membrane potential and PD helps in the selective passage of calcium ions through the channel pore. The S4 helix of the VSD encompasses several conserved positively charged residues, whereas, the S1–S3 helices are dominated by negatively charged amino acids. When the membrane is depolarized, the movement of the S4 helices is transmitted to the cytoplasmic ends of the S5 and S6 helices, through the S4–S5 linkers, resulting in the opening of the activation gate formed by the S6 helices on the inner side of the channel [3, 13].

The membrane-associated P-loop in each domain between the two helices, S5 and S6, form the selective filter of the channel. The selectivity of calcium channels relies on the P-loops domains and their calcium ion binding sites. The selectivity filter of VGCC includes conserved glutamate residues (E–E–E–E) in the P-loop region [5]. Their side chains can restrain Ca<sup>2+</sup> at the right coordination and let Ca<sup>2+</sup> enter into the pore region. The recent research identified three aspartic acid residues along the selectivity filter from extracellular to intracellular. Amino acid substitution and crystallization, has helped in locating the three binding sites for the Ca<sup>2+</sup> ions [5]. Although the bacterial calcium channel is different from the mammalian LTCCs in their amino acid sequence and structural features, the structure of CavAb has provided valuable insights into calcium ion selectivity conferred by the selectivity filter.

The N-terminus and C-terminus region of LTCC are both located in the cytosolic space. Although the major sequence of the N-terminus is composed of random loops, it also includes a calmodulin interaction domain, known as N-terminal spatial Ca<sup>2+</sup> transforming elements (NSCaTE) [23]. The length of the C-terminus is much longer than N-terminus and contains several binding sites for various proteins that modulate the LTCCs activity (shown in **Figure 3**). Proteolytic cleavage of the C-terminal domain generates two fragments, the proximal C-terminal regulatory domain (PCRD) and the distal C-terminal regulatory domain (DCRD). The upstream sequence of the cleaved site contains the PCRD, IQ domain, pre-IQ domain, and the EF-hand motif. This region is important for Ca<sup>2+</sup>/CaM binding and regulation.



**Figure 3.** The secondary structure topology of the  $\alpha_1$ -subunit of LTCCs. The N-terminal domain is followed by four homologous transmembrane domains and the C-terminal domain. Each of the transmembrane domains is made of six helices and a membrane associated P-loop. The orange, purple, red, and gray dots indicate the location of NSCaTE, PCRD, AKAP binding domain, and DCRD, respectively [3, 22]. The linker of DI and DII, colored in yellow, is the alpha-binding domain (ABD). The sequence from C1 to C2 and from C3 to C4 shows the two EF-hand motifs. Sequence from the end of C4 to the end of C6 colored in light blue is pre-IQ and IQ domain. The cleavage site is located in the sequence between DCRD and PCRD. The secondary structure is based on the PDBsum database.

The downstream sequence from the cleavage site includes the A-kinase-anchoring-protein (AKAP) binding domain (ABD) and DCRD [3]. When the DCRD is proteolytically cleaved, the cleaved fragment can remain non-covalently bound to the PCRD, thus allowing the two regions of the C-terminal domain to interact with each other and perform the auto-inhibitory function for the LTCCs [24]. The DCRD serves as an effective auto-inhibitory domain for the LTCCs or as a transcriptional modular when it enters the nucleus [24]. The ABD of the distal C-terminus plays a vital role in PKA-induced phosphorylation of the DCRD. The AKAP binds with the ABD and helps PKA identify the phosphorylation sites in the cleaved fragment. The phosphorylation shuts down the auto-inhibition of LTCC and facilitates the  $\text{Ca}^{2+}$  influx [13].

Coexpression and co-assembly of  $\text{CaV}\beta$  and  $\text{CaV}\alpha_2\delta$  subunits with  $\text{CaV}\alpha_1$  have a significant role in LTCCs trafficking [25]. The  $\text{CaV}\beta$  subunit, which belongs to the membrane-associated guanylate kinase (MAGUK) protein family is composed of three domains similar to that of the MAGUK family, except for the missing PDZ in the N-terminus. The two conserved structural domains of the  $\text{CaV}\beta$ , the SH3 and the guanylate-kinase (GuK) like domain are linked together by a HOOK domain. The HOOK domain of the  $\text{CaV}\beta$  isoforms has variable lengths and share a relatively low overall amino acid identity and plays an important role in the  $\text{CaV}\beta$  interaction with other proteins [26]. Similar to the DCTD, the HOOK domain possesses sites for phosphorylation and alters the conduction state of LTCCs. The  $\text{CaV}\beta$  subunit interacts with the 18-residue long DI-II linker (or the alpha interaction domain (AID)) of the  $\alpha_1$  subunit. The  $\alpha$ -binding pocket (ABP), a hydrophobic groove formed by the surrounding  $\alpha$ -helices, in the GuK domain of the  $\text{CaV}\beta$  subunit interacts with the AID [27]. The high-affinity association between AID and ABP markedly influences the cell surface expression of functional channels [26].



Another important co-expressed protein component of the LTCC complex is the  $\text{CaV}\alpha_2\delta$  subunit. The  $\alpha_2\delta$  subunit remains to be a promising target for the treatment of neuropathic pain and mutations that affect the function of  $\text{CaV}\alpha_2\delta$ -1 were found to cause cardiac dysfunctions [25]. The  $\text{CaV}\alpha_2\delta$  subunit is a disulfide-linked polypeptide that interacts with the  $\alpha_1$  subunit on the extracellular space through its'  $\alpha_2$  segment, while the  $\delta$  segment serves as an anchor fixing the subunit to the membrane. The  $\text{CaV}\alpha_2\delta$  contains a similar domain arrangement to various plasma proteins, which includes Von Willebrand factor type-A (VWFA) and the calcium channel and chemotaxis (CACHE) domain [28]. The VWFA domain found in  $\text{CaV}\alpha_2$  promotes the trafficking of the  $\alpha_1$  subunit to the membrane and acts as a receptor for the extracellular ligands, such as thrombospondins. This VWFA domain also contains a metal ion-dependent adhesion site (MIDAS), which allows precise coordination of the VWFA domain with bound protein ligand [29]. Mutation of this site can result in the loss of  $\text{CaV}\alpha_2\delta$  subunits' regulatory function to the  $\text{CaV}1.2$ ,  $\text{CaV}2.1$ , and  $\text{CaV}2.2$ . Nevertheless, the  $\text{CaV}\alpha_2\delta$  subunit can still help in trafficking the  $\text{CaV}\alpha_1$  subunit to the cytoplasmic membrane. The CACHE domain is located at the downstream sequence of VWFA domain in the extracellular side. This domain is known to have a possible role in small-molecule recognition [21, 28].

### 3. Three-dimensional structures of LTCCs

Elucidating the three-dimensional (3D) structure of membrane proteins is challenging due to their intricate environmental conditions. Until now, there are no complete 3D structures available for the human voltage-gated calcium channels. The 3D structures of two specific regions of VGCCs in complex with their auxiliary subunits have been resolved, the AID- $\text{CaV}\beta$  complex and the IQ domain-calmodulin ( $\text{Ca}^{2+}/\text{CaM}$ ) complex. Recently, the structure of *Arcobacter butzleri* calcium channel ( $\text{CaVAb}$ ) and the mammalian  $\text{CaV}1.1$  were determined using crystallography and cryo-electron microscopy (EM) techniques, respectively. These structures have provided significant insights on the ion selectivity and drug-binding sites in the calcium channels.

#### 3.1. The AID- $\text{CaV}\beta$ complex

The crystal structures of three isoforms of  $\text{CaV}\beta$  have been resolved in complex with the AID (i.e., short polypeptides from the DI-II linker of  $\text{CaV}\alpha_1$ ) from different species [30]. The 2.2 Å resolution structure of rabbit  $\text{CaV}\beta_2$  isoform was crystallized in complex with an 18-residue long polypeptide, corresponding to the AID of  $\text{CaV}1.1\alpha_1$  (PDB ID: 1T3L). The core region of rat  $\text{CaV}1.2\beta_3$  isoform was crystallized (PDB ID: 1VYV) with a polypeptide (49 AAs) at 2.6 Å resolution. Chen et al. crystallized the single structure of  $\text{CaV}\beta_4$  isoform at 3 Å resolution (PDB ID: 1VYU) [30]. Their core structures, which includes the SH3 and GuK domains, exhibit high similarity. A chimeric complex of rat  $\text{CaV}\beta_2$  isoform and first 16 residues of human  $\text{CaV}1.2$  AID region was crystallized at 1.97 Å resolution (PDB ID: 1T0J) [26]. Mutation analysis showed that three  $\text{CaV}1.2$  AID residues, Tyr447, Trp440, and Ile441 are important for the interaction between the  $\text{CaV}\beta$  subunit and the AID [26, 30].

In 2012, a 2.0 Å resolution crystal complex of rabbit CaV1.2 DI-DII linker and CaVβ<sub>2</sub> isoform was determined [27]. Not until recently, the 3D structure of the last isoform of CaVβ subunit, the CaVβ<sub>1</sub>, has been identified in a complex with the complete cryo-EM model of rabbit CaV1.1. The mechanism that CaVβ regulates CaVα<sub>1</sub> is achieved through the transmitted motions of DI-S6. Before association with CaVβ, AID is in a coil-type structure. The CaVβ acts as a chaperone and helps AID undergo a coil to helix transition during the binding [31]. The α-helix of AID propagates the upstream sequence of DI-S6. They form a rigid connection between the GuK domain of the CaVβ and the channel pore, and mechanically transduce their binding to channel gating states [30]. The N-terminus of the CaVβ is anchored to the membrane, which restricts the motion and orientation of the CaVβ binding to the AID and connecting the DI-S6 segment. These coupled motions help CaVβ effectively regulate the gating properties of calcium channel.

### 3.2. The IQ domain-calmodulin (CaM) complex

Calmodulin (CaM) is a small and conserved calcium-binding messenger protein that plays an essential role in all the HVA channels. In the case of LTCCs, binding with Ca<sup>2+</sup>/CaM is known to pronounce calcium-dependent inhibition of the channel current. Calmodulin, being localized in the cytosolic region, detects the changes in the levels of intracellular Ca<sup>2+</sup> and modulates the interaction of LTCCs with other proteins. Four EF-hand motifs distributed equally on the N- and C-terminus of the CaM works as the calcium ion sensor. Each of EF-hand motifs is composed of two alpha helices and is connected by a flexible loop with the Ca<sup>2+</sup> binding site located in the middle. The Ca<sup>2+</sup>/CaM has a higher binding affinity to LTCC and therefore associates with the LTCC complex even at low cytoplasmic Ca<sup>2+</sup> concentrations. The IQ domain and the pre-IQ domain, upstream sequence of the IQ domain, serve as the binding site for the calmodulin. CaM is known to play a regulatory role in the calcium-dependent inactivation of LTCCs. However, the trafficking function of Ca<sup>2+</sup>/CaM remains controversial, due to inconsistent results in different expression systems [32]. In hippocampal neurons, CaV1.2 trafficking to the distal dendrites is accelerated by the presence of Ca<sup>2+</sup>/CaM, and not by the apo-CaM [33].

From 2005 to 2012, several structures containing a short polypeptide from CaV1.1 or CaV1.2 and calcium-bound calmodulin (Ca<sup>2+</sup>/CaM) were determined. In 2005, three structures of the CaV1.2 IQ domain bound to the hydrophobic pocket of the Ca<sup>2+</sup>/CaM protein were resolved [34, 35]. In those complexes, Ca<sup>2+</sup>/CaM exists in a 2:1 ratio with the IQ domain [36]. IQ domain engages itself in the hydrophobic pockets, present in the N-terminal and C-terminal Ca<sup>2+</sup>/CaM lobes, through sets of conserved 'aromatic anchors'. In the CaV1.2, three residues (Tyr1627, Phe1628, and Phe1631) downstream of IQ domain bind the hydrophobic Ca<sup>2+</sup>/C lobe pockets. The three upstream residues (Phe1618, Tyr1619, and Phe1622) bind the Ca<sup>2+</sup>/N lobe pockets [34]. The lengths of CaV1.2α<sub>1</sub> IQ domains vary among the resolved structures. For example, the 3D structures of human IQ domain have been resolved with 37 residues (PDB ID: 2BE6), and 21 residues (PDB ID: 2F3Z, PDB ID: 2VAY) [37], and 21 residues from *Cavia porcellus* (PDB ID: 2F3Y). In 2009, Fallon et al. resolved the extended structure of IQ domain to include the pre-IQ domain, which comprised of 77 residues from human CaV1.2 C-terminus (PDB ID: 3G43) [38]. In 2010, the structure of PreIQ and IQ domain from human CaV1.2 containing 78 residues (PDB ID: 3OXQ) was crystallized in complex with Ca<sup>2+</sup>/CaM at 2.55 Å resolution [36]. In 2012, Liu and Vogel reported a novel-binding motif (NSCaTE) from N-terminus of CaV1.2

and CaV1.3 to have a higher affinity for binding Ca<sup>2+</sup>/CaM when compared to that of the binding region in C-terminus [23]. Using NMR, they reported the 3D structure of a 24-residue long NSCaTE motif in complex with the Ca<sup>2+</sup>/CaM (PDB ID: 2LQC). Until now, the Ca<sup>2+</sup>/CaM complex structure has only been resolved with CaV1.1 and CaV1.2 of the LTCCs. Although CaV1.4 binds to Ca<sup>2+</sup>/CaM, their interaction has not been reported to have any functional regulation.

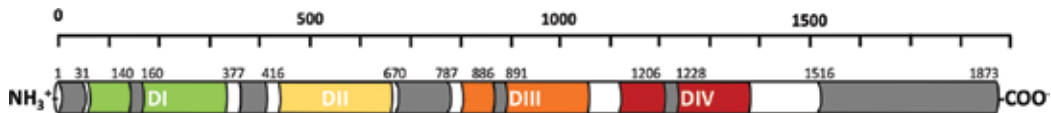
### 3.3. The structure of bacterial CaV channel

In 2014, the first structure of a bacterial calcium channel (CaVAb) was resolved by performing specific mutations on the *Arcobacter butzleri* sodium channel (NaVAb) [5]. The quaternary structure of CaVAb is a symmetrical homo-tetramer, which is similar to its NaVAb prototype. Four identical domains assemble to form the main structure of the channel, with each of the domain (containing 237 residues) encompassing six transmembrane helices. The topological features of the transmembrane domain of the CaVAb are similar to that of the LTCC. Tang et al. performed several mutations to elucidate the structural basis of Ca<sup>2+</sup> selectivity and reported the crystal structures of 13 variants that conferred different mutations in NaVAb.

Each monomer is composed of a voltage-sensing domain (S1–S4) and a pore-forming domain (S5–S6). Four positively charged arginines in the voltage-sensing domain detect the changes in the membrane potential. The voltage-sensor movements are transmitted to the pore-forming domain through a cytoplasmic linker that connects the S4 and S5 helices. Three negatively charged aspartate residues at the selectivity filter (Asp177, Asp178, and Asp181) were found to be essential for binding the Ca<sup>2+</sup> ion and render selectivity to the channel. The paper revealed that the ion-selective mechanism is based on three Ca<sup>2+</sup> binding sites, site-1 (Asp178), site-2 (Asp177, Leu176), and site-3 (Thr175). A single substitution at site-177, from Glu to Asp, enhanced the calcium selectivity by 1000 times over sodium, which was sufficient to convert the sodium channel to calcium channel. Although 181D is not directly involved in Ca<sup>2+</sup> coordination and lies outside of the ion-conducting pore, it generates an electronegative environment to attract the extracellular cations. Binding of one Ca<sup>2+</sup> blocks the pore and prevents the entry of the monovalent cations. The entry of second Ca<sup>2+</sup> induces electrostatic repulsion on the first Ca<sup>2+</sup>, thereby forcing it to flux into the cytoplasm. Thus, the extracellular calcium ions fluently permeate into the intracellular side in response to the concentration gradient [5].

### 3.4. Structure of CaV1.1

In 2015, Wu et al. reported the complete structure of the mammalian CaV1.1 complex at 4.2 Å resolution using the cryo-EM technique [39]. Three auxiliary subunits were isolated from the rabbit skeletal muscle, the pore-forming  $\alpha_1$ -subunit, the extracellular  $\alpha_2\delta$ -subunit, and the transmembrane  $\gamma$ -subunit. The fourth auxiliary subunit was included in the complex by docking the crystal structure of rat CaV $\beta_2$  (PDB ID: 1T0J) on the AID of CaV1.1 $\alpha_1$  subunit. Following this complex, two rabbit CaV1.1 complexes at resolution 3.9 Å (PDB ID: 5GJW) and 3.6 Å (PDB ID: 5GJV) were reported [40]. This CaV1.1 construct included 1873 amino acid residues. While the 3D coordinates of most parts of the CaV1.1  $\alpha_1$ -subunit were resolved, some of the cytoplasmic (N-terminus: 1–31, DI–DII linker: 377–416, DII–DIII linker: 670–787, and C-terminus 1516–1873) and extracellular segments (DI S3–S4: 140–160, DIII S3–S4: 886–891, and DIV S3–S4: 1206–1228) were found to be missing (**Figure 4**).



**Figure 4.** The missing residues in the rabbit CaV1.1- $\alpha_1$  structure (PDB ID: 5GJV) shaded in gray.

The rabbit CaV1.1 is composed of four inter-connected homologous domains, each of which includes the voltage-sensing and pore-forming domain. The S4 helix of the VSD is composed of six charged residues when compared to four residues in human CaVs [41]. Remarkably, the asymmetric pore-region of CaV1.1 is formed by the four S5, and S6 bundles and the tightly packed inner gate showcased a closed conformation and inactivated conduction-state of the CaV1.1 channel. The auxiliary CaV $\alpha_2$  subunit included four tandem cache domains and one VWA domain. The cysteine residues, Cys1074 in CaV $\delta$  and Cys406 in CaV $\alpha_2$  formed a disulfide bond at the binding region between VWA domain and CaV $\delta$ . In the VWA domain, the MIDAS residues (Ser263, Ser265, Asp261, Thr333, and Asp365) and CaV $\alpha_1$  DI S1–S2 residue (Asp78) are bound to a calcium ion. Both the previous and latest 3D structures identified for the CaV $\gamma$  subunit included four transmembrane  $\alpha$ -helices, however, in this CaV1.1 structure, additional extracellular  $\beta$ -sheets have been resolved together with the regions of the two termini. The second and third transmembrane-helices in CaV $\gamma$  and DIV S3–S4 in CaV $\alpha_1$  are directly involved in interactions through hydrophobic forces. The Cryo-EM structure of the rabbit CaV1.1, have thus brought novel insights on the multi-domain structure of VGCC, especially the association of CaV with the auxiliary proteins.

### 3.5. Computational modeling

Computational modeling and simulation remain to be a promising technique to reveal fundamental biological mechanisms, biomolecular interactions and predicting the effects of modulators. In CaV, modeling-based studies were previously performed to understand how LTCC blockers bind the calcium channel [42–44]. Tikhonov and Zhorov generated homology models of the open- and closed-state conformation of the pore-forming domains of CaV1.2 using the crystal structure of the KvAP and KCSA channels as the template [45]. The generated models were used to dock three types of LTCC blockers, benzothiazepine, phenylalkylamine, and dihydropyridine. The docking analysis showed that the all the three ligands bind near the S5–S6 helices of domain III and IV and the CaV residues, tyrosine in S6-DIII, tyrosine in S6-DIV, and glutamine in S5-DIII, are important for binding these ligands close to the pore domain of the channel. Since no experimentally-resolved structure of small molecule-CaV was available, *in silico* the docking analysis performed in this study provided useful insights for understanding ligand-binding in CaV.

Adiban et al. used the structure of the CaVAb (PDB ID: 4MVQ) to model the selectivity filter of the CaV with defined charges. They performed molecular dynamics (MD) simulation to calculate the potential of mean force and showed that the affinity for Ca<sup>2+</sup> in site-2 (Asp177, Leu176) is higher than that within the two other sites, site-1 (Asp178) and site-3 (Thr175). Their study also showed that, in the absence of calcium ions, the CaVAb could allow the passage of Na<sup>+</sup> ions, but not Cl<sup>-</sup> ions [46]. This study using the structure of CaVAb, was helpful in understanding the structure–function relationships of the calcium channel.

All of the computational models built for CaV until now were based on templates with low sequence identity (<30%). Studying molecular systems built with low-identity templates is quite challenging since the accuracy of the model is highly dependent on the similarity between the template and the target protein [47]. While the oligomeric structures of bacterial homologs are useful for modeling the transmembrane domains (TMDs), building the large intracellular domains that connect the TMDs using these structures is not feasible. With the availability of the CaV1.1 complex and other structural data, obtaining better quality homology-based models for the human CaV channels, especially the LTCCs, is now possible. Nevertheless, sophisticated methods and high-performance computing would be needed for modeling the multi-domain architecture of the human CaVs. Building these models can be helpful in understanding the structure-function-dynamic properties, the Ca<sup>2+</sup> influx mechanisms and effects of small molecules on these channels [48, 49].

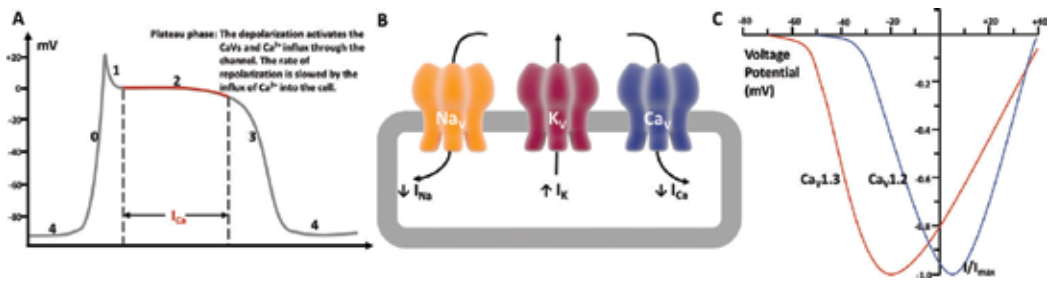
## 4. Activation mechanisms of LTCCs

LTCC, being a voltage-gated ion channel, remains mostly sensitive to the changes in the membrane potential and the VSD (S1–S4 helices) of the LTCCs play a crucial role in sensing the voltage changes across the membrane. In addition to the voltage-dependent gating mechanisms, the channel's conductivity also depends on the intracellular Ca<sup>2+</sup> concentration, and thus is modulated by both self-regulatory and extrinsic mechanisms.

### 4.1. Voltage-dependent activation/inactivation mechanism

The cardiac action potential is a classic example of the voltage-dependent mechanism. During the action potential, the ions channels undergo several conformational transitions and regulate the exchange of ions across the membrane. When the intracellular gates of the channel are open, the channel is referred to be conducting. The smooth passage of ions through the open-pore of the channel generates the electrical current across the membrane. When the membrane depolarizes, the inactivation gates of the channel are closed, while the intracellular gates are still open to allow the decay of current levels. Inactivation is a way to decrease the availability of the open-state of the channel at more depolarized membrane potentials [50]. The closed state of the channel corresponds to the closed intracellular gates, which hinders the ion passage, and results in a non-conducting state.

The action potential can be divided into five phases (Phase 0–4, shown in **Figure 5**) and the concerted activities of various ion channels in the heart help in maintaining the cardiac rhythm. In simple terms, at phase 0, the membrane is initially at the resting potential (–90 mV), where the LTCCs are in a closed-state (no Ca<sup>2+</sup> ion passage). When depolarization occurs, and the membrane potential reaches a threshold voltage of –70 mV, the inward sodium ion (Na<sup>+</sup>) channels are activated allowing the flow of the I<sub>Na</sub> current. This current flow further increases the membrane potential to a more positive value and reaches a peak, when the activation of LTCCs are initiated, and the sodium channels are inactivated. During phase 1, early and rapid repolarization occurs by the brief activation of K<sup>+</sup> channels and the LTCCs remain in a pre-open state. After phase 1, the opening of the LTCCs (open/activated state) slows the



**Figure 5.** (A) Cardiac action potential (left) [54]. (B) Activities of three types cation channels during phase 2. The inward sodium and calcium current decays with time; the outward potassium current is activated allowing the cell to move to resting state [55]. (C) CaV1.2 and CaV1.3 voltage potential amplitude. Plot re-generated from Xu and Lipscombe data [56].

repolarization down. This phase of the cardiac action potential, the phase 2, is called a plateau phase and is maintained by the balancing act of the Ca<sup>2+</sup> and K<sup>+</sup> ions (shown in **Figure 5**). This Ca<sup>2+</sup> influx that occur during phase 2 initiates the contractile function of the cardiac cells. Close to the end of phase 2, when more Ca<sup>2+</sup> ions are released an auto-inhibitory signal is triggered resulting in a non-conducting state or closed state of the calcium channel.

During phase 3, the cell tries to return to the resting state by the gradual inactivation of the calcium channels (inactivated state) and continued efflux of K<sup>+</sup> ions [51]. At the end of phase 3 inward rectifying K<sup>+</sup> channels are activated to reset the membrane potential to the resting state. The last phase of the action potential, in phase 4, the membrane returns to resting potential (−90 mV), which allows the LTCCs to transit from the inactivated state to the closed state for the next cycle of events. This resting potential of the membrane is maintained by the continued leak of the K<sup>+</sup> ions.

Given the tissue-specific localization of the members of LTCCs and their different functional roles relevant to the region of expression, these channels also have different activation threshold and kinetics. For example, the CaV1.1 and CaV1.2 require a depolarized threshold of +7 and −30 mV, for their activation [2, 52]. The CaV1.3 and CaV1.4 do not require a depolarized threshold as strong as CaV1.1 and CaV1.2, to be activated and have relatively low activation thresholds of about −55 and −40 mV (**Figure 5**), respectively. Similarly, CaV1.3 channels are known to activate with fast kinetics when compared to that of the CaV1.1 [53]. Although CaV1.3 is closely related to CaV1.2, it seems to share more similar properties with CaV1.4, including rapid activation kinetics, low activation threshold, and lower sensitivity to 1,4-DHPs [53].

#### 4.2. Calcium-dependent activation/inactivation mechanism

The calcium-dependent channel regulation process requires the participation of multiple segments, such as the β-subunit [57], Ca<sup>2+</sup>/CaM [58], CaMKII [59], N-terminal and C-terminal regions of the LTCC CaVα<sub>1</sub>. Calcium-dependent inactivation serves as the autoinhibitory control for the LTCCs to control the levels of intracellular calcium. It is mediated by the interactions between the Ca<sup>2+</sup>/CaM and CaV pre-IQ/IQ domains. Disruption to this interaction has

been known to attenuate the calcium-dependent inactivation process. At the resting potential, apo-CaM associates with the alpha-subunit of the channel. When  $\text{Ca}^{2+}$  ions bind the CaM, the fully charged CaM with four  $\text{Ca}^{2+}$  ions allow the two polarized lobes of the CaM, the  $\text{Ca}^{2+}$ /N lobe, and the  $\text{Ca}^{2+}$ /C lobe, to envelope the alpha-binding helix. Specific interactions of two lobes with the IQ domain initiate different calcium-dependent regulations. For example, in CaV1.2 and CaV1.3, CDI is caused by the interaction between the IQ domain and the  $\text{Ca}^{2+}$ /C-lobe, while CDF is facilitated by the interaction of the  $\text{Ca}^{2+}$ /N-lobe and the IQ domain [24, 35]. In contrary, the IQ domain interactions with the  $\text{Ca}^{2+}$ /N-lobe and the  $\text{Ca}^{2+}$ /C-lobe in the CaV2.1 channel, lead to CDF and CDI, respectively [60, 61].

Ferreira et al. [62] reported that calcium-dependent mechanisms could speed up the inactivation process. They used barium in the place of calcium ion and found that the channels undergo rapid activation and slow inactivation due to the lack of intracellular calcium. Their result showed that voltage-dependent mechanisms alone in the absence of calcium-dependent mechanisms would lead to slower inactivation [24, 53]. While CaM promotes calcium-dependent inactivation, the  $\text{Ca}^{2+}$ /calmodulin-dependent protein kinase II (CaMKII) counteracts the above process and helps in the re-activation of the channel in a calcium-dependent way. CaMKII phosphorylates the CaV $\beta$  subunit and the C-terminus of CaV $\alpha_1$  at their specific phosphorylation sites, resulting in the disruption of CaM-CaV channel interactions. Increase in the intracellular calcium ion level activates the CaMKII and reduces the effects of CDI [12, 59]. CaMKII enables the channel gates to be frequently left in the open state for a long time thus, prolonging the plateau phase of the action potential at high frequency.

## 5. L-type calcium channels modulators

The LTCCs are considered as an important target for the treatment of various diseases [9, 63–66]. CaV1.1, the major isoform of the skeletal LTCCs is reported to correlate with hypokalemic periodic paralysis, which is characterized by muscular weakness or paralysis [63]. CaV1.2 and CaV1.3, being more expressed in the heart and the brain, their dysfunction results in severe disease states, such as Timothy's syndrome, cardiac arrhythmia [6], bipolar disorder, and autism [64, 65]. Any abnormality in the cardiac LTCCs leads to long-QT syndrome (LQTS), where the QT interval of the cardiac action potential is prolonged, a condition that causes heart arrhythmias or sudden cardiac death (SCD) [67]. The Timothy Syndrome (TS), is an extremely rare multisystem LQTS subtype, that is mainly caused by the dysfunctions of LTCC and  $\text{Ca}^{2+}$  handling proteins. As the only LTCC subtype in the retinal cells, mutations in the CaV1.4 gene are known to weaken the normal visual functions and cause night blindness. Modulating LTCCs, therefore, remains to be an important avenue for the treatment of several diseases.

### 5.1. Small molecule modulators

Fleckenstein showed that small organic molecules, like verapamil, specifically inhibited the  $\text{Ca}^{2+}$  current from LTCCs [66]. Since then, several small-molecule modulators of the LTCCs

have been identified. Most LTCC drugs can be grouped into one of these three groups, phenylalkylamines, benzothiazepines, and dihydropyridines [9]. All LTCCs exhibit a similar pharmacological profile upon treatment with the drug, including the high-affinity frequency-dependent block [9]. These three classes of drugs bind to three allosterically linked receptor sites on the LTCCs and block the inward calcium current [68]. Previous studies showed that these three classes of drugs bind at three distinct sites, however with overlapped binding domains [43, 69]. All three binding sites are close to the pore and are located within the S5 and S6 helices of DIII and S6 helix of DIV [68]. Tikhonov and Zhorov choose the KvAP and KcsA crystal structure as the template to model the open state and the close state of CaV1.2, respectively. Based on this template, they investigated the binding mode of dihydropyridine [43] and benzothiazepine [42] and confirmed their binding in this region. However, the co-crystallized structure of CaVAb-verapamil complex suggests that the verapamil-like phenylalkylamines can bind within the pore of the channel [6].

#### 5.1.1. DHPs and related drugs

The 1,4-dihydropyridine (1,4-DHP) is an effective and specific LTCCs blocker that is commonly used for the treatment of cardiovascular diseases, such as vasodilation, angina, and hypotension [45, 68]. DHP-derived drugs, such as amlodipine, clevidipine, and felodipine are also used for the treatment of cardiac diseases [7]. Nimodipine, another DHP-based drug, regulates the LTCCs distributed in neurons and helps in improving the outcomes of neurological treatments [7, 65]. Most DHP-based antagonists prefer binding to the inactivated states of the channel and stabilize them to block the  $\text{Ca}^{2+}$  influx. Since most 1,4-DHPs are lipophilic, they also tend to bind on the outer surface of the channel facing the lipid molecules and form interactions with the S6 of DIII and DIV [53]. Four DIII residues (Tyr1152, Ile1153, Ile1156, Met1161) and one DIV residue (Asn1472) were found to be important for binding DHP-based drugs. Amino acid substitutions on the residues mentioned above were found to cause more than a five-fold decrease in the binding affinity of these compounds. Also, substitutions in the DIII and DIV residues of CaV1.2 (Phe1158, Phe1159, Met1160, Tyr1463, Met1464, Ile1471) are known to cause the about two- to fivefold decreases in the binding affinity [69].

#### 5.1.2. Phenylalkylamine and related drugs

Verapamil is the prototype phenylalkylamine and is the only drug currently available from this class for clinical use [9, 68]. It is widely used for the treatment of hypertension. The significant differences in the binding affinities of phenylalkylamine towards the different conduction states of the channel show that these drugs, similar to DHPs, most likely bind to the inactivated state of LTCCs [7, 66, 68]. It has been shown that phenylalkylamine binding causes the channel to hardly recover from the repolarization [68, 69]. It is known from the co-crystallized structure of CaVAb that phenylalkylamine binds in the central cavity of the pore on the intracellular side of the selectivity filter [6]. Upon binding, the drug results in the physical blockade of the channel and thus, preventing the passage of calcium ions. The Br-verapamil interacts with the surrounding residues, including Met174, Leu176, and two Thr206, from the S6 helices of each domain.



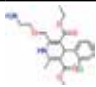
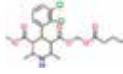
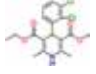
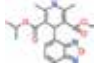
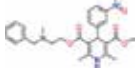
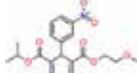
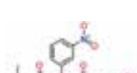

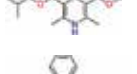
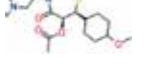
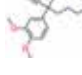
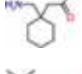
### 5.1.3. Benzothiazepine and related drugs

Diltiazem, a clinically approved LTCC antagonist from the benzothiazepine class, is used for the treatment of arrhythmias. The diltiazem exhibits modest selectivity for LTCCs in vascular smooth muscle over cardiac muscle. Similar to the other two types, benzothiazepine tends to bind the inactivated state of LTCCs and share similar binding site as that of the 1,4-DHPs. Based on the photoaffinity labeling experiments, the binding sites of diltiazem was located within the S6 of DIII and DIV. Specific amino acid residues, Tyr1463, Ala1467, and Ile1470 that are present in the S6 helix of the DIV have been identified to be important for benzothiazepine blocking [68].

In addition to the  $\alpha_1$ -subunit, the  $\alpha_2\delta$ -subunit of LTCCs are also considered as a promising target for regulating the channel functions [70]. Pregabalin and gabapentin are  $\alpha_2\delta$ -subunit targeting small molecules that are being used for the treatment of chronic neuropathic pain [9, 29]. It has been shown that these two molecules are sensitive only to  $\text{CaV}\alpha_2\delta_1$  and  $\text{CaV}\alpha_2\delta_2$  and not to other isoforms of  $\text{CaV}\alpha_2\delta$  [21]. These drugs work through the association of  $\text{CaV}\alpha_2\delta$  and  $\text{CaV}\alpha_1$  and inhibit the calcium channel activity in two ways. First, the association of  $\text{CaV}\alpha_2\delta$  and  $\text{CaV}\alpha_1$  increases the current amplitude. Binding with ligands inhibits this effect. Second, these drugs modify the channel activation by affecting the channel surface trafficking [71]. Interactions with ligands decrease the  $\alpha_2\delta$ -subunit surface expression and LTCC trafficking, which in turn reduces the overall calcium inward currents [70]. Using alanine-scanning mutagenesis these drugs have been identified to bind to an arginine residue (Arg217) on the extracellular side of the channel. Due to their extracellular binding characteristics, these drugs are not required to enter the cell to bind their target, which makes them an attractive alternative therapy for the treatment of neurological diseases [7]. **Table 2** summarizes the binding region, targeted disease, and chemical structure of LTCC targeting drugs.

## 5.2. Peptide modulators

Apart from the small molecular modulators, few natural toxin proteins have been known to specifically block the LTCCs. Two groups of toxins that selectively block the  $\text{CaV}2$  subfamily have been identified: the  $\omega$ -conotoxin family of pore blockers and the functionally heterogeneous  $\omega$ -agatoxin family of pore blockers [8]. Recently, Findeisen et al. reported a peptide-based inhibitor for the  $\text{CaV}$ . The  $\text{CaV}\beta$  subunit exhibits a chaperone-like function and induces a helical conformation on the AID from its' coiled structure, upon binding. The helix-conformation of AID has a higher binding affinity towards the  $\text{CaV}\beta$  subunit [27, 72]. Based on this mechanism, Findeisen et al. [57] developed a stapled meta-xylyl (m-xylyl) AID, that is compatible to bind the  $\text{CaV}\beta$  subunit. The stapled peptide, having a higher helix propensity had a higher chance to bind the  $\text{CaV}\beta$  when compared to that of the native AID. This peptide inhibited the interaction between the AID and  $\text{CaV}\beta$  ( $K_d$   $\text{CaV}1.2$ -AID:  $6.6 \pm 2.0$  nM,  $K_d$  AID-CEN:  $5.2 \pm 1.5$  nM) and served as an antagonist for the calcium channel. The crystal structure of the stapled peptide in complex with the AID region of the human  $\text{CaV}1.2$ , and the rat  $\text{CaV}\beta_2$  was resolved at 1.7 and 2.0 Å resolution, respectively (PDB ID: 5V2Q, 5V2P). Thus, peptide-based inhibitors are also of interest in modulating the  $\text{CaV}$  channel.

Drug	Drug class	Binding region	Targeted disease	2D-structure
Amlodipine	1,4-Dihydropyridine	CaV $\alpha$ 1 IIIS5-S6, IIIS6, IVS6	Hypertension, chronic stable angina	
Clevidipine	1,4-Dihydropyridine	CaV $\alpha$ 1 IIIS5-S6, IIIS6, IVS6	Hypertension	
Felodipine	1,4-Dihydropyridine	CaV $\alpha$ 1 IIIS5-S6, IIIS6, IVS6	Hypertension	
Isradipine	1,4-Dihydropyridine	CaV $\alpha$ 1 IIIS5-S6, IIIS6, IVS6	Hypertension	
Nicardipine	1,4-Dihydropyridine	CaV $\alpha$ 1 IIIS5-S6, IIIS6, IVS6	Hypertension, chronic stable angina	
Nifedipine	1,4-Dihydropyridine	CaV $\alpha$ 1 IIIS5-S6, IIIS6, IVS6	Hypertension, vasospastic angina, chronic stable angina	
Nimodipine	1,4-Dihydropyridine	CaV $\alpha$ 1 IIIS5-S6, IIIS6, IVS6	Improve neurologic outcome	
Nisoldipine	1,4-Dihydropyridine	CaV $\alpha$ 1 IIIS5-S6, IIIS6, IVS6	Hypertension	
Diltiazem	Benzothiazepine	CaV $\alpha$ 1 IIIS6, IVS6	Hypertension	
Verapamil	Phenylalkylamine	CaV $\alpha$ 1 IS6, IIS6, IIIS6, IVS6	Hypertension, chronic stable angina, cluster headache	
Pregabalin	Gamma-aminobutyric acid (GABA)	CaV $\alpha$ 2 $\delta$	Neuropathic pain, epilepsy, generalized anxiety disorder	
Gabapentin	Gamma-aminobutyric acid (GABA)	CaV $\alpha$ 2 $\delta$	Epilepsy, neuropathic pain	

**Table 2.** Common L-type calcium channel inhibitors. The list of drugs and the 2D structures are obtained from the Drugbank database.

## 6. Discussion

Voltage-gated calcium channels (VGCCs), which are responsible for the calcium flux in cells, play a key role in many physiological processes, including neurotransmission, cell cycle, muscular contraction, cardiac action potential, gene expression, and protein modulation.

Their abnormal functions result in increased intracellular calcium levels and trigger serious pathological effects from cardiovascular and neuronal diseases to cancer. VGCCs are therefore considered as a significant target and development of isoform-specific modulators for VGCCs remain promising in pharmaceutical research.

The diverse expression patterns of the L-type and T-type channels show that these channels are pharmacologically important in several cancers, Parkinson's disease, sensory diseases and cardiac diseases. The N-type channels, although present in different organs, is known for their activity in the nervous system and are considered as a target for pain and nervous disorders. On the other hand, the P/Q-type, which is preferably expressed in the neuronal cells, is attributed to neurological diseases, such as migraine, Alzheimer's and ataxia. For several decades, non-selective calcium channel blockers have been used for targeting the calcium channels for various treatments. The FDA approval of ziconotide (N-type channel blocker) and the specificity of  $\omega$ -agatoxin to P-/Q-type channels have attracted the development of more isoform-specific blockers [9]. Given the diversity in the roles and expression of calcium channels, specific targeting of these channels seems to be a promising strategy for therapeutic innovations.

## 7. Conclusion

In this chapter, we provide a comprehensive overview of the different types of VGCCs, especially the LTCCs, their sequence, structure, distribution, functional, and biophysical/biochemical variations. Numerous studies have reported these key features, including the structural and functional properties of different CaV channels. For instance, the recent structures of CaVA<sub>b</sub> and the rabbit CaV1.1 paved the way for understanding the structure–function connections of ion-selectivity mechanism, self-regulation, and small-molecule interactions. However, till date, the complete structures of the human CaV isoforms have not been resolved, which remains to be a hurdle for understanding the intrinsic disease-related mechanisms of the channel. With the advent and application of various technologies, such as cryo-EM, NMR, crystallography, molecular modeling, and molecular dynamics, it could be possible to resolve the complete structure of the human isoforms. Having this structural information in-hand would help in understanding the structure–function relationships of these channels, and thereby in the development of isoform-specific calcium channel modulators.

## Author details

Tianhua Feng<sup>1</sup>, Subha Kalyanamoorthy<sup>1</sup> and Khaled Barakat<sup>1,2,3\*</sup>

\*Address all correspondence to: [kbarakat@ualberta.ca](mailto:kbarakat@ualberta.ca)

1 Faculty of Pharmacy and Pharmaceutical Sciences, University of Alberta, Edmonton, Alberta, Canada

2 Li Ka Shing Institute of Virology, University of Alberta, Edmonton, Alberta, Canada

3 Li Ka Shing Applied Virology Institute, University of Alberta, Edmonton, Alberta, Canada

## References

- [1] Prakash P, Hancock JF, Gorfe AA. Binding hotspots on K-ras: Consensus ligand binding sites and other reactive regions from probe-based molecular dynamics analysis. *Proteins*. 2015;**83**(5):898-909. DOI: 10.1002/prot.24786
- [2] Dolphin AC. A short history of voltage-gated calcium channels. *British Journal of Pharmacology*. 2006;**147**(Suppl 1):S56-S62. DOI: 10.1038/sj.bjp.0706442
- [3] Catterall WA. Voltage-gated calcium channels. *Cold Spring Harbor Perspectives in Biology*. 2011;**3**(8):a003947. DOI: 10.1101/cshperspect.a003947
- [4] Hess P, Lansman JB, Tsien RW. Different modes of Ca channel gating behaviour favoured by dihydropyridine Ca agonists and antagonists. *Nature*. 1984;**311**(5986):538-544
- [5] Tang L et al. Structural basis for Ca<sup>2+</sup> selectivity of a voltage-gated calcium channel. *Nature*. 2014;**505**(7481):56-61. DOI: 10.1038/nature12775
- [6] Tang L et al. Structural basis for inhibition of a voltage-gated Ca<sup>2+</sup> channel by Ca<sup>2+</sup> antagonist drugs. *Nature*. 2016;**537**(7618):117-121. DOI: 10.1038/nature19102
- [7] Godfraind T. Discovery and development of calcium channel blockers. *Frontiers in Pharmacology*. 2017;**8**:286. DOI: 10.3389/fphar.2017.00286
- [8] Protti DA, Uchitel OD. Transmitter release and presynaptic Ca<sup>2+</sup> currents blocked by the spider toxin omega-Aga-IVA. *Neuroreport*. 1993;**5**(3):333-336
- [9] Zamponi GW et al. The physiology, pathology, and pharmacology of voltage-gated calcium channels and their future therapeutic potential. *Pharmacological Reviews*. 2015;**67**(4):821-870. DOI: 10.1124/pr.114.009654
- [10] Teng J et al. Ion-channel blocker sensitivity of voltage-gated calcium-channel homologue Cch1 in *Saccharomyces cerevisiae*. *Microbiology*. 2008;**154**(Pt 12):3775-3781. DOI: 10.1099/mic.0.2008/021089-0
- [11] Gomes B et al. Lymphocyte calcium signaling involves dihydropyridine-sensitive L-type calcium channels: Facts and controversies. *Critical Reviews in Immunology*. 2004;**24**(6):425-447
- [12] Hofmann F et al. L-type CaV1.2 calcium channels: From in vitro findings to in vivo function. *Physiological Reviews*. 2014;**94**(1):303-326. DOI: 10.1152/physrev.00016.2013
- [13] Striessnig J et al. L-type Ca<sup>2+</sup> channels in heart and brain. *Wiley Interdisciplinary Reviews: Membrane Transport and Signaling*. 2014;**3**(2):15-38. DOI: 10.1002/wmts.102
- [14] Temme SJ, Murphy GG. The L-type voltage-gated calcium channel CaV1.2 mediates fear extinction and modulates synaptic tone in the lateral amygdala. *Learning & Memory*. 2017;**24**(11):580-588. DOI: 10.1101/lm.045773.117
- [15] Mangoni ME et al. Functional role of L-type Cav1.3 Ca<sup>2+</sup> channels in cardiac pacemaker activity. *Proceedings of the National Academy of Sciences of the United States of America*. 2003;**100**(9):5543-5548. DOI: 10.1073/pnas.0935295100

- [16] Baumann L et al. Functional characterization of the L-type Ca<sup>2+</sup> channel Cav1.4alpha1 from mouse retina. *Investigative Ophthalmology & Visual Science*. 2004;**45**(2):708-713
- [17] Catterall WA et al. International Union of Pharmacology. XLVIII. Nomenclature and structure-function relationships of voltage-gated calcium channels. *Pharmacological Reviews*. 2005;**57**(4):411-425. DOI: 10.1124/pr.57.4.5
- [18] Karaki H et al. Calcium movements, distribution, and functions in smooth muscle. *Pharmacological Reviews*. 1997;**49**(2):157-230
- [19] Artalejo CR, Adams ME, Fox AP. Three types of Ca<sup>2+</sup> channel trigger secretion with different efficacies in chromaffin cells. *Nature*. 1994;**367**(6458):72-76. DOI: 10.1038/367072a0
- [20] Bodi I. The L-type calcium channel in the heart: The beat goes on. *Journal of Clinical Investigation*. 2005;**115**(12):3306-3317. DOI: 10.1172/jci27167
- [21] Dolphin AC. The alpha(2)delta subunits of voltage-gated calcium channels. *Biochimica et Biophysica Acta-Biomembranes*. 2013;**1828**(7):1541-1549. DOI: 10.1016/j.bbamem.2012.11.019
- [22] Tuluc P et al. Molecular interactions in the voltage sensor controlling gating properties of CaV calcium channels. *Structure*. 2016;**24**(2):261-271. DOI: 10.1016/j.str.2015.11.011
- [23] Liu Z, Vogel HJ. Structural basis for the regulation of L-type voltage-gated calcium channels: Interactions between the N-terminal cytoplasmic domain and Ca<sup>2+</sup>-calmodulin. *Frontiers in Molecular Neuroscience*. 2012;**5**:38. DOI: 10.3389/fnmol.2012.00038
- [24] Hulme JT et al. Autoinhibitory control of the CaV1.2 channel by its proteolytically processed distal C-terminal domain. *The Journal of Physiology*. 2006;**576**(Pt 1):87-102. DOI: 10.1113/jphysiol.2006.111799
- [25] Simms BA, Zamponi GW. Trafficking and stability of voltage-gated calcium channels. *Cellular and Molecular Life Sciences*. 2012;**69**(6):843-856. DOI: 10.1007/s00018-011-0843-y
- [26] Van Petegem F et al. Structure of a complex between a voltage-gated calcium channel beta-subunit and an alpha-subunit domain. *Nature*. 2004;**429**(6992):671-675. DOI: 10.1038/nature02588
- [27] Almagor L et al. The role of a voltage-dependent Ca<sup>2+</sup> channel intracellular linker: A structure-function analysis. *The Journal of Neuroscience*. 2012;**32**(22):7602-7613. DOI: 10.1523/JNEUROSCI.5727-11.2012
- [28] Briot J et al. Three-dimensional architecture of the L-type calcium channel: Structural insights into the CaV $\alpha$ 2 $\delta$ 1 auxiliary protein. *Biochemistry & Molecular Biology Journal*. 2016;**02**(03):1-7. DOI: 10.21767/2471-8084.100025
- [29] Eroglu C et al. Gabapentin receptor alpha2delta-1 is a neuronal thrombospondin receptor responsible for excitatory CNS synaptogenesis. *Cell*. 2009;**139**(2):380-392. DOI: 10.1016/j.cell.2009.09.025
- [30] Chen YH et al. Structural basis of the alpha1-beta subunit interaction of voltage-gated Ca<sup>2+</sup> channels. *Nature*. 2004;**429**(6992):675-680. DOI: 10.1038/nature02641

- [31] Buraei Z, Yang J. Structure and function of the beta subunit of voltage-gated Ca<sup>2+</sup> channels. *Biochimica et Biophysica Acta*. 2013;**1828**(7):1530-1540. DOI: 10.1016/j.bbamem.2012.08.028
- [32] Bourdin B et al. Molecular determinants of the CaVbeta-induced plasma membrane targeting of the CaV1.2 channel. *The Journal of Biological Chemistry*. 2010;**285**(30):22853, 22863. DOI: 10.1074/jbc.M110.111062
- [33] Stroffekova K. Ca<sup>2+</sup>/CaM-dependent inactivation of the skeletal muscle L-type Ca<sup>2+</sup> channel (Cav1.1). *Pflugers Arch*. 2008;**455**(5):873-884. DOI: 10.1007/s00424-007-0344-x
- [34] Van Petegem F, Chatelain FC, Minor DL Jr. Insights into voltage-gated calcium channel regulation from the structure of the CaV1.2 IQ domain-Ca<sup>2+</sup>/calmodulin complex. *Nature Structural & Molecular Biology*. 2005;**12**(12):1108-1115. DOI: 10.1038/nsmb1027
- [35] Fallon JL et al. Structure of calmodulin bound to the hydrophobic IQ domain of the cardiac Ca(v)1.2 calcium channel. *Structure*. 2005;**13**(12):1881-1886. DOI: 10.1016/j.str.2005.09.021
- [36] Kim EY et al. Multiple C-terminal tail Ca<sup>2+</sup>/CaMs regulate Ca(V)1.2 function but do not mediate channel dimerization. *The EMBO Journal*. 2010;**29**(23):3924-3938. DOI: 10.1038/emboj.2010.260
- [37] Halling DB et al. Determinants in CaV1 channels that regulate the Ca<sup>2+</sup> sensitivity of bound calmodulin. *The Journal of Biological Chemistry*. 2009;**284**(30):20041-20051. DOI: 10.1074/jbc.M109.013326
- [38] Fallon JL et al. Crystal structure of dimeric cardiac L-type calcium channel regulatory domains bridged by Ca<sup>2+</sup> center dot calmodulins. *Proceedings of the National Academy of Sciences of the United States of America*. 2009;**106**(13):5135-5140. DOI: 10.1073/pnas.0807487106
- [39] Wu J et al. Structure of the voltage-gated calcium channel Cav1.1 complex. *Science*. 2015;**350**(6267):aad2395. DOI: 10.1126/science.aad2395
- [40] Wu J et al. Structure of the voltage-gated calcium channel Ca(v)1.1 at 3.6 Å resolution. *Nature*. 2016;**537**(7619):191-196. DOI: 10.1038/nature19321
- [41] Burashnikov E et al. Mutations in the cardiac L-type calcium channel associated with inherited J-wave syndromes and sudden cardiac death. *Heart Rhythm*. 2010;**7**(12):1872-1882. DOI: 10.1016/j.hrthm.2010.08.026
- [42] Tikhonov DB, Zhorov BS. Molecular modeling of benzothiazepine binding in the L-type calcium channel. *The Journal of Biological Chemistry*. 2008;**283**(25):17594-17604. DOI: 10.1074/jbc.M800141200
- [43] Tikhonov DB, Zhorov BS. Structural model for dihydropyridine binding to L-type calcium channels. *The Journal of Biological Chemistry*. 2009;**284**(28):19006-19017. DOI: 10.1074/jbc.M109.011296
- [44] Cheng RC, Tikhonov DB, Zhorov BS. Structural model for phenylalkylamine binding to L-type calcium channels. *The Journal of Biological Chemistry*. 2009;**284**(41):28332-28342. DOI: 10.1074/jbc.M109.027326

- [45] Shaldam MA et al. 1,4-dihydropyridine calcium channel blockers: Homology modeling of the receptor and assessment of structure activity relationship. *ISRN Medicinal Chemistry*. 2014;**2014**:1-14. DOI: 10.1155/2014/203518
- [46] Adiban J, Jamali Y, Rafii-Tabar H. Modeling ion permeation through a bacterial voltage-gated calcium channel CaVAb using molecular dynamics simulations. *Molecular BioSystems*. 2016;**13**(1):208-214. DOI: 10.1039/c6mb00690f
- [47] Tramontano A. Homology modeling with low sequence identity. *Methods*. 1998;**14**(3):293-300. DOI: 10.1006/meth.1998.0585
- [48] Jalily Hasani H et al. Effects of protein-protein interactions and ligand binding on the ion permeation in KCNQ1 potassium channel. *PLoS One*. 2018;**13**(2):e0191905. DOI: 10.1371/journal.pone.0191905
- [49] Ahmed M et al. Modeling the human Nav1.5 sodium channel: Structural and mechanistic insights of ion permeation and drug blockade. *Drug Design, Development and Therapy*. 2017;**11**:2301-2324. DOI: 10.2147/DDDT.S133944
- [50] Bahring R, Covarrubias M. Mechanisms of closed-state inactivation in voltage-gated ion channels. *The Journal of Physiology*. 2011;**589**(Pt 3):461-479. DOI: 10.1113/jphysiol.2010.191965
- [51] Di Virgilio F et al. Voltage-dependent activation and inactivation of calcium channels in PC12 cells. Correlation with neurotransmitter release. *The Journal of Biological Chemistry*. 1987;**262**(19):9189-9195
- [52] Tuluc P et al. A CaV1.1 Ca<sup>2+</sup> channel splice variant with high conductance and voltage-sensitivity alters EC coupling in developing skeletal muscle. *Biophysical Journal*. 2009;**96**(1):35-44. DOI: 10.1016/j.bpj.2008.09.027
- [53] Lipscombe D, Helton TD, Xu W. L-type calcium channels: The low down. *Journal of Neurophysiology*. 2004;**92**(5):2633-2641. DOI: 10.1152/jn.00486.2004
- [54] Saad M et al. Ranolazine in cardiac arrhythmia. *Clinical Cardiology*. 2016;**39**(3):170-178. DOI: 10.1002/clc.22476
- [55] Grant AO. Cardiac ion channels. *Circulation. Arrhythmia and Electrophysiology*. 2009;**2**(2):185-194. DOI: 10.1161/CIRCEP.108.789081
- [56] Xu WF, Lipscombe D. Neuronal Ca(v)1.3 alpha(1) L-type channels activate at relatively hyperpolarized membrane potentials and are incompletely inhibited by dihydropyridines. *Journal of Neuroscience*. 2001;**21**(16):5944-5951
- [57] Findeisen F et al. Stapled voltage-gated calcium channel (CaV) alpha-interaction domain (AID) peptides act as selective protein-protein interaction inhibitors of CaV function. *ACS Chemical Neuroscience*. 2017;**8**(6):1313-1326. DOI: 10.1021/acchemneuro.6b00454
- [58] Pitt GS. Calmodulin and CaMKII as molecular switches for cardiac ion channels. *Cardiovascular Research*. 2007;**73**(4):641-647. DOI: 10.1016/j.cardiores.2006.10.019
- [59] Abiria SA, Colbran RJ. CaMKII associates with CaV1.2 L-type calcium channels via selected beta subunits to enhance regulatory phosphorylation. *Journal of Neurochemistry*. 2010;**112**(1):150-161. DOI: 10.1111/j.1471-4159.2009.06436.x

- [60] Kim EY et al. Structures of CaV2 Ca<sup>2+</sup>/CaM-IQ domain complexes reveal binding modes that underlie calcium-dependent inactivation and facilitation. *Structure*. 2008;**16**(10): 1455-1467. DOI: 10.1016/j.str.2008.07.010
- [61] Mori MX et al. Crystal structure of the CaV2 IQ domain in complex with Ca<sup>2+</sup>/calmodulin: High-resolution mechanistic implications for channel regulation by Ca<sup>2+</sup>. *Structure*. 2008;**16**(4):607-620. DOI: 10.1016/j.str.2008.01.011
- [62] Ferreira G et al. Ion-dependent inactivation of barium current through L-type calcium channels. *Journal of General Physiology*. 1997;**109**(4):449-461. DOI: 10.1085/jgp.109.4.449
- [63] Bidaud I et al. Voltage-gated calcium channels in genetic diseases. *Biochimica et Biophysica Acta*. 2006;**1763**(11):1169-1174. DOI: 10.1016/j.bbamcr.2006.08.049
- [64] Berger SM, Bartsch D. The role of L-type voltage-gated calcium channels Cav1.2 and Cav1.3 in normal and pathological brain function. *Cell and Tissue Research*. 2014;**357**(2): 463-476. DOI: 10.1007/s00441-014-1936-3
- [65] Ortner NJ, Striessnig J. L-type calcium channels as drug targets in CNS disorders. *Channels (Austin, Tex.)*. 2016;**10**(1):7-13. DOI: 10.1080/19336950.2015.1048936
- [66] Striessnig J, Ortner NJ, Pinggera A. Pharmacology of L-type calcium channels: Novel drugs for old targets? *Current Molecular Pharmacology*. 2015;**8**(2):110-122
- [67] Giudicessi JR, Ackerman MJ. Calcium revisited: New insights into the molecular basis of long-QT syndrome. *Circulation. Arrhythmia and Electrophysiology*. 2016;**9**(7):e002480. DOI: 10.1161/CIRCEP.116.002480
- [68] Hockerman GH et al. Molecular determinants of drug binding and action on L-type calcium channels. *Annual Review of Pharmacology and Toxicology*. 1997;**37**:361-396. DOI: 10.1146/annurev.pharmtox.37.1.361
- [69] Striessnig J et al. Structural basis of drug binding to L Ca<sup>2+</sup> channels. *Trends in Pharmacological Sciences*. 1998;**19**(3):108-115
- [70] Offord J, Isom LL. Drugging the undruggable: Gabapentin, pregabalin and the calcium channel alpha2delta subunit. *Critical Reviews in Biochemistry and Molecular Biology*. 2015;**51**(4):246-256. DOI: 10.3109/10409238.2016.1173010
- [71] Dolphin AC. Calcium channel auxiliary alpha2delta and beta subunits: Trafficking and one step beyond. *Nature Reviews. Neuroscience*. 2012;**13**(8):542-555. DOI: 10.1038/nrn3311
- [72] Opatowsky Y et al. Structural analysis of the voltage-dependent calcium channel beta subunit functional core and its complex with the alpha 1 interaction domain. *Neuron*. 2004;**42**(3):387-399. DOI: 10.1016/S0896-6273(04)00250-8



---

# Transient Receptor Potential (TRP)

---



---

# TRP Ion Channels: From Distribution to Assembly

---

Wei Cheng

Additional information is available at the end of the chapter

<http://dx.doi.org/10.5772/intechopen.76479>

---

## Abstract

Transient receptor potential (TRP) ion channel superfamily is widely distributed from neuronal to non-neuronal tissues by serving as cellular sensors via interacting with a wide spectrum of physical and chemical stimuli. TRP ion channels are tetrameric protein complexes. Accordingly, TRP subunits can form functional both homomeric channels and heteromeric channels which either in the same subfamily or in the different subfamilies to diversify TRP channel functions. In this chapter, we will briefly introduce this fascinating ion channel superfamily. Further, we will summarize current knowledge on mammalian TRP ion channels distribution in tissues and organs as well as assembly of these ion channel subunits. Implications and related physiological roles regarding distribution and assembly will be overviewed as well.

**Keywords:** assembly, expression, interaction, ion channel, tetramer, TRP

---

## 1. Introduction

Mammalian TRP ion channel superfamily comprises 28 members, which belong to 6 subfamilies including TRPC (TRPC1-7), TRPV (TRPV1-6), TRPM (TRPM1-8), TRPML (TRPML1-3), TRPA (TRPA1) and TRPP (TRPP2, TRPP3 and TRPP5). Most of the TRPs are non-selective cationic ion channels, which permeate to  $\text{Ca}^{2+}$ ,  $\text{Mg}^{2+}$  and  $\text{Na}^{+}$  cations, and involve in a plethora of physiological and pathological functions.

Despite as low abundant membrane proteins, TRP ion channels are widely distributed in tissues and organs in mammals. TRPs can be activated by diverse physical or chemical stimuli in nature which make these ion channels as multifunctional cellular sensors [1].

TRP ion channels are tetrameric cation channels. Structurally, each TRP subunit harbors six transmembrane segments with a pore-forming region. Both N and C termini are located intracellularly. Most of the TRPs have an ankyrin repeat domain in N terminal and a TRP box in C terminal by modulation of protein-protein interactions that allowing intra- and inter-cellular associations. The long N and C termini of TRPs also contain several additional regulatory regions, which are relatively conserved in most of the TRP channels.

## 2. Distribution and function of TRP channels in tissues and organs

### 2.1. TRPs in nervous system

#### 2.1.1. Distribution patterns

TRP ion channels are widely distributed in nervous system harboring members among subfamilies of TRPC, TRPV, TRPM, TRPA and TRPML. These TRPs can be detected both within central and peripheral nervous system. Briefly, TRPCs are extensively distributed in various parts of mammalian brain and DRG neurons. Specifically, TRPC1 is characterized distributed in mammalian brain, including human fetal and adult brain, rat brain as well as rat embryonic brain [2].

For TRPVs, all members of this subfamily are expressed in central nervous system. TRPV1 has been detected in mammalian brain, especially one study revealed that TRPV1 exhibited highly restricted distribution in central neuronal system in rat, monkey and human by using in situ hybridization as well as electrophysiological recordings [3]. Recent studies reported that TRPV5 was detected in olfactory bulb, cortex, hippocampus, hypothalamus, midbrain, brainstem and cerebellum of the rat [4]. In addition, TRPV6 was found in lamina terminalis, olfactory bulb, amygdala, hippocampus, brainstem and cerebellum of the mouse [5].

Among TRPM subfamily, TRPM1 and TRPM2 are widely expressed in mammalian brain. Moreover, other members of this TRPM subfamily, including TRPM3, TRPM4, TRPM5, TRPM7 and TRPM8, were all identified expressed in rat, mouse and human brain [6].

Further, TRPA1 was extensively found in mammalian sensory ganglia, trigeminal sensory afferents and spinal dorsal horn, even in astrocytes [6, 7]. TRPV4 and TRPA1 were detected in pancreatic nerve fibers and in dorsal root ganglia neurons innervating the pancreas, which may contribute to inflammatory pain in mice [8].

The three members of TRPML are all expressed in mouse brain [9].

#### 2.1.2. Specific molecular sensors

Based on the distribution pattern of TRP ion channels in nervous system, their multi-functions as cellular sensors are consistent with the complexity of nervous network. Specifically, TRPV1, TRPV2, TRPV3, TRPV4 and TRPM2, TRPM3, TRPM4, TRPM5 are characterized as

heat and warm sensors of body so far, while TRPC5, TRPM8 and TRPA1 are responsible for cold or cool sensing [10]. Meanwhile, continuous studies revealed that TRPM1, TRPM4, TRPC1, TRPC3, TRPC5 and TRPC6 may involve in auditory mechanosensation [11–13]. TRP ion channels serving as cellular sensors are also involved in taste via TRPM5, pain by TRPV1, TRPV2 and TRPA1 [14]. In addition, most TRP ion channels may involve in olfactory transduction by widely distributed in olfactory bulb [15].

## 2.2. TRPs in skeletal system and implications

### 2.2.1. Distribution patterns

In general, skeletal system consists of bone, joint and skeletal muscles. Recent studies have been elucidated that several members of TRPCs, TRPVs and TRPMs are distributed in these organs and tissues. Specifically, TRPC1 and TRPC4 have been detected in bone and skeletal muscles [16, 17].

Further, TRPV2 was detected in osteoclasts in bone [18]. TRPV4 has been found in mandibular condylar chondrocytes, osteoclasts and osteoblasts of the rat [19, 20]. TRPV5 appeared in the ruffled border membrane of the mouse osteoclasts, and TRPV6 was observed widely expressed in bone cells but was not crucial for bone mineralization in mice [21].

Moreover, human TRPM7 has been found in bone, and recent study revealed that TRPM7 regulated  $Mg^{2+}$  ions to promote the osteoinduction of human osteoblast via PI3K pathway [22].

### 2.2.2. Roles and implications

The distribution of functional TRP ion channels in skeletal system interrelate both calcium ions and cytosolic calcium sensing elements closely. Studies indicate that distribution of TRPC1 and TRPC4 in bone and skeletal muscles may involve in regulating cell differentiation and osteoclast formation via modulating calcium homeostasis [16, 17], and TRPV2 can regulate osteoclastogenesis via calcium oscillations [18]. The study indicates that TRPV4 plays a role in regulating bone mass as well as mastication-associated pain at the temporomandibular joint [19, 20]. Despite studies identified that TRPV4 mutations can lead to osteoarticular pathology, the mechanism underlying TRPV4 modulation remains unclear.

## 2.3. TRPs in digestive system

### 2.3.1. Distribution patterns

To date, accumulated documentations indicate that members within four subfamilies (including TRPC, TRPV, TRPM and TRPML) of TRPs appear in digestive system. TRPC1, TRPC2, TRPC3, TRPC4, TRPC5, TRPC6 and TRPC7 are widely distributed in the stomach of mouse. TRPC1 has been detected in liver by using specific antibody [23]. For TRPC4, widely distributed in stomach, intestine and pancreas and low level in liver of human have been observed [24]. Also TRPC4 and TRPC5 have been detected in murine jejunum and colon [25]. TRPC6

has been found to distribute in smooth muscle of stomach, colon and esophagus [25, 26]. However, the roles of TRPCs within these tissues and organs are incompletely understood.

For TRPV subfamily, TRPV1, TRPV2, TRPV3 and TRPV4 are all expressed in the larynx epithelium of mice [27]. TRPV3 is found in nose, stomach, colon and small intestine in mice, especially in the epithelium of the tongue and nose. TRPV4 is expressed in stomach, small intestine and colon [28]. Other studies also revealed that TRPV4 was distributed in bile duct [29]. The murine and human TRPV6 was distributed in pancreas and gastrointestinal tract, including esophagus, stomach, duodenum, jejunum and colon [30].

Among TRPM subfamily, TRPM2 is widely expressed in several digestive organs, including stomach, intestine and low level in liver [31]. TRPM5 is found in pancreas as well as in sparse chemosensory cells located throughout the digestive track. Within the gastrointestinal system, TRPM5 was detected in the stomach, small intestine and colon, and it may regulate several physiological functions of the gastrointestinal tract. TRPM6 transcripts are detected in the intestine and colon. Furthermore, TRPM8 has been found expressed in liver [28].

The TRPMLs are all expressed in digestive system including stomach, colon, small intestine, liver and pancreas. However, the physiological roles of these distributions are still missing.

### 2.3.2. Roles and implications

Distributions of TRPs throughout the alimentary canal are relevant to digestive and absorptive function of mediating the whole body homeostasis of metabolism. It seems that TRPV5 and TRPV6 are involved in mediating intestinal calcium uptake and TRPM5 is involved in regulation of glucose stimulated insulin secretion [28]. TRPM2 participates in pathogenesis of bowel disease and salivary gland fluid secretion [32].

## 2.4. TRPs in immune system and their physiological relevance

### 2.4.1. Distribution patterns

In immune system, recent studies indicate broad distribution of TRPs in this system, including TRPC, TRPV, TRPM and TRPML subfamilies. Mammalian TRPC2 transcripts were detected in spleen and rat thyroid cells [33, 34]. Employing immune cells, physiological roles either of TRPC3 channels or TRPC3/6 heteromeric channel were identified to involve in  $Ca^{2+}$  signaling mechanism [35, 36]. TRPC6 was also identified in other immune cells of the lungs like alveolar macrophages [37]. Most interestingly, ovalbumin-challenged *Trpc6* knockout mice exhibited reduced allergic responses in the bronchoalveolar lavage [38]. However, the precise functional roles of TRPCs in these cells are still elusive.

For TRPVs, TRPV2 is abundantly expressed in the cells of the immune system. Study indicates that mRNA of TRPV2 was strongly expressed in the spleen [39]. TRPV2 was detected in macrophages and Kupffer cells [40]. In addition, TRPV2 was observed in mast cells [41], neutrophils [42], hematopoietic stem cells as well as both T with CD4+ and CD8+ and B with CD19+ lymphocytes. In hematopoietic stem cells, TRPV2 was observed with CD34+ [43]. TRPV4 has been detected in mast cells [44] and endolymphatic sac [45]. Meanwhile, both TRPV5 and

TRPV6 were found in lymphocytes, Jurkat leukemia T cells [46] and leukemia K562 cells [47] and may contribute to store-operated calcium entry.

Most of the TRPMs, including TRPM2, TRPM4, TRPM5, TRPM6 and TRPM7, are all expressed in the bone marrow and spleen. Specifically, TRPM2 appears in immune cells (including neutrophils, megakaryocytes, monocytes, macrophages, B lymphoblast cells, T lymphocytes, dendritic cells and mast cells). TRPM4 and TRPM6 are detected in mast cells and leukocytes, respectively [48, 49]. However, the physiological roles remain unclear.

For TRPMLs, they are all distributed in spleen and thymus of mouse. TRPML2 mRNA was detected in B cells, T cells, mastocytoma, myeloma cell lines and primary splenocytes by RT-PCR technique [50].

#### 2.4.2. Roles and implications

Although TRPC1 has not been detected in immune system yet, but *Trpc1* deletion could reduce T helper type 2 (Th2) cells to stimuli in vivo. In vitro, proliferation and receptor-induced IL-2 production are significantly attenuated in *Trpc1* knockout splenocytes. Thus, TRPC1 may be involved in proinflammation and could be therapeutic target in immune diseases [51]. Since TRPV2 is expressed in various types of cells in immune system, it may be involved in both innate and adaptive immune responses. Moreover, TRPM2 may act as a mediator for inflammation via stimulus-induced  $\text{Ca}^{2+}$  influx in immune system, and TRPM4 in T cells may be relevant to immune response for interleukin-2 production [52].

### 2.5. TRPs in reproductive system

#### 2.5.1. Distribution patterns

Based on accumulated studies so far, there are five subfamilies of TRPs distributed in the reproductive system, including TRPC, TRPV, TRPM, TRPML and TRPP. It seems that TRPCs extensively appear in reproductive system including prostate, placenta, testis, ovary, uterus, myometrium and sperm [53, 54]. Specifically, TRPC1, TRPC2 and TRPC7 are distributed in testis and sperm. TRPC3 and TRPC5 are expressed in ovary, uterus, sperm and testis. Moreover, TRPC4, TRPC7 are found in myometrium. In addition, TRPC4 is widely observed in human prostate, placenta, rat testis, ovary, human and mouse sperm. And TRPC6 is found in ovary, uterus, placenta and sperm.

All TRPVs are expressed in prostate. Specifically, TRPV1 appears in testis and prostate and TRPV2 shows in prostate. For TRPV3, it is observed in rat prostate, human placenta and testis. TRPV4 is expressed in sperm and prostate. Furthermore, TRPV5 and TRPV6 are expressed in human placenta, sperm, prostate and the epididymis. Meanwhile, TRPV4 was also detected broadly distributed in female reproductive tract [55] and oviduct [56], and these TRPV channels may function as a link between  $\text{Ca}^{2+}$  transport and  $\text{Ca}^{2+}$  signaling.

For TRPMs, all members seem to appear in prostate, testis, placenta and sperm. TRPM2 is expressed in placenta endometrium, sperm and prostate. TRPM3 is distributed in ovary, testis, sperm and prostate [57]. TRPM6 is highly expressed in testis and prostate. Moreover,

humans have strong TRPM7 expression in testis, prostate and placenta. The TRPM8 transcript was originally identified in the testis and prostate tissue [58]. In addition, TRPM8 is also expressed in human sperm.

TRPMLs are all expressed in human testis and uterus. TRPML1 is also observed in human placenta and the role is still unknown.

For TRPP subfamily, TRPP2 (*PKD2*) and TRPP3 (*PKD2L1*) transcripts were both found in many fetal and adult tissues, testis and ovary [59]. In contrast, TRPP5 (*PKD2L2*) transcription appears to be mostly restricted to the testis.

### 2.5.2. Roles and implications

Little is known about the roles of TRPs in reproductive system. Studies imply that TRPC2 may modulate pheromone sensory signaling transduction and TRPM8 can be a biomarker for prostate cancer.

## 2.6. TRPs in cardiovascular system

### 2.6.1. Distribution patterns

Studies have identified that five subfamilies (TRPC, TRPV, TRPM, TRPML and TRPP) of TRPs are distributed in cardiovascular system, especially in cardiomyocytes, smooth cells and endothelium cells, and these TRP ion channels may involve in hypertension as well as cardiac hypertrophy. Briefly, TRPC1, TRPC3, TRPC4, TRPC5, TRPC6 and TRPC7 are all expressed in heart of both human and mouse. Specifically, TRPC2 expression on the plasma membrane has been found in murine erythroblasts and heart [24, 60]. TRPC4, TRPC5 and TRPC7 have been observed in endothelial cells of coronary arteries [61]. The roles of these distributions are still unclear.

For TRPVs, TRPV2, TRPV4 and TRPV6 are observed in mouse heart. Specifically, TRPV1 has been found expressed in arteriolar smooth muscle [3]. TRPV2 was detected in cardiovascular system, including arterial smooth muscle cells, venous smooth muscle cells, endothelial cells and cardiomyocytes [62]. Moreover, TRPV4 was observed broadly expressed in heart as well as arteries [55].

TRPM2, TRPM3, TRPM4, TRPM6 and TRPM7 are all distributed in mouse heart. Meanwhile, all the subfamily members except TRPM8 appear in human heart. TRPM3 has been observed to express in saphenous vein, pulmonary artery, coronary artery, mesenteric artery, and femoral artery. TRPM4 was described in cardiac myocytes, vascular smooth muscle cells, vascular endothelial cells and red blood cells [62]. Furthermore, expression of TRPM8 has been reported in rat myocytes isolated from large arteries [63].

All TRPMLs are expressed in mouse heart and no relevant roles have been proved.

Both TRPP2 (*PKD2*) and TRPP3 (*PKD2L1*) are distributed in heart and the related physiological functions are still in the air to date.



### 2.6.2. Roles and implications

The study shows that TRPC4 and TRPC5 may regulate endothelial permeability and agonist-dependent vasorelaxation and TRPV1 could control blood flow in skeletal muscle. Moreover, TRPV2 may act as a stretch sensor and TRPM8 may involve in the regulation of vascular tone.

## 2.7. TRPs in urinary system

### 2.7.1. Distribution patterns

There are five subfamilies of TRPs appear to express in urinary system, including TRPCs, TRPVs, TRPMs, TRPMLs and TRPPs. Specifically, TRPC1, TRPC2, TRPC3, TRPC4, TRPC5, TRPC6 and TRPC7 are all expressed in kidney. Moreover, TRPC4 was found in renal epithelial cells, preglomerular resistance vessels, bladder and urothelium [64], and the specific roles are still lacking.

For TRPVs, TRPV2, TRPV4, TRPV5 and TRPV6 are all observed in mouse kidney. TRPV1, TRPV2, TRPV3 and TRPV4 were detected in bladder epithelial cells [64]. Furthermore, TRPV4 is described broadly expressed in urinary bladder and kidney [55].

Human TRPM2, TRPM3, TRPM4, TRPM5, TRPM6 and TRPM7 are all expressed in kidney, while TRPM3, TRPM4, TRPM6 and TRPM7 are found in kidney of mouse. Specifically, TRPM4 was detected in mammalian renal tubule [65], and TRPM8 has been characterized in the bladder urothelium and male urogenital tract [66].

The TRPMLs are all distributed in mouse kidney and the relevant roles are still lacking.

Both TRPP2 (*PKD2*) and TRPP3 (*PKD2L1*) are expressed in kidney and relevant roles remain unclear.

### 2.7.2. Roles and implications

The roles of TRPs in urinary system remain to be elucidated. TRPV1 channel was proposed to regulate bladder contractions by mediating urothelial ATP release in response to stretch [67]. TRPV2 and TRPV4 may be involved in sensing mechanical stimuli and TRPMLs could be related to urinary dysfunctions.

## 2.8. TRPs in respiratory system

### 2.8.1. Distribution patterns

Recent documented studies indicate that subfamilies for TRPC, TRPV, TRPM, TRPA, TRPML and TRPP are all distributed in respiratory system, especially in lung and other respiratory organs. Specifically, the expressions of TRPC3, TRPC6 and TRPC7 are observed in the lung of human and mouse.

For TRPVs, TRPV1, TRPV2, TRPV3 and TRPV4 are expressed in mouse respiratory epithelium. TRPV2, TRPV4 and TRPV6 are detected in lung. Specifically, TRPV1 and TRPV4 were observed in trachea and bronchi [68–70].

TRPM2, TRPM4, TRPM6 and TRPM7 are widely expressed in lung. TRPM8 with altered N-terminus has been found in human bronchial epithelial cells which localized in the endoplasmic reticulum [71].

TRPA1 was found presented in non-neuronal tissues, including human and mouse lung [72].

TRPML1, TRPML2 and TRPML3 are all distributed in the lung of mouse. While the functions related to these distribution are still lacking.

TRPP2 (*PKD2*) and TRPP3 (*PKD2L1*) are expressed in lung and the functional roles remain to be elucidated.

### *2.8.2. Roles and implications*

The functional roles of TRPs in respiratory system need more efforts. Studies indicate that TRPC3, TRPC6 and TRPC7 may enhance respiratory rhythm regularity and TRPV1 and TRPV4 may facilitate receptor-operated calcium entry.

## **2.9. TRPs in endocrine system**

### *2.9.1. Distribution patterns*

Since lacking investigation employed for TRP ion channels in endocrine system, only several references for TRPs can be provided in this chapter. The expression of TRPC3 mRNA has been detected in pituitary gland [24] and the relevant roles are still unclear.

For TRPV subfamily, TRPV2 is abundantly expressed in the epithelium of the pancreatic duct, mammary gland, parotid gland and submandibular gland. Meanwhile, TRPV2 has also been detected in chromogranin-positive neuroendocrine cells in the stomach, duodenum and intestine [73]. In the pancreas, TRPV2 was found expressed in insulin-produced  $\beta$ -cells [74]. TRPV4 has been found in the mammary gland [75].

For TRPM subfamily, TRPM2 appears in pancreatic  $\beta$ -cells of endocrine system, and the channel involves in glucose-induced insulin release and cell apoptosis triggered by application of  $H_2O_2$  [76, 77]. TRPM4 was detected to express in white and brown adipocytes [78, 79] and the roles are still missing. Recent studies reported that TRPM8 and TRPV1 are expressed in brown adipose tissues [80, 81].

### *2.9.2. Roles and implications*

TRPs in endocrine system may be involved in sensing stimulus from cellular milieu of physical or chemical resources. Recent study shows that TRPV1 participated in the modulation of clock gene oscillations in response to light-dark cycle. Meanwhile, cold-sensing TRPM8 channel involves in the regulation of clock and clock-controlled genes and thermogenesis in brown adipose tissues [80, 81].

### 3. Assembly of TRP channels and its implications

TRP ion channels have been found heterogeneity in native tissues and organs due to channel subunits heteromerization. Meanwhile, wide assembly of TRP ion channel subunits of either the same subfamily or different subfamilies has been detected in heterologous expression system.

#### 3.1. Heteromerization of TRPs with specificity

Recent investigations indicate that subunits extensively heteromultimerize in the TRPC subfamily. Accordingly, the overlapped distribution patterns of TRPC proteins in the hippocampus and peripheral tissues are also coincident with the heteromerization. Specifically, formation of heteromeric complexes by both TRPC5 and another member of the same subfamily, TRPC4, with the TRPC1 subunit (TRPC1/5 and TRPC1/4) has been identified in mammalian cells. Using quantitative high-resolution mass spectrometry, TRPC1, TRPC4 and TRPC5 were demonstrated to assemble into heteromultimers with each other in the mouse brain and hippocampus [82]. In HEK293 cells, cotransfection of TRPC1 and TRPC4 yielded novel nonselective cationic channels. Heteromeric TRPC1/4 channel showed dynamic gating property depending on TRPC1 isoform subtypes and receptor stimulation system. [83]. Using GST pull-down assays, heteromerization of TRPC1 with TRPC3 was examined and the ankyrin repeats (AR) region of TRPC3 could mediate the heteromeric TRPC1/3 formation. Furthermore, the heteromeric TRPC1/3 may participate in regulating the resting cytosolic  $Ca^{2+}$  levels in skeletal muscle [84]. Coassembly of TRPC1 and TRPC5 in hippocampal neurons and in HEK293 cells resulted in a novel nonselective cation channel with a voltage dependence similar to NMDA receptor channels. Similar associations were reported between TRPC1 and TRPC3 via an N-termini domain interaction in salivary gland cells. In addition, heteromerization of TRPC3 and TRPC4 seems to produce channels with a distinct pore structure clearly different from those of the homomeric TRPC3 and TRPC4 channels. Moreover, study also revealed that TRPC1/3/7 can interact to form a store-operated channel complex [85].

For TRPV subfamily, using fluorescence resonance energy transfer (FRET) as well as single-channel recording, widespread interaction between any two members of TRPV1–4 has been identified [86]. This study provided evidence that thermosensitive TRPV channel subunits can form heteromeric channels with intermediate conductance levels and gating kinetic properties compared to homomeric channels. Moreover, colocalization and association between TRPV1 and TRPV2, TRPV1 and TRPV3 as well as TRPV5 and TRPV6 can form heteromeric channel complexes. Recent study identified that TRPV4 could facilitate with TRPV1 in some sensory neurons [87].

Heteromerization of TRPM subunits remains far less clear. Association between TRPM6 and TRPM7 formed heteromeric channels with intermediate conductance and gating properties. Recent study uncovered heteromeric TRPM6/7 channels with altered pharmacology and sensitivity to intracellular Mg-ATP compared with homomeric TRPM7. Furthermore, TRPM6 kinase domain modulated heteromeric channel sensitivity of intracellular Mg-ATP concentrations [88].

The mucolipin TRPML family exhibited low similarity to other TRPs. Montell and coworkers demonstrated that TRPMLs can assemble to form heteromultimers with intermediate

conductance and kinetic properties. Moreover, the presence of either TRPML1 or TRPML2 specifically modulates TRPML3 trafficking from endoplasmic reticulum to lysosomes [85].

### 3.2. Assembly of TRPs in different subfamilies

Extensive studies revealed widespread heteromerization within the mammalian TRP channel superfamily. Heteromeric TRPP2/TRPC1 channel complexes with a stoichiometry of 2:2 exhibited a new receptor-operated channel property. TRPP2 selectively assembled with TRPC1 and TRPC4 to form channel complexes mediating angiotensin II-induced  $\text{Ca}^{2+}$  responses in mesangial cells. Heteromeric cation channels composed of the TRPP2 mutant and the TRPC3 or TRPC7 protein enhanced receptor-activated  $\text{Ca}^{2+}$  influx that may lead to dysregulated cell growth in autosomal dominant polycystic kidney disease. Using coimmunoprecipitation, the composition of TRPP2/TRPC5, TRPP3/TRPC1, TRPP3/TRPC5, TRPP5/TRPC1 and TRPP5/TRPC5 was also identified. TRPP2 and TRPV4, which formed heteromeric channel complex, have been reported both *in vivo* and *in vitro*. Then, heteromeric TRPP2/TRPV4 complex with a 2:2 stoichiometry and alternating subunit arrangement was identified using atomic force microscopy approach [85]. The study indicates that TRPV4 could form heteromeric channels with TRPC1 in vascular endothelial cells. Then,  $\text{Ca}^{2+}$  store depletion enhanced the trafficking of TRPV4/TRPC1 channels into the plasma membrane, thus contributed to mediate store-operated current and store-operated calcium ion entry [89]. TRPV4 can form a heteromeric channel with TRPC6 in the pulmonary artery smooth muscle cell, and TRPV4 plays a critical role in hypoxic pulmonary vasoconstriction potentially via cooperation with TRPC6 [90]. TRPV6 exhibited substantial colocalization and *in vivo* interaction with TRPC1, and functional interaction of TRPV6 with TRPC1 negatively regulates  $\text{Ca}^{2+}$  influx in HEK293 cells [91]. Heteromeric TRPV5 and TRPML3 channels with novel conductance were detected under conditions that did not activate either TRPML3 or TRPV5 [92].

Moreover, novel combination of TRPC1/TRPC6/TRPV4 may mediate mechanical hyperalgesia and primary afferent nociceptor sensitization. Subsequently, TRPV4, TRPC1 and TRPP2 have been reported to form a flow-sensitive heteromeric channel in primary cultured rat mesenteric artery endothelial cells as well as HEK293 cells. Moreover, heteromeric TRPV4/TRPC1/TRPP2 channel can mediate the flow-induced  $\text{Ca}^{2+}$  increase in native vascular endothelial cells [93].

### 3.3. Assembly between TRPP channels and receptor-like polycystin-1 family proteins

PKD1 and PKD2 have been identified as the genes mutated in autosomal dominant polycystic kidney disease (ADPKD). The TRPP ion channel subfamily (PKD2-like group) contains three members of TRPP2 (PKD2), TRPP3 (PKD2L1) and TRPP5 (PKD2L2). The receptor like polycystin-1 family proteins (PKD1-like group) contains five members, including PKD1, PKDREJ, PKD1L1, PKD1L2 and PKD1L3. TRPP subunits not only assemble into functional homomeric ion channels but also assemble with polycystin-1 family members to form heteromeric receptor-channel complexes.

Heteromeric interaction between TRPP2 and PKD1 has been identified by several groups throughout the past decade. TRPP3 can also interact with PKD1, and the interaction is essential for TRPP3 trafficking and channel formation. Along these lines, studies also showed that TRPP3

and PKD1L3 colocalized in taste receptor cells. Heteromeric complex with three TRPP3 and one PKD1L3 functions as an acid sensor. Single amino acid mutations in the putative pore region of both proteins alter ion selectivity of the channel. A TRPP3 C-terminal coiled-coil domain forms a trimer in regulating assembly and surface expression of the TRPP3/PKD1L3 complex [94]. Moreover, heteromeric TRPP3/PKD1L3 channel complex in mice and humans regulated translocation and expression of hedgehog pathway proteins through modulation of ciliary calcium concentration [95]. Recent study found that extracellular loops between the first and second transmembrane segments of TRPP2 and TRPP3 associated with the extracellular loops between the sixth and seventh transmembrane segments of PKD1 and PKD1L3, respectively, and the associations between these loops are essential for the trafficking and function of the complexes [96].

### 3.4. Implications of assembly of TRPs

It is clear that coassembly of ion channel subunits yields a variety of diverse channel complexes. Heteromultimerization among mammalian TRP subunits produces novel channel types with functional properties distinct from their homomeric counterparts. Heteromerization of mammalian TRPV1/3, TRPV5/6, TRPML1/2, TRPC1/3, TRPC1/4, TRPC1/5, TRPC3/4, TRPC4/5, TRPV5 and TRPML3 has been identified to produce channels with novel or altered properties.

Meanwhile, TRPP2 coassembled with TRPC1 to form heteromultimeric channels that exhibit new receptor-operated property implicated in mechanosensation. Furthermore, association between TRPP2 and TRPV4 produces a channel with mechanosensitive and thermosensitive roles. Recent study indicates that heteromultimers of TRPC1/4, TRPC1/5 and TRPC4/5 in the mouse brain and hippocampus involved in regulation of spatial working memory and flexible relearning by facilitating proper synaptic transmission [82]. TRPC1 and TRPC6 with TRPV4 are frequently coexpressed in DRG neurons; TRPC1 and TRPC6 subunits are incorporated with TRPV4 to mediate mechanical hyperalgesia and primary afferent nociceptor sensitization. Interestingly, TRPV4 is required for itch signaling in some sensory neurons via facilitation of TRPV1. The formation of heteromeric complexes could be a prevalent mechanism by which the vast array of somatosensory information is encoded in sensory neurons [87]. In addition, functional interaction between the noxious cold-sensitive TRPA1 channel subunit and the noxious heat-sensitive TRPV1 channel subunit could contribute to TRPA1-mediated responses in trigeminal sensory neurons. Moreover, colocalization of PKD1L3 with TRPP3 (PKD2L1) in taste receptor cells may involve in taste sensory transduction. In summary, heteromerization of TRPs to novel channel complexes extends TRP channel distribution and function.

## 4. Discussion

### 4.1. More distribution relevance of TRPs need to be fully elucidated

TRP ion channels are almost expressed in all types of mammalian cells and their functions are also diverse as their distributions in tissues and organs. TRP channels not only act as polymodal cellular sensors, which are involved in cellular sensing from somatosensation, hearing, taste and olfaction [14], but also participate in many other physiological and pathological

process from metabolism, homeostasis and even carcinogenesis. To date, the puzzle of relevant roles regarding TRP distribution in tissues and organs remains incompletely understood.

Specifically, the functions of TRPCs in mammalian are involved in temperature perception, mechanosensation, proinflammation, pheromone modulation, vasorelaxation as well as respiratory rhythm regulation. Furthermore, they also regulate cell differentiation and bone mass via calcium involving. However, the distribution relevance of TRPs in digestive as well as urinary system needs more and deeper investigation.

For TRPVs, the distribution relevance is mostly related to somatosensation such as thermosensation, mechanosensation and nociception [1]. Meanwhile, TRPVs distribution also acts as sensory channels for receptor-operated calcium entry. But the related roles in immune system, urinary system as well as respiratory system remain elusive.

The subfamily of TRPM is extensively distributed in nervous system, skeletal system, digestive system, immune system, reproductive system, cardiovascular system, urinary system, respiratory system and endocrine system. Their functions are involved in warm or cold perception as well as thermogenesis, auditory mechanoreception, taste, metabolism, vascular tone regulation and inflammation. In addition, TRPM8 can be a biomarker for carcinogenesis of prostate. Further investigations regarding functional relevance of TRPMs' distributions need to be deeply elucidated, in particular in urinary system as well as respiratory system.

TRPA1 is mostly expressed in nervous system. Its functions involve in thermosensation, auditory mechanosensation as well as olfactory transduction. Meanwhile, TRPMLs are expressed in brain, heart, kidney and lung. Moreover, they appear in digestive system, immune system and reproductive system. But the relevance of the distribution is still missing. Little is known about the related roles of TRPPs in reproductive system, cardiovascular system, urinary system and respiratory system.

Despite TRPs have been explored extensively for almost half of century, our understanding of the implications related to TRPs distribution is still missing a lot of pieces. Further investigation regarding this relevance needs to be elusive urgently.

#### **4.2. Heteromerizations tangle the elucidation for distributions and functions**

The intracellular distributions of TRP ion channels may be dynamically regulated by cytosolic changes. However, little is known about whether and how TRP channels change subunit composition in response to environmental stimuli. So far, most published studies focused on the static TRP ion channels subunit composition. How does the cell determine how and when subunits are coassembled? To what extent does extra or intracellular milieu affect the molecular sensitivity of the neuron? In fact, the coassembly of TRP ion channel subunits in living cells is dynamically regulated. Studies indeed sustain that the distribution of TRP ion channel in cells changes dramatically upon stimulation [97, 98]. Thus, when we study the distribution and function of TRPs, the dimension for dynamic influences has to be considered.

Furthermore, the extensive studies focus on TRP ion channels heteromerization, while much remains to be elucidated about the physiological consequences of heteromultimerization

among TRP subunits. Practical approach and advanced technique to monitor assembly of dynamic TRP ion channel subunits should be explored. Moreover, distribution of heteromeric TRP complexes involving in physiological and pathophysiological processes calls for more solid and careful investigations.

## 5. Conclusions and outlook

In this chapter, we described our understanding in distribution and assembly of TRP ion channels based on recent references. Haboring a superfamily of ion channels protein, TRPs exhibit ubiquitously distributions in mammals which depict a diverse and fascinating network. This makes the investigation more painstaking for grasp both the correct expression pattern and the roles of these TRPs. With recent technological advances of gene sequencing combines high throughput screening, breakthrough in this area will be likely achieved. Moreover, reporter genes as well as high resolution technique provide more precise location of where the TRPs really are.

Understanding TRPs from distribution to assembly not only help us to comprehend the physiological roles of TRPs but also can widen the perspective of taking TRPs as potential therapeutic targets with their pathological relevance.

Although many aspects have been deciphered through focused studies regarding TRP ion channels expression and assembly during past decades, our knowledge on the implication of TRPs distribution and assembly remains limited. There are still gaps and bewildered controversies in our understanding of these TRPs. The whole scope of TRP distribution and assembly needs more thorough and scrutinized investigation, and new technical approach applied for TRP channel investigations needs to be developed.

## Acknowledgements

This work was supported by part of the grant from the National Natural Science of Foundation in China (81301720 to W. Cheng).

## Conflict of interest

No competing financial interests exist.

## Author details

Wei Cheng

Address all correspondence to: [wcheng@dmu.edu.cn](mailto:wcheng@dmu.edu.cn)

Institute of Cancer Stem Cell, Dalian Medical University, Dalian, Liaoning Province, PR China

## References

- [1] Clapham DE. TRP channels as cellular sensors. *Nature*. 2003;**426**:517-524
- [2] Wes PD, Chevesich J, Jeromin A, Rosenberg C, Stetten G, Montell C. TRPC1, a human homolog of a *Drosophila* store-operated channel. *Proceedings of the National Academy of Sciences of the United States of America*. 1995;**92**:9652-9656
- [3] Cavanaugh DJ, Chesler AT, Jackson AC, Sigal YM, Yamanaka H, Grant R, et al. Trpv1 reporter mice reveal highly restricted brain distribution and functional expression in arteriolar smooth muscle cells. *The Journal of Neuroscience*. 2011;**31**:5067-5077. DOI: 10.1523/JNEUROSCI.6451-10.2011
- [4] Kumar S, Singh U, Goswami C, Singru PS. Transient receptor potential vanilloid 5 (TRPV5), a highly Ca(2+) -selective TRP channel in the rat brain: Relevance to neuroendocrine regulation. *Journal of Neuroendocrinology*. 2017;**29**:1-23. DOI: 10.1111/jne.12466
- [5] Kumar S, Singh U, Singh O, Goswami C, Singru PS. Transient receptor potential vanilloid 6 (TRPV6) in the mouse brain: Distribution and estrous cycle-related changes in the hypothalamus. *Neuroscience*. 2017;**344**:204-216. DOI: 10.1016/j.neuroscience.2016.12.025
- [6] Vennekens R, Menigoz A, Nilius B. TRPs in the brain. *Reviews of Physiology, Biochemistry and Pharmacology*. 2012;**163**:27-64. DOI: 10.1007/112\_2012\_8
- [7] Lee SM, Cho YS, Kim TH, Jin MU, Ahn DK, Noguchi K, et al. An ultrastructural evidence for the expression of transient receptor potential ankyrin 1 (TRPA1) in astrocytes in the rat trigeminal caudal nucleus. *Journal of Chemical Neuroanatomy*. 2012;**45**:45-49. DOI: 10.1016/j.jchemneu.2012.07.003
- [8] Ceppa E, Cattaruzza F, Lyo V, Amadesi S, Pelayo JC, Poole DP, et al. Transient receptor potential ion channels V4 and A1 contribute to pancreatitis pain in mice. *American Journal of Physiology Gastrointestinal and Liver Physiology*. 2010;**299**:G556-G571. DOI: 10.1152/ajpgi.00433.2009
- [9] Samie MA, Grimm C, Evans JA, Curcio-Morelli C, Heller S, Slaugenhaupt SA, et al. The tissue-specific expression of TRPML2 (MCOLN-2) gene is influenced by the presence of TRPML1. *Pflügers Archiv*. 2009;**459**:79-91. DOI: 10.1007/s00424-009-0716-5
- [10] Voets T. TRP channels and thermosensation. *Handbook of Experimental Pharmacology*. 2014;**223**:729-741
- [11] Gerka-Stuyt J, Au A, Peachey NS, Alagramam KN. Transient receptor potential melastatin 1: A hair cell transduction channel candidate. *PLoS One*. 2013;**8**:e77213. DOI: 10.1371/journal.pone.0077213
- [12] Sakuraba M, Murata J, Teruyama R, Kamiya K, Yamaguchi J, Okano H, et al. Spatiotemporal expression of TRPM4 in the mouse cochlea. *Journal of Neuroscience Research*. 2014;**92**:1409-1418. DOI: 10.1002/jnr.23410



- [13] Sexton JE, Desmonds T, Quick K, Taylor R, Abramowitz J, Forge A, et al. The contribution of TRPC1, TRPC3, TRPC5 and TRPC6 to touch and hearing. *Neuroscience Letters*. 2016;**610**:36-42. DOI: 10.1016/j.neulet.2015.10.052
- [14] Voets T, Talavera K, Owsianik G, Nilius B. Sensing with TRP channels. *Nature Chemical Biology*. 2005;**1**:85-92
- [15] Dong HW, Davis JC, Ding S, Nai Q, Zhou FM, Ennis M. Expression of transient receptor potential (TRP) channel mRNAs in the mouse olfactory bulb. *Neuroscience Letters*. 2012;**524**:49-54. DOI: 10.1016/j.neulet.2012.07.013
- [16] Sabourin J, Lamiche C, Vandebrouck A, Magaud C, Rivet J, Cognard C, et al. Regulation of TRPC1 and TRPC4 cation channels requires an alpha1-syntrophin-dependent complex in skeletal mouse myotubes. *The Journal of Biological Chemistry*. 2009;**284**:36248-36261. DOI: 10.1074/jbc.M109.012872
- [17] Ong EC, Nesin V, Long CL, Bai CX, Guz JL, Ivanov IP, et al. A TRPC1 protein-dependent pathway regulates osteoclast formation and function. *The Journal of Biological Chemistry*. 2013;**288**:22219-22232. DOI: 10.1074/jbc.M113.459826
- [18] Kajiyama H, Okamoto F, Nemoto T, Kimachi K, Toh-Goto K, Nakayama S, et al. RANKL-induced TRPV2 expression regulates osteoclastogenesis via calcium oscillations. *Cell Calcium*. 2010;**48**:260-269. DOI: 10.1016/j.ceca.2010.09.010
- [19] Chen Y, Williams SH, McNulty AL, Hong JH, Lee SH, Rothfus NE, et al. Temporomandibular joint pain: A critical role for Trpv4 in the trigeminal ganglion. *Pain*. 2013;**154**:1295-1304. DOI: 10.1016/j.pain.2013.04.004
- [20] Masuyama R, Mizuno A, Komori H, Kajiyama H, Uekawa A, Kitaura H, et al. Calcium/calmodulin-signaling supports TRPV4 activation in osteoclasts and regulates bone mass. *Journal of Bone and Mineral Research : The Official Journal of the American Society for Bone and Mineral Research*. 2012;**27**:1708-1721. DOI: 10.1002/jbmr.1629
- [21] van der Eerden BC, Weissgerber P, Fratzl-Zelman N, Olausson J, Hoenderop JG, Schreuders-Koedam M, et al. The transient receptor potential channel TRPV6 is dynamically expressed in bone cells but is not crucial for bone mineralization in mice. *Journal of Cellular Physiology*. 2012;**227**:1951-1959. DOI: 10.1002/jcp.22923
- [22] Zhang X, Zu H, Zhao D, Yang K, Tian S, Yu X, et al. Ion channel functional protein kinase TRPM7 regulates Mg ions to promote the osteoinduction of human osteoblast via PI3K pathway: In vitro simulation of the bone-repairing effect of Mg-based alloy implant. *Acta Biomaterialia*. 2017;**63**:369-382. DOI: 10.1016/j.actbio.2017.08.051
- [23] Brereton HM, Chen J, Rychkov G, Harland ML, Barritt GJ. Maitotoxin activates an endogenous non-selective cation channel and is an effective initiator of the activation of the heterologously expressed hTRPC-1 (transient receptor potential) non-selective cation channel in H4-IIIE liver cells. *Biochimica et Biophysica Acta*. 2001;**1540**:107-126

- [24] Riccio A, Medhurst AD, Mattei C, Kelsell RE, Calver AR, Randall AD, et al. mRNA distribution analysis of human TRPC family in CNS and peripheral tissues. *Brain Research Molecular Brain Research*. 2002;**109**:95-104
- [25] Walker RL, Hume JR, Horowitz B. Differential expression and alternative splicing of TRP channel genes in smooth muscles. *American Journal of Physiology. Cell Physiology*. 2001;**280**:C1184-C1192
- [26] Wang J, Laurier LG, Sims SM, Preiksaitis HG. Enhanced capacitative calcium entry and TRPC channel gene expression in human LES smooth muscle. *American Journal of Physiology Gastrointestinal and Liver Physiology*. 2003;**284**:G1074-G1083. DOI: 10.1152/ajpgi.00227.2002
- [27] Hamamoto T, Takumida M, Hirakawa K, Takeno S, Tatsukawa T. Localization of transient receptor potential channel vanilloid subfamilies in the mouse larynx. *Acta Oto-Laryngologica*. 2008;**128**:685-693
- [28] Holzer P. TRP channels in the digestive system. *Current Pharmaceutical Biotechnology*. 2011;**12**:24-34
- [29] Gradilone SA, Masyuk AI, Splinter PL, Banales JM, Huang BQ, Tietz PS, et al. Cholangiocyte cilia express TRPV4 and detect changes in luminal tonicity inducing bicarbonate secretion. *Proceedings of the National Academy of Sciences of the United States of America*. 2007;**104**:19138-19143. DOI: 10.1073/pnas.0705964104
- [30] Peng JB, Chen XZ, Berger UV, Weremowicz S, Morton CC, Vassilev PM, et al. Human calcium transport protein CaT1. *Biochemical and Biophysical Research Communications*. 2000;**278**:326-332. DOI: 10.1006/bbrc.2000.3716
- [31] Fonfria E, Murdock PR, Cusdin FS, Benham CD, Kelsell RE, McNulty S. Tissue distribution profiles of the human TRPM cation channel family. *Journal of Receptor and Signal Transduction Research*. 2006;**26**:159-178. DOI: 10.1080/10799890600637506
- [32] Matsumoto K, Takagi K, Kato A, Ishibashi T, Mori Y, Tashima K, et al. Role of transient receptor potential melastatin 2 (TRPM2) channels in visceral nociception and hypersensitivity. *Experimental Neurology*. 2016;**285**:41-50. DOI: 10.1016/j.expneurol.2016.09.001
- [33] Sukumaran P, Lof C, Pulli I, Kempainen K, Viitanen T, Tornquist K. Significance of the transient receptor potential canonical 2 (TRPC2) channel in the regulation of rat thyroid FRTL-5 cell proliferation, migration, adhesion and invasion. *Molecular and Cellular Endocrinology*. 2013;**374**:10-21. DOI: 10.1016/j.mce.2013.03.026
- [34] Wissenbach U, Schroth G, Philipp S, Flockerzi V. Structure and mRNA expression of a bovine trp homologue related to mammalian trp2 transcripts. *FEBS Letters*. 1998;**429**:61-66
- [35] Carrillo C, Hichami A, Andreoletti P, Cherkaoui-Malki M, del Mar Cavia M, Abdoul-Azize S, et al. Diacylglycerol-containing oleic acid induces increases in  $[Ca^{2+}]_i$  via

- TRPC3/6 channels in human T-cells. *Biochimica et Biophysica Acta*. 2012;**1821**:618-626. DOI: 10.1016/j.bbali.2012.01.008
- [36] Philipp S, Strauss B, Hirnet D, Wissenbach U, Mery L, Flockerzi V, et al. TRPC3 mediates T-cell receptor-dependent calcium entry in human T-lymphocytes. *The Journal of Biological Chemistry*. 2003;**278**:26629-26638. DOI: 10.1074/jbc.M304044200
- [37] Finney-Hayward TK, Popa MO, Bahra P, Li S, Poll CT, Gosling M, et al. Expression of transient receptor potential C6 channels in human lung macrophages. *American Journal of Respiratory Cell and Molecular Biology*. 2010;**43**:296-304. DOI: 10.1165/rcmb.2008-0373OC
- [38] Sel S, Rost BR, Yildirim AO, Sel B, Kalwa H, Fehrenbach H, et al. Loss of classical transient receptor potential 6 channel reduces allergic airway response. *Clinical and Experimental Allergy: Journal of the British Society for Allergy and Clinical Immunology*. 2008;**38**:1548-1558. DOI: 10.1111/j.1365-2222.2008.03043.x
- [39] Caterina MJ, Rosen TA, Tominaga M, Brake AJ, Julius D. A capsaicin-receptor homologue with a high threshold for noxious heat. *Nature*. 1999;**398**:436-441. DOI: 10.1038/18906
- [40] Link TM, Park U, Vonakis BM, Raben DM, Soloski MJ, Caterina MJ. TRPV2 has a pivotal role in macrophage particle binding and phagocytosis. *Nature Immunology*. 2010;**11**:232-239. DOI: 10.1038/ni.1842
- [41] Zhang D, Spielmann A, Wang L, Ding G, Huang F, Gu Q, et al. Mast-cell degranulation induced by physical stimuli involves the activation of transient-receptor-potential channel TRPV2. *Physiological Research*. 2012;**61**:113-124
- [42] Heiner I, Eisfeld J, Luckhoff A. Role and regulation of TRP channels in neutrophil granulocytes. *Cell Calcium*. 2003;**33**:533-540
- [43] Santoni G, Farfariello V, Liberati S, Morelli MB, Nabissi M, Santoni M, et al. The role of transient receptor potential vanilloid type-2 ion channels in innate and adaptive immune responses. *Frontiers in Immunology*. 2013;**4**:34. DOI: 10.3389/fimmu.2013.00034
- [44] Kim KS, Shin DH, Nam JH, Park KS, Zhang YH, Kim WK, et al. Functional expression of TRPV4 Cation channels in human mast cell line (HMC-1). *The Korean Journal of Physiology & Pharmacology: Official Journal of the Korean Physiological Society and the Korean Society of Pharmacology*. 2010;**14**:419-425. DOI: 10.4196/kjpp.2010.14.6.419
- [45] Kumagami H, Terakado M, Sainoo Y, Baba A, Fujiyama D, Fukuda T, et al. Expression of the osmotically responsive cationic channel TRPV4 in the endolymphatic sac. *Audiology & Neuro-Otology*. 2009;**14**:190-197. DOI: 10.1159/000180290
- [46] Vassilieva IO, Tomilin VN, Marakhova II, Shatrova AN, Negulyaev YA, Semenova SB. Expression of transient receptor potential vanilloid channels TRPV5 and TRPV6 in human blood lymphocytes and Jurkat leukemia T cells. *The Journal of Membrane Biology*. 2013;**246**:131-140. DOI: 10.1007/s00232-012-9511-x

- [47] Semenova SB, Vassilieva IO, Fomina AF, Runov AL, Negulyaev YA. Endogenous expression of TRPV5 and TRPV6 calcium channels in human leukemia K562 cells. *American Journal of Physiology. Cell Physiology*. 2009;**296**:C1098-C1104. DOI: 10.1152/ajpcell.00435.2008
- [48] Walder RY, Landau D, Meyer P, Shalev H, Tsolia M, Borochowitz Z, et al. Mutation of TRPM6 causes familial hypomagnesemia with secondary hypocalcemia. *Nature Genetics*. 2002;**31**:171-174. DOI: 10.1038/ng901
- [49] Vennekens R, Olausson J, Meissner M, Bloch W, Mathar I, Philipp SE, et al. Increased IgE-dependent mast cell activation and anaphylactic responses in mice lacking the calcium-activated nonselective cation channel TRPM4. *Nature Immunology*. 2007;**8**:312-320. DOI: 10.1038/ni1441
- [50] Lindvall JM, Blomberg KE, Wennborg A, Smith CI. Differential expression and molecular characterisation of *Lmo7*, *Myo1e*, *Sash1*, and *Mcoln2* genes in Btk-defective B-cells. *Cellular Immunology*. 2005;**235**:46-55. DOI: 10.1016/j.cellimm.2005.07.001
- [51] Yildirim E, Carey MA, Card JW, Dietrich A, Flake GP, Zhang Y, et al. Severely blunted allergen-induced pulmonary Th2 cell response and lung hyperresponsiveness in type 1 transient receptor potential channel-deficient mice. *American Journal of Physiology Lung Cellular and Molecular Physiology*. 2012;**303**:L539-L549. DOI: 10.1152/ajplung.00389.2011
- [52] Launay P, Cheng H, Srivatsan S, Penner R, Fleig A, Kinet JP. TRPM4 regulates calcium oscillations after T cell activation. *Science*. 2004;**306**:1374-1377. DOI: 10.1126/science.1098845
- [53] Gotz V, Qiao S, Beck A, Boehm U. Transient receptor potential (TRP) channel function in the reproductive axis. *Cell Calcium*. 2017;**67**:138-147. DOI: 10.1016/j.ceca.2017.04.004
- [54] Babich LG, Ku CY, Young HW, Huang H, Blackburn MR, Sanborn BM. Expression of capacitative calcium TrpC proteins in rat myometrium during pregnancy. *Biology of Reproduction*. 2004;**70**:919-924. DOI: 10.1095/biolreprod.103.023325
- [55] Everaerts W, Nilius B, Owsianik G. The vanilloid transient receptor potential channel TRPV4: From structure to disease. *Progress in Biophysics and Molecular Biology*. 2010;**103**:2-17. DOI: 10.1016/j.pbiomolbio.2009.10.002
- [56] Andrade YN, Fernandes J, Vazquez E, Fernandez-Fernandez JM, Arniges M, Sanchez TM, et al. TRPV4 channel is involved in the coupling of fluid viscosity changes to epithelial ciliary activity. *The Journal of Cell Biology*. 2005;**168**:869-874. DOI: 10.1083/jcb.200409070
- [57] Jang Y, Lee Y, Kim SM, Yang YD, Jung J, Oh U. Quantitative analysis of TRP channel genes in mouse organs. *Archives of Pharmacal Research*. 2012;**35**:1823-1830. DOI: 10.1007/s12272-012-1016-8
- [58] Tsavaler L, Shapero MH, Morkowski S, Laus R. Trp-p8, a novel prostate-specific gene, is up-regulated in prostate cancer and other malignancies and shares high homology

- with transient receptor potential calcium channel proteins. *Cancer Research*. 2001; **61**:3760-3769
- [59] Veldhuisen B, Spruit L, Dauwerse HG, Breuning MH, Peters DJ. Genes homologous to the autosomal dominant polycystic kidney disease genes (PKD1 and PKD2). *European Journal of Human Genetics*. 1999; **7**:860-872. DOI: 10.1038/sj.ejhg.5200383
- [60] Liman ER, Corey DP, Dulac C. TRP2: A candidate transduction channel for mammalian pheromone sensory signaling. *Proceedings of the National Academy of Sciences of the United States of America*. 1999; **96**:5791-5796
- [61] Yip H, Chan WY, Leung PC, Kwan HY, Liu C, Huang Y, et al. Expression of TRPC homologs in endothelial cells and smooth muscle layers of human arteries. *Histochemistry and Cell Biology*. 2004; **122**:553-561. DOI: 10.1007/s00418-004-0720-y
- [62] Yue Z, Xie J, Yu AS, Stock J, Du J, Yue L. Role of TRP channels in the cardiovascular system. *American Journal of Physiology. Heart and Circulatory Physiology*. 2015; **308**: H157-H182
- [63] Johnson CD, Melanaphy D, Purse A, Stokesberry SA, Dickson P, Zholos AV. Transient receptor potential melastatin 8 channel involvement in the regulation of vascular tone. *American Journal of Physiology. Heart and Circulatory Physiology*. 2009; **296**:H1868-H1877. DOI: 10.1152/ajpheart.01112.2008
- [64] Yu W, Hill WG, Apodaca G, Zeidel ML. Expression and distribution of transient receptor potential (TRP) channels in bladder epithelium. *American Journal of Physiology. Renal Physiology*. 2011; **300**:F49-F59. DOI: 10.1152/ajprenal.00349.2010
- [65] Hurwitz CG, Hu VY, Segal AS. A mechanogated nonselective cation channel in proximal tubule that is ATP sensitive. *American Journal of Physiology. Renal Physiology*. 2002; **283**:F93-F104. DOI: 10.1152/ajprenal.00239.2001
- [66] Stein RJ, Santos S, Nagatomi J, Hayashi Y, Minnery BS, Xavier M, et al. Cool (TRPM8) and hot (TRPV1) receptors in the bladder and male genital tract. *The Journal of Urology*. 2004; **172**:1175-1178. DOI: 10.1097/01.ju.0000134880.55119.cf
- [67] Birder LA, Nakamura Y, Kiss S, Nealen ML, Barrick S, Kanai AJ, et al. Altered urinary bladder function in mice lacking the vanilloid receptor TRPV1. *Nature Neuroscience*. 2002; **5**:856-860. DOI: 10.1038/nn902
- [68] Lorenzo IM, Liedtke W, Sanderson MJ, Valverde MA. TRPV4 channel participates in receptor-operated calcium entry and ciliary beat frequency regulation in mouse airway epithelial cells. *Proceedings of the National Academy of Sciences of the United States of America*. 2008; **105**:12611-12616. DOI: 10.1073/pnas.0803970105
- [69] Watanabe N, Horie S, Michael GJ, Spina D, Page CP, Priestley JV. Immunohistochemical localization of vanilloid receptor subtype 1 (TRPV1) in the Guinea pig respiratory system. *Pulmonary Pharmacology & Therapeutics*. 2005; **18**:187-197. DOI: 10.1016/j.pupt.2004.12.002

- [70] Li J, Kanju P, Patterson M, Chew WL, Cho SH, Gilmour I, et al. TRPV4-mediated calcium influx into human bronchial epithelia upon exposure to diesel exhaust particles. *Environmental Health Perspectives*. 2011;**119**:784-793. DOI: 10.1289/ehp.1002807
- [71] Sabnis AS, Shadid M, Yost GS, Reilly CA. Human lung epithelial cells express a functional cold-sensing TRPM8 variant. *American Journal of Respiratory Cell and Molecular Biology*. 2008;**39**:466-474. DOI: 10.1165/rcmb.2007-0440OC
- [72] Kunert-Keil C, Bisping F, Kruger J, Brinkmeier H. Tissue-specific expression of TRP channel genes in the mouse and its variation in three different mouse strains. *BMC Genomics*. 2006;**7**:159. DOI: 10.1186/1471-2164-7-159
- [73] Kowase T, Nakazato Y, Yoko OH, Morikawa A, Kojima I. Immunohistochemical localization of growth factor-regulated channel (GRC) in human tissues. *Endocrine Journal*. 2002;**49**:349-355
- [74] Hisanaga E, Nagasawa M, Ueki K, Kulkarni RN, Mori M, Kojima I. Regulation of calcium-permeable TRPV2 channel by insulin in pancreatic beta-cells. *Diabetes*. 2009;**58**:174-184. DOI: 10.2337/db08-0862
- [75] Jung C, Fandos C, Lorenzo IM, Plata C, Fernandes J, Gene GG, et al. The progesterone receptor regulates the expression of TRPV4 channel. *Pflügers Archiv*. 2009;**459**:105-113. DOI: 10.1007/s00424-009-0706-7
- [76] Uchida K, Tominaga M. The role of thermosensitive TRP (transient receptor potential) channels in insulin secretion. *Endocrine Journal*. 2011;**58**:1021-1028
- [77] Ishii M, Shimizu S, Hara Y, Hagiwara T, Miyazaki A, Mori Y, et al. Intracellular-produced hydroxyl radical mediates H<sub>2</sub>O<sub>2</sub>-induced Ca<sup>2+</sup> influx and cell death in rat beta-cell line RIN-5F. *Cell Calcium*. 2006;**39**:487-494. DOI: 10.1016/j.ceca.2006.01.013
- [78] Halonen J, Nedergaard J. Adenosine 5'-monophosphate is a selective inhibitor of the brown adipocyte nonselective cation channel. *The Journal of Membrane Biology*. 2002;**188**:183-197. DOI: 10.1007/s00232-001-0184-0
- [79] Ringer E, Russ U, Siemen D. Beta(3)-adrenergic stimulation and insulin inhibition of non-selective cation channels in white adipocytes of the rat. *Biochimica et Biophysica Acta*. 2000;**1463**:241-253
- [80] Moraes MN, Mezzalira N, de Assis LV, Menaker M, Guler A, Castrucci AM. TRPV1 participates in the activation of clock molecular machinery in the brown adipose tissue in response to light-dark cycle. *Biochimica et Biophysica Acta*. 2017;**1864**:324-335. DOI: 10.1016/j.bbamcr.2016.11.010
- [81] Moraes MN, de Assis LVM, Henriques FDS, Batista Jr ML, Guler AD, Castrucci AML. Cold-sensing TRPM8 channel participates in circadian control of the brown adipose tissue. *Biochimica et Biophysica Acta*. 2017;**1864**:2415-2427. DOI: 10.1016/j.bbamcr.2017.09.011
- [82] Broker-Lai J, Kollewe A, Schindeldecker B, Pohle J, Nguyen Chi V, Mathar I, et al. Heteromeric channels formed by TRPC1, TRPC4 and TRPC5 define hippocampal

- synaptic transmission and working memory. *The EMBO Journal*. 2017;**36**:2770-2789. DOI: 10.15252/embj.201696369
- [83] Kim J, Kwak M, Jeon JP, Myeong J, Wie J, Hong C, et al. Isoform- and receptor-specific channel property of canonical transient receptor potential (TRPC)1/4 channels. *Pflügers Archiv*. 2014;**466**:491-504. DOI: 10.1007/s00424-013-1332-y
- [84] Woo JS, Lee KJ, Huang M, Cho CH, Lee EH. Heteromeric TRPC3 with TRPC1 formed via its ankyrin repeats regulates the resting cytosolic Ca<sup>2+</sup> levels in skeletal muscle. *Biochemical and Biophysical Research Communications*. 2014;**446**:454-459. DOI: 10.1016/j.bbrc.2014.02.127
- [85] Cheng W, Sun C, Zheng J. Heteromerization of TRP channel subunits: Extending functional diversity. *Protein & Cell*. 2010;**1**:802-810. DOI: 10.1007/s13238-010-0108-9
- [86] Cheng W, Yang F, Takanishi CL, Zheng J. Thermosensitive TRPV channel subunits coassemble into heteromeric channels with intermediate conductance and gating properties. *The Journal of General Physiology*. 2007;**129**:191-207. DOI: 10.1085/jgp.200709731
- [87] Kim S, Barry DM, Liu XY, Yin S, Munanairi A, Meng QT, et al. Facilitation of TRPV4 by TRPV1 is required for itch transmission in some sensory neuron populations. *Science Signaling*. 2016;**9**:ra71. DOI: 10.1126/scisignal.aaf1047
- [88] Zhang Z, Yu H, Huang J, Faouzi M, Schmitz C, Penner R, et al. The TRPM6 kinase domain determines the Mg<sup>2+</sup>ATP sensitivity of TRPM7/M6 heteromeric ion channels. *The Journal of Biological Chemistry*. 2014;**289**:5217-5227. DOI: 10.1074/jbc.M113.512285
- [89] Ma X, Cheng KT, Wong CO, O'Neil RG, Birnbaumer L, Ambudkar IS, et al. Heteromeric TRPV4-C1 channels contribute to store-operated Ca<sup>2+</sup> entry in vascular endothelial cells. *Cell Calcium*. 2011;**50**:502-509. DOI: 10.1016/j.ceca.2011.08.006
- [90] Goldenberg NM, Wang L, Ranke H, Liedtke W, Tabuchi A, Kuebler WM. TRPV4 is required for hypoxic pulmonary vasoconstriction. *Anesthesiology*. 2015;**122**:1338-1348. DOI: 10.1097/ALN.0000000000000647
- [91] Schindl R, Fritsch R, Jardin I, Frischauf I, Kahr H, Muik M, et al. Canonical transient receptor potential (TRPC) 1 acts as a negative regulator for vanilloid TRPV6-mediated Ca<sup>2+</sup> influx. *The Journal of Biological Chemistry*. 2012;**287**:35612-35620. DOI: 10.1074/jbc.M112.400952
- [92] Guo Z, Grimm C, Becker L, Ricci AJ, Heller S. A novel ion channel formed by interaction of TRPML3 with TRPV5. *PLoS One*. 2013;**8**:e58174. DOI: 10.1371/journal.pone.0058174
- [93] Du J, Ma X, Shen B, Huang Y, Birnbaumer L, Yao X. TRPV4, TRPC1, and TRPP2 assemble to form a flow-sensitive heteromeric channel. *The FASEB Journal*. 2014;**28**:4677-4685. DOI: 10.1096/fj.14-251652
- [94] Yu Y, Ulbrich MH, Li MH, Dobbins S, Zhang WK, Tong L, et al. Molecular mechanism of the assembly of an acid-sensing receptor ion channel complex. *Nature Communications*. 2012;**3**:1252. DOI: 10.1038/ncomms2257

- [95] Delling M, DeCaen PG, Doerner JF, Febvay S, Clapham DE. Primary cilia are specialized calcium signalling organelles. *Nature*. 2013;**504**:311-314. DOI: 10.1038/nature12833
- [96] Salehi-Najafabadi Z, Li B, Valentino V, Ng C, Martin H, Yu Y, et al. Extracellular loops are essential for the assembly and function of polycystin receptor-ion channel complexes. *The Journal of Biological Chemistry*. 2017;**292**:4210-4221. DOI: 10.1074/jbc.M116.767897
- [97] Kun J, Szitter I, Kemeny A, Perkecz A, Kereskai L, Pohoczky K, et al. Upregulation of the transient receptor potential ankyrin 1 ion channel in the inflamed human and mouse colon and its protective roles. *PLoS One*. 2014;**9**:e108164. DOI: 10.1371/journal.pone.0108164
- [98] Vetter I, Cheng W, Peiris M, Wyse BD, Roberts-Thomson SJ, Zheng J, et al. Rapid, opioid-sensitive mechanisms involved in transient receptor potential vanilloid 1 sensitization. *The Journal of Biological Chemistry*. 2008;**283**:19540-19550. DOI: 10.1074/jbc.M707865200



---

# Anions

---



---

# Lifting the Fog over Mitochondrial Chloride Channels

---

Katarina Mackova, Anton Misak and  
Zuzana Tomaskova

Additional information is available at the end of the chapter

<http://dx.doi.org/10.5772/intechopen.76419>

---

## Abstract

The current through mitochondrial chloride channels was first described in 1987. Subsequently, several types of ion channels permeable to chloride and other anions were found in the mitochondria of different origins. The increasing number of electrophysiological studies, however, yielded only more ambiguity rather than order in the field of chloride channels. This uncertainty was slightly reduced by two different studies: experiments that showed a significant role of chloride channels in the process of mitochondrial membrane potential oscillations and experiments that localized chloride intracellular ion channel (CLIC) proteins in cardiac mitochondrial membranes. Our recently published single-channel electrophysiological experiments are well in line with the channel activity of recombinant CLIC proteins. The experimental evidence seems to be inevitably, though slowly converging on a connection between single-channel activity and the identity of the mitochondrial chloride channel protein.

**Keywords:** chloride channel, mitochondria, cardiomyocyte, inner membrane anion channel—IMAC, chloride intracellular ion channel—CLIC

---

## 1. Introduction

Ion channels permeable to anions were underrated for a long time concerning their role in the life of a cell. The role of chloride channels in mitochondria was particularly underrated. This chapter focuses on the chloride channels of the inner mitochondrial membrane. The different electrophysiological descriptions of these channels that have appeared since 1987 are compared. In addition to single-channel current measurements, measurements of mitochondrial membrane potential oscillations in whole cardiomyocytes provided information about the role of the mitochondrial chloride channel. At the molecular level, super-resolution fluorescence

---

imaging and Western blot analysis yielded invaluable information about the localization of chloride intracellular channel (CLIC) isoforms in the mitochondrial membrane. The results from these different fields of research are discussed and combined to identify a connection between measured chloride channel activities and the identity of the corresponding proteins.

## 2. First chloride channels on (electrophysiological) stage

One of the earliest studies of anion channel activity was reported in 1979 by White and Miller [1]. The authors used membrane vesicles from the electric organ of *Torpedo californica* fish and fused these vesicles into a planar lipid bilayer to measure the single-channel current. The fascinating story about the discovery of these channels was recounted by Miller [2]. Indeed, the reconstitution of intracellular ion channels in planar lipid bilayers in combination with the single-channel patch-clamp approach was extensively used to characterize ion channels of different origins and cellular localizations. The following years were fruitful with discoveries of new chloride channels. At present, chloride channels are classified into several groups; some are based on the genetic information known about the channel proteins, and others are defined only according to the described single-channel electrophysiological properties [3]. The first member of the 'chloride channel' (ClC) family was cloned more than 20 years ago [4]. Since then, several other members have been identified [5]. When the ClC homologues from *Escherichia coli* and *Salmonella typhimurium* were crystallized, the dimeric structure of these channels was revealed; each of the two monomers has its own conducting pore [6]. This 'double-barrel' structure is reflected at the level of electrophysiological measurements by the presence of two open-channel levels with equal conductances of approximately 10 pS each [1, 7–9]. Another chloride channel group contains ligand-regulated channels, such as glycine and  $\gamma$ -aminobutyric acid (GABA) receptors [10, 11]; these two channels have a neuronal origin, and they were described at the single-channel level in 1983. The cAMP-activated cystic fibrosis transmembrane conductance regulator (CFTR) group represents a separate chloride channel family localized in epithelial cells [12, 13]. The CFTR channel was purified, reconstituted into liposomes and measured at the single-channel level in 1992 [14]. The last of the chloride channel groups to be genetically distinguished was the group of chloride intracellular ion channels (CLICs); the first member of this group was described at the single-channel level in 1987 [15]. We return to CLICs later, in part 6. In addition, finally, there are channels that have unknown encoding genes—swelling-activated chloride channels [16] or calcium-activated chloride channels [17, 18]; both channel types were described at the beginning of the 1990s. In the following sections, we focus on the chloride channels localized in the inner mitochondrial membrane.

## 3. A multitude of chloride channels

One of the presumptions of Mitchell's chemiosmotic hypothesis is that the inner mitochondrial membrane is impermeable to ions other than protons [19]; however, with the development

of experimental approaches that allowed the detection of ion transport through the mitochondrial membrane, evidence showing that the mitochondrial membrane is crowded with ion transporters accumulated (rev. in [20]). At the beginning of the 1980s, the commonly used methods were rather indirect: the uptake of the radioactive isotope  $^{36}\text{Cl}^-$  was measured [21], or the light scattering from swollen mitochondria was monitored [22, 23], although the biophysical approach for single-channel current measurement was already available [24–26].

### 3.1. Anion fluxes in mitochondria

The anion transport through inner mitochondrial membranes of mammalian origin was described for the first time in 1979 by Selwyn et al. [27]. This chloride uniporter was later named ‘inner membrane anion channel’ (IMAC) [28]. IMAC was characterized by light-scattering measurements of swollen mitochondria in the presence of rotenone, which inhibits complex I of the respiratory chain [28–32]. Beavis and Garlid showed that the transport of anions was strongly dependent on pH when  $\text{Mg}^{2+}$  ions were depleted from the mitochondria by the A23187 ionophore; in the presence of  $\text{Mg}^{2+}$ , the transport rate was low and could be increased by alkaline pH [22]. A role for IMAC in the regulation of mitochondrial volume after pathological swelling has been suggested [28]. The group of Beavis looked for the putative identity of IMAC and searched for pharmacological similarities between IMAC and adenine nucleotide translocase (ANT) [33]. They found that several nucleotide analogues (e.g. Cibacron Blue) partially inhibit the flux of small anions and block the flux of malonate [33], whereas at low doses, these compounds stimulate the flux. The most important difference between IMAC and ANT was the effect of the selective ANT inhibitor carboxyatractyloside, which did not affect IMAC in any way [33]. The researchers concluded that IMAC is not identical to ANT. Later, in 1996, Beavis and Davatol-Hag studied the effect of several stilbene-2,2'-disulfonates [34], which are known as nonspecific chloride channel inhibitors [3, 34]. 4,4'-Diisothiocyano-2,2'-stilbenedisulfonic acid (DIDS) is most often used to inhibit chloride channels. These researchers showed that DIDS, which was applied from the side of the intermembrane space, partially inhibited the flux of chloride by 30%. The inhibitory effect was more pronounced for malonate transport. A possible mechanism of IMAC inhibition by large anionic molecules (DIDS, nucleotide analogues) has been proposed [33] where these molecules bind to a binding site within the conductive pathway. This hypothesis is based on the fact that neither of the compounds could completely block the flux of small ions, which is in contrast to the inhibition of flux of larger anions such as malonate. The conductive pathway seems to be large enough to enable the entrance (at least partial) of complex compounds such as DIDS, as IMAC is also permeable to large anions [22]. The most recent publications concerning IMAC, which was measured by the light-scattering technique, appeared in 2004. One of these studies evaluated the combined effect of temperature and  $\text{Mg}^{2+}$  on IMAC [35], and the second one measured the activation of IMAC by fatty acids [36]. Schonfeld et al. [36] showed that fatty acids activated the chloride flux through IMAC. The positive effect of fatty acids on activity was confirmed by single-channel measurements. The authors suggested that long-chain fatty acids directly remove the  $\text{Mg}^{2+}$  ions from the binding sites of the IMAC protein or that these fatty acids form complexes with  $\text{Mg}^{2+}$  ions, thus lowering their matrix concentration. However, the described single-channel experiments provide questionable support for the proposed mechanism of activation. On the

other hand, the A23187 ionophore [22] caused the depletion of the  $Mg^{2+}$  matrix pool [36], leading to IMAC activation. The inhibitory effect of  $Mg^{2+}$  ions on IMAC activity was not only pH-dependent but also temperature-dependent [35]. At 25°C, the flux through IMAC was blocked by  $Mg^{2+}$  ions at physiological pH. Researchers have opined that the activation of IMAC in physiological processes is unlikely and that its role under these conditions is unclear [37, 38]. Beavis and Powers estimated that at physiological  $Mg^{2+}$  concentrations and 37°C, IMAC activity is ~7% of its maximum. The authors concluded that other factors regulating the activity of IMAC are probably involved and are waiting to be discovered [35].

### 3.2. Electrophysiology measurements of the inner mitochondrial membrane

The largest advance in the study of anion transport in mitochondria occurred in 1987 when the current through giant mitoplasts, that is, mitochondria deprived of the outer membrane [39], was first measured by a relatively novel (at the time) electrophysiological patch-clamp method [25]. To obtain the giant mitoplasts necessary to allow the stable connection of the patch pipette to the mitoplast membrane, mice were fed cuprizone. The researchers observed a slightly selective anion channel, with voltage-dependent activity and a mean single-channel conductance of 107 pS (in 150 mM KCl); this channel was later named the centum-pS channel [40]. This channel was also found in the inner membrane of the liver and heart mitochondria of oxen and mice that were not treated with cuprizone [41]. The centum-pS channel responds to nanomolar concentrations of mitochondrial benzodiazepine receptor (mBzR) ligands. The channel activity is completely inhibited by protoporphyrin IX, PK11195 and Ro5-4864 (4-chlorodiazepam) with  $IC_{50}$  values in the nanomolar range. The high affinity of the benzodiazepine ligands to this channel suggests a putative association of the channel protein with the mBzR present in the outer membrane of mitochondria [40, 42]. Apart from the voltage-sensitive centum-pS channel [43, 44], Kinnally et al. also observed a 15-pS channel (low conductance channel, LCC) in the inner mitochondrial membrane patches; this channel was activated by alkaline pH and was inhibited by the presence of  $Mg^{2+}$  ions, and the authors suggested that this channel corresponds to IMAC [44]. With the increasing number of electrophysiological experiments on mitoplasts or isolated submitochondrial vesicles, the number of observed anion channel types has multiplied. There are actually several slightly differing anion channels that have been described, although one cannot conclude with certainty which of them could correspond to IMAC [44–49]. The anion channels were measured from mitochondrial membranes of different origin.

Anion channels in the inner membrane of brown adipose tissue mitochondria were characterized by a conductance of 108 pS in 150 mM KCl solution [45, 49]. These channels were measured by the patch-clamp technique in mitoplast-attached mode. Klitsch and Siemen [45] showed that this channel is inhibited by a low concentration of purine nucleotides; however, the channel is not identical to the uncoupling protein (UCP) [45, 50, 51]. UCP from brown adipose tissue mitochondria was also shown to behave as a chloride channel, with two steps of 75-pS conductance (in 100 mM KCl), to be sensitive to voltage and to be inhibited by nucleotides and DIDS. UCP is unaffected by pH changes and  $Mg^{2+}$  ions [50]. According to Borecky et al., the 108-pS channel may be a candidate for IMAC because of several properties: the most convincing ones are the pH dependence of the channel activity (quantified as the open probability of the channel) and the inhibition by  $Mg^{2+}$  ions [49]. Its activity was inhibited by propranolol [52], similar to the anion fluxes through IMAC [53].

In yeast mitochondria, a 45-pS channel (in 150 mM KCl) was detected; this channel was characterized by low activity, which was only slightly affected by voltage. The channel could be inhibited by ATP [47, 54].

A more thorough description of anion channels derived from sheep cardiac mitoplasts was given by Hayman et al. [46, 55]. Channels permeable to chloride were observed after the incorporation of vesicles into a planar lipid bilayer; one type of channel had a conductance of 100 pS in 150 mM KCl, was named intermediate conductance mitochondrial anion channel (INMAC), and had multiple subconductance states; the other type of channel had 50-pS conductance, had two distinct subconductance states, and was named small conductance mitochondrial anion channel (SMAC). Both channels were more selective for anions than for the potassium cation ( $P_{Cl}/P_K \sim 7-9$ ). The responses of INMAC channels to pH changes were consistent with those of the brown adipose tissue 108-pS channel [49]; however, the response was not sensitive to ATP,  $Mg^{2+}$  ions or voltage [46].

Native chloride channel with a conductance of 129 pS in 250 mM KCl [56] and 97 pS in 150 mM KCl [57] were detected in purified rat cardiac mitochondria. These channels were

Name (citations)	Origin	Method	G [Ps] ([KCl])	$P_{Cl}/P_K$	Kinetic features	Substates
IMAC [34, 53]		Light scattering of swollen mitoplasts	Not defined for IMAC flux			
Centum pS [39, 40]	Mouse liver	Patch clamp	107 (150 mM)	~4.5	Bursts	
Centum pS [41]	Mouse heart and liver, ox heart	Patch clamp	~100 (150 mM)			
108 pS [45]	Brown adipose tissue	Patch clamp	108 (150 mM)			✓
108 pS [49]	Brown adipose tissue	Patch clamp	108 (150 mM)		Bursts	
UCP [50]	Brown adipose tissue	Patch clamp	2 × 75 (100 mM)	~17		
45 pS [47, 54]	Yeast	Patch clamp	45 (150 mM)	~3.2		
INMAC [46, 55]	Sheep heart	BLM	100 (150 mM)	~9		✓
SMAC [46, 55]	Sheep heart	BLM	50 (150 mM)	~7		✓
97-pS [56, 57]	Rat heart	BLM	97 (150 mM)	~3	Burst	✓
LCC [44, 52]	Rat liver	Patch clamp	15 (150 mM)			
CLIC5 [21, 83, 85]	Recombinant	BLM	26–400 (140 mM)	~0.5–9		✓

BLM is the method of ion channel reconstitution into a planar lipid bilayer. The conductance (G) and the selectivity for chloride over potassium ions ( $P_{Cl}/P_K$ ) are summarized in columns 4 and 5, respectively. The concentration of KCl in which the conductance was determined is shown next to the value of conductance. Some channels possess a typical kinetic feature—bursts (column 6). The final column shows the presence of subconductance states (substates). The cells are empty when the corresponding information is missing.

**Table 1.** Origin, method of detection and biophysical parameters of different chloride channels from the inner mitochondrial membrane.

Name	Voltage	Mg <sup>2+</sup>	pH	DIDS
IMAC [34, 53]		Inhibition	Acidic pH—inhibition Alkaline pH—activation	Partial inhibition
Centum pS [39, 40]	Sensitive	(Mg <sup>2+</sup> not present in the solutions)	Insensitive	
Centum pS [41]	Sensitive			Insensitive
108 pS [45]				
108 pS [49]	Sensitive	Inhibition	Acidic pH—inhibition Alkaline pH—high activity	
UCP [50]	Sensitive	Insensitive	Insensitive	Inhibition
45 pS [47, 54]	Minimal	Insensitive		
INMAC [46, 55]	Slightly sensitive or insensitive	Insensitive	Acidic pH—inactivation Alkaline pH—active channel	
SMAC [46, 55]		Decrease in amplitude	Insensitive	
97 pS [56, 57]	Sensitive	Activation	Acidic pH—slow ↑ G followed by inhibition Alkaline pH—high activity, ↓ G	One-sided inhibition
LCC [44, 52]	Insensitive	Inhibition	Activation by alkaline pH No activity at acidic pH	
CLIC5 [21, 83, 85]				

The table summarizes the effect of voltage, Mg<sup>2+</sup> ions, pH and the nonspecific anion channel inhibitor DIDS on the activity of the chloride channels. Regulation by pH also affected the conductance of the channels (G); the arrows indicate the change in conductance. The cells are empty when the corresponding information is missing.

**Table 2.** Regulation of chloride channels from the inner mitochondrial membrane.

also permeable to large anions such as acetate. Concerning the selectivity of these channels, the channels were slightly selective for anions over potassium ions ( $P_{Cl^-}/P_K \sim 3$ ) and practically nonselective among several tested types of anions. The channels responded to pH changes by changing their ionic conductance. An alkaline environment caused an immediate decrease in conductance but did not affect the activity. On the other hand, acidification induced a slow increase in conductance, as well as an abrupt inhibition after a delay of approximately 1 min [56]. A similar effect of pH on channel activity was seen in the study of the centum-pS channel from brown adipose tissue mitochondria [49], but no changes in conductance due to pH shifts were reported. The pH dependence of the conductance of the rat mitochondrial chloride channels was also measured with the gluconate anion, which was impermeant at 7.4 pH. Interestingly, gluconate conductance appeared at acidic pH and gradually increased with the acidity of the environment [56]. However, it seems



that in addition to the spatial dimensions of the anion size, the change in conductance can be a consequence of the change in hydration energy at different pH values and/or the change in the surface charge in the pore vestibule [58]. As mentioned before, DIDS is commonly used as a nonspecific inhibitor of anion channels, although not all of these channels are sensitive to DIDS. The chloride channels from rat cardiac mitochondria are inhibited by DIDS from one side only, with  $IC_{50}$  of  $\sim 12 \mu\text{M}$ . DIDS affected the complicated kinetics of these channels, which was previously described in detail [57]. In native mitochondrial chloride channels, the dependence of the activity on voltage has an approximately bell-shaped character [57], and these channels are more active in the presence of  $1 \text{ mM Mg}^{2+}$  ions than in  $\text{Mg}^{2+}$ -free solution [56]. Again, for these channels, some but not all properties correspond to IMAC.

The origin, methodical approach, biophysical properties and regulation of the inner mitochondrial membrane chloride channels are summarized in **Tables 1** and **2**. In these tables, the frequent value of  $\sim 100\text{-pS}$  conductance (in  $150 \text{ mM KCl}$ ) and the similar selectivities suggest that the  $108\text{-pS}$  channel, INMAC and the channel from purified rat cardiac mitochondria might all represent the centum-pS channel. Nevertheless, these studies did not lead to a definitive conclusion about the identity of IMAC and did not provide an ultimate match at a single-channel level. In addition, the potential role or roles of these channels are mostly unclear (rev. in [59]). In the first years of the third millennium, the interest in mitochondrial chloride channels began to slowly fade. At this time, the group of Brian O'Rourke published a set of studies on the oscillations of the mitochondrial membrane potential in whole cardiomyocytes, which revived interest in IMAC by indicating its importance in this phenomenon [60–62].

#### **4. Role of mitochondrial chloride channels in mitochondrial membrane potential oscillations**

Changes in the cardiac action potential (AP) duration lead to ventricular arrhythmias [42]. The pattern of AP is also determined by sarcolemmal ATP-sensitive potassium channels ( $\text{sarcK}_{\text{ATP}}$ ) [63], whose activity responds to changes in ATP levels in the cytoplasm. Thus, the perturbation of mitochondrial bioenergetics can be one cause of AP heterogeneity because mitochondria produce the majority of cellular ATP [42]. A decrease in mitochondrial membrane potential ( $\Delta\Psi_m$ ) is associated with a lowered ATP production, which affects the  $\text{sarcK}_{\text{ATP}}$  that regulate the action potential duration [61, 64]. Several years ago, it was shown that metabolic stress can induce a collapse in  $\Delta\Psi_m$  [60]; this collapse could be abolished by different inhibitors of ion channels of the inner mitochondrial membrane that are permeable to anions [37]. Arrhythmias can also arise as a consequence of the oxidative stress caused by ischemia/reperfusion [42]. A decrease, oscillations and even a collapse of  $\Delta\Psi_m$  were observed in isolated cardiomyocytes exposed to oxidative stress [61]. Oxidative stress can be experimentally induced by exposing a small volume of the cell to a laser flash. The energy provided by the laser light induces a local increase in the production of reactive oxygen species (ROS) in the mitochondria in the flashed region. In 2000, Zorov et al. published a study showing that local ROS production can lead to a synchronous collapse of  $\Delta\Psi_m$

in whole cardiomyocytes [65]. The increased ROS concentration in the mitochondria causes the release of excess ROS into the cytoplasm, in parallel with a fast depolarization of mitochondrial membrane potential. This process was named ROS-induced ROS release [65]. Before the ROS are scavenged by superoxide dismutase, the ROS cause depolarization of neighboring mitochondria. It is assumed that the prevailing form of the ROS responsible for this effect is the superoxide radical. Under physiological conditions, local  $\Delta\Psi_m$  oscillations are characterized by a broad frequency range, and mitochondria act as oscillators that are weakly coupled by ROS.  $\Delta\Psi_m$  oscillations, which are induced by oxidative stress or by insufficient concentrations of substrate, are characterized by one dominant frequency and a high amplitude (up to tens of millivolts) [61]. These oscillations spread into the whole cardiomyocyte [66]. Aon et al. showed that the ROS produced at complex III of the electron transport chain are from the main part responsible for synchronous  $\Delta\Psi_m$  oscillations. The authors provided evidence that the superoxide radical is the ROS involved in the oscillations and their propagation throughout the cell. The role of IMAC in the process of  $\Delta\Psi_m$  regulation was highlighted by the fact that inhibitors of anion channels (DIDS, 4'-chlorodiazepam) prevented the oscillations and collapse of  $\Delta\Psi_m$  [61]. The presence of an anion channel inhibitor locked the ROS within the mitochondria exposed to a laser flash. These results led the authors to assume a double role of IMAC in both the dissipation of energy that causes  $\Delta\Psi_m$  depolarization and the pathway that allows superoxide radicals to leave the matrix [61].  $\Delta\Psi_m$  changes are also accompanied by redox potential oscillations in the whole cell [61]. The redox pair reduced/oxidized glutathione (GSH/GSSG) is the major indicator of the cellular redox state [67]. It has been proved experimentally that the GSH/GSSG ratio determines the trend of  $\Delta\Psi_m$  changes and their reversibility [68]. The GSH/GSSG ratio and the absolute concentration of these two compounds in cardiomyocytes affect the chloride fluxes in mitochondria under conditions of oxidative stress [68]. A computer model of a mitochondrial oscillator was based on oxidative phosphorylation, the cytoplasmic ROS-scavenging system, ROS and IMAC [62]. The results of this model are in good agreement with experimental data. IMAC, whose identity remains uncertain, was included in this model as an escape route for ROS. The conductance of IMAC was set as the conductance of the yeast 108-pS channel [49]. The model assumes that IMAC is activated in a positive feedback loop by the leaking of ROS from the matrix, where high concentrations of ROS accumulate under oxidative stress conditions. IMAC mediates the release of ROS from mitochondria if the ROS production in the matrix is increased to a critical value. The release of ROS provides communication within the mitochondrial network, which results in synchronous  $\Delta\Psi_m$  oscillations throughout the whole cardiomyocyte [62, 69]. According to the model, the flux of anions through IMAC is responsible for the fast depolarization phase during the  $\Delta\Psi_m$  oscillations [62, 66].

The role of IMAC in the process of mitochondrial membrane potential oscillations inspired a further search for evidence of the identity of the native chloride channels from highly purified rat cardiomyocyte mitochondria.

## 5. Kinetics, subconductance states and inferred channel structure

The basic biophysical properties and regulation of many of the described mitochondrial chloride channels are not consistently in agreement among themselves and with the accepted

properties of the IMAC pathway, but the gating and permeation through the channel pore seem to be more useful properties for comparison of these channels.

The 108-pS channel from brown adipose tissue mitochondria is characterized by bursts of fast flickering at negative voltages and long openings at positive voltages [49]. A similar behavior, but with inverse polarity, is visible in the traces of sheep chloride channels. These channels were reconstituted in a planar lipid bilayer; at an applied voltage of  $-50$  mV, the openings were long, and the transitions to the closed state were infrequent. By contrast, the channel under  $+50$  mV applied potential also exhibited bursts of fast events (see Figures 2 and 3 in [55]). The different polarities of this effect can be caused by different orientations of the channel in the measuring system. The bursting behavior was also reported for the chloride channels of rat cardiac mitochondria [57]. A report that the gating kinetics was affected by voltage was also found for the 45-pS yeast mitochondria channel [47]. It is unfortunate that the gating kinetics was not thoroughly described for many of the reported mitochondrial chloride channels; this information might have been helpful for comparison of these channels, which differ in pharmacological regulation in many cases.

In general, ion channels can have not only a main conducting state but also states with lower than maximal conductance, which are called subconductance states (or simply substates). The presence of substates was described and analyzed in native chloride channels from rat cardiac mitochondria [70], which are similar to the chloride channels from sheep cardiac mitochondria [55]. Three distinct substates were detected in the chloride channels of rat origin, and their conductances corresponded to 29, 50 and 74% of the maximal conductance. The occupancy of states with a lower conductance is small and less than 2% for each state. SMACs from sheep mitochondria displayed substates with 25 and 50% of the maximal conductance. The occupancy of the 75% substate was rare and below 1% [55]. Hayman proposed that the channel is formed by four subunits. INMACs exhibited several substates, but these states were not described in more detail [46].

An unusual observation of the decomposition of the chloride channel of rat cardiac mitochondria into substates was described by Tomasek et al. [70]. This channel is characterized by the absence of a maximal conducting state and an increased gating frequency between substates, leading to complete loss of the channel activity. The behavior of the channels was in line with the suggested model of four conducting subunits that cooperate as one channel. The gating of the four units is synchronized, and it seems that the subunits are unstable when they do not work in the cooperating complex.

As the occupancy of substates that were analyzed is low, it is not surprising that the occupancy has not been described or even mentioned in other studies of chloride channels from the inner mitochondrial membranes. On the other hand, the presence of substates was described for some chloride intracellular channels called CLICs [71].

## 6. CLIC localization

Thirty years ago, chloride intracellular channel (CLIC) proteins were isolated from bovine kidney cortex membrane vesicles for the first time [15]. The protein was isolated using a high-affinity ligand of chloride channels, indanyloxyacetic acid (IAA-94), and the transport through

the channel was detected by the uptake of the  $^{36}\text{Cl}^-$  isotope. In 1989, CLIC proteins were purified from bovine kidney cortexes and the apical membranes of bovine trachea and reconstituted into lipid vesicles; the single-channel properties of CLIC were measured in a planar lipid bilayer system [21]. Since then, the family of CLIC proteins has grown, and it contains six vertebrate members, three invertebrate members and at least four plant members [71]. These proteins can adopt two forms—soluble and integral membrane [72]. The soluble form of CLIC1 was crystallized, and the obtained structure is a structural homologue of the glutathione-S-transferase superfamily [72, 73]. The CLIC1 isoform was also crystallized in the presence of glutathione (GSH), for which these proteins possess a binding site [72]. CLIC1 has been thoroughly studied at the single-channel level, but an extremely broad range of channel conductances from 17 to 160 pS has been reported for this isoform [71, 72, 74–78]. The channel activity was not affected by the presence of 1 mM  $\text{Ca}^{2+}$  or 1 mM  $\text{Mg}^{2+}$ , although the activity was blocked by both the oxidized and reduced forms of glutathione [74], which is consistent with the presence of a glutathione-binding site. This channel is localized in intracellular membranes, as are other CLIC family members, and in plasma membranes [71]. The conductance of expressed CLIC4 channels was measured in several studies, and the conductance spanned a broad range of values from 1 [79] up to 43 pS [80, 81]. Although the conductance varies among these studies, there is an agreement concerning the selectivity of the channel, which is poorly selective for anions over cations ( $P_{\text{Cl}^-}/P_{\text{choline}} \sim 3$ ) [79, 80]. Littler et al. resolved the structure of CLIC4 at 1.8 Å resolution [81], indicating that CLIC4 is a monomeric protein, and it was structurally similar to CLIC1 with a difference in the domain of CLIC1 that undergoes structural changes upon oxidation. It was shown, however, that CLIC4 also responds to redox agents. Incubation with  $\text{H}_2\text{O}_2$  favored the fusion of CLIC4 into the planar lipid bilayer; on the other hand, pretreatment with DTT resulted in no channel activity [81]. Intriguingly, the CLIC4 expressed in HEK293 cells was not affected by the nonspecific chloride channel inhibitor DIDS [82]. The absence of DIDS inhibition was also found for the centum-pS channel [41], and a one-sided effect was reported for anion channels derived from rat cardiac mitochondrial membranes [57].

The recombinant CLIC5 isoform was also studied at the single-channel level [83]. Similar to other CLIC isoforms, CLIC5 is poorly selective for monovalent ions (either negatively or positively charged), and several values of conductance ranging between 26 and 400 pS were reported [21, 84, 85]. Different substates were observed in single-channel current recordings of CLIC1 and CLIC5 proteins incorporated into planar lipid bilayers [77, 83]. The observed broad range of conductance values was interpreted to indicate a cluster of functioning chloride channel pores [71, 86].

CLIC proteins possess two peculiar properties. One already mentioned property is that CLIC proteins can exist in two different forms: a soluble protein form and an integral membrane protein form, which is unusual as the structural characteristics of integral proteins differ from those of soluble proteins. This double structure is deduced from the fact that CLIC proteins were found in both the aqueous phase and the membrane fraction during the process of protein isolation [87]. However, the crystallographic structure of the integral form has not yet been determined. The second peculiarity is that these proteins lack the conserved mitochondrial targeting sequence [88–90]; nevertheless, in 2016, the research group of H. Singh reported that some CLIC isoforms are localized in the mitochondria of cardiomyocytes [89, 90].

Indeed, this finding was a breakthrough after three decades of searching for the identity of chloride channel proteins in the inner mitochondrial membrane. The CLIC4 and CLIC5 isoforms were detected on mitochondrial membranes using immunofluorescence imaging and colocalization of fluorescent markers for CLIC isoforms 1, 4 and 5 and MitoTracker dye via a super-resolution STED microscope. The presence of the corresponding proteins was detected by Western blot analysis of the purified mitochondrial fraction. Interestingly, the CLIC5 and CLIC4 proteins do not have the same distribution in the mitochondrial membrane. The CLIC4 isoform has a cluster distribution similar to that of a voltage-dependent anion channel of the outer mitochondrial membrane, VDAC1 [91]. Higher levels of the CLIC4 isoform were found in the outer mitochondrial membrane, while CLIC5 had a uniform distribution mainly concentrated in the inner mitochondrial membrane.

## 7. Discussion of the identity of the mitochondrial chloride channel

The spectrum of chloride channels found in the native inner mitochondrial membranes seems to be broad, and there are many experimental inconsistencies among these channels. Some properties are nevertheless notable when one is searching for the identity of the channel. The discussed channels were all measured either from highly purified mitochondrial membrane fractions fused to planar lipid bilayers or from patched mitoplasts. The most frequently reported channel has ~100-pS conductance [39, 41, 46, 49, 57]. Several of the channels share a bursting pattern of single-channel activity, voltage-dependent activity and gating kinetics. In addition, some of these channels maintain the pH regulation described for the anion flux through IMAC [49, 53, 56]. An anion channel having a 100-pS conductance was successfully incorporated in a model of the process of ROS-induced ROS release and synchronized mitochondrial membrane potential oscillations [62]. This model describes well the measured experimental data.

The only chloride channel protein detected in the inner mitochondrial membrane is the CLIC5 channel. Naturally, the question arises as to whether the CLIC5 channel is identical to the channel with the measured single-channel currents described in several studies. To answer this question now, we can consider only the available (and not very abundant) experimental data from recombinant CLIC5 single-channel measurements [21, 84, 85]. The inhibitory effect of IAA-94, which was studied with native mitochondrial chloride channels of the rat heart [56], favors a connection between these channels and CLICs. The hints of the structural features of native channels of both rat [70] and sheep [55] origin are also in good agreement with the structural model suggested for CLICs [71]. Rat mitochondrial chloride channels, which are similar in many ways to the centum-pS channel, suggest that these channels correspond to IMACs, and the rat mitochondrial chloride channels were reported to be redox-sensitive [70]. Unfortunately, the redox regulation has not been thoroughly described, but the behavior of the channels in reduced and oxidized environments seems to be consistent with the CLIC redox sensitivity. Both CLICs and (the many) mitochondrial chloride channels are poorly selective, and the conductance of all the discussed chloride channels is within the broad range reported for CLIC channels [71].

## 8. Conclusion and future prospects

There is one crucial task ahead of us to reach the ultimate convergence point: the connection between the native inner mitochondrial membrane chloride channels and the CLIC protein must be proved unambiguously. If this connection was proven, the experimentation on the mitochondrial membrane potential can progress to a completely new level. This progression might provide important knowledge concerning the process of cardiac arrhythmias caused by  $\Delta\Psi_m$  oscillations, with a potential clinical impact in the future. The use of molecular genetic techniques, such as silencing or conditional knock-out, and studies on the structure-function relationship will be feasible. Once the gene for the mitochondrial chloride channel is known, many options for experimentation will become available. The Janus kinase/signal transducer and activator of transcription (JAK/STAT) pathway can provide benefits against ischemia/reperfusion injury via changes in the expression or activity of some proteins, including the proteins of the respiratory chain [92]. In the context of the ROS-induced  $\Delta\Psi_m$  oscillations that occur during mitochondrial stress, it seems to be causally important to minimize ROS formation by improving mitochondrial function. STATs, which were also identified in cardiomyocyte mitochondria, can be useful for this task. In addition to being involved in mitochondrial respiratory function [93], STAT3 may regulate the mitochondrial permeability transition pore [94, 95]. It would be of interest to know whether the inner membrane mitochondrial chloride channel is also affected by STAT3 or the STAT3 activation pathway under conditions of ischemia/reperfusion.

## Acknowledgements

This work was supported by the Scientific Grant Agency of MESRaS and SAS, namely grants VEGA 2/0146/16 and VEGA 2/0090/18, and by the Slovak Research and Development Agency (grant APVV-15-0371). This manuscript was edited for English language by American Journal Experts (AJE). I thank my dear colleagues and friends Karol Ondrias, Marian Grman and Milan Tomasek for fruitful and passionate discussions. I also thank Ludo Varecka and Katka Polcicova for their critical comments and inspiring remarks.

## Conflict of interest

There is no conflict of interest.

## Author details

Katarina Mackova<sup>1</sup>, Anton Misak<sup>2</sup> and Zuzana Tomaskova<sup>1\*</sup>

\*Address all correspondence to: zuzana.tomaskova@savba.sk

<sup>1</sup> Institute of Molecular Physiology and Genetics, Center of Biosciences, Slovak Academy of Sciences, Bratislava, Slovak Republic

<sup>2</sup> Institute of Clinical and Translational Research, Biomedical Research Center, Slovak Academy of Sciences, Bratislava, Slovak Republic

## References

- [1] White MM, Miller C. A voltage-gated anion channel from the electric organ of *Torpedo californica*. The Journal of Biological Chemistry. 1979;**254**(20):10161-10166
- [2] Miller C. In the beginning: A personal reminiscence on the origin and legacy of ClC-0, the "Torpedo Cl(-) channel. The Journal of Physiology. 2015;**593**(18):4085-4090
- [3] Jentsch TJ et al. Molecular structure and physiological function of chloride channels. Physiological Reviews. 2002;**82**(2):503-568
- [4] Jentsch TJ, Steinmeyer K, Schwarz G. Primary structure of *Torpedo marmorata* chloride channel isolated by expression cloning in *Xenopus* oocytes. Nature. 1990;**348**(6301):510-514
- [5] Jentsch TJ, Neagoe I, Scheel O. CLC chloride channels and transporters. Current Opinion in Neurobiology. 2005;**15**(3):319-325
- [6] Dutzler R et al. X-ray structure of a ClC chloride channel at 3.0 Å reveals the molecular basis of anion selectivity. Nature. 2002;**415**(6869):287-294
- [7] Bauer CK et al. Completely functional double-barreled chloride channel expressed from a single *Torpedo* cDNA. Proceedings of the National Academy of Sciences of the United States of America. 1991;**88**(24):11052-11056
- [8] Hanke W, Miller C. Single chloride channels from *Torpedo* electroplax. Activation by protons. The Journal of General Physiology. 1983;**82**(1):25-45
- [9] Miller C. Open-state substructure of single chloride channels from *Torpedo* electroplax. Philosophical Transactions of the Royal Society of London. Series B, Biological Sciences. 1982;**299**(1097):401-411
- [10] Sakmann B, Hamill OP, Bormann J. Patch-clamp measurements of elementary chloride currents activated by the putative inhibitory transmitter GABA and glycine in mammalian spinal neurons. Journal of Neural Transmission. Supplementum. 1983;**18**:83-95
- [11] Hamill OP, Bormann J, Sakmann B. Activation of multiple-conductance state chloride channels in spinal neurones by glycine and GABA. Nature. 1983;**305**(5937):805-808
- [12] Schultz BD et al. Pharmacology of CFTR chloride channel activity. Physiological Reviews. 1999;**79**:S109-S144
- [13] Anderson MP et al. Generation of cAMP-activated chloride currents by expression of CFTR. Science. 1991;**251**(4994):679-682
- [14] Bear CE et al. Purification and functional reconstitution of the cystic fibrosis transmembrane conductance regulator (CFTR). Cell. 1992;**68**(4):809-818
- [15] Landry DW et al. Epithelial chloride channel. Development of inhibitory ligands. The Journal of General Physiology. 1987;**90**(6):779-798
- [16] Baumgarten CM, Clemo HF. Swelling-activated chloride channels in cardiac physiology and pathophysiology. Progress in Biophysics and Molecular Biology. 2003;**82**(1-3):25-42

- [17] Dixon DM, Valkanov M, Martin RJ. A patch-clamp study of the ionic selectivity of the large conductance, Ca-activated chloride channel in muscle vesicles prepared from *Ascaris suum*. *The Journal of Membrane Biology*. 1993;**131**(2):143-149
- [18] Jones K et al. Electrophysiological characterization and functional importance of calcium-activated chloride channel in rat uterine myocytes. *Pflügers Archiv*. 2004;**448**(1):36-43
- [19] Mitchell P. Coupling of phosphorylation to electron and hydrogen transfer by a chemiosmotic type of mechanism. *Nature*. 1961;**191**:144-148
- [20] Ponnalagu D, Singh H. Anion channels of mitochondria. *Handbook of Experimental Pharmacology*. 2016;**240**:71-101
- [21] Landry DW et al. Purification and reconstitution of chloride channels from kidney and trachea. *Science*. 1989;**244**(4911):1469-1472
- [22] Beavis AD, Garlid KD. The mitochondrial inner membrane anion channel. *The Journal of Biological Chemistry*. 1987;**262**(5):15085-15093
- [23] Warhurst IW, Dawson AP, Selwyn MJ. Inhibition of electrogenic anion entry into rat liver mitochondria by N,N'-dicyclohexylcarbodiimide. *FEBS Letters*. 1982;**149**(2):249-252
- [24] Miller C. Integral membrane channels: Studies in model membranes. *Physiological Reviews*. 1983;**63**(4):1209-1242
- [25] Neher E, Sakmann B, Steinbach JH. The extracellular patch clamp: A method for resolving currents through individual open channels in biological membranes. *Pflügers Archiv*. 1978;**375**(2):219-228
- [26] Schein SJ, Colombini M, Finkelstein A. Reconstitution in planar lipid bilayers of a voltage-dependent anion-selective channel obtained from paramecium mitochondria. *The Journal of Membrane Biology*. 1976;**30**(2):99-120
- [27] Selwyn MJ, Dawson AP, Fulton DV. An anion-conducting pore in the mitochondrial inner membrane [proceedings]. *Biochemical Society Transactions*. 1979;**7**(1):216-219
- [28] Garlid KD, Beavis AD. Evidence for the existence of an inner membrane anion channel in mitochondria. *Biochimica et Biophysica Acta*. 1986;**853**(3-4):187-204
- [29] Halle-Smith SC, Murray AG, Selwyn MJ. Palmitoyl-CoA inhibits the mitochondrial inner membrane anion-conducting channel. *FEBS Letters*. 1988;**236**(1):155-158
- [30] Zernig G et al. Mitochondrial Ca<sup>2+</sup> antagonist binding sites are associated with an inner mitochondrial membrane anion channel. *Molecular Pharmacology*. 1990;**38**(3):362-369
- [31] Powers MF, Beavis AD. Triorganotin inhibit the mitochondrial inner membrane anion channel. *The Journal of Biological Chemistry*. 1991;**266**(26):17250-17256
- [32] Beavis AD. Properties of the inner membrane anion channel in intact mitochondria. *Journal of Bioenergetics and Biomembranes*. 1992;**24**(1):77-90
- [33] Powers MF, Smith LL, Beavis AD. On the relationship between the mitochondrial inner membrane anion channel and the adenine nucleotide translocase. *The Journal of Biological Chemistry*. 1994;**269**(14):10614-10620



- [34] Beavis AD, Davatol-Hag H. The mitochondrial inner membrane anion channel is inhibited by DIDS. *Journal of Bioenergetics and Biomembranes*. 1996;**28**(2):207-214
- [35] Beavis AD, Powers M. Temperature dependence of the mitochondrial inner membrane anion channel: The relationship between temperature and inhibition by magnesium. *The Journal of Biological Chemistry*. 2004;**279**(6):4045-4050
- [36] Schonfeld P et al. Fatty acids induce chloride permeation in rat liver mitochondria by activation of the inner membrane anion channel (IMAC). *Journal of Bioenergetics and Biomembranes*. 2004;**36**(3):241-248
- [37] O'Rourke B. Pathophysiological and protective roles of mitochondrial ion channels. *The Journal of Physiology*. 2000;**529**(Pt 1):23-36
- [38] Jung DW, Brierley GP. Matrix free Mg(2+) and the regulation of mitochondrial volume. *The American Journal of Physiology*. 1999;**277**(6 Pt 1):C1194-C1201
- [39] Sorgato MC, Keller BU, Stuhmer W. Patch-clamping of the inner mitochondrial membrane reveals a voltage-dependent ion channel. *Nature*. 1987;**330**(6147):498-500
- [40] Kinnally KW et al. Mitochondrial benzodiazepine receptor linked to inner membrane ion channels by nanomolar actions of ligands. *Proceedings of the National Academy of Sciences of the United States of America*. 1993;**90**(4):1374-1378
- [41] Sorgato MC et al. Further investigation on the high-conductance ion channel of the inner membrane of mitochondria. *Journal of Bioenergetics and Biomembranes*. 1989;**21**(4):485-496
- [42] Brown DA, O'Rourke B. Cardiac mitochondria and arrhythmias. *Cardiovascular Research*. 2010;**88**:241-249
- [43] Kinnally KW et al. Calcium modulation of mitochondrial inner membrane channel activity. *Biochemical and Biophysical Research Communications*. 1991;**176**(3):1183-1188
- [44] Kinnally KW, Antonenko YN, Zorov DB. Modulation of inner mitochondrial membrane channel activity. *Journal of Bioenergetics and Biomembranes*. 1992;**24**(1):99-110
- [45] Klitsch T, Siemen D. Inner mitochondrial membrane anion channel is present in brown adipocytes but is not identical with the uncoupling protein. *The Journal of Membrane Biology*. 1991;**122**(1):69-75
- [46] Hayman KA, Spurway TD, Ashley RH. Single anion channels reconstituted from cardiac mitoplasts. *The Journal of Membrane Biology*. 1993;**136**(2):181-190
- [47] Ballarin C, Sorgato MC. An electrophysiological study of yeast mitochondria: Evidence for two inner membrane anion channels sensitive to ATP. *Journal of Biological Chemistry*. 1995;**270**(33):19262-19268
- [48] De Marchi U et al. A maxi-chloride channel in the inner membrane of mammalian mitochondria. *Biochimica et Biophysica Acta*. 2008;**1777**(11):1438-1448
- [49] Borecky J, Jezek P, Siemen D. 108-pS channel in brown fat mitochondria might be identical to the inner membrane anion channel. *The Journal of Biological Chemistry*. 1997;**272**(31):19282-19289

- [50] Huang SG, Klingenberg M. Chloride channel properties of the uncoupling protein from brown adipose tissue mitochondria: A patch-clamp study. *Biochemistry*. 1996;**35**(51):16806-16814
- [51] Jezek P, Orosz DE, Garlid KD. Reconstitution of the uncoupling protein of brown adipose tissue mitochondria. Demonstration of GDP-sensitive halide anion uniport. *The Journal of Biological Chemistry*. 1990;**265**(31):19296-19302
- [52] Antonenko YN et al. Selective effect of inhibitors on inner mitochondrial membrane channels. *FEBS Letters*. 1991;**285**(1):89-93
- [53] Beavis AD, Powers MF. On the regulation of the mitochondrial inner membrane anion channel by magnesium and protons. *The Journal of Biological Chemistry*. 1989;**264**(29):17148-17155
- [54] Ballarin C, Sorgato MC. Anion channels of the inner membrane of mammalian and yeast mitochondria. *Journal of Bioenergetics and Biomembranes*. 1996;**28**(2):125-130
- [55] Hayman KA, Ashley RH. Structural features of a multisubstate cardiac mitoplast anion channel: Inferences from single channel recording. *The Journal of Membrane Biology*. 1993;**136**(2):191-197
- [56] Misak A et al. Mitochondrial chloride channels: Electrophysiological characterization and pH induction of channel pore dilation. *European Biophysics Journal*. 2013;**42**(9):709-720
- [57] Tomaskova Z et al. Inhibition of anion channels derived from mitochondrial membranes of the rat heart by stilbene disulfonate—DIDS. *Journal of Bioenergetics and Biomembranes*. 2007;**39**(4):301-311
- [58] Misak A. Mitochondriove chloridove kanaly: Od izolacie membranovych vezikul a elektrofyziologickej charakterizacie ku modulacii bioaktivnymi zdrojmi H<sub>2</sub>S [thesis]. Univerzita P.J.Safarika Kosice; 2014
- [59] Tomaskova Z, Ondrias K. Mitochondrial chloride channels—What are they for? *FEBS Letters*. 2010;**584**(10):2085-2092
- [60] Romashko DN, Marban E, O'Rourke B. Subcellular metabolic transients and mitochondrial redox waves in heart cells. *Proceedings of the National Academy of Sciences of the United States of America*. 1998;**95**(4):1618-1623
- [61] Aon MA et al. Synchronized whole cell oscillations in mitochondrial metabolism triggered by a local release of reactive oxygen species in cardiac myocytes. *The Journal of Biological Chemistry*. 2003;**278**:44735-44744
- [62] Cortassa S et al. A Mitochondrial oscillator dependent on reactive oxygen species. *Biophysical Journal*. 2004;**87**:2060-2073
- [63] Faivre JF, Findlay I. Action potential duration and activation of ATP-sensitive potassium current in isolated guinea-pig ventricular myocytes. *Biochimica et Biophysica Acta*. 1990;**1029**(1):167-172
- [64] O'Rourke B, Ramza BM, Marban E. Oscillations of membrane current and excitability driven by metabolic oscillations in heart cells. *Science*. 1994;**265**(5174):962-966

- [65] Zorov DB et al. Reactive oxygen species (ROS)-induced ROS release: A new phenomenon accompanying induction of the mitochondrial permeability transition in cardiac myocytes. *The Journal of Experimental Medicine*. 2000;**192**(7):1001-1014
- [66] Aon MA et al. From mitochondrial dynamics to arrhythmias. *The International Journal of Biochemistry & Cell Biology*. 2009;**40**:1940-1948
- [67] Schafer FQ, Buettner GR. Redox environment of the cell as viewed through the redox state of the glutathione disulfide/glutathione couple. *Free Radical Biology & Medicine*. 2001;**30**(11):1191-1212
- [68] Aon MA et al. Sequential opening of mitochondrial ion channels as a function of glutathione redox thiol status. *The Journal of Biological Chemistry*. 2007;**282**:21889-21900
- [69] Zhou L et al. A Reaction-diffusion model of ROS-induced ROS release in a mitochondrial network. *PLoS Computational Biology*. 2010;**6**(1):e1000657
- [70] Tomasek M et al. Subconductance states of mitochondrial chloride channels: Implication for functionally-coupled tetramers. *FEBS Letters*. 2017;**591**(15):2251-2260
- [71] Singh H. Two decades with dimorphic chloride intracellular channels (CLICs). *FEBS Letters*. 2010;**584**(10):2112-2121
- [72] Harrop SJ et al. Crystal structure of a soluble form of the intracellular chloride ion channel CLIC1 (NCC27) at 1.4-Å resolution. *The Journal of Biological Chemistry*. 2001;**276**(48):44993-45000
- [73] Cromer BA et al. From glutathione transferase to pore in a CLIC. *European Biophysics Journal*. 2002;**31**(5):356-364
- [74] Tulk BM, Kapadia S, Edwards JC. CLIC1 inserts from the aqueous phase into phospholipid membranes, where it functions as an anion channel. *American Journal of Physiology. Cell Physiology*. 2002;**282**:C1103-C1112
- [75] Tulk BM et al. CLIC-1 functions as a chloride channel when expressed and purified from bacteria. *The Journal of Biological Chemistry*. 2000;**275**(35):26986-26993
- [76] Tonini R et al. Functional characterization of the NCC27 nuclear protein in stable transfected CHO-K1 cells. *The FASEB Journal*. 2000;**14**(9):1171-1178
- [77] Singh H, Ashley RH. Redox regulation of CLIC1 by cysteine residues associated with the putative channel pore. *Biophysical Journal*. 2006;**90**(5):1628-1638
- [78] Littler DR et al. The intracellular chloride ion channel protein CLIC1 undergoes a redox-controlled structural transition. *The Journal of Biological Chemistry*. 2004;**279**(10):9298-9305
- [79] Proutski I, Karoulias N, Ashley RH. Overexpressed chloride intracellular channel protein CLIC4 (p64H1) is an essential component of novel plasma membrane anion channels. *Biochemical and Biophysical Research Communications*. 2002;**297**(2):317-322
- [80] Duncan RR et al. Rat brain p64H1, expression of a new member of the p64 chloride channel protein family in endoplasmic reticulum. *The Journal of Biological Chemistry*. 1997;**272**(38):23880-23886

- [81] Littler DR et al. Crystal structure of the soluble form of the redox-regulated chloride ion channel protein CLIC4. *The FEBS Journal*. 2005;**272**(19):4996-5007
- [82] Bridges RJ et al. Stilbene disulfonate blockade of colonic secretory Cl<sup>-</sup> channels in planar lipid bilayers. *The American Journal of Physiology*. 1989;**256**(4 Pt 1):C902-C912
- [83] Singh H, Cousin MA, Ashley RH. Functional reconstitution of mammalian 'chloride intracellular channels' CLIC1, CLIC4 and CLIC5 reveals differential regulation by cytoskeletal actin. *The FEBS Journal*. 2007;**274**(24):6306-6316
- [84] Edwards JC, Tulk B, Schlesinger PH. Functional expression of p64, an intracellular chloride channel protein. *Journal of Membrane Biology*. 1998;**163**(2):119-127
- [85] Weber-Schurholz S et al. Indanyloxyacetic acid-sensitive chloride channels from outer membranes of skeletal muscle. *The Journal of Biological Chemistry*. 1993;**268**(1):547-551
- [86] Singh H, Ashley RH. CLIC4 (p64H1) and its putative transmembrane domain form poorly selective, redox-regulated ion channels. *Molecular Membrane Biology*. 2007;**24**(1):41-52
- [87] Tulk BM, Edwards JC. NCC27, a homolog of intracellular Cl<sup>-</sup> channel p64, is expressed in brush border of renal proximal tubule. *American Journal of Physiology-Renal Physiology*. 1998;**274**(6):F1140-F1149
- [88] Omura T. Mitochondria-targeting sequence, a multi-role sorting sequence recognized at all steps of protein import into mitochondria. *Journal of Biochemistry*. 1998;**123**(6):1010-1016
- [89] Ponnalagu D et al. Data supporting characterization of CLIC1, CLIC4, CLIC5 and DmCLIC antibodies and localization of CLICs in endoplasmic reticulum of cardiomyocytes. *Data in Brief*. 2016;**7**:1038-1044
- [90] Ponnalagu D et al. Molecular identity of cardiac mitochondrial chloride intracellular channel proteins. *Mitochondrion*. 2016;**27**:6-14
- [91] Singh H et al. Visualization and quantification of cardiac mitochondrial protein clusters with STED microscopy. *Mitochondrion*. 2012;**12**(2):230-236
- [92] Meier JA, Larner AC. Toward a new STATE: The role of STATs in mitochondrial function. *Seminars in Immunology*. 2014;**26**(1):20-28
- [93] Heusch G et al. Mitochondrial STAT3 activation and cardioprotection by ischemic postconditioning in pigs with regional myocardial ischemia/reperfusion. *Circulation Research*. 2011;**109**(11):1302-1308
- [94] Boengler K et al. Inhibition of permeability transition pore opening by mitochondrial STAT3 and its role in myocardial ischemia/reperfusion. *Basic Research in Cardiology*. 2010;**105**(6):771-785
- [95] Boengler K et al. The STAT3 inhibitor stattic impairs cardiomyocyte mitochondrial function through increased reactive oxygen species formation. *Current Pharmaceutical Design*. 2013;**19**(39):6890-6895



*Edited by Kaneez Fatima Shad*

Ion channels are proteins that make pores in the membranes of excitable cells present both in the brain and the body. These cells are not only responsible for converting chemical and mechanical stimuli into the electrical signals but are also liable for monitoring vital functions.

All our activities, from the blinking of our eyes to the beating of our heart and all our senses from smell to sight, touch, taste and hearing are regulated by the ion channels. This book will take us on an expedition describing the role of ion channels in congenital and acquired diseases and the challenges and limitations scientist are facing in the development of drugs targeting these membrane proteins.

Published in London, UK

© 2018 IntechOpen  
© markusblanke / iStock

**IntechOpen**

